

Microbial communities in biogas reactors and their link to stability and performance

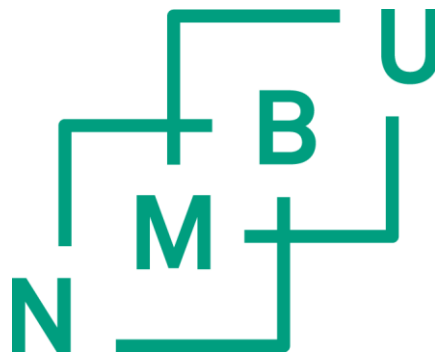
Mikrobielle samfunn i biogass reaktorer og deres kobling til stabilitet og ytelse

Philosophiae Doctor (PhD) Thesis

Live Heldal Hagen

Department of Chemistry, Biotechnology and Food Science
Faculty of Veterinary Medicine and Bioscience
Norwegian University of Life Sciences

Ås (2016)



Thesis number 2016:60
ISSN 1894-6402
ISBN 978-82-575-1380-1

Table of Contents

ACKNOWLEDGEMENTS	III
SUMMARY	V
SAMMENDRAG	VII
ABBREVIATIONS	XI
LIST OF PAPERS	IX
1 INTRODUCTION	1
1.1 BIOGAS PRODUCTION FOR A SUSTAINABLE BIO-ECONOMY	1
1.2 <i>Biogas in Europe and Norway</i>	2
1.2 THE BIOGAS REACTOR	4
1.2.1 <i>Feedstock</i>	5
1.2.2 <i>Process parameters influencing the process stability</i>	6
1.3 FROM WASTE TO ENERGY – A MICROBIAL PROCESS	8
1.3.1 <i>The study of complex microbial communities</i>	14
2 OUTLINE AND AIM OF THESIS	17
3 MAIN RESULTS AND DISCUSSION	19
3.1 DYNAMICS IN A MICROBIAL COMMUNITY UNDERGOING DISTURBANCE (PAPER I)	19
3.2 EFFECT OF STORAGE CONDITION ON INOCULUM MICROBIAL COMMUNITY COMPOSITION AND PERFORMANCE (PAPER II)	21
3.3 EFFECT OF TEMPERATURE AND RECIRCULATION ON MICROBIAL COMMUNITY COMPOSITION AND PERFORMANCE (PAPER III)	23
3.4 CHARACTERIZATION OF THE MICROBIAL COMMUNITY IN A STABLE FULL-SCALE BIOGAS PLANT (PAPER IV)	25
4 CONCLUDING REMARKS	28
5 APPLICATION AND FUTURE PERSPECTIVES	30
REFERENCES	32
PAPERS	I-IV

ACKNOWLEDGEMENTS

The present work was carried out during the period 2013-2016 in the Protein Engineering and Proteomics (PEP) group, Department of Chemistry, Biotechnology and Food Science at The Norwegian University of Life Sciences (NMBU). The PhD study was part of two projects: “Robust processes for biogas production using manure and by-products from agriculture and agro-industry” (RobuBiogas) and “Biogas from organic residues and livestock manure as a vehicle fuel” (BiogasFuel), both funded by the Research Council of Norway.

First of all, I would like to express gratitude to my main supervisor, Professor Svein Jarle Horn for supporting and encouraging me. You always keep your door open, and I truly appreciate that you have taken the time to patiently answer my questions. I would also like to thank co-supervisor Dr. Phillip Pope for opening the door to the PEP-corridor in the first place and for sharing valuable advises. A special thanks to co-supervisor Professor Vincent Eijssink, your endless knowledge and enthusiasm is a true inspiration.

I would also like to express my gratefulness to Vivekanand Vivekanand and Mirzaman Zamanzadeh. Thank you for sharing of your biogas processing knowledge, and for collecting samples for microbial analysis. A special thanks to Jeremy Frank, for helpful support with the bioinformatics.

Anne-Cath and Ellen, you are the core of the PEP group, and how you can keep track on everyone and everything in the lab is a mystery to me! I would also like to thank all members of the PEP-group, with a very special thanks to Trine for always keeping the door open for me and my frustrations, both research-related and private matter, and Kasia for always keeping the door closed (literally), and for creating an energetic atmosphere in our office. You make work fun!

A special thanks to Professor Jon Fredrik Hanssen, who opened my eyes to the intriguing microbial world. You are my hero.

Thanks to my family for letting me be myself - it seems like my stubbornness paid off. A special thanks to my “Afghan family” for the sweetest cakes, the warmest hugs and perspective on life. And then, last but not least, a very special thanks to my friends. Throughout the years, you have given me good laughs and valuable memories. During the last period of this work, you have also given me a support that I am eternally grateful for. You are simply the best.

Live

SUMMARY

The Anaerobic digestion (AD) of organic material gathers a great interest worldwide due to the global needs for waste recycling and renewable energy production. Biogas, the end product of an AD process, is a mixture of methane and carbon dioxide. Biogas can be used for heating, electricity or upgraded to pure methane for vehicle fuels. It could also serve as a part of the cycle in biorefineries. Although widely applied for energy production, an improved knowledge regarding the underlying microbial community is desired to ensure stable and efficient energy production. Therefore, the studies described in this thesis aimed to increase the knowledge base of microbial community in biogas reactors and relate this to stability and performance of the digestion process.

We analyzed 16S rRNA gene sequences from samples collected of both unstable and stable laboratory-scale biogas reactors, and studied the community profile and dynamics of bacteria and archaea. In particular, we evaluated the balance between acidogenesis and methanogenesis in reactors fed with an easy degradable substrate. We also evaluated how the microbial composition linked to performance was affected by different storage conditions on inoculum, as well as temperature and recirculation of effluent. The microbial community collected from a stable thermophilic industrial-scale reactor was further exposed using a combined meta-omics approach. This allowed us to map quantitative metaproteomics data to phylotype-specific genomic bins, in order to study the microbial network and metabolic pathways.

The interaction between different participating bacterial and archaeal groups have a significant impact on the stability of a biogas process. Volatile fatty acid (VFA) accumulation and a reduced biogas production was related to an unbalance between the acidogenesis and methanogenesis in both mesophilic and thermophilic reactors, caused either by a too fast hydrolysis due to overloading, or a too slow methanogenesis due to ammonia inhibition. Our results related the presence of several microbial groups to the accumulation and depletion of fatty acids. We also observed that recirculation of effluent had a negative effect on the thermophilic processes, with severe accumulation of VFAs and ammonia. While recirculation had only minor effects on the biogas production and performance under mesophilic operation, the microbial community composition changed. This indicates a substantial functional redundancy in the mesophilic microbiome, making

the community more resilient. The results also indicate that the inoculum may be stored up to one month without severe loss of microbial activity. Importantly, the deep characterization of microbial community revealed a synergic network, including a putative novel syntrophic acetate oxidizing bacteria.

Overall, the findings reported in this thesis provides increased insight into microbial community and the ecological roles of different microbial groups in relation to stability and performance of the AD process. Improved understanding about this intricate microbial network can be used to monitor and control the AD process, to ensure stable and efficient biogas production.

SAMMENDRAG

Anaerob nedbrytning av organisk materiale har stor interesse verden over på grunn av det globale behovet for resirkulering av avfall og generering av fornybar energi. Biogass, som er sluttproduktet etter en anaerob nedbrytningsprosess, består av en blanding metan og karbondioksid. Biogassen kan brukes til varme, strøm eller oppgraderes til ren metan og brukes som biodrivstoff. Den kan også tjene som en del av syklusen i et bioraffineri. Selv om anaerob nedbrytning for energiproduksjon er en godt etablert prosess, er økt forståelse om det underliggende mikrobielle samfunnet ønskelig for å sikre stabil og effektiv energiproduksjon. Studiene som beskrives i denne avhandlingen tar derfor sikte på å øke kunnskapsbasen rundt mikrobielle samfunn i biogassreaktorer, og relatere dette til stabilitet og ytelse i nedbrytningsprosessen.

Vi analyserte 16S rRNA gensekvensene i prøver tatt fra både ustabile og stabile laboratorie-skala biogassreaktorer, og studerte samfunnsprofilen og dynamikken av bakterier og arker. Mer spesifikt evaluerte vi balansen mellom acidogenesen og metanogenesen i reaktorer foret med lett nedbrytbart substrat. Vi evaluerte også hvilken effekt ulike lagringsforhold av inokulumet, så vel som temperatur og resirkulering, hadde på den mikrobielle sammensetningen og ytelsen. Det mikrobielle samfunnet i en stabil, termofil industrireaktor ble videre studert ved å benytte en kombinert meta-omiks tilnærming. Dette gjorde det mulig å relatere kvantitativ metaproteomikkdata til spesifikke fylotyper, og dermed avdekke mikrobielle nettverk og sentrale metabolske synteseveier.

Samspeillet mellom de ulike bakterie- og arkengruppene har stor innvirkning på stabiliteten til en biogass prosess. Akkumulering av flyktige fettsyrer og redusert biogassproduksjon ble relatert til ubalanse mellom acidogenesen og metanogenesis, som resultat av for rask hydrolyse på grunn av overføring, eller for sakte metanogenesis på grunn av ammonium hemming. Våre resultater kobler tilstedeværelsen av flere mikrobielle grupper til akkumulering eller nedbryting av fettsyrer. Resultatene viser også at resirkulering av effluenten kan ha negativ effekt på biogassproduksjonen i termofile reaktorer. Resirkulering hadde derimot liten innvirkning på biogass produksjonen i de mesofile reaktorene, til tross for stor forandring i sammensetningen av det mikrobielle samfunnet. Dette tyder på at en funksjonell redundans i den mesofile mikrobiotaen, noe som gjøre samfunnet mer spenstig. Resultatene tyder også på at inokulum kan lagres opptil en måned uten å miste mikrobiell

aktivitet. En dyp karakterisering av det mikrobielle samfunnet avdekket et synergisk nettverk, som inkluderte en antatt ny syntrofisk acetatoksiderende bakterie.

Samlet sett øker funnene rapportert i denne avhandlingen innsikten til det mikrobielle samfunnet og de økologiske rollene til ulike mikrobielle grupper i relasjon til stabilitet og ytelse i nedbrytningsprosessen. En økt forståelse om dette intrikate mikrobielle nettverket kan videre brukes til å overvåke og kontrollere den anaerobe nedbrytningsprosessen, for å sikre stabil og effektiv biogass produksjon.

LIST OF PAPERS

Paper I

Hagen, L.H., Vivekanand, V., Linjordet, R., Pope, P.B., Eijsink, V.G.H., Horn, S.J., 2014, Microbial community structure and dynamics during co-digestion of whey permeate and cow manure in continuous stirred tank reactor systems. *Bioresource Technology*, **171**, 350-359.

Paper II

Hagen, L.H., Vivekanand, V., Pope, P.B., Eijsink, V.G.H., Horn, S.J., 2015, The effect of storage conditions on microbial community composition and biomethane potential in a biogas starter culture. *Applied Microbiology and Biotechnology*, **99**, 5749-5761.

Paper III

Zamanzadeh, M., **Hagen, L.H.**, Svensson K., Linjordet, R., Horn, S.J., 2016, Anaerobic digestion of food waste – Effect of recirculation and temperature on performance and microbiology. *Water Research*, **96**, 246-254.

Paper IV

Hagen, L.H., Frank, J.A., Zamanzadeh, M., Eijsink, V.G.H., Pope, P.B., Horn, S.J., Arntzen, M., 2016, Quantitative metaproteomics highlight the metabolic contribution of uncultured phylotypes in a thermophilic anaerobic digestion; submitted manuscript.

In addition to Papers I-IV, the author contributed to the following papers within the timeframe of this thesis work:

Salgado-Flores, A., **Hagen, L.H.**, Ishaq, S. L., Zamanzadeh, M., Wright, A.D.G., Pope, P.B., Sundset, M.A., 2016, Rumen and Cecum Microbiomes in Reindeer (*Rangifer tarandus tarandus*) Are Changed in Response to a Lichen Diet and May Affect Enteric Methane Emissions. *PloS one*, **11**, doi:10.1371/journal.pone.0155213

Salgado-Flores, A., Bockwoldt, M., **Hagen, L. H.**, Pope, P.B., Sundset, M.A., 2016, A first insight into the fecal microbiota of the high Arctic muskoxen (*Ovibos moschatus*). *Microbial Genomics*, Published Ahead of Print April 29, 2016, doi: 10.1099/mgen.0.000066

Frank, J.A., Arntzen, M., Sun, L., **Hagen, L.H.**, McHardy, A., Horn, S.J., Eijsink, V.G.H., Schnürer, A., Pope, P.B., 2016. Novel syntrophic populations dominate ammonia-tolerant methanogenic microbiomes; submitted to *mSystems*.

ABBREVIATIONS

16S rRNA	16S ribosomal ribonucleic acid
ATP	Adenosine triphosphate
AD	Anaerobic digestion
BMP	Biochemical methane potential
CSTR	Continuously stirred tank reactors
GHG	Greenhouse gas
HTR	Hydraulic retention time
SAB	Syntrophic acetogenic bacteria
SAO	Syntrophic acetate oxidation
SAOB	Syntrophic acetate oxidizing bacteria
VFA	Volatile fatty acids

1 INTRODUCTION

1.1 Biogas production for a sustainable bio-economy

The increasing energy demand is a global challenge that at the present time is predominantly met by fossil fuel. Fossil fuel driven energy generation has several negative impacts on the environment, and the concentration of greenhouse gases (GHG) rises rapidly as a direct consequence the combustion of fossil fuel. Moreover, the fossil fuel resources are finite, and many of the reservoirs are found in politically unstable regions making this an unreliable energy source for the future. A transition from a fossil-based to a bio-based economy with use of stable and long term energy sources without negative impact on the environment is therefore desirable.

The vision of bio-economy is to create a resource-efficient economic system where food, material, chemicals, energy and fuel are produced from a renewable feedstock. The increased focus on sustainability have led to the development of new technologies, and in this context, production of energy and fuel from anaerobic digestion of biomass has gained increased focus during the recent years. Anaerobic digestion (AD) is a biologically mediated process that under anaerobic conditions converts organic material to biogas. This gas is a mixture of the energy carrier methane (CH_4 ; 50-70%) and carbon dioxide (CO_2 ; 30-50%), in addition to a small amount of trace gases (e.g. H_2S). The produced biogas can be used directly for electricity- and heat production, or, when upgraded to biomethane, as a vehicle fuel or as a feedstock in the speciality chemicals industry (paints, plastics, detergents). In addition to lowering the GHG emission by replacing fossil fuels with renewable methane, controlled AD of organic waste will also reduce spontaneous emissions of ammonia and CH_4 from stored waste. Release of CH_4 to the atmosphere from e.g. natural wetlands, landfills and livestock manure storage, is very problematic since CH_4 is a 20 times more potent GHG than CO_2 . Notably, CH_4 from sources associated with agricultural activities are contributing a significant portion of the global anthropogenic GHG emission (Weiss & Leip, 2012). A cost efficient reduction of GHG emission otherwise released to the atmosphere have therefore been an important driving force for establishing stable and efficient AD systems. An additional benefit of AD is that the residues from the process can be utilized as a fertilizer on agricultural land, substituting mineral fertilizers (Holm-Nielsen et al., 2009; Weiland, 2010). This leads to recirculation of nutrients and a reduction of nitrogen loss, as the anaerobic process converts

organically bound nitrogen to ammonium, readily accessible to plants (Massé et al., 2011; Möller & Müller, 2012). A high potential is also seen in linking biogas production to other aspects of the bio-based economy (such as production of ethanol, cosmetics, processed food) in a cascade of conversion processes. In this way, material that have traditionally been classified as “waste” can be recycled to valuable “green” products, fuel and energy with minimal waste generation and GHG emission, moving the society towards a sustainable bio-economy.

1.2 Biogas in Europe and Norway

Generation of combustible gas from decaying organic matter in absence of oxygen has been a known phenomenon for several centuries. The first anaerobic digesters were constructed to treat wastewater already late in the 19th century and the first biogas reactor treating wastewater from a whole city was established in 1895 (Exeter, UK). The use of anaerobic treatment continued to develop over the following century, with a main focus on treatment of domestic wastewater and with an initial objective of reducing sludge volume. The energy crisis in 1970 stimulated a rapid boost in the application of AD, this time also with a focus on energy production and reduction of dependence of fossil fuel. Today, AD of waste streams from agriculture comprises the main feedstock in European biogas plants (71%, EBA Biogas Report 2014), but AD treatment of organic waste originating from households and food processing industries are also well established. The application of biogas production from organic waste for electricity and heat production is common in Europe, and according to the latest report from European Biogas Association (EBA Biomethane & Biogas Report 2015), 17 240 biogas plants and 367 biomethane plants were operated within EU by the end of 2014. Germany is a pioneer in biogas production among the European countries, responsible for approx. half of the biogas production, followed by United Kingdom (UK) and Italy (EurObserv'er, 2014). Germany is also leading in the use of biomethane as a fuel, followed by Sweden that by the end of 2014 used 78% of its 1 303 GWh production of biomethane to run almost 50 000 vehicles (EBA Biomethane & Biogas Report 2015). Globally about $25 \cdot 10^9$ m³ methane is produced each year, but if the available portion of the world agricultural byproducts and domestic residues were anaerobically digested this could be increased to more than $1000 \cdot 10^9$ m³, potentially replacing a quarter of current natural gas consumption. While

most biogas currently is used for heat and power, about 17 million vehicles worldwide are running on natural gas which could be switched to biomethane.

In 2014, the Norwegian Ministry of Climate and Environment presented a new ‘Norwegian strategy for biogas, where the objective was to stimulate more production of biogas in Norway. A significant driving force is to reduce GHG emission. The current production of biogas in Norway is about $63 \cdot 10^6 \text{ m}^3 \text{ CH}_4$ (630 GWh), but the production potential is much larger. Agriculture is a large biomass resource in Norway, where the methane production potential from manure is more than $200 \cdot 10^6 \text{ m}^3 \text{ CH}_4$. An equally large biogas potential is held by the aquaculture industry along the Norwegian coast. Fish sludge (feces, feed rests) is extremely high in energy, but using fish waste as feed to biogas production is nevertheless challenging due to the high N level (low C:N ratio, as described in the forthcoming section), potentially leading to ammonia accumulation and process instability (Aspé et al., 2001; Gebauer, 2004). However, as both fish sludge and manure are rich in nutrition and have a high N-content, and they represent good substrate for co-digestion with carbon-rich residues generated in lignocellulosic biorefineries.

In total 48 biogas plants (number from ENOVA, 2014) are operating in Norway, with several others under construction. These are mainly degrading waste and residues from household, food processing industry and agriculture in addition to a large fraction of sewage sludge. Most of the biogas produced in Norway have traditionally been used for power and heat, but a clear trend the recent years is that the plants are upgrading biogas to vehicle biofuel. Purified biogas can easily replace the use of natural gas driven vehicle fuel, and about 100 buses are running on biogas derived biofuel in Norway today – an number expected to double in the near future. Another potential use of biogas is the production of hydrogen, primarily as a renewable emission free vehicle fuel, but also as a chemical feedstock to biorefineries.

1.2 The biogas reactor

A biogas reactor is in principle a closed system, constructed with an inlet for the substrate, an outlet for the effluent and a system for collecting the produced biogas. Different process types of biogas reactor configuration can be applied for AD, and the reactor size can vary from large-scale reactors treating municipal waste or household waste from entire cities, to small-scale reactors located at farms to utilize cattle manure *on site* for energy production. Laboratory-scale reactors are often used to study the biogas process and to evaluate different feedstocks. A typical system to study is continuously stirred tank reactors (CSTR), where the substrate is pumped continuously or semi-continuously into the process, simultaneously with removal of digestion residues (the effluent) (Figure 1). Batch systems, where the feedstock initially is added to a closed reactor system and then digested, is suitable for evaluation of biochemical methane potential (BMP) of specific substrates. The hydraulic retention time (HTR) is the average time the liquid remains in the reactor, and plays a crucial role in CSTR due to the continuously loss of active microbial biomass. Optimal HTR have been suggested in the range of 15-30 days for AD under mesophilic (30-40 °C) conditions, and 10-20 days under thermophilic conditions (Angelidaki et al., 2011), although even shorted HTR have been reported for high-rate thermophilic (50-60 °C) digesters (Ho et al., 2014).



Figure 1. Laboratory-scale semi-continuously stirred tank reactors (CSTR)

The AD process is carried out by a complex microbial community, where the whole process can be divided into four stages: Hydrolysis, Acidogenesis, Acetogenesis and Methanogenesis. A diverse group of anaerobe and facultative anaerobe bacteria performs the three first, while a specific group of methane producing archaea (methanogens) performs the final stage (Gujer & Zehnder, 1983) (An overview is given in Figure 2). These four groups work closely together, where in particular microorganisms from the first and second groups as well as the third and fourth group are linked closely together (Schink, 1997). In order to ensure an efficient and stable AD process, the operating parameters have to accommodate the growth requirements of the participating microorganism in terms of nutrients, temperature and pH (Weiland, 2010). This can be challenging, as the microbial consortia usually are very diverse and have different requirements. A separation of the two first stages (hydrolysis and acidogenesis) from the two last (acetogenesis and methanogenesis) have been demonstrated as promising to improve hydrolysis without inhibiting the methanogenesis (Blonskaja et al., 2003; Liu et al., 2006; Lv et al., 2010; Schmit & Ellis, 2001; Zhang & Noike, 1991). However, two-stage digestion process requires additional operational costs, and more research is needed to evaluate the potential benefits of implementation in commercial systems.

1.2.1 Feedstock

In a balanced AD process, the degradation rate of the first two steps equals the degradation rate in the two final steps. A well-constructed process adapted to the feedstock material is therefore essential to ensure an optimal biogas production. Typical substrates for AD includes sludge from wastewater treatment plants, agriculture by-products and manure, crop silage, food waste from households and by-products from food processing industry. In general, biomass rich in proteins and fats, such as food waste and slaughterhouse waste, have a higher biogas potential than biomass with high level of soluble carbohydrates (Schnürer & Jarvis, 2009; Wagner et al., 2013; Weiland, 2010). Since microorganism utilizes carbon faster than nitrogen, and a carbon-to-nitrogen (C:N) ratio in the range between 15:1 and 30:1 is often desired to maintain a balanced degradation (Hills, 1979; Panichnumsin et al., 2010; Wu et al., 2010; Zhang et al., 2013). Whereas high C:N ratio will give less methane, too low C:N ratio might cause accumulation of ammonia, and eventually a pH exceeding the growth range for methanogens (Wang et al., 2012). In addition to carbon and nitrogen, phosphate and minor-nutrients (trace elements) is essential to support the microbial growth. Anaerobic co-digestion

has been shown as an efficient way to achieve a suitable C:N ratio and nutrient composition in the feedstock, and the synergic effect utilizing several different substrates is well documented (Astals et al., 2012; Diaz et al., 2011; Hartmann & Ahring, 2005a; Mata-Alvarez et al., 2011; Vivekanand et al., 2012; Wang et al., 2012; Wu et al., 2010). Moreover, different pretreatment methods (enzymatic, physical or chemical) have been successfully applied to enhance the degradation rate of recalcitrant substrates, such as lignocellulosic biomass (Risberg et al., 2013).

1.2.2 Process parameters influencing the process stability

Most of the biogas reactors are operating at a temperature ranging from 30 – 40 °C (mesophilic) or 50-60 °C (thermophilic). Mesophilic operation are often the preferred configuration in industry, as it requires less energy input for heating than the thermophilic (Gallert & Winter, 1997). The microbial populations found in mesophilic biogas reactors are also relative resilient, with a higher tolerance to fluctuations and inhibitory compounds in the environment (Angelidaki & Ahring, 1994; Sanchez et al., 2000). Several studies have reported that the microbial community in thermophilic reactors typically are less diverse than mesophilic populations, and therefore more vulnerable to environmental stress and operational changes (Karakashev et al., 2005; Leven et al., 2007). Moreover, ammonia toxicity increases with increasing temperatures, especially inhibiting the methanogenic population (Angelidaki & Ahring, 1993), as discussed further in the forthcoming sections. On the other hand, an increased metabolic activity of the microorganisms is achieved under thermophilic temperature, allowing shorter HRT and a higher efficiency in degradation of organic matter (Sanchez et al., 2000; Zabranska et al., 2000). Digestion under thermophilic conditions also benefit from sufficient sanitation of the organic waste (Bagge et al., 2005; Sahlström, 2003; Zabranska et al., 2000).

An AD process generally have a pH range from 6.0 to 8.5. Several bacteria may tolerate acidic pH conditions, while it is widely accepted that the methanogenic population will be inhibited at lower pH (Boone & Xun, 1987; Weiland, 2010). Volatile fatty acids (VFAs) are important fermentation intermediates in AD and accumulation of VFAs, e.g. as a result of high organic loading rate or free ammonia inhibition, can potentially lead to a critical drop in pH (acidification). Acidification resulting from VFA accumulation is the most common AD

process failure, where methanogenesis becomes the rate-limiting step leading to a decreased methane production (Akuzawa et al., 2011; Barredo & Evison, 1991; Goux et al., 2015; Koster & Cramer, 1987). Thus VFA concentrations, especially butyrate, propionate and acetate, are often monitored to spot possible process problems (Ahring et al., 1995; Nielsen et al., 2007). It should nevertheless be noted that the accumulation of VFAs does not necessary lead to decreased pH, depending of the buffer capacity in the substrate (Shehu et al., 2012).

The inoculum serves as an initial start culture, and is usually the slurry (effluent) from operative well performing biogas reactor, rich in active anaerobic microorganisms. The inoculum composition have been proven as a key determinant of the final microbial community and performance of the AD (Cortes-Tolalpa et al., 2016). Studies have shown that microbial communities can adapt to stress, and remain tolerant over several generations (Fotidis et al., 2013). Thus, depending on the history of the inoculum source, the inoculum may introduce a microbial community core adapted to specific operational conditions or to stress, such as elevated ammonia levels (De Vrieze et al., 2015). The degradation efficiency may also be directly reflected by the inoculum selection, as the microbial community will be inherited to the feedstock and temperature that it was exposed to in the source (Moset et al., 2015). Thus, selecting an inoculum source that contains a collection of microorganism suitable for the desired degradation process is important to ensure a stable and efficient biogas production. Moreover, designing ‘elastic’ microbial start cultures, with ability to quickly respond on environmental changes or that possess the functional machinery needed for degradation of recalcitrant material (e.g. lignocellulose) might be relevant for future applications.

1.3 From waste to energy – a microbial process

Despite the worldwide application of biogas reactors, the microbial community responsible for the AD process has for a long time been a black box. The increased application of AD for energy production have motivated researchers to investigate the underlying microbial community, and it is now clear that we can divide the whole AD process into the four major steps previously mentioned (Figure 2).

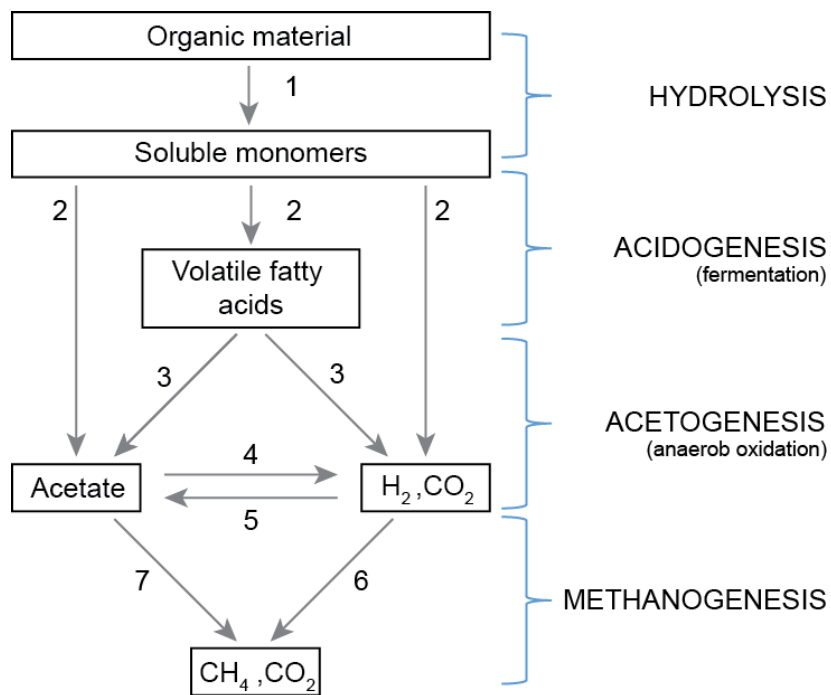


Figure 2. Anaerobic digestion of organic material to methane and carbon dioxide proceeds through four main steps: Hydrolysis (1), Acidogenesis (2), Acetogenesis (3; Syntrophic oxidation of VFAs, 4; Syntrophic acetate oxidation, 5; Hydrogen oxidation) and Methanogenesis (6; Hydrogenotrophic methanogenesis, 7; Acetoclastic methanogenesis).

In the first step, degradation of biopolymers to monomers takes place (Hydrolysis). Depending on the biomass material, different microorganisms secrete specialized enzymes for breaking down polymeric material to compounds small enough to enter the bacterial cells. Insoluble carbohydrates are hydrolyzed into soluble carbohydrates, proteins are hydrolyzed into amino acids and lipids are converted to glycerol and oleate. These compounds are then fermented to fatty acids, secondary alcohols, CO₂ and hydrogen (second step; Acidogenesis). Fatty acids and secondary alcohols are syntrophically converted to hydrogen, CO₂ and acetate

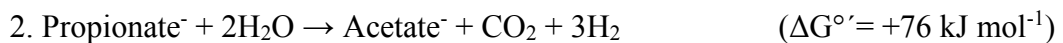
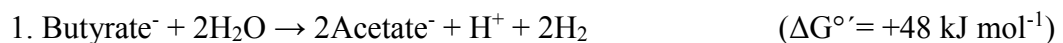
(third step; Acetogenesis) (Angelidaki et al., 1999). While a large consortium of bacteria carries out the three first steps of anaerobe degradation, a more specialized group of archaea collectively called methanogens performs the final step (Methanogenesis). Hydrogenotrophic methanogens utilize H_2 to reduce CO_2 to CH_4 , while acetoclastic methanogens converts acetate to methane through formation of acetyl coenzyme A (CoA) (Thauer, 1998). Most of the described methanogens are hydrogenotrophic (e.g. the *Methanobacteriales*, *Methanococcales* and *Methanomicrobiales* orders). The group of acetoclastic methanogens are restricted to species belonging to the order *Methanosarcinales*, with *Methanosaeta* and *Methanosarcina* as important genera. *Methanosarcina* can additionally grow on CO_2 and H_2 . An alternative pathway for converting acetate to methane is through a syntrophic association between the hydrogen consuming microorganisms (i.e. hydrogenotrophic methanogens) and a specialized group of homoacetogenic bacteria, called syntrophic acetate oxidizing bacteria (SAOB).

1.2.2 Syntrophic degradation of fermentation intermediates

For a microbe, the energy generated from degradation of organic matter in an anaerobic process is low compared to aerobic degradation or anaerobic respiration. Thus, a complete conversion of complex organic compounds to biogas in anaerobic environments depends upon an efficient and well-working cooperation between several metabolic types of microorganism. The degree of dependency between members in the metabolic network varies, from utilizing the metabolic product from the organism ahead in the food chain as substrate supply to being entirely dependent on the metabolic behavior of another microorganism. In syntrophy, such cooperation is obligate between two metabolically different microorganisms. One syntrophic partner rely on the other for substrate availability, while keeping the concentration of the intermediates at a minimum making the first reaction possible. The metabolism often involves interspecies transfer of either hydrogen or formate. A classic example is the discovery of the “*Methanobacillus omelianskii*” culture, a classified organism shown to convert ethanol to CH_4 . Later, it turned out that *Methanobacillus omelianskii* was not a pure culture, but rather a co-culture of two syntrophic partners that in cooperation through interspecies hydrogen transfer made the conversion of ethanol to CH_4 thermodynamically possible (McInerney et al., 2008). Under standard conditions, the Gibbs free energy changes (ΔG) of the oxidative fermentation of ethanol is a hydrogen releasing,

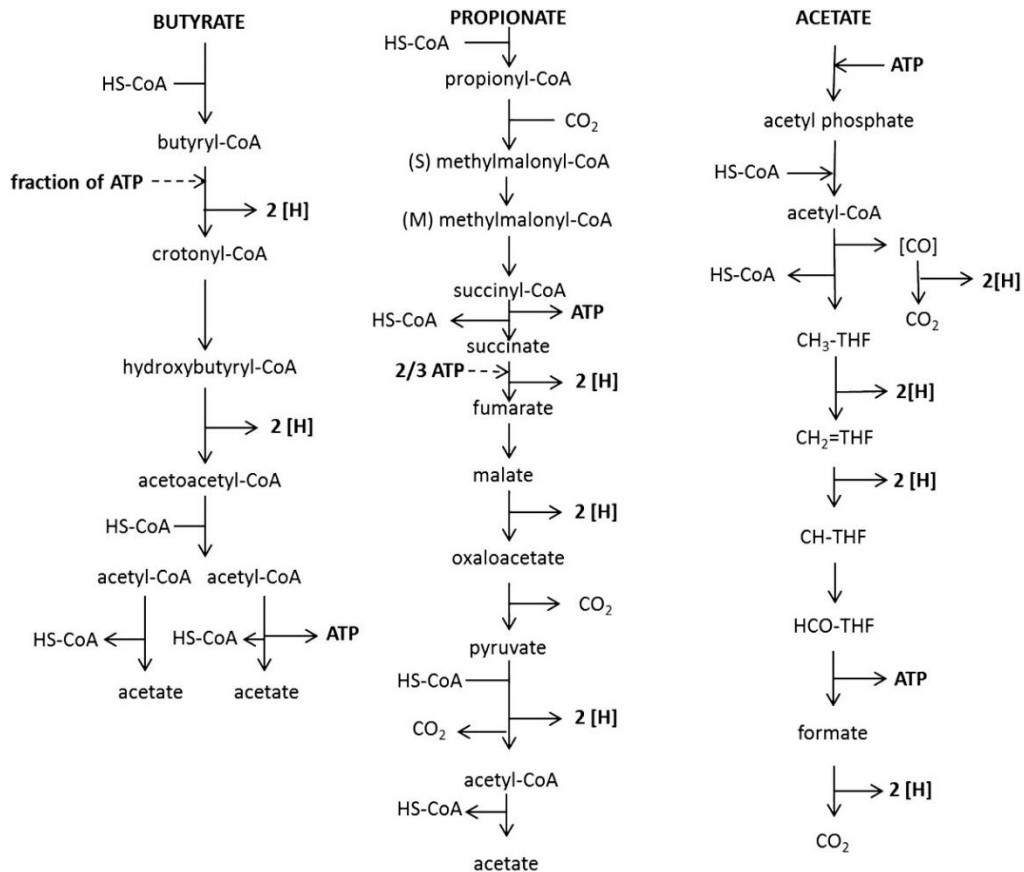
endergonic reaction (+19 kJ per 3 mol of Etanol). Thus, in a pure culture, this reaction would go in the energetic favorable direction producing ethanol. However, with the action of the hydrogen scavenger keeping the hydrogen partial pressure low, the hydrogen production becomes thermodynamically favorable.

Depending on the substrate combination and how active the hydrogen-utilizing population in an AD is, a portion of VFAs are generated from the fermentation of carbohydrates, amino acids and lipids. Butyrate, propionate and acetate are the most common fermentation products, and a rapid removal of these are critical to avoid build-up of VFA that may result in a drop in pH, process inhibition and eventually process collapse. Degradation of fatty acids is even more endergonic under standard condition (shown by the positive Gibbs free energy changes in equation 1-3. The values are adapted from Schink et al., 1997) than ethanol degradation. The hydrogen partial pressure required is lower than what hydrogenotrophic methanogens can maintain, and this conversion is balancing on the limit of what is thermodynamically possible (Schink, 1997; Thauer et al., 1977). In addition to relying on a hydrogen-consuming counterpart keeping the partial pressure of H₂ at a minimum, degradation of VFA therefore requires a mechanism for reversed electron transport (Schink, 1997; Sieber et al., 2010; Worm et al., 2014).



Equations (1-3)

Oxidation of fermentation products yields low free energy change even under optimal syntrophic growth conditions. Moreover, the available energy is shared between several partial reactions and two or more organism, leaving very small amount of energy (ATP) left for cell maintenance and growth, resulting in a very slow growth of syntrophic organisms. All known syntrophic butyrate degraders, e.g. *Syntrophomonas wolfei* (McInerney et al., 1981), *Syntrophothermus lipocalidus* (Sekiguchi et al., 2000) and *Syntrophus aciditrophicus* (Jackson et al., 1999) oxidize butyrate via the β -oxidation pathway (Figure 3). This pathway includes one reaction generating ATP, that partly have to be invested in the conversion of butyrate-CoA to crotonyl-CoA. Longer fatty acids are also degraded through several β -oxidation cycles, where the fatty acids are truncated by two carbons for each cycle. Depending on the carbon chain of the fatty acid, acetyl-CoA (degradation of even-numbered fatty acids) or propanoyl-CoA (degradation of odd-numbered fatty acids) is the end product. Propionate is also major product from glycerol degradation, and most of the described syntrophic propionate degraders utilize the methylmalonyl-CoA (MMC) pathway (Kosaka et al., 2006) (Figure3). In this pathway, one ATP is generated through substrate level phosphorylation generates one ATP, of which a large fraction is invested in the oxidation of succinate to fumarate. Only a few syntrophic propionate oxidizing bacteria been characterized, amongst them *Syntrophobacter wolinii* (Boone & Bryant, 1980) and *Pelotomaculum thermopropionicum* (Kosaka et al., 2006). An alternative route, the dismutation pathway, to butyrate and acetate have been reported for the propionate degrader *Smithella propionica* (de Bok et al., 2001).



Beta-oxidation Methylmalonyl-CoA pathway Wood-Ljungdahl pathway

Figure 3 Metabolic pathways that are used for syntrophic degradation of butyrate and longer chain fatty acids (β -oxidation), propionate (methylmalonyl CoA pathway) and acetate (Wood-Ljungdahl pathway) (Adapted from Worm et al., 2014).

Acetate is the main product of several catabolic conversion process, such as glycolysis, amino acid degradation, and oxidation of butyrate, propionate and longer chain fatty acids as described above. In a well working biogas reactor with an active subculture of acetoclastic archaea, acetate is converted directly to methane through the acetoclastic methanogenesis. Elevated concentrations of free ammonia are toxic for several microorganisms, either as inhibitory to enzyme activity, or directly pernicious to the cell, and acetoclastic methanogens have in particular been shown to be sensitive (Schnürer et al., 1999). A feedstock composed of protein rich material will lead to a release of ammonia from amino acid degradation, while a large fraction of easily degradable carbohydrates will cause a rapid production of VFA. In

such instances, conversion of acetate to methane may occur through a two-step mechanism involving the action of a syntrophic acetate oxidizing bacteria (SAOB) generating CO₂ and hydrogen from acetate, followed by hydrogenotrophic methanogenesis (Figure 4). This syntrophic acetate oxidation (SAO) pathway enables a complete degradation of organic matters to methane even under thermodynamically unfavorable conditions. Investigations have demonstrated that the SAOBs utilizes a reverse (reductive) direction of the Wood Ljungdahl pathway (Hattori et al., 2005; Lee & Zinder, 1988a), or alternatively by combining the methyl branch of the Wood Ljungdahl pathway with a glycine cleavage system (Nobu et al., 2015). Despite the importance the SAO pathway might play in AD processes, very few cultivable representatives from SAOBs have been described. The first acetogen (strain AOR) capable of syntrophic acetate oxidation was isolated from a thermophilic (60 °C) methanogenic environment (Lee & Zinder, 1988b; Zinder & Koch, 1984). This acetogen was unfortunately lost, and it took more than ten years until a new SAOB, *Clostridium ultunense* was isolated (Schnürer et al., 1996). A few additional SAOBs have been isolated and characterized, namely *Thermacetogenium phaeum* (Hattori et al., 2000), *Syntrophacetius schinkii* (Westerholm et al., 2010), *Tepidanaerobacter acetatoxidans* (Westerholm et al., 2011) and *Thermotoga lettinga* (Balk et al., 2002). Additionally, newer molecular technology (e.g. high throughput techniques) have revealed novel SAOBs (Mosbæk et al., 2016; Müller et al., 2016; Nobu et al., 2015).

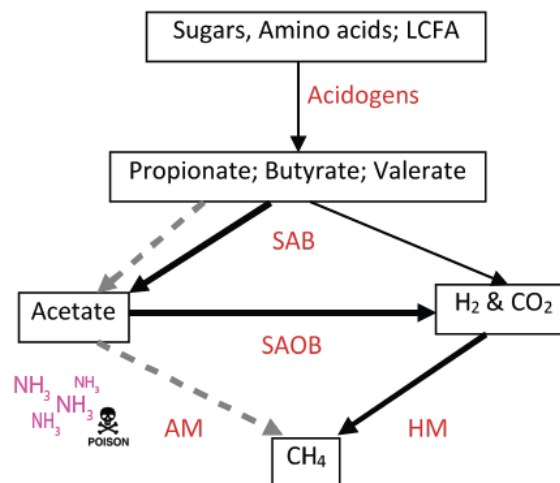


Figure 4. Methane production pathways. Dashed arrows illustrates acetate conversion via acetoclastic methanogenesis. If the acetoclastic methanogenes (AM) are inhibited e.g. free ammonia, acetate oxidation in a two-step conversion (solid black arrow) from syntrophic acetate oxidizing bacteria (SAOB) and hydrogenotrophic methanogenes (HM) becomes crucial.

1.3.1 The study of complex microbial communities

Cultivation have traditionally been the only method to characterize and classify microorganisms, and cultivation-depended methods have given us a valuable insight regarding the key populations in AD processes. Isolation of pure cultures or enrichments of co-cultures of two or more species from AD are still an important and widely applied method for characterization of novel bacteria and archaea. Nevertheless, many of the microbes found in complex microbial communities often have complex metabolic requirements or depend on the presence of other microbial species, such as the syntrophs described above. Moreover, the activity and characteristics of a phylotype might be very different in a monoculture than within a complex community. Cultivating obligate or facultative anaerobic organisms is therefore both challenging and time consuming and likely biased as microbial activity and function are influenced by environmental factors and the presence of other microbes.

During the last decade, development and application of different culture-independent techniques have enabled us to get novel insights about complex microbial communities in environmental samples. The sequencing technology, boosted by the “the human genome project” (Turnbaugh et al., 2007), have developed rapidly and sequencing of whole communities directly from the environment is now frequently documented. High throughput sequencing of conserved marker genes, mostly 16S rRNA genes, have been extensively used during the recent years to uncover the phylogenetic diversity in e.g. AD reactors. This has provided information about microbial communities and their relationship to process conditions and feedstock (e.g. Ziganshin et al., 2013), novel bacterial and archaeal strains (e.g. Hahnke et al., 2014; Westerholm et al., 2011) and given grounds for proposal for a core microbiome for AD (Riviere et al., 2009). It has also become possible to study low abundant microorganisms of the microbial community as the sequencing resolution have increased.

While 16S rRNA data can indicate who is present and in what amount, metagenomics additionally provide information regarding the metabolic potential of the microorganisms. Thus, metagenomics, random sequencing of the entire genomic content in the sample, is a powerful tool for gathering information regarding the genomic diversity and functional complexity. Metagenomic studies have shown the functional traits of the core microbiome, e.g. *Firmicutes*'s

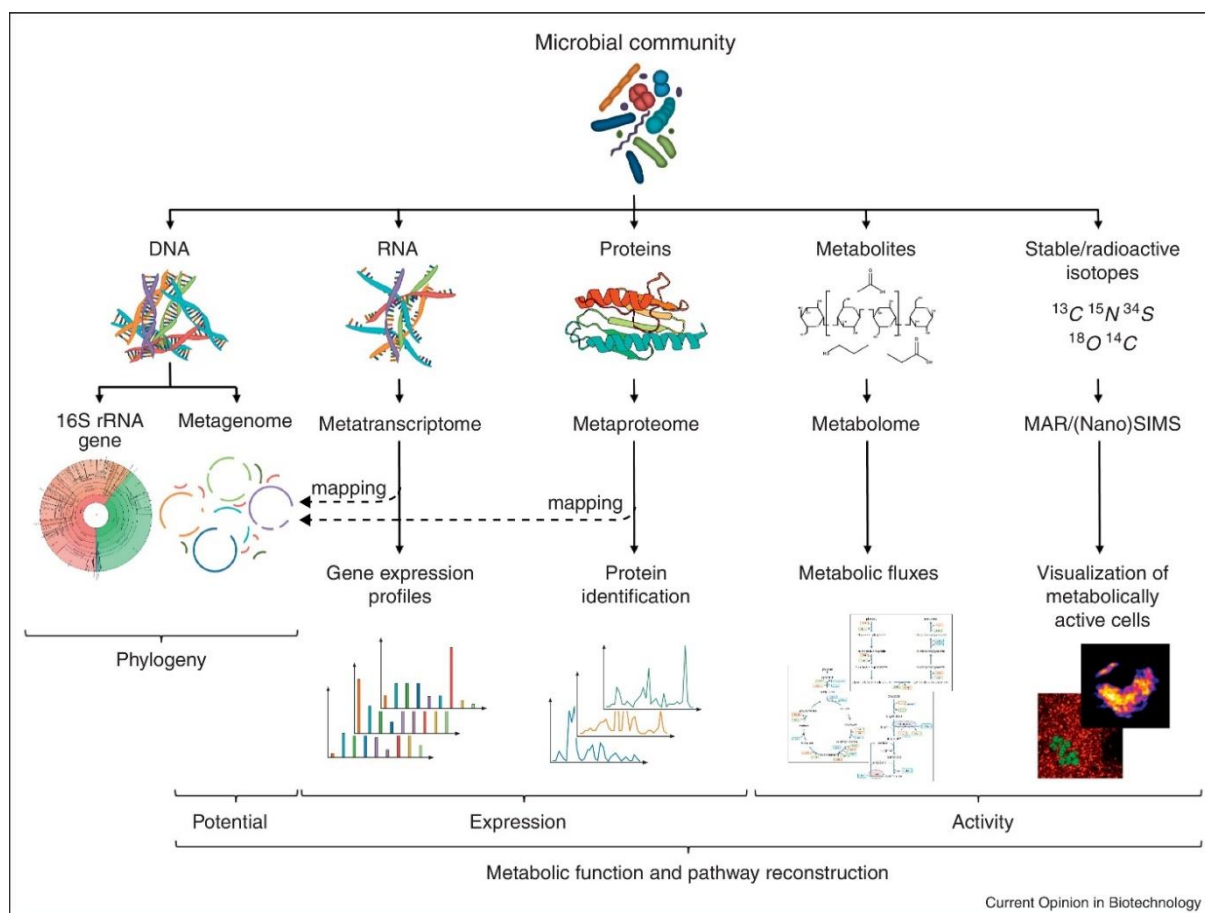


Figure 5. Combination of several molecular, isotope labeling and microscopy methods provides a powerful tool for determining the phylogenetic and functional diversity of a microbial community in e.g. AD. Adapted from (Vanwonterghem et al., 2014).

role in fermentation and ability to break down polysaccharides together with members of *Bacteroidetes*, and characterization of *Clostridia* as the most important class involved in Acetogenesis (Wood-Ljungdahl pathway) (Jaenicke et al., 2011; Solli et al., 2014). Recently, a few studies have also reconstructed draft genomes of uncharacterized, novel bacteria from extensive metagenomics shot gun sequencing (Campanaro et al., 2016; Nobu et al., 2015), giving a opportunity to explored the functional potential of uncultivated microorganisms. Furthermore, by analyzing the transcriptome (Nolla-Ardèvol et al., 2015; Tveit et al., 2014; Zakrzewski et al., 2012), metabolites or proteins expressed (Heyer et al., 2015), we are now also able to get an insight into the activity of a microbial community. Moreover, combination of several meta-omic based techniques makes it possible to characterize the phylogeny of microbial communities, interspecies interactions and synergic relationship, and link this to metabolic function (Hultman et al., 2015; Mosbæk et al., 2016; Nobu et al., 2016; Xia et al.,

2014; Zhou et al., 2014) (Figure 5). This will lead to a deeper understanding of how the microbial community structure influence anaerobic digester efficiency and stability.

2 OUTLINE AND AIM OF THESIS

Characterization of the microbial community structures in anaerobic digesters have demonstrated the presence of complex interspecies food-chains, and identification of key microorganisms have been the prelude to e.g. application of bioaugmentation to successfully increase methane production. However, large variations in the microbial communities have been observed, depending on the substrate, inoculum and process conditions. The development in DNA sequencing technologies and bioinformatics the recent decade, allowing characterization of uncultivated microorganisms, have revolutionized microbial ecology. Biogas digesters are engineered systems intended for waste treatment and energy production. By applying the new tools for microbial community analyses, we should be able to understand the digestion process much better and hopefully increase the stability and enhance the performance of the biogas process. This thesis is a contribution in this regard. The overall aim of the study was **to increase the knowledge base of microbial communities in biogas reactors and relate this to stability and performance of the digestion process**. To achieve this, several different biogas systems was investigated, spanning from unstable laboratory scale biogas reactors to a stable full-scale biogas plant. More specifically the following factors has been evaluated: 1) balance between acidogenesis and methanogenesis in reactors fed with an easy degradable substrate (Paper I), 2) effect of storage conditions on inoculum microbial community and performance (Paper II), 3) Effect of temperature and recirculation on microbial community composition and performance (Paper III), and 4) deep characterization of the microbial community in a stable full-scale biogas plant (Paper IV).

In the first part of this study, described in Paper I, 16S rRNA gene sequencing was applied in a time course study of two initially parallel CSTR reactors fed a co-substrate of cheese whey and cow manure to investigate microbial community dynamics from start-up to stable operation. As a consequence of high organic load of a readily degradable substrate, major process instability was observed in the form of fatty acid accumulation. One of the reactors recovered, while the other collapsed. This gave a unique opportunity to study the dynamics of the microbial community in an AD process apparently operating close to the edge of stability. The biogas performance was correlated to the community structure, demonstrating that accumulation and depletion of fatty acids was related to several bacterial groups.

Paper II describes a systematic storage experiment conducted on inoculum material, used as a biogas starter culture. The aim was to study how the microbial community composition and biomethane potential of an inoculum was affected by different storage conditions. This study led to identification of robust and vulnerable microorganism, and demonstrated a storage-mediated shift in the methanogenic pathway. The results indicated that inoculum may be stored up to 1 month without major loss of methanogenic activity.

In Paper III, the performance and the microbial community in four ADs operating at mesophilic (37 °C) and thermophilic (55°C) conditions with and without digestate recirculation was studied. While the recirculation had significant impact on the mesophilic microbial community, the community profile in the two thermophilic digesters were rather similar. The results showed different impact of ammonia inhibition depending on configuration and temperature, with lowest methane yield in the thermophilic biogas reactor with recirculation.

All three abovementioned papers were based on 16S rRNA gene sequencing technology; the two first were conducted on a 454 pyrosequencing platform, the latter on the Illumina MiSeq platform. In the final study (Paper IV), a deeper characterization utilizing a combination of 16S rRNA gene sequencing, metagenomics and metaproteomics was applied to identify key organisms and metabolic pathways in a stable thermophilic (60°C) commercial biogas reactor. In particular, this data demonstrated a thermophilic uncultured bacterium that seemingly utilizes the β -oxidation to degrade longer chain fatty acids to acetyl-CoA, followed by a further oxidation to CO₂ through the reductive Wood-Ljungdahl pathway. Overall, Paper IV addresses the ecological roles of several uncultured phylotypes reported to be widespread in anaerobic digesters.

3 MAIN RESULTS AND DISCUSSION

3.1 Dynamics in a microbial community undergoing disturbance (paper I)

In the study described in the first paper (Paper I), we got the opportunity to gain insight into the dynamics and changes of a mesophilic microbiota in an AD process responding on organic overload. Two initially parallel CSTR were fed with a mixture of cow manure and cheese whey. Manure was used as a co-substrate to introduce more recalcitrant material and a higher N-content to the feedstock. The initial aim was to examine the biogas potential of co-digesting whey and cow manure, and characterize the dynamics of the microbial community. Thus, samples were collected once a week from both reactors for microbial analysis. During the first half of the experimental period, instability in the reactors was observed, measured as a decrease in biogas production and accumulation of VFAs, mainly propionate, as shown in Figure 1 and 2 (respectively) in Paper I. As discussed in the Introduction of this thesis, accumulation of VFAs is a typical a sign of an unbalance between the acidogenesis and methanogenesis step. One of the two parallel reactors (R1) recovered when the organic loading rate was reduced; the other (R2) did not.

The microbial community was investigated by 16S rRNA gene sequencing of samples taken on weekly basis throughout a period of 100 days. Not surprisingly, the results showed different microbial community dynamics in the two reactors, where in general more variation was observed in the unstable reactor (R2). While the microbial community in R1 underwent a gradual dynamic succession, more fluctuations were seen for the microbial community in R2. Changes within the archaeal community was greater compared to bacteria, presumably explained by the higher sensitivity towards VFA among methanogens than bacteria. As previously introduced, acetoclastic methanogens tends to be more liable to toxicity than hydrogenotrophic methanogens. Accordingly, only a minor fraction of the archaea 16S rRNA gene sequences was assigned to acetoclastic methanogens (i.e. *Methanosarcina*, *Methanosaeta*) in both R1 and R2 after 20 days of operation, whereas hydrogenotrophic methanogens dominated (Figure 4 in Paper I).

Propionate is in general an important intermediate in AD, and in a well-working, balanced AD process with low hydrogen concentration, propionate will be further converted to succinate, fumarate and eventually acetate via the methylmalonyl-CoA (MMC) pathway. While a depletion of propionic acids was observed in the recovered reactor (R1), the

concentration accumulated rapidly in R2 indicating an inhibited or absent propionic acid oxidizing population. As a step to imply the driving forces governing the microbial changes, including the observed fraction of uncultured phylotypes, the correlations between variations of process data and abundance of microorganism was examined (Figure 5 and 6 in Paper I). Interestingly, both the network map and the redundancy analysis (RDA) plot showed significant correlation between the abundance of several bacterial groups and the concentration of propionic acid, among them the phylotype *Candidatus Cloacomonas*. *Candidatus Cloacomonas* belongs to the candidate phyla WWE1, and is widely represented in anaerobic digesters (e.g. Solli et al., 2014; Stolze et al., 2015). At the time when Paper I was published, one study reported that the genome of *Candidatus Cloacomonas acidaminovorans* contained all genes involved in the MMC pathway (Pelletier et al., 2008). A more recent study, published after Paper I, also demonstrated that another uncultivated organism within the same candidate division, referred to as Ca. Cloacimonetes also expressed an MMC pathway (Nobu et al., 2015). This further supports our initial hypothesis that the present phylotype *Candidatus Cloacomonas* was in fact responsible for the propionate depletion in R1. In another recent study, three parallel CSTR reactors were exposed to organic overloading with sugar beet pulp in order to examine the effect of inhibitory VFA accumulation followed by recovery (Goux et al., 2015); while acetate was the major VFA during the period of overloading, propionate constituted the majority of measured VFA in the recovery phase. An increased relative abundance of WWE1-affiliated phylotype was seen in the overload phase, reinforcing our hypothesis of *Candidatus Cloacomonas* involvement in VFA degradation. In comparison to the findings reported in Paper I, these three reactors also showed a dominance of

In an attempt to recover the AD process in both reactors, the OLR was reduced. This did indeed result in a temporal drop of propionate concentration in both reactors. However, when the original feeding regime was resumed, a new accumulation of propionic acid was observed in R2, this time seemingly followed by a subsequent conversion of propionic acid to acetic acid. A temporary increase of acetic acid concentration was also observed in R1, yet to a lesser extent than in R2. Overall, the correlation analysis applied in this study revealed that the variation in VFA concentration (i.e. acetate and propionate) was linked to several groups of organism.

3.2 Effect of storage condition on inoculum microbial community composition and performance (Paper II)

Inoculum, the starter culture of a biogas reactor, provides an active microbial community and its quality is of high importance regarding the startup phase and the long-term stability of a biogas reactor (De Vrieze et al., 2015; Moset et al., 2015). Usually, the inoculum originates from existing AD processes and it is generally recommended to use fresh inoculum for the start-up of a biogas process. However, it is not unusual to store the inoculum material to be used in laboratory-scale reactors for some time. To the best of our knowledge, no standardized guidelines or testing of appropriate storage conditions were available when this study was conducted. Thus, in the goal of Paper II was to investigate how inoculum quality is affected by storage at different temperatures and time.

The storage conditions compared was room temperature (RT), 4 °C and freezing at -20 °C for 1 week, 1, 2, 6 and 11 months, and the effect was tested by initiating AD in batch reactors of cellulose subsequent to storage. The digestion was performed at mesophilic temperature (37 °C) and the experimental period continued for 40 days, although most of the cellulose degradation was completed already after 20 days (Figure 2 in Paper II). The different storage conditions had clear impacts on both the microbial community composition and on the biogas activity of the inoculum. The highest total biogas yields were observed in inocula stored for up to 1 month, indicating that inoculum should not be preserved for longer times. Furthermore, a lower methane yield in the initial phase of digestion with inocula stored at -20 °C showed that the microbial community was recovering slowly after freezing. Overall, the results showed that time of storage in general had greater influence on the microbial community than temperature, although the combination of longer storage times and lower temperatures had the biggest effect. VFA concentrations in all samples (after AD) were very low, indicating that the hydrolysis step might have been rate-limiting in the reactors with low BMP.

Moreover, the relationship between storage conditions and microbial communities and biogas production was evaluated, and one of the objectives was to identify key microorganisms sensitive, or robust, to storing. The microbial analysis showed that members of *Bacteroidetes*, which were abundant in the fresh inoculum sample, decreased with more extreme (longtime storage at cold temperature) storage, and seemingly handled storage poorer than members of

Firmicutes. The *Candidatus* Clacimonas, suggested to be involved in fatty acid (propionate) consumption in Paper I, also seemed to handle storage poorly. So did the hydrogenotrophic methanogens (e.g. genus *Methanocelleus*), which were dominant in the original inoculum. Interestingly, *Candidatus* Clacimonas have also, by others, been suggested to play a crucial role in syntrophic degradation of acetic acid in cooperating with hydrogen consumers (Chouari et al., 2005; Solli et al., 2014). If this is correct, it demonstrates a shift in the degradation route of acetate to methane; from the two-step conversion via syntrophic acetate oxidation, to a direct conversion of acetate to methane by acetoclastic methanogens. The seemingly most robust methanogen was *Methanosarcina*, comprising < 60 % of the total archaeal sequences in samples stored for longer time (Figure 4 and 5 in Paper II).

Studies attempting to assess the impact of sample storage on microbial communities have reported inconsistent results. Soil samples were affected by preservation only to a minor extent (Lauber et al., 2010; Rubin et al., 2013), while considerable changes were observed after storage of soil and fecal samples (Ott et al., 2004; Tzeneva et al., 2009). In contrast to other sample storage experiments, this study also addresses the microbial community after anaerobic degradation, thus investigating the viability and activity of the organisms. The results presented in Paper II clearly showed that extensive preservation of the inoculum lead to changes in the microbial community that correlated to lower biogas production.

3.3 Effect of temperature and recirculation on microbial community composition and performance (paper III)

In the next study, described in Paper III, the effect of temperature and recirculation of digestate was tested on AD of food waste. Food waste has a high solids content and dilution is often needed prior to AD. Since diluting with water is in some areas both costly and limited, the use of recirculated digestate for dilution may be an alternative.

The results clearly indicated that while the mesophilic biogas process was hardly affected by recirculation, the digestate recirculation had a negative impact on the performance in the thermophilic process. The thermophilic CSTR digesters had in general poorer performance than the mesophilic, most likely due to ammonia inhibition as described in the Introduction of this thesis. *Methanosaeta*, which is widely accepted as sensitive to free ammonia, is therefore most common at mesophilic conditions, although both mesophilic and thermophilic species have been characterized (Kato et al., 2014; Kendall & Boone, 2006; Patel & Sprott, 1990). Accordingly, while *Methanosaeta* was the most abundant methanogen in MD (0.8% of the total reads) and MD+R (4%), this genus was below detection level in both thermophilic reactors (TD, TD+R) (Figure 3 and 4 in Paper III). While low VFA concentration in the mesophilic reactors demonstrated an efficient removal of intermediates, both thermophilic reactors experienced an accumulation of VFAs (Figure 2 in Paper III). While organic overloading was the assumed reason for propionate accumulation in the study reported in Paper I, these ADs most likely suffer from ammonia inhibition of the methanogenic population. Notably, while propionate was the most abundant VFA in TD+R, acetate dominated in TD presumably as a result of ammonia-inhibited acetoclastic methanogen population. This suggested that methane was generated from acetate through the previously described two-step SAO pathway. Indeed, a genus (*Thermacetogenium*) which comprises one characterized SAOB (*Thermaceogenium phaeum*) (Hattori et al., 2000) was detected in TD and TD+R, with higher relative abundance in the latter (Figure 4 in Paper III).

The most striking result when comparing the microbial communities in the mesophilic reactors with and without recirculation (MD+R and MD, respectively) was the inconsistency of the most dominant bacteria (Figure 3 in Paper III). While 53% of all 16S rRNA gene sequences in MD were assigned to candidate genus T78 within the phylum *Chloroflexi*, only 5% was assigned to this phylotype in MD+R. On the contrary, 48% was assigned to

Clostridium (phylum *Firmicutes*) in MD+R, while only 1% in MD. Considering the similar performance of the two reactors, it seems likely that they share the same functional niche, assumingly related to carbohydrate degradation as discussed in the paper. In contrast to the mesophilic digesters, the microbial communities in the thermophilic digesters were rather similar, consisting mainly of the phyla *Firmicutes*, *Thermotoga*, *Syntergistetes* and the hydrogenotrophic methanogen *Methanothermobacter* (Figure 4 in Paper III). This could be explained by a lower risk of microbial biomass wash-out in thermophilic digester without recirculation, as higher temperatures generally enhance the microbial growth rate. In conclusion, Paper III demonstrated the recirculation of digestate is a good strategy for diluting food waste feedstock in mesophilic condition, this despite a relatively high level of ammonia.

Moreover, while GS FLX 454 pyrosequencing was utilized to characterize the microbial communities in the two other studies described above (Paper II and Paper III), the current work was conducted on Illumina MiSeq platform. Although 454 pyrosequencing provided longer reads, this sequencing technology is decommissioned in favor of the superior sequencing depth provided by the Illumina platform. Thus, a procedure for Illumina MiSeq sample preparation and bioinformatics-workflow was established for the study described in Paper III. That work provided the basis for other subsequent microbial community analysis conducted in our laboratory.

3.4 Characterization of the microbial community in a stable full-scale biogas plant (paper IV)

In the final paper, a deeper characterization of the microbial community in a biogas reactor located on a commercial waste-treating plant in southern Norway was described. Particularly, this study provides insight to the metabolic roles of scarcely described microbial groups and uncultured phylotypes, amongst them a novel bacteria believed to degrade longer chain fatty acids all the way to CO₂ and H₂.

Even though 16S rRNA gene sequencing provides information on the microorganisms present, the technique is restricted to describing phylogenetic abundance. In order to gain increased knowledge regarding the microbial process, Paper IV presents a study where a combination of several high-throughput technologies were applied. More precise, 16S rRNA gene sequencing and total metagenomics analysis was used to recover genomic bins. This data was then combined with quantitative metaproteomics, allowing us to assign protein abundance values to specific proteins for each genomic bin. The aim of the study was to predict the activity of the microbial groups participating in the AD, and explore synergistic relationship conceivably playing a key role in the process stability. While the other papers formerly described in this thesis involves digestion processes in laboratory-scale CSTR reactors (paper I and III) or batch reactors (paper II), this study was conducted on a commercial full-scale reactor operating under thermophilic conditions. AD of waste and crops at thermophilic conditions are commonly applied in Europe, although mesophilic reactors are dominating. Running thermophilic processes have, as mentioned in the Introduction, several advantages over mesophilic processes, e.g. enhanced hydrolysis of particulate matter and increased degradation efficiency, higher total biogas produced and reduction of pathogens (Bolzonella et al., 2012; Leven et al., 2007; Zabranska et al., 2000). The reactor studied in paper IV was operating at 60 °C. This temperature is higher than usually reported for thermophilic biogas reactors at commercial plants, although a few attempts on equivalent temperatures have been tested in pilot scale reactors previously with varying degree of success (Hartmann & Ahring, 2005b; Ho et al., 2014). A relatively high level of free ammonia (367 mg NH₃-N/L) was observed in the reactor, probably as an effect of the high temperature and proteinaceous feedstock (mainly food waste).

During the last years, a number of studies based on combinations of functional and phylogenetic analysis describing the microbial community and the general flow of carbon in an AD have been published (e.g. Campanaro et al., 2016; Nobu et al., 2015). Only a few studies based on combination of metagenomics and metaproteomics was reported prior the planning stage and execution of the study described in Paper IV (Hultman et al., 2015; Lauro et al., 2011; Ng et al., 2010; Zhou et al., 2014). Although only lightly touched upon in the paper, the establishment of the methods used to analyze the microbial community was a large part of this study. Accordingly, a newly established strategy combining Illumina and Pacific Biosciences (PacBio) long and high accuracy circular consensus sequencing (CCS) reads was applied, to improve the assembly and taxonomic binning (Frank et al., 2016). Illumina MiSeq (300 bp) was chosen over Illumina HiSeq (to date maximum 150 bp) for longer reads, yet sacrificing sequencing depth compared to HiSeq. Two approaches for assembly of the generated MiSeq and PacBio sequencing reads were tested, one where the reads from each sequencing technology were assembled into contigs separately, followed by second assembly of the contigs from both sets. The other strategy applied an assembler (MiRA version 4.0) that allowed for assembly of raw reads from different platforms. The outcome showed that the latter alternative yielded increased contig length and this method was therefore chosen for downstream analysis. One major challenge was the assembly of the dominant bacteria in the community. The addition of PacBio reads significantly improved the assembly, compared to the initial attempts using the MiSeq dataset only. Nevertheless, an enlarged number of contigs making up the genomic bins for the most dominant bacteria, especially *C. proteolyticus*, was observed. This resulted in a genomic bin size that exceeded the expected genome size by more than tenfold. This was most likely due to multiple strains, and oligotyping (Eren et al., 2011) confirmed the presence of up to 11 polymorphs within the genomic bin of *C. proteolyticus*. Thus, this introduces an additional level of complexity seldom reported in biogas reactors.

The most dominant bacteria genus *Coprothermobacter*, comprised 76 % of all 16S rRNA gene sequences in the amplicon dataset. *C. proteolyticus* is recognized as an indicator of a well-working processes, and successful attempts of using this bacterium for bioaugmentation have been reported (Lü et al., 2014). Moreover, an enhanced degradation of proteins was seen when grown in co-culture with the hydrogenotrophic methanogen *Methanothermobacter thermoautotrophicus* (Sasaki et al., 2011). *M. thermoautotrophicus* was indeed the most dominating methanogen in the biogas plant, but the overall relative abundance of

methanogens was very low (<0.1 % of the total 16S rRNA reads) (Figure 1 in Paper IV). Nevertheless, as discussed in the paper, in contrast to the low phylogenetic abundance, a relatively high abundance of proteins affiliated to the hydrogenotrophic methanogenesis was detected. Albeit lower protein abundance, proteins affiliated to the obligate acetoclastic methanogen *Methanosaeta thermophila* (reference genome according to supplementary table S1 in Paper IV) was also detected, indicating metabolic activity of a *Methanosaeta*-phylogroup acclimatized to elevated ammonia levels (Figure 2 in Paper IV).

Importantly, the paper describes the functional reconstruction of a novel bacterium (called unFirm02_FrBGR in paper IV) that apparently have the enzymatic machinery to degrade longer-chain fatty acids by a β -oxidation pathway to acetyl-CoA or acetate, then further converting the acetyl-CoA to CO₂ and H₂ via the reductive Wood-Ljungdahl pathway (Figure 3 in Paper IV). This combination of pathways is documented for non-syntrophic sulphate reducers, but to the best of our knowledge not for the characterized SAOBs. No genes for sulphate reduction was found in the genomic annotation of unFirm02_FrBGR, indicating that this bacteria was not a sulphate reducer. unFirm02_FrBGR also expressed Fe-S oxidoreductase and a subsequent electron transfer flavoprotein (α - and β - subunits) previously shown to serve as a reverse electron transfer in syntrophic fatty acid oxidizing bacteria (e.g. *S. wolfei* (Sieber et al., 2010), giving more supporting our assumptions of a syntrophic lifestyle. However, cultivation based effort is needed to completely validate the proposed metabolic traits of unFirm02_FrBGR. While the work of Paper IV was ongoing, a few other studies were published, indicating that the occurrence of unknown SAOB is widespread across anaerobic digesters. Thus, the result from this thesis, and those reported by (Mosbæk et al., 2016) and (Müller et al., 2016), provides evidence of the importance of this poorly understood microbial group in anaerobic digesters operating at elevated levels of free ammonia.

4 CONCLUDING REMARKS

During the work presented in this thesis, several different biogas reactors have been studied; two mesophilic CTSR reactors run at the same conditions (Paper I), batch reactors for BMP tests (Paper II), four CSTR reactors run at different temperatures and with or without recirculation, (Paper III) and one large-scale industrial thermophilic biogas reactor (Paper IV). The primary objectives of this work was to study microbial communities in relation to process conditions, performance and stability.

A congruent observation in all systems investigated was the expected correlation between less efficient reactors and high levels of VFAs. The imbalance between the fermenting bacteria and the methanogens, leading to accumulation of VFAs, in particular propionate and acetate, was presumably the reason for the reduced performance of the AD described in both Paper I and Paper III. This underpins the importance of a well-balanced microbial community with an active syntrophic population degrading fermentation intermediates, to ensure stable and efficient biogas production. Interestingly, findings from both Paper I and the mesophilic reactors in Paper III indicates that *Candidatus Cloacimonas* is serving as a syntrophic propionate oxidizer, playing a crucial role in AD to keep the level of propionate down. *Candidatus Cloacimonas* was also abundant in the microbial community studied in paper II, and seemed to handle storage poorly. The higher methane yield in the mesophilic contra the thermophilic lab scale reactors was also in accordance with the literature, as mesophilic reactors often have a more resilient microbial community, that is more robust to withstand environmental changes and stresses. This was demonstrated by a general higher microbial diversity in the mesophilic ADs. The elevated levels of free ammonia, observed in both thermophilic CSTRs and the mesophilic CSTR with recirculation (Paper III), and in the commercial thermophilic reactor (Paper IV) was not necessary related to poor anaerobic digester performance, thus indicating that a microbial population may acclimatize to ammonia stress. Prevalence of uncultured and scarcely described microorganisms was significant in all the AD systems described in this thesis, emphasizing the need for more investigations to grasp a more complete picture of the microbial community. For instance, the uncultured candidate bacterium *Atribacteria* (OP9) was found in several of the studies included in this thesis. Paper IV also indicates the findings of a novel SAOB. This bacterium was anticipated, from comparison of metagenomics and metaproteomics data, to syntrophically oxidize longer chain fatty acids via acetate to CO₂ and H₂.

As discussed in the Introduction of this thesis, syntrophic oxidation of acetate and longer chain fatty acids are thought to play an essential role in biogas reactors, especially under circumstances where the acetoclastic methanogens are inhibited or absent. Instability have major negative impact for commercial biogas plant, and increased understanding of the underlying microbial cause/response might help preventing process failures. More research is needed to grasp a complete picture, but the findings in the studies described in this thesis contributed to get a glimpse of the microbial community in relation to stability and performance of the anaerobic digestion process.

5 APPLICATION AND FUTURE PERSPECTIVES

AD of biomass offers a considerable potential for generation of sustainable energy and fuel, and could replace large fractions of the energy currently supplied by fossil fuels. The goals for biobased energy production in Europe is ambitious; by 2020 the EU goal is to supply 20% of its energy needs from renewable sources, of which 10% should in the transport sector. A strategy for European bioeconomy ('Innovation for sustainable growth: a bioeconomy for Europe's) was launched by the European commission in 2012, aiming to support research and innovation to develop biorefining technologies, and reduce the dependency on fossil fuels. In this transition from a fossil-based economy to a more sustainable bioeconomy, biogas production clearly has a natural and important role. Although the biogas process parameters of an AD are well described, the influence of the underlying microbial community on process stability and biogas yield is less understood. A deeper insight into the microbial community in biogas reactors might lead to increased knowledge of how to establish stable and efficient biogas production. The observations during this work emphasized that the microbial community structure is an important element in AD processes.

Currently, the concentration of VFAs is often used as an indicator of reactor disturbance, but often at a stage when it too late to save the process. With the rapidly improving and faster high-throughput sequencing technologies, it could also be possible to use a diagnostic approach to monitor the microbial community and identify lack of key microorganisms before the instability is fatal. Culture-independent techniques is a powerful tool to study the microbiome of environmental samples, and such data may be used to monitor the health of an AD process and for process control. Bioaugmentation, where specific microorganisms are added to the system have been shown as a promising solution to improve the performance, although several obstacles must be overcome. From the industrial point of view, the addition of SAOBs to save an ammonia-stressed microbial population in AD fed protein-rich material could be a way to increase the energy yield, or prevent costly process failures. Importantly, identification of key microbial "populations" is essential order to select good candidate for bioaugmentation, e.g. *Candidatus Cloacomoans* for propionate degradation, as well as potential SAOBs detected by modern culture independent techniques referred to throughout this thesis.

A clear trend the recent years have been to integrate biogas production in biorefineries, where waste from side streams in the refinery serves as the feedstock for the AD. This will be particularly important in the future, as the volume of the side streams increases with the rapidly increasing number of biorefineries. Examples of biorefineries are traditional pulp and paper mills, 1st generation bioethanol from sugarcane and corn, and recently the commercialization of cellulosic bioethanol. Lignocellulose biomass is suitable as substrate in biorefineries as this biomass does not compete with food or feed industry. Bioethanol production will always result in organic residues, and in a true circular biorefinery, this residue is used as feedstock for biogas production. The biogas produced can be utilized *on site* to run produce heat and power for the facility, or the biogas could be upgraded to biomethane, which can enter existing natural gas grid or used as a fuel. The biorefinery circle process can be completed by returning the effluent from the biogas process back to agricultural soil.

In addition to the natural role biogas can play in a biorefinery, biogas can also play a role in the context of the overall renewable energy sector, including renewables such as solar, wind, hydrothermal and geothermal. Since energy supply from e.g. solar and wind is intermittent, there is a demand for flexible technologies that can supply the energy grid when it is dark or when the wind is not blowing. One relatively novel idea is to combine flexible biogas production (and power generation) with other renewable energy sources in order to balance energy availability. Flexible biogas production can in principle be achievable by regulating the feeding regime to match the variation in the intermittent energy production, and a few recent studies on this is found in the literature (Hahn et al., 2014; Mauky et al., 2015). The study on the effect of inoculum storage (Paper II) contributes in this regard, and suggest that feeding of substrate once a month is sufficient to maintain a highly active biogas microbial community. However, to ensure stability and efficiency during ramping up and “dormant” biogas production, aspects around the feedstock selection (substrate), the microbial community and the operating parameters needs to be investigated in more details.

References

- Ahring, B.K., Sandberg, M., Angelidaki, I. 1995. Volatile fatty acids as indicators of process imbalance in anaerobic digestors. *Applied Microbiology and Biotechnology*, **43**(3), 559-565.
- Akuzawa, M., Hori, T., Haruta, S., Ueno, Y., Ishii, M., Igarashi, Y. 2011. Distinctive responses of metabolically active microbiota to acidification in a thermophilic anaerobic digester. *Microbial ecology*, **61**(3), 595-605.
- Angelidaki, I., Ahring, B. 1994. Anaerobic thermophilic digestion of manure at different ammonia loads: effect of temperature. *Water Research*, **28**(3), 727-731.
- Angelidaki, I., Ahring, B.K. 1993. Thermophilic anaerobic digestion of livestock waste: the effect of ammonia. *Applied Microbiology and Biotechnology*, **38**(4), 560-564.
- Angelidaki, I., Ellegaard, L., Ahring, B.K. 1999. A comprehensive model of anaerobic bioconversion of complex substrates to biogas. *Biotechnology and Bioengineering*, **63**(3), 363-372.
- Angelidaki, I., Karakashev, D., Batstone, D.J., Plugge, C.M., Stams, A.J.M. 2011. Biomethanation and its potential. in: *Methods in Enzymology: Methods in Methane Metabolism, Pt A*, (Eds.) A.C. Rosenzweig, S.W. Ragsdale, Vol. 494, pp. 327-351.
- Aspé, E., Martí, M., Jara, A., Roeckel, M. 2001. Ammonia inhibition in the anaerobic treatment of fishery effluents. *Water environment research*, 154-164.
- Astals, S., Nolla-Ardèvol, V., Mata-Alvarez, J. 2012. Anaerobic co-digestion of pig manure and crude glycerol at mesophilic conditions: Biogas and digestate. *Bioresource Technology*, **110**, 63-70.
- Bagge, E., Sahlström, L., Albihn, A. 2005. The effect of hygienic treatment on the microbial flora of biowaste at biogas plants. *Water research*, **39**(20), 4879-4886.
- Balk, M., Weijma, J., Stams, A.J. 2002. *Thermotoga lettingae* sp. nov., a novel thermophilic, methanol-degrading bacterium isolated from a thermophilic anaerobic reactor. *International Journal of Systematic and Evolutionary Microbiology*, **52**(4), 1361-1368.
- Barredo, M., Evison, L. 1991. Effect of propionate toxicity on methanogen-enriched sludge, *Methanobrevibacter smithii*, and *Methanospirillum hungatii* at different pH values. *Applied and environmental microbiology*, **57**(6), 1764-1769.
- Blonskaja, V., Menert, A., Vilu, R. 2003. Use of two-stage anaerobic treatment for distillery waste. *Advances in Environmental Research*, **7**(3), 671-678.
- Bolzonella, D., Cavinato, C., Fatone, F., Pavan, P., Cecchi, F. 2012. High rate mesophilic, thermophilic, and temperature phased anaerobic digestion of waste activated sludge: A pilot scale study. *Waste management*, **32**(6), 1196-1201.
- Boone, D.R., Bryant, M.P. 1980. Propionate-degrading bacterium, *Syntrophobacter wolinii* sp. nov. gen. nov., from methanogenic ecosystems. *Applied and Environmental Microbiology*, **40**(3), 626-632.
- Boone, D.R., Xun, L. 1987. Effects of pH, temperature, and nutrients on propionate degradation by a methanogenic enrichment culture. *Applied and Environmental Microbiology*, **53**(7), 1589-1592.
- Campanaro, S., Treu, L., Kougias, P.G., Francisci, D., Valle, G., Angelidaki, I. 2016. Metagenomic analysis and functional characterization of the biogas microbiome using high throughput shotgun sequencing and a novel binning strategy. *Biotechnology for biofuels*, **9**(1), 1.

- Chouari, R., Le Paslier, D., Dauga, C., Daegelen, P., Weissenbach, J., Sghir, A. 2005. Novel major bacterial candidate division within a municipal anaerobic sludge digester. *Applied and environmental microbiology*, **71**(4), 2145-2153.
- Cortes-Totalpa, L., Jiménez, D.J., Brossi, M.J., Salles, J.F., van Elsas, J.D. 2016. Different inocula produce distinctive microbial consortia with similar lignocellulose degradation capacity. *Applied microbiology and biotechnology*, 1-13.
- de Bok, F.A., Stams, A.J., Dijkema, C., Boone, D.R. 2001. Pathway of Propionate Oxidation by a Syntrophic Culture of *Smithella propionica* and *Methanospirillum hungatei*. *Applied and environmental microbiology*, **67**(4), 1800-1804.
- De Vrieze, J., Gildemyn, S., Vilchez-Vargas, R., Jáuregui, R., Pieper, D.H., Verstraete, W., Boon, N. 2015. Inoculum selection is crucial to ensure operational stability in anaerobic digestion. *Applied microbiology and biotechnology*, **99**(1), 189-199.
- Diaz, J.P., Reyes, I.P., Lundin, M., Horvath, I.S. 2011. Co-digestion of different waste mixtures from agro-industrial activities: Kinetic evaluation and synergetic effects. *Bioresource Technology*, **102**(23), 10834-10840.
- ENOVA. <http://www.enova.no>
- EurObserv`ER(2014). *Biogas barometer*
- European Biogas Association (2016) EBA annual Report for 2015
- Eren, A.M., Zozaya, M., Taylor, C.M., Dowd, S.E., Martin, D.H., Ferris, M.J. 2011. Exploring the diversity of *Gardnerella vaginalis* in the genitourinary tract microbiota of monogamous couples through subtle nucleotide variation. *PloS one*, **6**(10), e26732.
- Fotidis, I.A., Karakashev, D., Kotsopoulos, T.A., Martzopoulos, G.G., Angelidaki, I. 2013. Effect of ammonium and acetate on methanogenic pathway and methanogenic community composition. *FEMS microbiology ecology*, **83**(1), 38-48.
- Frank, J.A., Pan, Y., Tooming-Klunderud, A., Eijnsink, V.G., McHardy, A.C., Nederbragt, A.J., Pope, P.B. 2016. Improved metagenome assemblies and taxonomic binning using long-read circular consensus sequence data. *Scientific reports.*, **6**. doi: 10.1038/srep25373
- Gallert, C., Winter, J. 1997. Mesophilic and thermophilic anaerobic digestion of source-sorted organic wastes: effect of ammonia on glucose degradation and methane production. *Applied Microbiology and Biotechnology*, **48**(3), 405-410.
- Gebauer, R. 2004. Mesophilic anaerobic treatment of sludge from saline fish farm effluents with biogas production. *Bioresource Technology*, **93**(2), 155-167.
- Goux, X., Calusinska, M., Lemaigre, S., Marynowska, M., Klocke, M., Udelhoven, T., Benizri, E., Delfosse, P. 2015. Microbial community dynamics in replicate anaerobic digesters exposed sequentially to increasing organic loading rate, acidosis, and process recovery. *Biotechnology for biofuels*, **8**(1), 1.
- Gujer, W., Zehnder, A.J.B. 1983. Conversion processes in anaerobic digestion. *Water Science & Technology*, **15**(8-9), 127-167.
- Hahn, H., Krautkremer, B., Hartmann, K., Wachendorf, M. 2014. Review of concepts for a demand-driven biogas supply for flexible power generation. *Renewable and Sustainable Energy Reviews*, **29**, 383-393.
- Hahnke, S., Striesow, J., Elvert, M., Mollar, X.P., Klocke, M. 2014. *Clostridium bornimense* sp. nov., isolated from a mesophilic, two-phase, laboratory-scale biogas reactor. *International journal of systematic and evolutionary microbiology*, **64**(Pt 8), 2792-2797.

- Hartmann, H., Ahring, B.K. 2005a. Anaerobic digestion of the organic fraction of municipal solid waste: Influence of co-digestion with manure. *Water Research*, **39**(8), 1543-1552.
- Hartmann, H., Ahring, B.K. 2005b. A novel process configuration for anaerobic digestion of source-sorted household waste using hyper-thermophilic post-treatment. *Biotechnology and bioengineering*, **90**(7), 830-837.
- Hattori, S., Galushko, A.S., Kamagata, Y., Schink, B. 2005. Operation of the CO dehydrogenase/acetyl coenzyme A pathway in both acetate oxidation and acetate formation by the syntrophically acetate-oxidizing bacterium *Thermacetogenium phaeum*. *Journal of bacteriology*, **187**(10), 3471-3476.
- Hattori, S., Kamagata, Y., Hanada, S., Shoun, H. 2000. *Thermacetogenium phaeum* gen. nov., sp. nov., a strictly anaerobic, thermophilic, syntrophic acetate-oxidizing bacterium. *International Journal of Systematic and Evolutionary Microbiology*, **50**(4), 1601-1609.
- Heyer, R., Kohrs, F., Reichl, U., Benndorf, D. 2015. Metaproteomics of complex microbial communities in biogas plants. *Microbial biotechnology*. doi: 10.1111/1751-7915.12276.
- Hills, D.J. 1979. Effects of carbon: nitrogen ratio on anaerobic digestion of dairy manure. *Agricultural wastes*, **1**(4), 267-278.
- Ho, D., Jensen, P., Batstone, D. 2014. Effects of temperature and hydraulic retention time on acetotrophic pathways and performance in high-rate sludge digestion. *Environmental science & technology*, **48**(11), 6468-6476.
- Holm-Nielsen, J.B., Al Seadi, T., Oleskowicz-Popiel, P. 2009. The future of anaerobic digestion and biogas utilization. *Bioresource technology*, **100**(22), 5478-5484.
- Hultman, J., Waldrop, M.P., Mackelprang, R., David, M.M., McFarland, J., Blazewicz, S.J., Harden, J., Turetsky, M.R., McGuire, A.D., Shah, M.B. 2015. Multi-omics of permafrost, active layer and thermokarst bog soil microbiomes. *Nature*, **521**(7551), 208-212.
- Jackson, B.E., Bhupathiraju, V.K., Tanner, R.S., Woese, C.R., McInerney, M.J. 1999. *Syntrophus aciditrophicus* sp. nov., a new anaerobic bacterium that degrades fatty acids and benzoate in syntrophic association with hydrogen-using microorganisms. *Archives of Microbiology*, **171**(2), 107-114.
- Jaenicke, S., Ander, C., Bekel, T., Bisdorf, R., Dröge, M., Gartemann, K.-H., Jünemann, S., Kaiser, O., Krause, L., Tille, F. 2011. Comparative and joint analysis of two metagenomic datasets from a biogas fermenter obtained by 454-pyrosequencing. *PLoS One*, **6**(1), e14519.
- Karakashev, D., Batstone, D.J., Angelidaki, I. 2005. Influence of environmental conditions on methanogenic compositions in anaerobic biogas reactors. *Applied and Environmental Microbiology*, **71**(1), 331-338.
- Kato, S., Sasaki, K., Watanabe, K., Yumoto, I., Kamagata, Y. 2014. Physiological and transcriptomic analyses of the thermophilic, acetoclastic methanogen *Methanosaeta thermophila* responding to ammonia stress. *Microbes and Environments*, **29**(2), 162-167.
- Kendall, M.M., Boone, D.R. 2006. The order methanosarcinales. in: *The prokaryotes*, Springer, pp. 244-256.
- Kosaka, T., Uchiyama, T., Ishii, S.-i., Enoki, M., Imachi, H., Kamagata, Y., Ohashi, A., Harada, H., Ikenaga, H., Watanabe, K. 2006. Reconstruction and regulation of the central catabolic pathway in the thermophilic propionate-oxidizing syntroph *Pelotomaculum thermopropionicum*. *Journal of bacteriology*, **188**(1), 202-210.

- Koster, I.W., Cramer, A. 1987. Inhibition of methanogenesis from acetate in granular sludge by long-chain fatty acids. *Applied and environmental microbiology*, **53**(2), 403-409.
- Lauber, C.L., Zhou, N., Gordon, J.I., Knight, R., Fierer, N. 2010. Effect of storage conditions on the assessment of bacterial community structure in soil and human-associated samples. *FEMS microbiology letters*, **307**(1), 80-86.
- Lauro, F.M., DeMaere, M.Z., Yau, S., Brown, M.V., Ng, C., Wilkins, D., Raftery, M.J., Gibson, J.A., Andrews-Pfannkoch, C., Lewis, M. 2011. An integrative study of a meromictic lake ecosystem in Antarctica. *The ISME journal*, **5**(5), 879-895.
- Lee, M.J., Zinder, S.H. 1988a. Carbon monoxide pathway enzyme activities in a thermophilic anaerobic bacterium grown acetogenically and in a syntrophic acetate-oxidizing coculture. *Archives of microbiology*, **150**(6), 513-518.
- Lee, M.J., Zinder, S.H. 1988b. Isolation and characterization of a thermophilic bacterium which oxidizes acetate in syntrophic association with a methanogen and which grows acetogenically on H₂-CO₂. *Applied and environmental microbiology*, **54**(1), 124-129.
- Leven, L., Eriksson, A.R.B., Schnurer, A. 2007. Effect of process temperature on bacterial and archaeal communities in two methanogenic bioreactors treating organic household waste. *Fems Microbiology Ecology*, **59**(3), 683-693.
- Liu, D.W., Liu, D.P., Zeng, R.J., Angelidaki, I. 2006. Hydrogen and methane production from household solid waste in the two-stage fermentation process. *Water Research*, **40**(11), 2230-2236.
- Lv, W., Schanbacher, F.L., Yu, Z. 2010. Putting microbes to work in sequence: recent advances in temperature-phased anaerobic digestion processes. *Bioresource technology*, **101**(24), 9409-9414.
- Lü, F., Li, T., Wang, T., Shao, L., He, P. 2014. Improvement of sludge digestate biodegradability by thermophilic bioaugmentation. *Applied microbiology and biotechnology*, **98**(2), 969-977.
- Massé, D.I., Talbot, G., Gilbert, Y. 2011. On farm biogas production: A method to reduce GHG emissions and develop more sustainable livestock operations. *Animal Feed Science and Technology*, **166**, 436-445.
- Mata-Alvarez, J., Dosta, J., Mace, S., Astals, S. 2011. Codigestion of solid wastes: A review of its uses and perspectives including modeling. *Critical Reviews in Biotechnology*, **31**(2), 99-111.
- Mauky, E., Jacobi, H.F., Liebetrau, J., Nelles, M. 2015. Flexible biogas production for demand-driven energy supply—Feeding strategies and types of substrates. *Bioresource technology*, **178**, 262-269.
- McInerney, M.J., Bryant, M.P., Hespell, R.B., Costerton, J.W. 1981. *Syntrophomonas wolfei* gen. nov. sp. nov., an anaerobic, syntrophic, fatty acid-oxidizing bacterium. *Applied and Environmental Microbiology*, **41**(4), 1029-1039.
- McInerney, M.J., Struchtemeyer, C.G., Sieber, J., Mouttaki, H., Stams, A.J.M., Schink, B., Rohlin, L., Gunsalus, R.P. 2008. Physiology, ecology, phylogeny, and genomics of microorganisms capable of syntrophic metabolism. in: *Incredible Anaerobes: From Physiology to Genomics to Fuels*, (Eds.) J. Wiegand, R.J. Maier, M.W.W. Adams, Vol. 1125, Blackwell Publishing. Oxford, pp. 58-72.
- Mosbæk, F., Kjeldal, H., Mulat, D.G., Albertsen, M., Ward, A.J., Feilberg, A., Nielsen, J.L. 2016. Identification of syntrophic acetate-oxidizing bacteria in anaerobic digesters by combined protein-based stable isotope probing and metagenomics. *The ISME Journal*. doi:10.1038/ismej.2016.39

- Moset, V., Al-zohairi, N., Møller, H.B. 2015. The impact of inoculum source, inoculum to substrate ratio and sample preservation on methane potential from different substrates. *Biomass and Bioenergy*, **83**, 474-482.
- Müller, B., Sun, L., Westerholm, M., Schnürer, A. 2016. Bacterial community composition and fhs profiles of low-and high-ammonia biogas digesters reveal novel syntrophic acetate-oxidising bacteria. *Biotechnology for biofuels*, **9**(1), 1.
- Möller, K., Müller, T. 2012. Effects of anaerobic digestion on digestate nutrient availability and crop growth: a review. *Engineering in Life Sciences*, **12**(3), 242-257.
- Ng, C., DeMaere, M.Z., Williams, T.J., Lauro, F.M., Raftery, M., Gibson, J.A.E., Andrews-Pfannkoch, C., Lewis, M., Hoffman, J.M., Thomas, T. 2010. Metaproteogenomic analysis of a dominant green sulfur bacterium from Ace Lake, Antarctica. *The ISME journal*, **4**(8), 1002-1019.
- Nielsen, H.B., Uellendahl, H., Ahring, B.K. 2007. Regulation and optimization of the biogas process: propionate as a key parameter. *Biomass and Bioenergy*, **31**(11), 820-830.
- Nobu, M.K., Dodsworth, J.A., Murugapiran, S.K., Rinke, C., Gies, E.A., Webster, G., Schwientek, P., Kille, P., Parkes, R.J., Sass, H. 2016. Phylogeny and physiology of candidate phylum 'Atribacteria' (OP9/JS1) inferred from cultivation-independent genomics. *The ISME journal*, **10**(2), 273-286.
- Nobu, M.K., Narihiro, T., Rinke, C., Kamagata, Y., Tringe, S.G., Woyke, T., Liu, W.-T. 2015. Microbial dark matter ecogenomics reveals complex synergistic networks in a methanogenic bioreactor. *The ISME journal*, **9**(8), 1710-1722.
- Nolla-Ardèvol, V., Strous, M., Tegetmeyer, H.E. 2015. Anaerobic digestion of the microalga *Spirulina* at extreme alkaline conditions: biogas production, metagenome, and metatranscriptome. *Frontiers in microbiology*, **6**. doi: 10.3389/fmicb.2015.00597
- Ott, S.J., Musfeldt, M., Timmis, K.N., Hampe, J., Wenderoth, D.F., Schreiber, S. 2004. *In vitro* alterations of intestinal bacterial microbiota in fecal samples during storage. *Diagnostic microbiology and infectious disease*, **50**(4), 237-245.
- Panichnumsin, P., Nopharatana, A., Ahring, B., Chaiprasert, P. 2010. Production of methane by co-digestion of cassava pulp with various concentrations of pig manure. *Biomass and Bioenergy*, **34**(8), 1117-1124.
- Patel, G.B., Sprott, G.D. 1990. *Methanosaeta concilii* gen. nov., sp. nov. ("Methanothrix concilii") and *Methanosaeta thermoacetophila* nom. rev., comb. nov. *International journal of systematic bacteriology*, **40**(1), 79-82.
- Pelletier, E., Kreimeyer, A., Bocs, S., Rouy, Z., Gyapay, G., Chouari, R., Rivière, D., Ganesan, A., Daegelen, P., Sghir, A. 2008. "Candidatus Cloacamonas acidaminovorans": genome sequence reconstruction provides a first glimpse of a new bacterial division. *Journal of bacteriology*, **190**(7), 2572-2579.
- Risberg, K., Sun, L., Levén, L., Horn, S.J., Schnürer, A. 2013. Biogas production from wheat straw and manure—impact of pretreatment and process operating parameters. *Bioresource technology*, **149**, 232-237.
- Riviere, D., Desvignes, V., Pelletier, E., Chaussonnerie, S., Guermazi, S., Weissenbach, J., Li, T., Camacho, P., Sghir, A. 2009. Towards the definition of a core of microorganisms involved in anaerobic digestion of sludge. *The ISME Journal*, **3**(6), 700-714.
- Rubin, B.E., Gibbons, S.M., Kennedy, S., Hampton-Marcell, J., Owens, S., Gilbert, J.A. 2013. Investigating the impact of storage conditions on microbial community composition in soil samples. *PloS one*, **8**(7), e70460.

- Sahlström, L. 2003. A review of survival of pathogenic bacteria in organic waste used in biogas plants. *Bioresource technology*, **87**(2), 161-166.
- Sanchez, E., Borja, R., Weiland, P., Travieso, L., Martin, A. 2000. Effect of temperature and pH on the kinetics of methane production, organic nitrogen and phosphorus removal in the batch anaerobic digestion process of cattle manure. *Bioprocess Engineering*, **22**(3), 247-252.
- Sasaki, K., Morita, M., Sasaki, D., Nagaoka, J., Matsumoto, N., Ohmura, N., Shinozaki, H. 2011. Syntrophic degradation of proteinaceous materials by the thermophilic strains *Coprothermobacter proteolyticus* and *Methanothermobacter thermautotrophicus*. *Journal of Bioscience and Bioengineering*, **112**(5), 469-472.
- Schink, B. 1997. Energetics of syntrophic cooperation in methanogenic degradation. *Microbiology and Molecular Biology Reviews*, **61**(2), 262-280.
- Schmit, K.H., Ellis, T.G. 2001. Comparison of temperature-phased and two-phase anaerobic co-digestion of primary sludge and municipal solid waste. *Water Environment Research*, **73**(3), 314-321.
- Schnürer, A., Jarvis, Å. 2009. Microbiological Handbook for Biogas Plants.
- Schnürer, A., Schink, B., Svensson, B.H. 1996. *Clostridium ultunense* sp. nov., a mesophilic bacterium oxidizing acetate in syntrophic association with a hydrogenotrophic methanogenic bacterium. *International journal of systematic bacteriology*, **46**(4), 1145-1152.
- Schnürer, A., Zellner, G., Svensson, B.H. 1999. Mesophilic syntrophic acetate oxidation during methane formation in biogas reactors. *Fems Microbiology Ecology*, **29**(3), 249-261.
- Sekiguchi, Y., Kamagata, Y., Nakamura, K., Ohashi, A., Harada, H. 2000. *Syntrophothermus lipocalidus* gen. nov., sp. nov., a novel thermophilic, syntrophic, fatty-acid-oxidizing anaerobe which utilizes isobutyrate. *International Journal of Systematic and Evolutionary Microbiology*, **50**(2), 771-779.
- Shehu, M.S., Abdul Manan, Z., Wan Alwi, S.R. 2012. Optimization of thermo-alkaline disintegration of sewage sludge for enhanced biogas yield. *Bioresource technology*, **114**, 69-74.
- Sieber, J.R., Sims, D.R., Han, C., Kim, E., Lykidis, A., Lapidus, A.L., McDonnald, E., Rohlin, L., Culley, D.E., Gunsalus, R. 2010. The genome of *Syntrophomonas wolfei*: new insights into syntrophic metabolism and biohydrogen production. *Environmental microbiology*, **12**(8), 2289-2301.
- Solli, L., Håvelsrud, O.E., Horn, S.J., Rike, A.G. 2014. A metagenomic study of the microbial communities in four parallel biogas reactors. *Biotechnology for Biofuels*, **7**(1).
- Stolze, Y., Zakrzewski, M., Maus, I., Eikmeyer, F., Jaenicke, S., Rottmann, N., Siebner, C., Pühler, A., Schlüter, A. 2015. Comparative metagenomics of biogas-producing microbial communities from production-scale biogas plants operating under wet or dry fermentation conditions. *Biotechnology for biofuels*, **8**(1), 1.
- Thauer, R.K. 1998. Biochemistry of methanogenesis: a tribute to Marjory Stephenson. *Microbiology*, **144**, 2377-2406.
- Thauer, R.K., Jungermann, K., Decker, K. 1977. Energy-conservation in chemotrophic anaerobic bacteria. *Bacteriological Reviews*, **41**(1), 100-180.
- Turnbaugh, P.J., Ley, R.E., Hamady, M., Fraser-Liggett, C.M., Knight, R., Gordon, J.I. 2007. The Human Microbiome Project. *Nature*, **449**(7164), 804-810.
- Tveit, A., Urich, T., Svenning, M.M. 2014. Metatranscriptomic analysis of Arctic peat soil microbiota. *Applied and environmental microbiology*, AEM. 01030-14.

- Tzeneva, V.A., Salles, J.F., Naumova, N., de Vos, W.M., Kuikman, P.J., Dolfing, J., Smidt, H. 2009. Effect of soil sample preservation, compared to the effect of other environmental variables, on bacterial and eukaryotic diversity. *Research in microbiology*, **160**(2), 89-98.
- Vanwonterghem, I., Jensen, P.D., Ho, D.P., Batstone, D.J., Tyson, G.W. 2014. Linking microbial community structure, interactions and function in anaerobic digesters using new molecular techniques. *Current opinion in biotechnology*, **27**, 55-64.
- Vivekanand, V., Eijsink, V.G.H., Horn, S.J. 2012. Biogas production from the brown seaweed *Saccharina latissima*: thermal pretreatment and codigestion with wheat straw. *Journal of Applied Phycology*, **24**(5), 1295-1301.
- Wagner, A.O., Lins, P., Malin, C., Reitschuler, C., Illmer, P. 2013. Impact of protein-, lipid- and cellulose-containing complex substrates on biogas production and microbial communities in batch experiments. *Science of the Total Environment*, **458**, 256-266.
- Wang, X., Yang, G., Feng, Y., Ren, G., Han, X. 2012. Optimizing feeding composition and carbon–nitrogen ratios for improved methane yield during anaerobic co-digestion of dairy, chicken manure and wheat straw. *Bioresource Technology*, **120**, 78-83.
- Weiland, P. 2010. Biogas production: current state and perspectives. *Applied Microbiology and Biotechnology*, **85**(4), 849-860.
- Weiss, F., Leip, A. 2012. Greenhouse gas emissions from the EU livestock sector: a life cycle assessment carried out with the CAPRI model. *Agriculture, ecosystems & environment*, **149**, 124-134.
- Westerholm, M., Roos, S., Schnürer, A. 2010. *Syntrophaceticus schinkii* gen. nov., sp. nov., an anaerobic, syntrophic acetate-oxidizing bacterium isolated from a mesophilic anaerobic filter. *FEMS microbiology letters*, **309**(1), 100-104.
- Westerholm, M., Roos, S., Schnürer, A. 2011. *Tepidanaerobacter acetatoxydans* sp. nov., an anaerobic, syntrophic acetate-oxidizing bacterium isolated from two ammonium-enriched mesophilic methanogenic processes. *Systematic and applied microbiology*, **34**(4), 260-266.
- Worm, P., Koehorst, J.J., Visser, M., Sedano-Núñez, V.T., Schaap, P.J., Plugge, C.M., Sousa, D.Z., Stams, A.J. 2014. A genomic view on syntrophic versus non-syntrophic lifestyle in anaerobic fatty acid degrading communities. *Biochimica et Biophysica Acta (BBA)-Bioenergetics*, **1837**(12), 2004-2016.
- Wu, X., Yao, W., Zhu, J., Miller, C. 2010. Biogas and CH₄ productivity by co-digesting swine manure with three crop residues as an external carbon source. *Bioresource technology*, **101**(11), 4042-4047.
- Xia, Y., Wang, Y., Fang, H.H., Jin, T., Zhong, H., Zhang, T. 2014. Thermophilic microbial cellulose decomposition and methanogenesis pathways recharacterized by metatranscriptomic and metagenomic analysis. *Scientific reports*, **4**. doi:10.1038/srep06708.
- Zabranska, J., Stepova, J., Wachtl, R., Jenicek, P., Dohanyos, M. 2000. The activity of anaerobic biomass in thermophilic and mesophilic digesters at different loading rates. *Water Science and Technology*, 49-56.
- Zakrzewski, M., Goesmann, A., Jaenicke, S., Jünemann, S., Eikmeyer, F., Szczepanowski, R., Al-Soud, W.A., Sørensen, S., Pühler, A., Schlüter, A. 2012. Profiling of the metabolically active community from a production-scale biogas plant by means of high-throughput metatranscriptome sequencing. *Journal of Biotechnology*, **158**(4), 248-258.
- Zhang, C., Xiao, G., Peng, L., Su, H., Tan, T. 2013. The anaerobic co-digestion of food waste and cattle manure. *Bioresource technology*, **129**, 170-176.

- Zhang, T.C., Noike, T. 1991. Comparison of one-phase and two-phase anaerobic digestion processes in characteristics of substrate degradation and bacterial population levels. *Water Science & Technology*, **23**(7-9), 1157-1166.
- Zhou, Y., Pope, P.B., Li, S., Wen, B., Tan, F., Cheng, S., Chen, J., Yang, J., Liu, F., Lei, X. 2014. Omics-based interpretation of synergism in a soil-derived cellulose-degrading microbial community. *Scientific reports*, **4**.doi: 10.1038/srep05288.
- Ziganshin, A.M., Liebetrau, J., Pröter, J., Kleinstüber, S. 2013. Microbial community structure and dynamics during anaerobic digestion of various agricultural waste materials. *Applied microbiology and biotechnology*, **97**(11), 5161-5174.
- Zinder, S.H., Koch, M. 1984. Non-aceticlastic methanogenesis from acetate: acetate oxidation by a thermophilic syntrophic coculture. *Archives of Microbiology*, **138**(3), 263-272.

Paper I



Microbial community structure and dynamics during co-digestion of whey permeate and cow manure in continuous stirred tank reactor systems



Live Heldal Hagen^a, Vivekanand Vivekanand^a, Roar Linjordet^b, Phillip B. Pope^a, Vincent G.H. Eijsink^a, Svein J. Horn^{a,*}

^a Department of Chemistry, Biotechnology and Food Science, Norwegian University of Life Sciences, P.O. Box 5003, N-1432 Ås, Norway

^b Bioforsk, Norwegian Institute for Agricultural and Environmental Research, Frederik A. Dahls vei 20, 1432 Ås, Norway

HIGHLIGHTS

- Community of *Bacteroidetes*, *Firmicutes*, *Methanobacteriales* and *Methanomicrobiales*.
- High feeding of whey led to bioreactors operating at the edge of stability.
- Parallel biogas reactors differed in performance and microbial communities.

ARTICLE INFO

Article history:

Received 10 July 2014

Received in revised form 21 August 2014

Accepted 22 August 2014

Available online 30 August 2014

Keywords:

Anaerobic digestion

Methane

Microbial community

High throughput sequencing

Co-digestion

ABSTRACT

Microbial community profiles in two parallel CSTR biogas reactors fed with whey permeate and cow manure were investigated. The operating conditions for these two reactors were identical, yet only one of them (R1) showed stable performance, whereas the other (R2) showed a decrease in methane production accompanied by accumulation of propionic acid and, later, acetic acid. This gave a unique opportunity to study the dynamics of the microbial communities in two biogas reactors apparently operating close to the edge of stability. The microbial community was dominated by *Bacteroidetes* and *Firmicutes*, and the methanogens *Methanobacteriales* and *Methanomicrobiales* in both reactors, but with larger fluctuations in R2. Correlation analyses showed that the depletion of propionic acid in R1 and the late increase of acetic acid in R2 was related to several bacterial groups. The biogas production in R1 shows that stable co-digestion of manure and whey can be achieved with reasonable yields.

© 2014 Elsevier Ltd. All rights reserved.

1. Introduction

In the face of global challenges such as fossil fuel depletion, increasing greenhouse gas emissions and climate change, anaerobic digestion of organic material to biogas has become an attractive strategy for renewable energy production and sustainable waste disposal. Agricultural residues, municipal solid waste and wastewater have traditionally been the main substrates for biogas production. In addition, various residuals from the food processing industry have been proposed as possible substrates for biogas generation, including by-products from the dairy industry (Luo and Angelidaki, 2013).

* Corresponding author. Tel.: +47 67232488; fax: +47 64965901.

E-mail address: svein.horn@nmbu.no (S.J. Horn).

Cheese whey is a by-product from cheese production. Between 115 and 160 million tons of whey are generated globally every year, half of which is transformed into food products or utilized for ethanol fermentation, while the rest is disposed (Guimarães et al., 2010). Due to its world-wide availability and high carbohydrate content, whey is considered a suitable substrate to produce biogas via anaerobic degradation. Whey proteins have a relatively high value and are typically removed from whey by ultrafiltration. Thus, it is mainly the whey permeate, i.e., a solution primarily composed of water, lactose and salts, that is available for anaerobic digestion. Co-digestion of whey permeate with cow manure or poultry waste has caught some interest because the latter feedstocks provide buffer capacity, nitrogen, and nutrients (Gelegenis et al., 2007). Furthermore, to prevent rapid growth of acid forming bacteria, the easily degradable lactose in whey permeate needs to be balanced by more recalcitrant substrates, such as lignocellulosic material in cow manure.

Anaerobic degradation of organic compounds to biogas is carried out by a relatively undefined microbial culture which varies according to its origin, substrate composition, operational conditions and environmental parameters. Generally, anaerobic degradation proceeds via four main steps: hydrolysis, fermentation, anaerobic oxidation and methanogenesis. The three first steps are carried out by a large consortium of bacteria, while specialized groups of methane producing archaea (methanogens) are responsible for the final step (Gujer and Zehnder, 1983). Efficient and successful conversion of organic matter to biogas relies on a close and balanced cooperation between the different groups of microorganisms.

The bacteria degrade organic substrates to acetate and longer-chain volatile fatty acids (VFAs), mainly propionate and butyrate, in addition to lactate and alcohols (hydrolysis & fermentation). Acetate can be directly utilized in the aceticlastic methanogenesis or in a two-step pathway comprised of acetate oxidation to hydrogen and carbon dioxide by syntrophic acetate oxidizing bacteria (SAOB) and a subsequent conversion of these products to methane by hydrogenotrophic methanogens (Schnürer et al., 1999). The other reduced intermediate compounds, including long-chain VFAs, must be oxidized to acetate, formate or hydrogen prior to methanogenesis. This anaerobic oxidation process, also called acetogenesis, is carried out by acetogens. Degradation of VFAs is generally thermodynamically unfavorable ($\Delta G^{\circ} < 0$), and the conversion is only possible if the hydrogen partial pressure is kept low, e.g., by hydrogen consuming methanogens. Interspecies hydrogen/formate transfer between sulfate reducing bacteria and methanogens is also widespread in nature, and may play an important role in degradation of long chain fatty acids (Schink, 1997). Thus, a syntrophic cooperation between bacteria and methanogens is critical for the process. The low growth rate and sensitivity to toxic compounds of methanogenic archaea compared to that of bacteria makes the complex microbial community in a biogas digester vulnerable to changes in operational parameters. For example, an increase in the organic loading rate of the system will speed up the hydrolysis-acidification process, whereas hydrogenotrophic methanogens may fail to consume all the hydrogen produced, thus leading to accumulation of reduced metabolites, such as VFAs.

The start-up phase of biogas reactors is considered as the most critical period, and comparisons of the microbial diversity in anaerobe reactors during start-up and steady-state conditions have revealed considerable shifts in community composition (Cardinali-Rezende et al., 2012). Generally, studies of biogas microbial communities have focused on stably performing reactors (e.g., Pope et al., 2013) and only a few recently published studies have explored the dynamic changes in microbial communities in response to instability and changes during the digestion period (Westerholm et al., 2012; Ziganshin et al., 2013). Here, the community dynamics in two parallel continuously stirred tank reactors (CSTR) co-digesting cheese whey permeate and cow manure was investigated. 16S rRNA gene sequencing was used to characterize the dynamics of the microbial community over a period of three months. Both reactors were continuously analyzed with regard to biogas production and accumulation of volatile fatty acids. Although the two reactors were technical parallels and ran under identical conditions, they differed in performance over time. This gave a unique opportunity to study the dynamics of the microbial

communities in two biogas reactors apparently operating close to the edge of stability.

2. Methods

2.1. Substrate and inoculum

Whey permeate obtained by ultrafiltration of whey was supplied by TINE SA, Norway. The dry matter content (DM) was 16.2% of which 90.8% were volatile solids (VS). Manure (11.3% DM and 85.9% VS) was supplied by the Department of Animal Sciences, Norwegian University of Life Sciences, Norway. These feedstocks were stored at 4 °C until required for the digestion experiments. The microbial inoculum for this study was obtained from a local biogas plant (Tomb Biogas, Norway), that runs large scale continuous anaerobic digestion of cow manure and food waste at mesophilic temperature (37 °C; pH 7.6). The DM content of the inoculum was 5.2% and VS was 68.5%. Prior to the experiments, the inoculum was incubated anaerobically (37 °C, 10 days) to reduce endogenous biogas production in the subsequent experiments. Chemical composition data for the whey, manure and inoculum is given in Table 1.

2.2. CSTR experiments and biogas production

Anaerobic digestion was carried out in laboratory-scale (10 L) continuously stirred tank reactors (CSTR, Dolly, Belach Bioteknik, Stockholm, Sweden) with a working volume of 6 L. Two parallel reactors (R1 and R2) for were filled with inoculum (6 L). Initially each reactor was fed with 0.5 g VS/L/day of a mixture of whey and manure (48.0% VS from manure). It was then gradually increased day by day to reach the final organic loading rate of 2.7 g VS/L/day 10 days after the first feeding, and the loading rate was then kept constant. Because accumulation of VFAs was observed, the whey/manure ratio in the feed was reduced after 44 days of operation. For R1 the feed was changed to 2.9 g VS/L/day (64.2% VS from manure) and kept constant for the rest of the period. R2, which showed a more severe accumulation of VFAs, was run in the following way: day 44–57, only manure, 1.9 VS/L/day; day 58–79, whey and manure, 2.9 g VS/L/day (64.2% VS from manure); day 80 to the end of the experiment, only manure, 1.9 VS/L/day. The operational conditions of the reactors were: 37 °C, initial pH 7.5, 180 rpm, and feeding 6 days a week with a hydraulic retention time (HRT) of 25 days. The HRT was kept constant by adding water to the substrate mixture. See Fig. S1 for a schematic diagram of experimental setup.

Continuous real-time monitoring of pH, stirrer speed, temperature, gas flow and gas volume produced was managed using the BIOPHANTOM© software (Belach Bioteknik, Stockholm, Sweden). Produced biogas was measured monitoring volume displacement in dedicated glass columns. Based on methane concentration and biogas volume the ideal gas law was used to calculate methane production.

2.3. VFA analysis

Samples for Volatile fatty acids (VFAs) determination were collected once a week, and stored at –20 °C before analysis. VFAs (e.g.,

Table 1

Chemical characteristics of the materials. Volatile Solids (VS) and elements are expressed as percentage of Dry Matter (DM). Oxygen content was calculated by subtracting C, N and H values from VS content.

Substrate	Total C (%)	Total H (%)	Total N (%)	Total O (%)	Dry matter (%)	Volatile solid (%)	pH
Whey	41.1	5.3	0.4	44.0	16.2	90.8	7.2
Manure	45.2	5.6	1.1	34.0	11.3	85.9	7.3
Inoculum	32.7	4.0	2.8	29.0	5.2	68.5	7.6

formate, acetate, propionate and butyrate) were quantified by HPLC using a Dionex Ultimate 3000 system (Dionex, Sunnyvale, CA, USA). VFA concentrations were quantified by running standards. The HPLC samples were prepared by centrifugation and filtration (0.2 µm Sarstedt Filtropur S) in HPLC vials and transferred to an autosampler. The column applied was a Zorbax Eclipse Plus C18 from Agilent Technologies, 150 × 2.1 mm column (3.5 µm particles), equipped with guard column 12.5 × 2.1 mm (5 µm particles). The column was operated at 40 °C at 0.3 mL/min and 1 µL injection.

The elution was performed stepwise with eluents A (Methanol) and B (2.5 mM H₂SO₄) starting with 100% B from 0 to 2.5 min, from 2.51 to 25 min at 85% B and then immediately back to 100% B and reconditioning for 10 min. Detection was performed by UV absorption at 210 nm.

2.4. Methane analysis

The biogas composition in the CSTRs was monitored with an SRI gas chromatograph (Model 8610 C) equipped with a thermal conductivity detector (TCD) and a 2 m Haysep-D column. Chromatography, data acquisition and integration were performed using the PeakSimple 3.88 software for Windows. The injector, detector, and column were operated at 41, 153 and 81 °C, respectively. Helium was used as a carrier gas at 20 ml min⁻¹. A standard gas mixture (CH₄/CO₂) at 65/35% was used for calibration.

2.5. Other analyses

The elemental composition of carbon, hydrogen and nitrogen was determined by combustion using a Leco CHN-1000 instrument (St. Joseph, Michigan, USA).

Dry matter (DM)/total solid (TS) and ash content were determined by drying and burning the samples at 105 °C and 550 °C overnight, respectively. The VS content was calculated by subtracting the ash from the DM content.

2.6. Sampling and DNA extraction

The microbial community structure was analyzed in each of the two parallel reactors. For each digester, samples of reactor slurry were collected every 6–7th day, starting at day 12 and continued until day 100, yielding a total of 14 sampling points. Sampling of the inoculum was also carried out. All samples were frozen at –20 °C immediately after collection, and stored until extraction of DNA was performed. Repetitive dissociation of the biogas reactor material and harvesting of cells was performed prior to DNA extraction to recover microorganism absorbed to the organic material. In brief, reactor material samples were resuspended in a dissociation buffer, followed by low-speed centrifugation enabling harvesting of cells dissociated from particles in the liquid fraction. Direct DNA extraction was carried out according to Rosewarne et al. (2010), with minor modifications. DNA quality was checked for protein impurities and DNA degradation on 1% agarose gels, and DNA was quantified using the QubitTM fluorometer and the Quant-iTTM dsDNA BR Assay Kit (Invitrogen, Carlsbad, CA, USA).

2.7. Amplification and sequencing

The 16S rRNA gene of the extracted DNA was amplified with the broadly conserved primer sets 8F-515R (5'-AGAGTTTGATCTGG-3'/5'-TTACCGCGCTGCT-3') for Bacteria (Hamady et al., 2008) and 340F-1000R (5'-CCCTAYGGGCGASCAG-3'/5'-GGCCATGCACYWCYTCTC-3') for Archaea (Gantner et al., 2011), targeting the V1–V3 regions. These primers contained the 454 Life Science primer A sequence and a unique 8 – nt multiplex identifier

(Hamady et al., 2008). Triplicate amplification of each sample was carried out under identical conditions, but with unique multiplex identifiers. The PCR was performed with an initial denaturation step at 98 °C for 30 s., followed by 30 (Bacteria) or 35 (Archaea) cycles consisting of 98 °C for 10 s, 58 °C for 30 s and 72 °C for 45 s., and completed by a final elongation step at 72 °C for 7 s. The concentration of bacterial amplicons was quantified using the QubitTM fluorometer and the Quant-iTTM dsDNA BR Assay Kit (Invitrogen, Carlsbad, CA, USA). Archaeal amplicon concentrations were quantified by agarose gel electrophoresis using the Quantity One[®] software (Bio-Rad Laboratories, Hercules, CA) as fluorometric based quantification led to overestimation of nucleic acid concentration due to primer-dimer formation of the archaea primer pair. Equimolar concentrations of bacterial and archaeal amplicons were pooled prior to purification with NucleoSpin[®] Extract II columns (Machery-Nagel, Düren, Germany). The 454/Roche GS FLX sequencing was performed at the Norwegian Sequencing Centre in Oslo (www.sequencing.uio.no), using LIB-L chemistry. All nucleotide sequences obtained in this study have been deposited in the NCBI Sequence read archive (<http://www.ncbi.nlm.nih.gov/GenBank/index.html>) under accession number SRP043455.

2.8. Phylogenetic analysis of 16S rRNA gene sequences

The reads were quality filtered using the Quantitative Insight Into Microbial Ecology (QIIME) software package (Caporaso et al., 2010). Error correction and chimera removal was performed, and reads were de novo clustered into operational taxonomic sequences (OTUs) with 97% sequence identity using USEARCH which incorporates UCHIME (Edgar et al., 2011). Ribosomal database project (RDP) classifier with a confidence threshold of 0.8 were used to assign taxonomy to each OTU. The datasets was then rarefied by random subsampling to the smallest library (sequences/sample), to normalize and remove sample heterogeneity. Phylogenetic distance (weighted and un-weighted UniFrac) was used to measure beta-diversity between all pairs of bacterial communities. Based on this, deviants of triplicate amplicons were excluded from further downstream analysis, as such variances might introduce unrepresentative phylogenetic diversity for the digestion sample (this filtering was performed only if one out of three replicates was clearly divergent from two replicates with high similarity, representing the same sample). Taxa and OTU tables were generated in QIIME and used in the downstream statistical analysis. Calypso version 3.4 (www.bioinfo.qimr.edu.au/calypso/) was then used for mining, comparing and visualization of community composition in correlation to environmental variables. Multivariate analysis was used to assess associations between reactor performance and community composition based on the 16S rRNA gene amplicon sequencing. For this, a redundancy discriminate analysis (RDA) was applied, with constrained ordination, to examine how much of the variance in one set of variables (community composition) could explain the variation in another set of variables (VFA concentration). Permutation tests were applied to assess the significance of constraints. In addition, co-occurrence and the metabolic functionality were inferred by correlation between genera and environmental variables (concentration of acetate and propionate) visualized by correlation network maps. Sequences occurring at <2% of the total reads in at least one sample were excluded in order to reduce the network complexity. A valid co-occurrence observation was considered as a robust correlation if the Pearson's correlation coefficient (r) was minimum 0.6 and statistically significant (for n samples = 14 per reactor, P-value <0.05, two tailed). In the datasets used for correlation analysis, the counts per OTU/phylo-type were summed up for each day of anaerobic digestion.

3. Results and discussions

3.1. Performance of the CSTR biogas reactors

Two parallel CSTR reactors (R1 and R2) were run for 100 days using a mixture of whey permeate and manure as substrate. While these two reactors were technical replicates, R2 showed lower biomethane production than R1 (Fig. 1). Likewise, while R1 had a relatively stable methane content in the biogas throughout the experimental period (53–56%), the methane content gradually dropped in R2 reaching 30% at the end of the experiment (data not shown). Fig. 2 shows the concentration (mM) of two volatile fatty acids (VFAs; acetic and propionic acid) during the digestion period for the two reactors. Propionic acid (PA) was the main VFA found in both reactors, probably produced from easily degradable lactose in the whey, but it reached a much higher concentration in R2. After 39 days of digestion, PA reached a maximum concentration of 55.7 mM in R1. Subsequently, PA was rapidly depleted to a level below 1 mM (Fig. 2), showing that the H_2 partial pressure was low enough for anaerobic oxidation of PA to take place. The maximum concentration of acetic acid (AA), probably

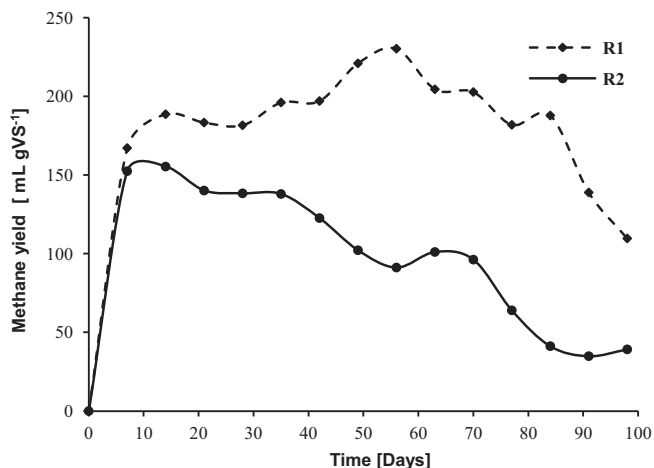


Fig. 1. Specific methane production for R1 and R2. Each point represents weekly average.

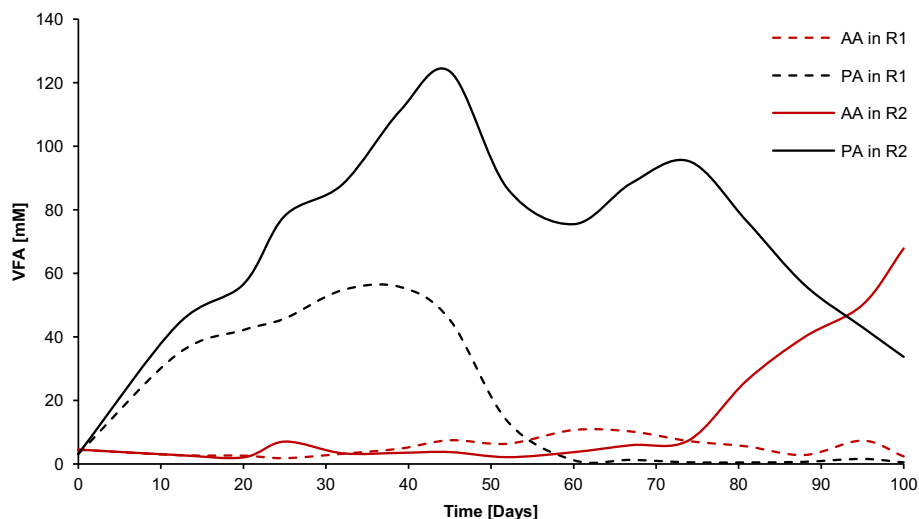


Fig. 2. Concentration of acetic and propionic acids in R1 (--) and R2 (—). From day 44 R1 was fed a lower whey/manure ratio, while R2 was fed only manure. R2 was again fed a whey/manure mixture in the period day 58–79, and then only manure again from day 80.

formed from propionate, was 10.7 mM after 60 days of digestion. At the end of the digestion period, the total concentration of VFAs in this stable R1 reactor was below 10 mM. The initial pH was approximately 7.6, which gradually decreased to pH 7.1 during the first 20 days (in both reactors; Fig. S2). In R1, this pH was maintained throughout the digestion period.

In R2, PA reached a maximum concentration of 123.5 mM on day 45. The concentration then gradually decreased, but it remained high, with a new peak of 95.3 mM appearing at day 74. The dip in PA concentration between day 45 and 74 correlates with changes in the feeding regime of R2 (feeding of whey permeate was stopped at day 43 and resumed at day 58) that were meant to stabilize the reactor. After day 75, the concentration of PA again showed a gradual decrease, but this time the decrease was accompanied by a rise in AA concentration. Thus, in this phase PA was converted to AA, but AA was apparently not further processed by the methanogens, perhaps as a consequence of a drop in pH, from approximately 7.0 to 6.0 (Fig. S2). Indeed, methane production went down quite dramatically in this period (Fig. 1). At the end of the digestion period, VFA levels in R2 were 67.9 mM and 33.7 mM for AA and PA, respectively. Microbial production of PA (fermentation) is driven by a variety of bacterial strains, for instance *Clostridium propionicum* and *Propionibacterium* spp., (Liu et al., 2012). These bacteria can utilize different carbon sources, such as glucose, glycerol, lactate and also lactose from whey (Hassan and Nelson, 2012). PA producing bacteria metabolize the carbon source into pyruvate, which is then converted to succinic acid and further degraded to PA. AA may be formed as a by-product (Morales et al., 2006). During anaerobic oxidation, PA is mainly oxidized via the methylmalonyl-CoA pathway yielding AA, H_2 and CO_2 (De Bok et al., 2004). In a stable biogas process AA is rapidly consumed by acetoclastic methanogens, or by SAOBs in synergy with a hydrogenotrophic methanogenic partner, to form methane. As the acetoclastic methanogens have been shown to be more sensitive to disturbance and toxic substances, syntrophic action of SAOBs and hydrogenotrophic methanogens were probably important in these reactors. Thus, when hydrogen/-formate regulating methanogens are active, hydrogen and formate concentration are low enough to make the degradation of fatty acids energetically favorable for the acetogens. An accumulation of volatile fatty acids, as seen in R2, is a typical consequence of unbalanced cooperation between the fermentative/acetogenic and methanogenic fractions of the microbial population.

Accumulation of VFAs is a well-known consequence of feeding too much of an easily digestible substrate, and a too high loading rate of the easily degradable whey lactose was probably the reason for the initial accumulation of PA in both reactors. Tolerable PA concentrations in biogas reactors vary according to operational parameters and substrate, ranging from lower than 20 mM to concentrations above 50 mM (Ahring et al., 1995; Barredo and Evison, 1991). The maximum concentration of PA seen in R1 (55.74 mM) has been reported as potentially inhibiting in other studies, but was not inhibitory in this study. However, the fact that R2, run under identical conditions, did never recover from the PA accumulation must mean that the feeding regime was so intense that the microbial community was operating close to the edge of stability.

3.2. Overall microbial diversity

Phylogenetic analysis of total bacterial and archaeal 16S rRNA genes was performed in order to characterize the microbial community composition in the two anaerobic digesters. In total, 374,505 bacterial and 353,074 archaeal raw reads with average length of approximately 560 bp and 520 bp, respectively, were obtained from the amplicon library originating from the two reactors and the inoculum sample. The inoculum was collected at Tomb biogas plant which is treating manure and food waste. 16S rRNA gene sequencing of the microbial consortia in the raw inoculum showed that it was composed of 40% *Firmicutes*, 36% *Bacteroidetes*, 12% *Chloroflexi*, 6% *Spirochaetes*, 2% *Synergistetes* in addition to 4% unclassified bacteria. The archaeal fraction comprised 46% *Methanobacteriales*, 45% *Methanosarcinales*, 5% *Methanomicrobiales*, 3% Miscellaneous Crenarchaeota group (MCG) and 1% *Thermoplasmata* of the uncultured group E2 (Fig. S3).

After filtering and normalization, 84,285 bacterial and 54,432 archaeal 16S rRNA sequences originating from R1 were clustered into 718 and 57 OTUs, respectively. The 113,088 and 58,512 reads obtained after filtering and normalization of the data for R2 were assigned to 663 and 38 bacterial and archaeal OTUs, respectively. The OTUs were then assigned to phylogenetic taxa, and for both reactors, *Firmicutes* and *Bacteroidetes* were the dominant bacteria phyla followed by *Spirochaetes*, *Chloroflexi* and *Synergistetes* (Fig. S4a and b). *Firmicutes* and *Bacteroidetes* are normally found in a wide range of different habitats, and have a high level of metabolic diversity. They are frequently observed, and often predominant, in biogas reactors running on a variety of substrates (Kampmann et al., 2012; Pope et al., 2013). *Synergistetes*, *Spirochaetes* and *Chloroflexi* have also been observed in a number of anaerobic processes, and Rivière et al. (2009) have defined *Chloroflexi* and *Synergistetes*, in addition to *Bacteroidetes*, as core microorganisms in anaerobic digestion.

For both reactors, archaeal representatives were less diverse than bacteria (Fig. S4c and d). The majority of the archaeal reads were assigned to the phylum *Euryarchaeota*. *Euryarchaeota* is a deep branch of archaea comprising methanogenic organisms, including hydrogenotrophic methanogens that dominated in both reactors. Only a minority of the total archaeal sequences belonged to *Methanosarcinales*. As *Methanosarcinales* are the only archaea observed in this study capable of performing acetate degradation to form methane, their low presence indicates that acetoclastic methanogenesis did hardly occur in the reactors. Since in R1 PA is converted to AA without accumulation of AA, it seems likely that SAOBs have played an important role for AA utilization. Recent studies have shown that SAOBs indeed are abundant in a range of different biogas plants (Sun et al., 2014), and bacteria potentially involved in degradation of fatty acids was also observed in both reactors in this study, as discussed in more detail below. A small fraction of archaea in R1 and R2 also belonged mainly to the *Thermoplasmata* (clone WCHD3-02), a class of *Euryarchaeota* frequently

found in anaerobic digestion processes and recently shown to have a methanogenic lifestyle (Paul et al., 2012).

3.3. Microbial community development and dynamics – bacteria

The OTUs originated from samples taken at different times during the digestion period, making it possible to monitor the development and dynamics of the microbial community structure. The relative proportion of the most abundant bacterial OTUs in R1 and R2 over time, assigned to class based on taxonomic classification with RDP, is provided in Fig. 3. Comparison of the bacterial community dynamics in reactors R1 and R2 revealed that the community structure varied considerably between the two reactors, despite the fact that they were run in parallel and originated from the same inoculum. In brief, more fluctuation of both dominating and less abundant bacteria and archaea was seen for R2. As shown in Fig. 3, *Bacteroidetes* and *Firmicutes* were predominant throughout the digestion period in both reactors. Overall, until day 52, the relative abundance of *Bacteroidetes* increased while *Firmicutes*, especially *Bacilli* decreased in both reactors. Moreover, a decrease of *Bacteroidetes* and an increase of *Bacilli* were observed in R2 after day 52, possibly as a response to the interruption in feeding whey permeate from day 52 to day 60. However, this trend in R2 went on also after feeding of whey permeate was continued at day 60 (Fig. 3). Most of the sequences belonging to the phylum *Bacteroidetes* in this study indicated high similarity to *Bacteroidia* (formerly referred to as class *Bacteroidetes*). Species of the *Bacteroidetes* phylum can serve several roles in anaerobic degradation processes. They are mostly known as sugar fermenters and plant cellulose degraders. In addition, protein degradation and subsequent amino acid fermentation to acetate, propionate and succinate among strains have been documented (Kampmann et al., 2012).

A majority of the sequences belonging to *Firmicutes* was classified as *Clostridia* and *Bacilli*. A significant proportion of *Firmicutes* was also assigned to unclassified members of the class *Clostridia*, with increasing abundance after day 52 in R2. The presence of the class *Clostridia* (here mainly comprising unclassified *Clostridia* and *Clostridiales*) in the reactors is in accordance with their abundance observed in several previous studies on anaerobic digestion process (e.g. Ziganshin et al., 2013). *Clostridia* are a highly versatile class of anaerobic bacteria, and represent a major group of hydrolyzing and fermentative bacteria, including acetogens and syntrophic acetate oxidizing bacteria (Schnürer et al., 1996). On genus level, a significant number of the sequences classified as *Clostridia* had high homology with *Clostridium*, with generally decreasing abundance throughout the digestion period (data not shown). A rapid rise of *Clostridia* was seen at day 74 in R2, which could reflect a response on the resumed loading of whey permeate from day 58.

A large fraction of the *Bacilli* sequences was associated with the genus *Streptococcus*, a group of lactic acid bacteria shown to ferment saccharides to produce a wide range of products (Hoskins et al., 2001). Most *Streptococcus* bacteria prefer growth on glucose, but strains (e.g., *Streptococcus suis* and *Streptococcus thermophilus*) with the ability to degrade lactose have also been isolated and could therefore potentially be participating in the degradation of the whey (Kilpper-Bälz and Schleifer, 1987). In this study, the relative abundance of *Bacilli* declined drastically in both reactors during the first weeks. Moreover, the growth of *Bacilli* seemed to be affected by the discontinuous feeding of whey in R2, as the relative abundance of *Bacilli* increased when reactor was fed only with cow manure. A major proportion (~99%) of the Candidate division WWE1 (phyla *Spirochaeta*) was assigned to *Cloacamonales* with high similarity to the phylotypes *Candidatus Cloacamonas* and Candidate division *Cloacamonaceae* clone BHB21. In R1, a gradual decrease in the proportion of *Candidatus Cloacamonas* was

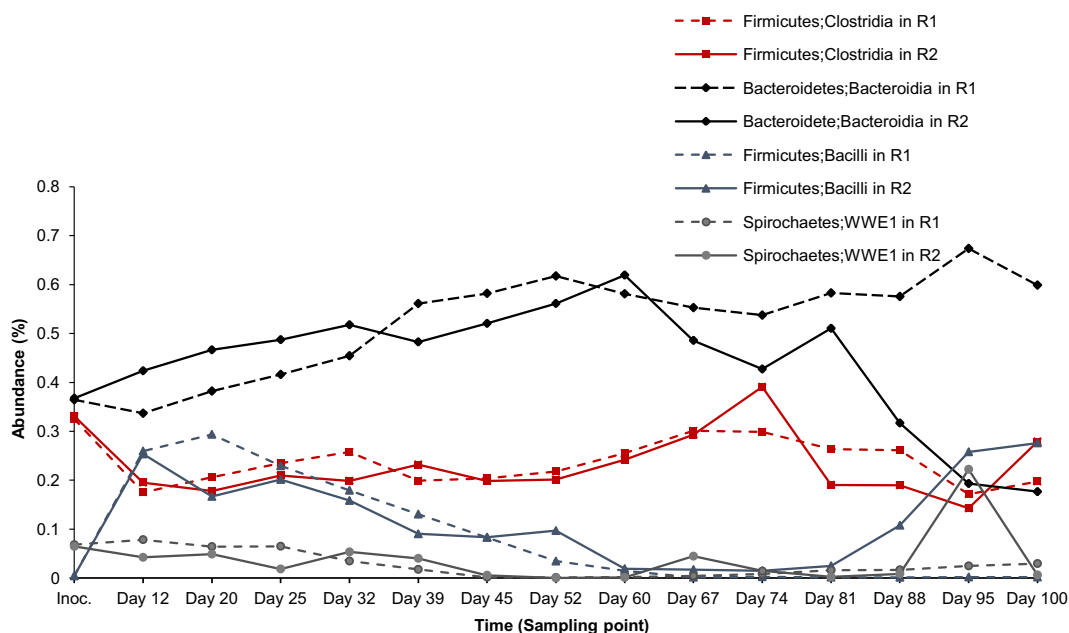


Fig. 3. Comparison of the bacterial community profiles during the anaerobic digestion period in R1 (--) and R2 (—). The relative abundance of dominant bacteria taxa; *Clostridia*, *Bacteroidia*, *Bacilli* and candidate division WWE1, is represented at class level with phylum lineage indicated. Values are given as the sum of triplicates, after filtration and rarefaction.

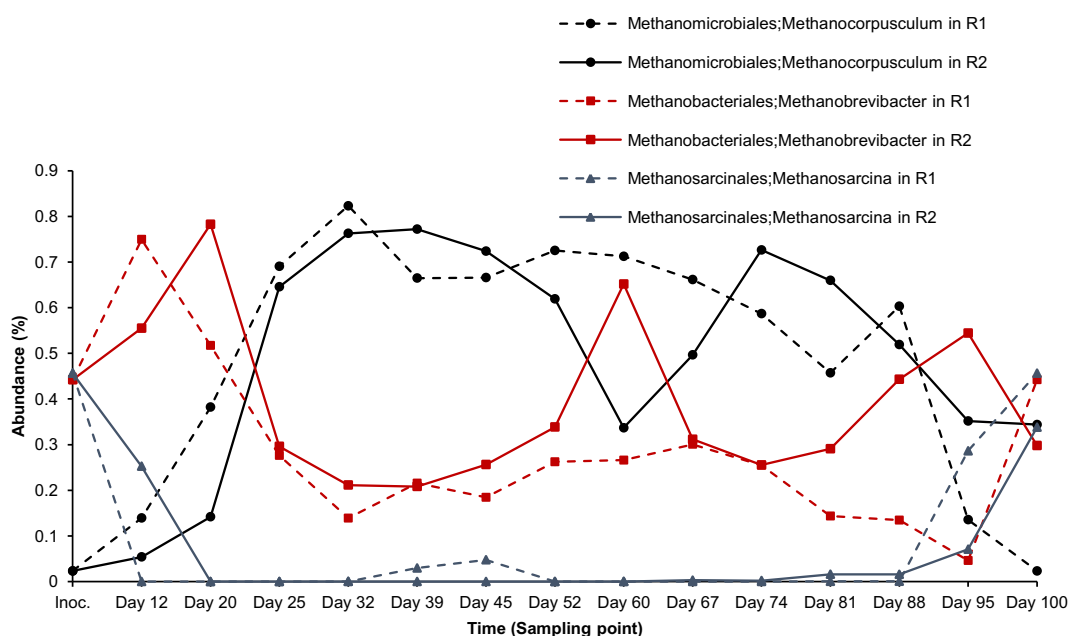


Fig. 4. Comparison of archaeal community profiles during the anaerobic digestion period in R1 (--) and R2 (—). The relative abundance of dominant methanogens; *Methanocorpusculum*, *Methanobrevibacter* and *Methanosarcina* is represented at genus level with order lineage indicated. Values are given as the sum of triplicates, after filtration and rarefaction.

observed during the first weeks until a minimum was reached after 52 days. In contrast, considerable fluctuation of *Candidatus* Cloacamonas was observed in R2, with a significant increase of abundance after 88 days. Relative abundance of sequences with high similarity to *Candidatus* Cloacamonaceae clone BHB21 increased considerable after 67 days of operation. Candidate phylum TM7 was also dynamically changing during the digestion time, with different development in the two reactors (data not shown).

Both these uncultured bacteria divisions have been frequently found in anaerobic processes. Knowledge regarding their metabolic functions is still poor, but members of *Spirochaeta* and Candidate phylum TM7 have been found to utilize glucose (Ariesyady et al., 2007). Furthermore, organisms related to *Candidatus* Cloacamonas have been identified in several anaerobic digesters and are proposed to be syntrophic (i.e., amino acid fermentation and oxidative propionate degradation) bacteria (Ganesan et al., 2008).

3.4. Microbial community development and dynamics – archaea

The results for the archaea community analysis are summarized in Fig. 4, providing dynamics of the most abundant archaeal groups (order and genus). As for bacteria, more fluctuations were observed in R2 than in the stable R1. A majority of the archaeal OTUs were affiliated to *Methanobacteriales* and *Methanomicrobiales*. In the initial phase, the archaeal population shows a clear shift from dominance of *Methanobacteriales* to dominance of *Methanomicrobiales* in both reactors. Apparently, *Methanobacteriales* that are dominant in the inoculum (Fig. S3b) are outcompeted in this phase. Also note that *Methanosarcinales* which was abundant in the inoculum quickly disappears in both reactors. *Methanomicrobiales* was mainly identified as the genus *Methanocorpusculum*. A significant fraction of the *Methanomicrobiales* sequences associated to the final sample

in R1 was affiliated to the recently established family lineage *Methanoregulaceae*, members of which have been isolated from propionic degrading enrichment cultures (Imachi et al., 2008; Sakai et al., 2012). *Methanobacteriales* was mainly assigned to the genus *Methanobrevibacter*, in addition to a minority of *Methanobacterium*. Almost all members of *Methanomicrobiales* and *Methanobacteriales* are hydrogenotrophic methanogens, converting carbon dioxide, carbon monoxide or formate to methane by using H₂. However, *Methanomicrobiales* are more metabolically versatile than *Methanobacteriales* and specific strains are, in addition to CO₂/H₂ utilization, able to grow on a variety of other carbon sources (Liu and Whitman, 2008). The majority of *Methanosarcinales* sequences had high homology to *Methanosarcina* on genus level, and a significant proportion of *Methanosarcina* was related to the last sample in both reactors. The gradual increase of the aceticlastic *Methanosarcina*

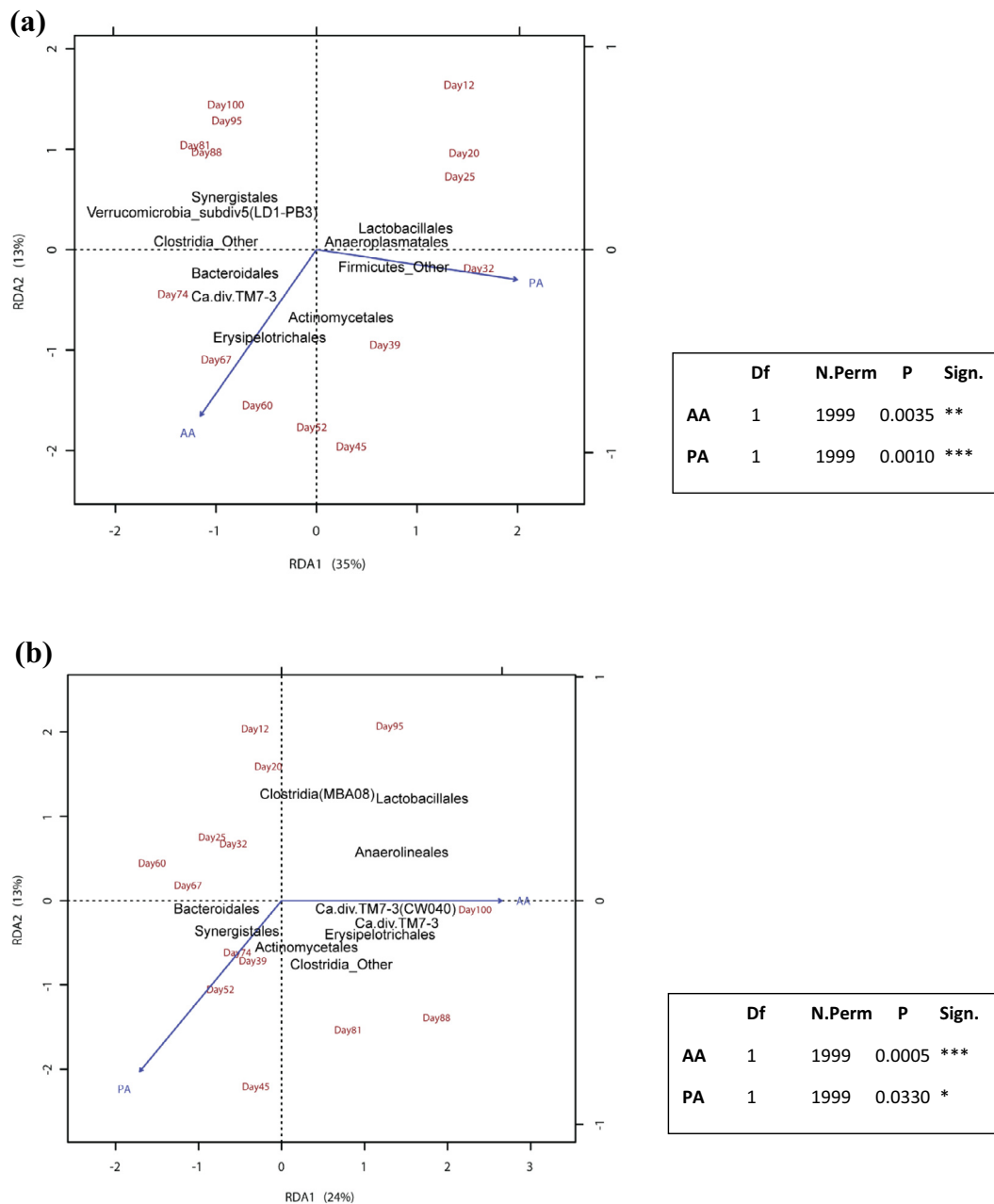


Fig. 5. Redundancy analysis (RDA), showing correlation between the relative abundance of a specific bacterial population and the concentration of propionic and acetic acid for R1 (a) and R2 (b). Each point (day) represents the composition of the bacterial community at the indicated time point. The 1st component (RDA1) explains 35% (R1) and 24% (R2) of the variance in the data while the 2nd (RDA2) explains 13% (R1 and R2). Sequences with 0.5% reads in at least one sample was filtered out.

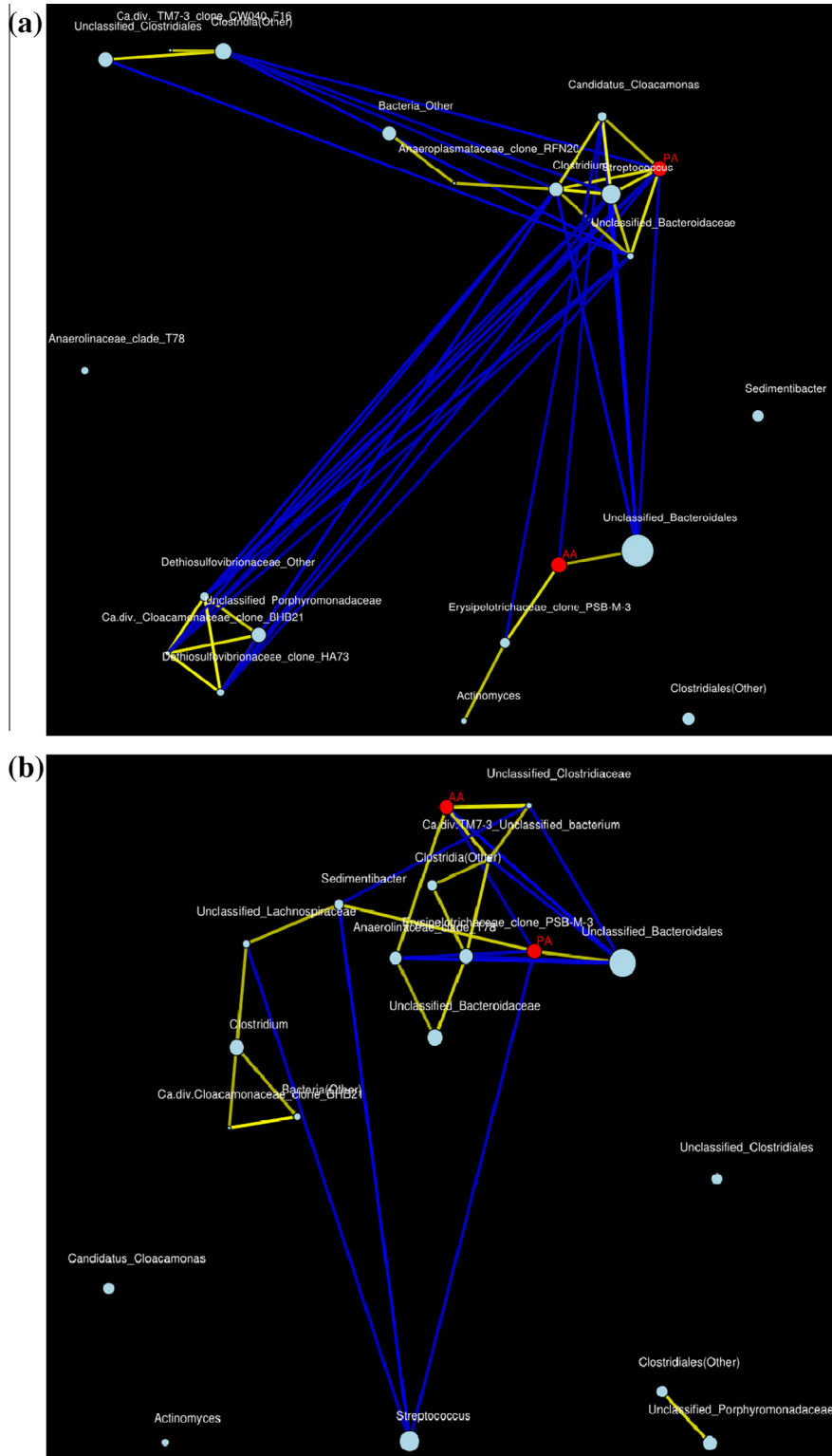


Fig. 6. Network map of bacteria (genus) and the two specific VFAs propionic acid and acetic acid, showing interactions between all samples of the stable reactor (R1:a) and the disturbed reactor (R2:b). Positive correlations are marked with yellow edge, showing co-occurring “events”, while negative correlations are demonstrated with a blue edge. Each phylotype is represented by dots, and the size of the dot reflects the relative number of sequenced found within the phylotype. Each connection between two nodes stands for a strong (Pearson’s $r > 0.6$) and significant (P -value < 0.05) correlation. Minimum proportion of 2% reads in at least one sample was used to reduce network complexity. Networks with min. proportion at 0.5% is provided in S.5.

during the last month of reactor operation in R2 was likely a result of increased concentration of acetic acid (Fig. 2). However, a drop in pH was observed in this period (Fig. S2), and this could also be the reason for increased relative abundance, as members of *Methanosarcinales* may tolerate pH down to 4–4.5. *Methanosarcinales* was

also present in the initial sample of R2, likely due to high abundance in the inoculum. Even though it is rather surprising that *Methanosarcina* is absent in the initial sample point (Day 12) for R1, as R1 and R2 initially was parallels, it should be noted that the CSTRs ran in 12 days before the first microbial sampling point, and that

the two reactors probably divergent before that, also seen from the specific methane production (Fig. 1).

The overall low abundance of acetoclastic methanogens (i.e., *Methanosarcina*, *Methanosaeta*) reinforces the impression provided by the VFA analysis (discussed in Section 3.1) that SAOBs participate in acetate conversion during co-digestion of whey and manure. Several *Clostridium* strains have been isolated and classified as SAOBs (Schnürer et al., 1996), and although no organisms was characterized on strain-level in this study, the presence of *Clostridium* in both reactors might indicate acetate consumption via syntrophic acetate oxidation.

3.5. Correlation between abundance of bacterial groups and concentrations of propionic and acetic acids

Multivariate analysis was used to evaluate potential correlations between the bacterial community structure and the concentration of volatile fatty acids. Redundancy Analysis (RDA) plots were calculated from the bacterial profiles on order level (Fig. 5). A permutation test (1999 permutations) was implemented to assess significance of constraints, showing that the concentration of PA and AA had influence on the bacterial distribution in R1 ($P < 0.01$). Significance influence was also predicted in R2, both for PA and AA ($P < 0.05$). The distribution of the samples (representing microbial community compositions at different time points) demonstrated that the community undergoes continuous dynamic succession in R1 (Fig. 5a). In contrast, the samples from R2 were scattered, indicative of an unstable microbial community with high variability. Correlation hypothesis established from the RDA analysis was further tested by exploring potential co-occurrence patterns through network analysis. Networks based on strong (Pearson's $r > 0.6$) and significant ($P < 0.05$) correlations are provided in Fig. 6, showing positive (yellow) and negative (blue) correlations between the different phylotypes at genus level, PA and AA.

The results from the constrained redundancy analysis showed that the variation in relative abundance of uncultured strains of *Firmicutes* could be explained by the variation in concentration of propionic acid in the stable reactor, R1. This was confirmed by a Pearson's correlation network with low abundant groups (min. prop. 0.5%, Fig. S5). The network map (Fig. 6a) also demonstrated a strong positive correlation between PA and *Streptococcus*, *Clostridium*, *Candidatus Cloacamonas* and an unclassified genus of *Bacteroidaceae*. In addition, a strong positive correlation between a syntrophic group (*Synergistales*; *Dethiosulfovibrionaceae*, *Dethiosulfovibrionaceae* clone HA73), unclassified *Porphyromonadaceae* of *Bacteroidetes* and Candidate division *Cloacamonaceae* clone BHB21 also suggest that their growth is enhanced by the presence of each other. Interestingly, this cluster had a negative correlation to PA, thus indicating that they are either sensitive to high propionic concentration, or responsible for keeping the level of propionate low in R1. Synergistic relationship including sulfate reducers growing on propionate have been described previously (e.g., Boone and Bryant, 1980) and it is tempting to suggest that the thio-sulfate- and sulfate-reducing bacterial family of *Dethiosulfovibrionaceae* may serve a central role in syntrophic propionate oxidation in R1. Additionally, both analyses suggested a significant correlation between AA and *Erysipelotrichales* in R1. In R2, co-occurrence of AA and *Anaerolineales* (phylum *Chloroflexi*) was observed (Figs. 5b and 6b). *Anaerolineales* (T78 clade) showed significant negative Pearson's correlation to PA, which in turn had a negative correlation to the concentration of AA. Even though members of *Anaerolineales* previously have been isolated from propionate-degrading consortia, growth on volatile fatty acids was not supported for the selected strains (Yamada et al., 2007). Acetate was shown to be a major product from growth on carbohydrates and it was also shown that growth of *Anaerolineales* is enhanced in

co-culture with hydrogenotrophic methanogens. The observed negative correlation of *Anaerolineales* to PA could therefore be an effect of inhibited methanogens rather than a cause of PA depletion, while the significant rise of acetic acid during the terminal period in R2 could be generated by members of *Chloroflexi*, together with Candidate division TM7-3. A significant correlation between Candidate division TM7-3 and AA concentration was observed for both reactors, indicating that this phylotype is playing a key role in acetic acid metabolism (Figs. 5a and b and 6b).

A microbial community in a habitat that undergoes major fluctuations in environmental variables would be expected to change, either causing or responding to the environmental changes. However, comparison of Pearson's correlation and redundancy analysis did not provide a consistent explanation of the PA concentration in R2. Rather, the variation of PA concentration seemed to be linked to several groups of organisms. Most strikingly, a strong positive correlation between PA and uncharacterized *Bacteroidetes* through Pearson's correlation was found, while PA seemed to be the driving force of variation of *Synergistales* in the redundancy analysis. Even though correlation plots can be particularly important in order to infer metabolic functionality and potential in a community determined by 16S rRNA, it should be kept in mind that interactions within anaerobic digesters are very complex, and underlying processes may not always be explained by statistical correlation analysis. While this study reveals relationships between volatile fatty acids and phylogenetic groups within the microbial community, the reason for such connections still remains largely unclear. For example, the positive correlation between propionic acid and unclassified strains of *Firmicutes* could be interpreted as either a microbial response to availability of propionic acid as substrate, or the cause of accumulation through metabolic activity.

4. Conclusions

The bioreactors in this study were operating on the boundary of tolerance due to intensive feeding of easily degradable material, resulting in critical levels of propionic acid in R2, while propionic acid was degraded leading to recovery of the process in R1. The depletion of PA in R1 was related to several bacterial groups, indicate that a synergistic propionic acid degrading consortium was established in the stable reactor. In general, the extent and complexity of synergistic interactions in the microbial world is largely unexplored and further research remains an essential step towards optimizing the microbial production of biogas.

Acknowledgements

This work was financially supported by the Norwegian Research Council (project No. 203402), Cambi ASA (Norway), TINE SA, and The Norwegian Farmers' Union. A great appreciation is extended to Tomb biogas plant for supplying this study with inoculum, and TINE SA for providing whey permeate.

Appendix A. Supplementary data

Supplementary data associated with this article can be found, in the online version, at <http://dx.doi.org/10.1016/j.biortech.2014.08.095>.

References

- Ahring, B.K., Sandberg, M., Angelidaki, I., 1995. Volatile fatty acids as indicators of process imbalance in anaerobic digesters. *Appl. Microbiol. Biotechnol.* 43 (3), 559–565.
- Ariesyady, H.D., Ito, T., Okabe, S., 2007. Functional bacterial and archaeal community structures of major trophic groups in a full-scale anaerobic sludge digester. *Water Res.* 41 (7), 1554–1568.

- Barredo, M., Evison, L., 1991. Effect of propionate toxicity on methanogen-enriched sludge, *Methanobrevibacter smithii*, and *Methanospirillum hungatii* at different pH values. *Appl. Environ. Microbiol.* 57 (6), 1764–1769.
- Boone, D.R., Bryant, M.P., 1980. Propionate-degrading bacterium, *Syntrophobacter wolinii* sp. nov. gen. nov., from methanogenic ecosystems. *Appl. Environ. Microbiol.* 40 (3), 626–632.
- Caporaso, J.G., Kuczynski, J., Stombaugh, J., Bittinger, K., Bushman, F.D., Costello, E.K., Fierer, N., Peña, A.G., Goodrich, J.K., Gordon, J.I., 2010. QIIME allows analysis of high-throughput community sequencing data. *Nat. Methods* 7 (5), 335–336.
- Cardinali-Rezende, J., Colturato, L.F., Colturato, T.D., Chartone-Souza, E., Nascimento, A., Sanz, J.L., 2012. Prokaryotic diversity and dynamics in a full-scale municipal solid waste anaerobic reactor from start-up to steady-state conditions. *Bioresour. Technol.* 119, 373–383.
- De Bok, F., Plugge, C., Stams, A., 2004. Interspecies electron transfer in methanogenic propionate degrading consortia. *Water Res.* 38 (6), 1368–1375.
- Edgar, R.C., Haas, B.J., Clemente, J.C., Quince, C., Knight, R., 2011. UCHIME improves sensitivity and speed of chimera detection. *Bioinformatics* 27 (16), 2194–2200.
- Ganesan, A., Chaussonnerie, S., Tarrade, A., Dauga, C., Bouchez, T., Pelletier, E., Le Paslier, D., Sghir, A., 2008. *Cloacibacillus evryensis* gen. nov., sp. nov., a novel asaccharolytic, mesophilic, amino-acid-degrading bacterium within the phylum 'Synergistetes', isolated from an anaerobic sludge digester. *Int. J. Syst. Evol. Microbiol.* 58 (9), 2003–2012.
- Gantner, S., Andersson, A.F., Alonso-Sáez, L., Bertilsson, S., 2011. Novel primers for 16S rRNA-based archaeal community analyses in environmental samples. *J. Microbiol. Methods* 84 (1), 12–18.
- Gelegenis, J., Georgakakis, D., Angelidaki, I., Mavris, V., 2007. Optimization of biogas production by co-digesting whey with diluted poultry manure. *Renewable Energy* 32 (13), 2147–2160.
- Guimarães, P.M., Teixeira, J.A., Domingues, L., 2010. Fermentation of lactose to bio-ethanol by yeasts as part of integrated solutions for the valorisation of cheese whey. *Biotechnol. Adv.* 28 (3), 375–384.
- Gujer, W., Zehnder, A.J.B., 1983. Conversion processes in anaerobic digestion. *Water Sci. Technol.* 15 (8–9), 127–167.
- Hamady, M., Walker, J.J., Harris, J.K., Gold, N.J., Knight, R., 2008. Error-correcting barcoded primers for pyrosequencing hundreds of samples in multiplex. *Nat. Methods* 5 (3), 235–237.
- Hassan, A., Nelson, B., 2012. *Invited review: anaerobic fermentation of dairy food wastewater*. *J. Dairy Sci.* 95 (11), 6188–6203.
- Hoskins, J., Alborn, W.E., Arnold, J., Blaszczyk, L.C., Burgett, S., DeHoff, B.S., Estrem, S.T., Fritz, L., Fu, D.-J., Fuller, W., 2001. Genome of the bacterium *Streptococcus pneumoniae* strain R6. *J. Bacteriol.* 183 (19), 5709–5717.
- Imachi, H., Sakai, S., Sekiguchi, Y., Hanada, S., Kamagata, Y., Ohashi, A., Harada, H., 2008. *Methanolinea tarda* gen. nov., sp. nov., a methane-producing archaeon isolated from a methanogenic digester sludge. *Int. J. Syst. Evol. Microbiol.* 58 (1), 294–301.
- Kampmann, K., Ratering, S., Kramer, I., Schmidt, M., Zerr, W., Schnell, S., 2012. Unexpected stability of *Bacteroidetes* and *Firmicutes* communities in laboratory biogas reactors fed with different defined substrates. *Appl. Environ. Microbiol.* 78 (7), 2106–2119.
- Kilpper-Bälz, R., Schleifer, K.H., 1987. *Streptococcus suis* sp. nov., nom. rev. *Int. J. Syst. Bacteriol.* 37 (2), 160–162.
- Liu, Y.C., Whitman, W.B., 2008. Metabolic, phylogenetic, and ecological diversity of the methanogenic archaea. In: Wiegand, J., Maier, R.J., Adams, M.W.W. (Eds.), *Incredible Anaerobes: From Physiology to Genomics to Fuels*, vol. 1125. Blackwell Publishing, Oxford, pp. 171–189.
- Liu, L., Zhu, Y., Li, J., Wang, M., Lee, P., Du, G., Chen, J., 2012. Microbial production of propionic acid from *Bacteroidetes*: current state, challenges and perspectives. *Crit. Rev. Biotechnol.* 32 (4), 374–381.
- Luo, G., Angelidaki, I., 2013. Co-digestion of manure and whey for in situ biogas upgrading by the addition of H₂: process performance and microbial insights. *Appl. Microbiol. Biotechnol.* 97 (3), 1373–1381.
- Morales, J., Choi, J.S., Kim, D.S., 2006. Production rate of propionic acid in fermentation of cheese whey with enzyme inhibitors. *Environ. Prog.* 25 (3), 228–234.
- Paul, K., Nonoh, J.O., Mikulski, L., Brune, A., 2012. "Methanoplasmatales", Thermoplasmatales-related archaea in termite guts and other environments, are the seventh order of methanogens. *Appl. Environ. Microbiol.* 78 (23), 8245–8253.
- Pope, P.B., Vivekanand, V., Eijsink, V.G., Horn, S.J., 2013. Microbial community structure in a biogas digester utilizing the marine energy crop *Saccharina latissima*. *Biotech* 3 (5), 407–414.
- Rivière, D., Desvignes, V., Pelletier, E., Chaussonnerie, S., Guermazi, S., Weissenbach, J., Li, T., Camacho, P., Sghir, A., 2009. Towards the definition of a core of microorganisms involved in anaerobic digestion of sludge. *The ISME Journal* 3 (6), 700–714.
- Rosewarne, C.P., Pope, P.B., Denman, S.E., McSweeney, C.S., O'Cuiv, P., Morrison, M., 2010. High-yield and phylogenetically robust methods of DNA recovery for analysis of microbial biofilms adherent to plant biomass in the herbivore gut. *Microb. Ecol.* 61 (2), 448–454.
- Sakai, S., Ehara, M., Tseng, I.-C., Yamaguchi, T., Bräuer, S.L., Cadillo-Quiroz, H., Zinder, S.H., Imachi, H., 2012. *Methanolinea mesophila* sp. nov., a hydrogenotrophic methanogen isolated from rice field soil, and proposal of the archaeal family Methanoregulaceae fam. nov. within the order Methanomicrobiales. *Int. J. Syst. Evol. Microbiol.* 62 (6), 1389–1395.
- Schink, B., 1997. Energetics of syntrophic cooperation in methanogenic degradation. *Microbiol. Mol. Biol. Rev.* 61 (2), 262.
- Schnürer, A., Schink, B., Svensson, B.H., 1996. *Clostridium ultunense* sp. nov., a mesophilic bacterium oxidizing acetate in syntrophic association with a hydrogenotrophic methanogenic bacterium. *Int. J. Syst. Bacteriol.* 46 (4), 1145–1152.
- Schnürer, A., Zellner, G., Svensson, B.H., 1999. Mesophilic syntrophic acetate oxidation during methane formation in biogas reactors. *FEMS Microbiol. Ecol.* 29 (3), 249–261.
- Sun, L., Müller, B., Westerholm, M., Schnürer, A., 2014. Syntrophic acetate oxidation in industrial CSTR biogas digesters. *J. Biotechnol.* 171, 39–44.
- Westerholm, M., Levén, L., Schnürer, A., 2012. Bioaugmentation of syntrophic acetate-oxidizing culture in biogas reactors exposed to increasing levels of ammonia. *Appl. Environ. Microbiol.* 78 (21), 7619–7625.
- Yamada, T., Imachi, H., Ohashi, A., Harada, H., Hanada, S., Kamagata, Y., Sekiguchi, Y., 2007. *Bellilinea caldifistulae* gen. nov., sp. nov. and *Longilinea arvorzyae* gen. nov., sp. nov., strictly anaerobic, filamentous bacteria of the phylum Chloroflexi isolated from methanogenic propionate-degrading consortia. *Int. J. Syst. Evol. Microbiol.* 57 (10), 2299–2306.
- Ziganshin, A.M., Liebetrau, J., Pröter, J., Kleinstüber, S., 2013. Microbial community structure and dynamics during anaerobic digestion of various agricultural waste materials. *Appl. Microbiol. Biotechnol.* 97 (11), 5161–5174.

Supplementary material

Microbial community structure and dynamics during co-digestion of whey permeate and cow manure in CSTR systems

Live Haldal Hagen¹, Vivekanand Vivekanand¹, Roar Linjordet², Phillip B. Pope¹, Vincent G.H. Eijsink¹, Svein J. Horn^{1*}

¹ Department of Chemistry, Biotechnology and Food Science, Norwegian University of Life Sciences, P. O. Box 5003, N-1432 Ås, Norway

² Bioforsk, Norwegian Institute for Agricultural and Environmental Research, Frederik A. Dahls vei 20, 1432 Ås, Norway.

*Corresponding author. Department of Chemistry, Biotechnology and Food Science, Norwegian University of Life Sciences, P. O. Box 5003, N-1432 Ås, Norway. Tel.: + 47 67232488; Fax: + 47 64965901. E-mail address: svein.horn@nmbu.no

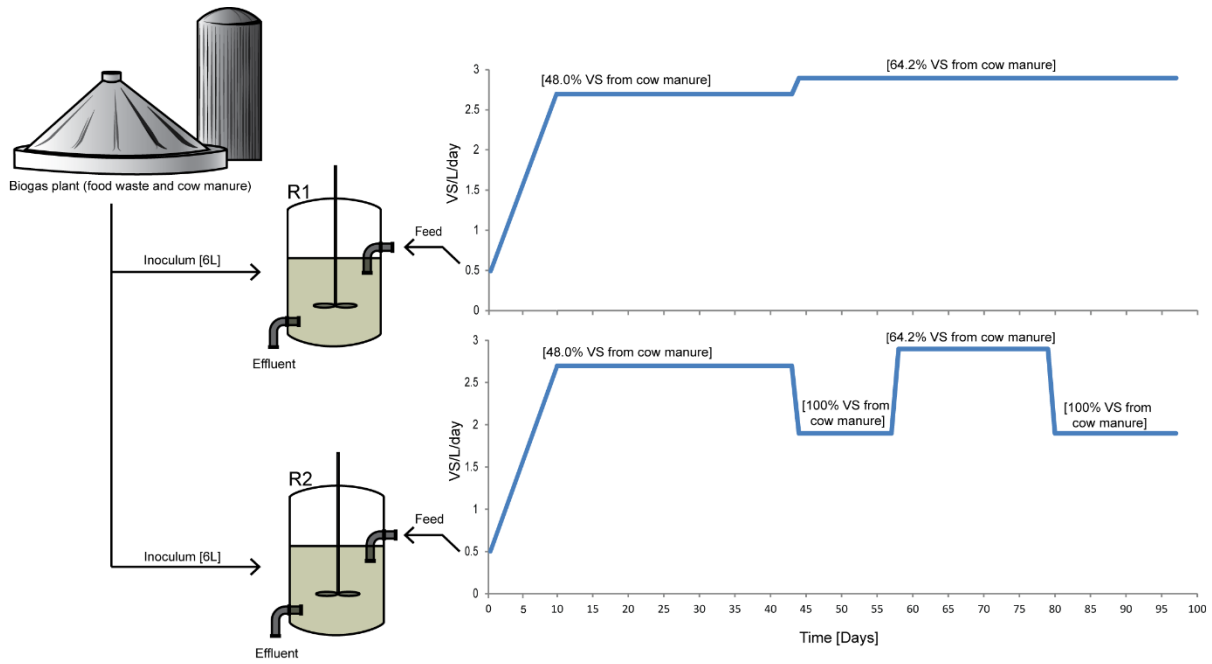


Figure S1: Schematic diagram of the experimental setup. Two laboratory-scale (10 L) continuously stirred tank reactors (CSTR) with a working volume of 6 L were running for 100 days at 37 °C, 180 rpm and a constant hydrolytic retention time of 25 days. Effluent from a biogas plant running on food waste and cow manure was used as inoculum, and both reactors were fed with a mixture of whey and cow manure, gradually increased to reach a final organic loading rate of 2.7 g VS/L/day. Sampling of material for microbial analysis was carried out every 6-7th day, starting at day 12. Changes in the feeding regime was introduced as a consequence of observed VFA accumulation in R2.

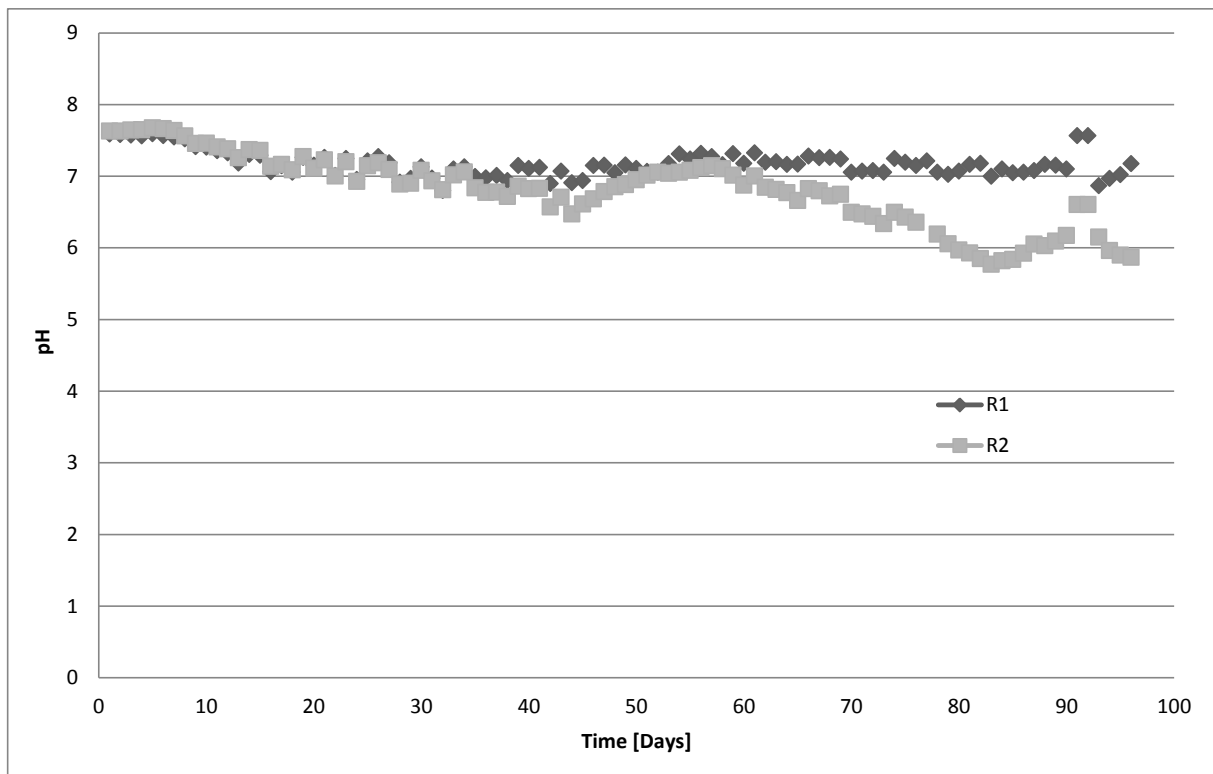
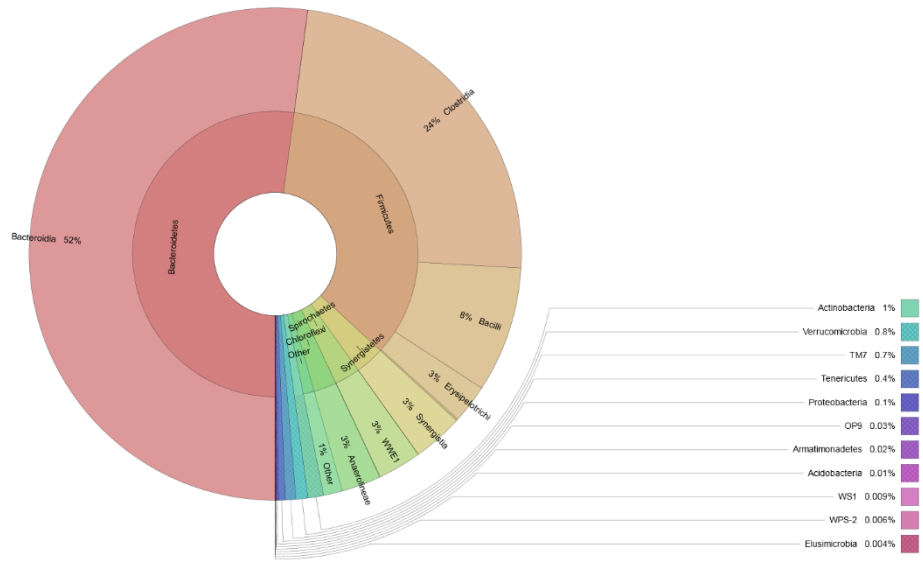
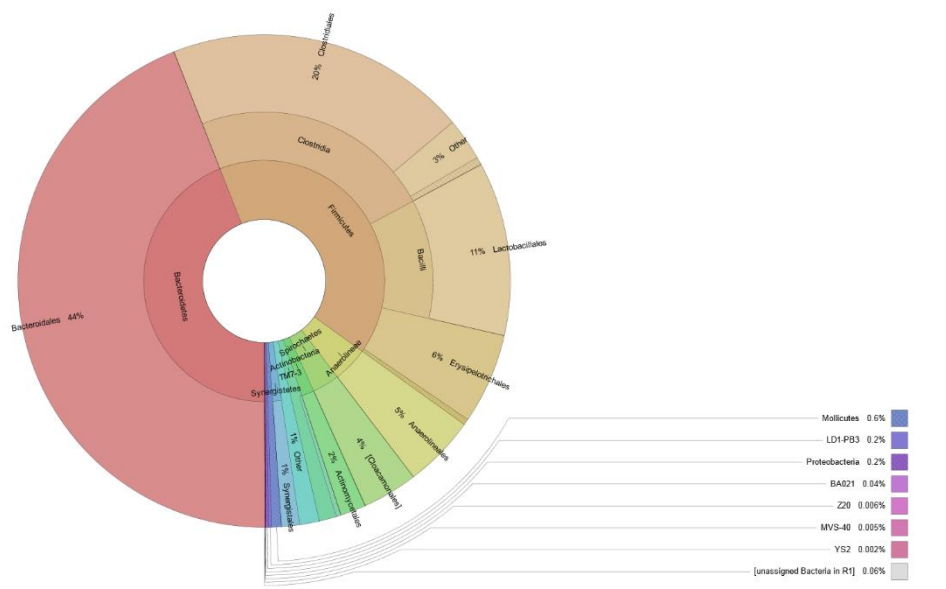


Figure S2. pH measurements for the CSTR reactors R1 and R2. The pH in the stable reactor (R1, black) and the unstable (R2, grey) reactor was continuously measured throughout the digestion period.

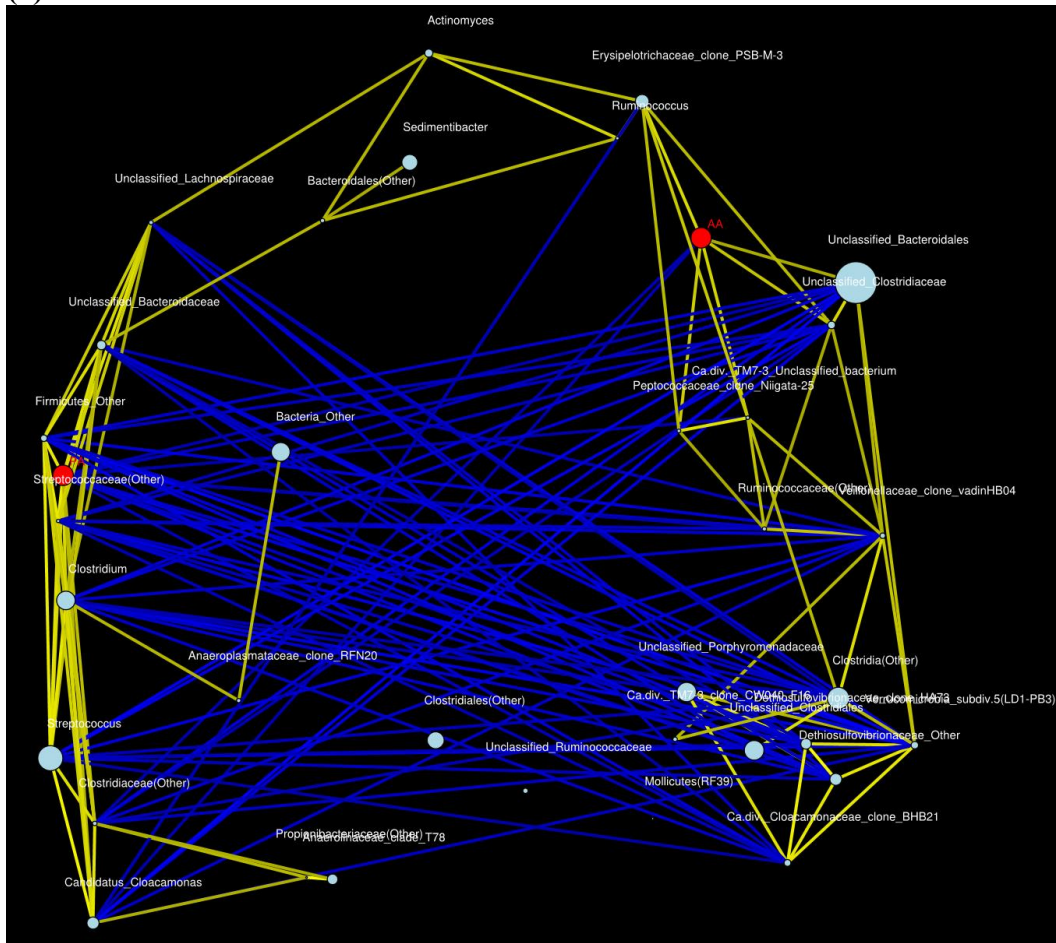
a)



b)



(a)



b)

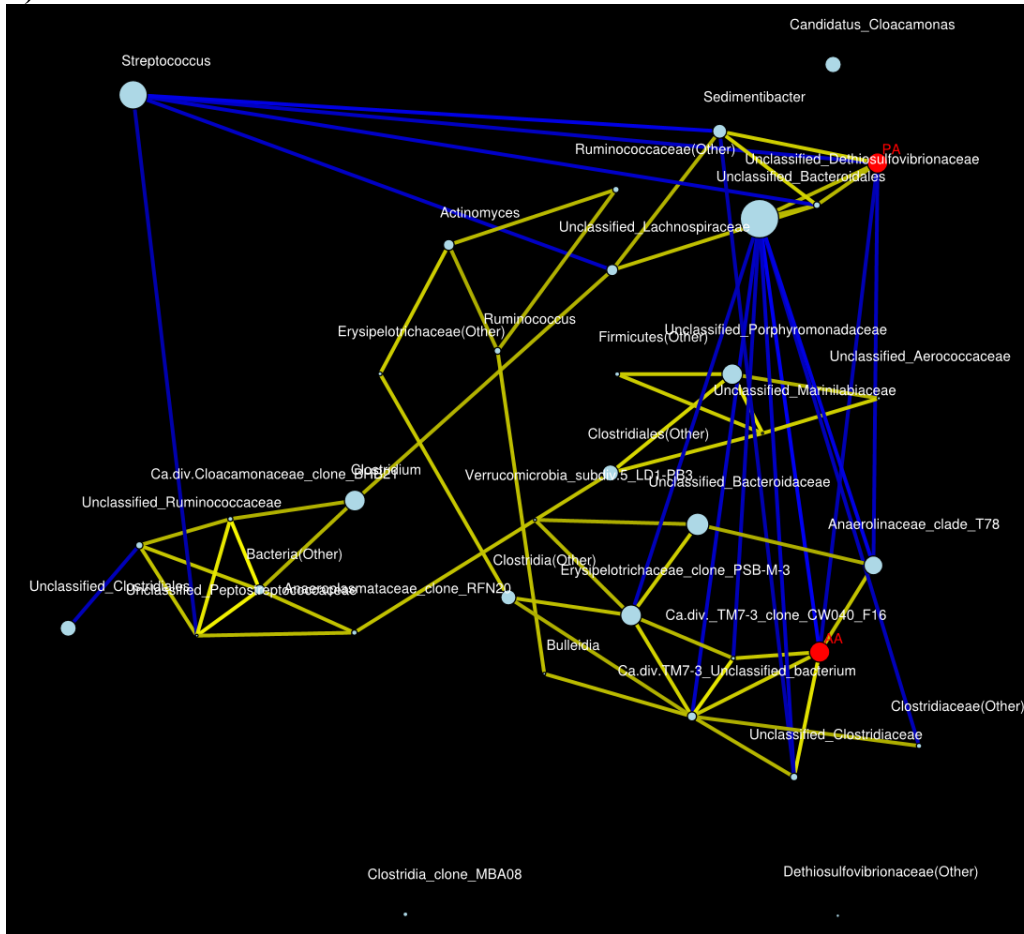


Figure S5. Network map with high abundant genus (>0.5%) Network map of bacteria (genus. Min. prop.: 0.5% reads in at least one sample) and the two specific VFAs propionic acid and acetic acid, showing interactions between all samples of the stable reactor, R1 (a) and the unstable reactor, R2 (b). Positive correlations are marked with yellow line showing co-occurring “events”, while negative correlations are shown as blue lines. Each phylotype is represented by dots, and the size of the dot reflects the relative number of sequences found for this phylotype. Each connection between two nodes stands for a strong (Pearson’s $r > 0.6$) and significant (P -value < 0.05) correlation.

Paper II

The effect of storage conditions on microbial community composition and biomethane potential in a biogas starter culture

Live Haldal Hagen¹ · Vivekanand Vivekanand¹ · Phillip B. Pope¹ · Vincent G. H. Eijsink¹ · Svein J. Horn¹

Received: 6 February 2015 / Revised: 14 April 2015 / Accepted: 18 April 2015 / Published online: 7 May 2015
© Springer-Verlag Berlin Heidelberg 2015

Abstract A new biogas process is initiated by adding a microbial community, typically in the form of a sample collected from a functional biogas plant. This inoculum has considerable impact on the initial performance of a biogas reactor, affecting parameters such as stability, biogas production yields and the overall efficiency of the anaerobic digestion process. In this study, we have analyzed changes in the microbial composition and performance of an inoculum during storage using barcoded pyrosequencing of bacterial and archaeal 16S ribosomal RNA (rRNA) genes, and determination of the biomethane potential, respectively. The inoculum was stored at room temperature, 4 and -20°C for up to 11 months and cellulose was used as a standard substrate to test the biomethane potential. Storage up to 1 month resulted in similar final methane yields, but the rate of methane production was reduced by storage at -20°C . Longer storage times resulted in reduced methane yields and slower production kinetics for all storage conditions, with room temperature and frozen samples consistently giving the best and worst performance, respectively. Both storage time and temperature affected the microbial community composition and methanogenic activity. In particular, fluctuations in the relative abundance of *Bacteroidetes* were observed. Interestingly, a shift from hydrogenotrophic methanogens to methanogens

with the capacity to perform acetoclastic methanogenesis was observed upon prolonged storage. In conclusion, this study suggests that biogas inocula may be stored up to 1 month with low loss of methanogenic activity, and identifies bacterial and archaeal species that are affected by the storage.

Keywords Inoculum · Anaerobic digestion · Methane · Biogas · Bioenergy · Microbial community

Introduction

Because of limited fossil fuel reserves and accumulation of greenhouse gases in the atmosphere, a transition away from fossil fuels is needed (Horn 2013). Thus, alternative energy technologies are under constant consideration, and the production of biogas through anaerobic degradation has become an important component in the global development of renewable fuels (Lorenz et al. 2013; Weiland 2010). Biogas has traditionally been produced by anaerobic digestion (AD) of manure, organic wastes and wastewater, but may also be produced from lignocellulosic biomass (Ahring et al. 2014; Kafle et al. 2013; Vivekanand et al. 2013). A complete anaerobic degradation of organic substrates to biogas is accomplished by a complex microbial community. Large polymers such as polysaccharides, proteins or lipids are hydrolyzed to smaller monomeric subunits (hydrolysis). These monomers are then fermented into organic acids (acidogenesis), and further degraded to simpler compounds such as acetate, formate, CO_2 and H_2 (acetogenesis). Hydrolysis, acidogenesis and acetogenesis are carried out by a large consortium of bacteria, while the final step, methanogenesis, is carried out by a group of specialized archaea called methanogens. Acetoclastic methanogens can utilize acetate directly to produce methane. Hydrogenotrophic methanogens

Electronic supplementary material The online version of this article (doi:10.1007/s00253-015-6623-0) contains supplementary material, which is available to authorized users.

✉ Svein J. Horn
svein.horn@nmbu.no

¹ Department of Chemistry, Biotechnology and Food Science, Norwegian University of Life Sciences, P. O. Box 5003, 1432 Ås, Norway

on the other hand, are exclusively using CO₂ and H₂, and can either utilize these compounds directly from the upstream metabolic network, or in a two-step pathway where the first step, acetate oxidation to CO₂ and H₂, is carried out by syntrophic acetate oxidizing bacteria (SAOB).

Efficient production of biogas depends on many factors including the type of biomass, the use of pretreatments, the digestion temperature, and the availability of nutrients and trace metals (Aubart and Bully 1984; Jimenez et al. 1989; Shehu et al. 2012). Moreover, the inoculum has a major impact on the kinetics, stability and yield of the AD process (Elbeshbishy et al. 2012; Lopes et al. 2004; Raposo et al. 2012). These inocula are usually slurries containing a rich anaerobic microbial community which are used for the start-up of the AD process in a reactor. The functionality of an inoculum may be tested by carrying out batch tests to determine of the biomethane potential (BMP) (Angelidaki et al. 2009) of one or several substrates.

Despite the fact that the inoculum quality is very important for the start-up of AD processes, studies related to storage and preservation of inocula are scarce in literature (Castro et al. 2002). Most of such studies have been carried out on anaerobic granular sludges (Bae et al. 1995; Shin et al. 1993; Wu et al. 1995). Usage of fresh inoculum is often recommended, although it is normally assumed that an inoculum may be stored for limited time periods (Angelidaki et al. 2009; Shelton and Tiedje 1984). To our knowledge, no systematic study has been published evaluating the effect of storage on inoculum performance. Moreover, while the general process of AD leading to methane formation is well known, knowledge regarding composition, interactions and dynamics of the microbial communities involved is still limited. In-depth studies of the phylogenetic diversity of the community may help understanding the process and its limiting factors, with the eventual aim of enhancing biogas production and avoid process failures (Hagen et al. 2014; Westerholm et al. 2012; Ziganshin et al. 2013). We present a systematic study of the effect of inoculum storage at room temperature (RT), 4 and –20 °C for different time periods (1 week; 1, 2, 6 and 11 months) on biogas production rates and yields. Additionally, we have characterized storage-induced changes in the inocula's bacterial and archaeal communities.

Materials and methods

Biogas inoculum

The inoculum used for the storage experiments was collected from a local biogas plant (Tomb Biogas plant, Norway) running large scale continuous anaerobic co-digestion of food waste and cow manure at mesophilic temperature. The inoculum was pre-incubated at 37 °C for 10 days in order to reduce

the residual bio-degradable organic fraction and, thus, endogenous biogas production. To make the inoculum slurry more homogeneous, it was passed through a sieve (5 mm) to remove large particles. The inoculum was then diluted three times with sterile water and 400 mL aliquots were added to 555 mL batch bottles. The diluted inoculum had a total solid (TS) concentration of 1.2 %; the pH was 7.6 and the ammonium concentration 948 ppm. The batch bottles with diluted inoculum (96 bottles) were sealed and immediately transferred to RT (36 bottles), 4 °C (30 bottles) or –20 °C (30 bottles) for storage (Fig. 1). During the inoculum handling described above efforts were made to minimize exposure to air in all steps. To ensure safety, pressure generated in the bottles during long time storage was regularly released by penetrating the septum with a needle. Six of the RT bottles were used immediately for analysis and AD, and are referred to as the fresh sample in this study.

Biogas production

To evaluate the impact of storage on the inoculum, BMP tests of fresh as well as stored samples were carried out. Cellulose (Avicel PH101, Sigma, USA) was used as standard substrate. All BMP tests were conducted in triplicates, meaning that cellulose was added to three bottles, whereas three other bottles used as a control contained the inoculum only. As substrate, 0.60 g of volatile solid (VS; cellulose) was added. The bottles were purged with nitrogen for 2 min to ensure anaerobic conditions, closed with rubber seals and aluminum screw caps and transferred to the shaker (Multitron Standard, Infors HT, Switzerland) for incubation (37 °C, 90 rpm, 40 days) (Vivekanand et al. 2013). The same procedure was followed for all the time points and storage conditions described above. The results are presented with standard deviations derived from the triplicate experiments.

Analysis

TS and ash contents were determined by drying and incinerating the samples at 105 and 550 °C overnight, respectively. The VS content was calculated by subtracting the ash from the TS content.

Gas composition and calculation

Gas composition analysis and calculations were performed as described by Vivekanand et al. (2013). In brief, biogas production was monitored by measuring the generated pressure in the bottle digesters using a digital pressure transducer (GMH 3161, Greisinger Electronic, Germany). Gas composition was analyzed in an Agilent micro gas chromatograph (Agilent Technologies 3000A, USA), equipped with a thermal conductivity (TCD) detector and a Poraplot

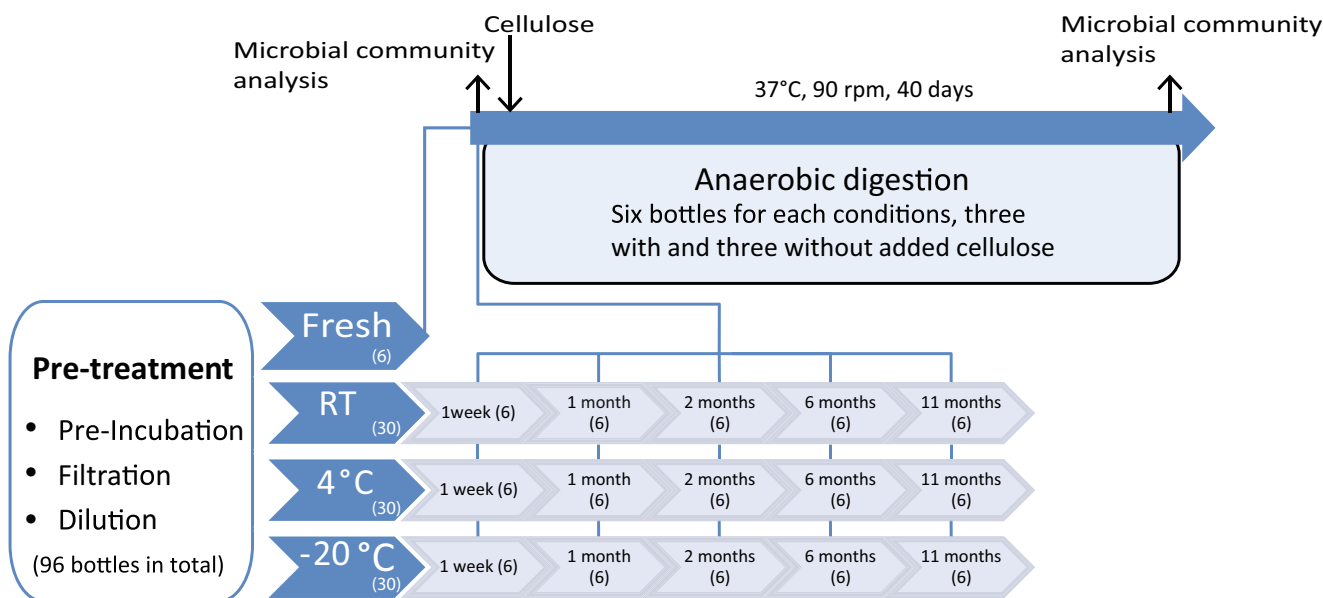


Fig. 1 Schematic illustration of the experimental design. Samples for microbial community analysis were collected immediately after storing and after a subsequent 40 days of AD in batch fermenters with cellulose as substrate. Each time point and storage condition required six bottles,

three with cellulose and three without added cellulose (to correct for endogenous methane production; these bottles were not sampled for community analysis). In total, the experiment required 96 batch bottles

Q column (8 m×0.32 mm; styrene–divinylbenzene polymer) kept at 45 °C.

A standard mixture of carbon dioxide (35 %) and methane (65 %) was utilized for single point calibration. Once the pressure and the gas composition had been analyzed, the overpressure in bottle digesters was released by penetrating the septum with a needle. Using the headspace volume of the bottles and measurements of methane concentrations as input, the ideal gas law was applied for calculating methane production during the experiments. The reported methane yields are the values obtained after subtracting endogenous methane production from the inoculum alone.

Sampling and 454 pyrosequencing

Slurry (1 ml) from the batch digesters was collected for microbial community analysis, both before addition of cellulose and after 40 days of AD. The three samples from the replicates were pooled and mixed thoroughly prior to DNA extractions. DNA was extracted according to Rosewarne et al. (2010), with minor modifications. Amplification of the variable region V1-V3 of bacteria and archaea was carried out with the broadly conserved primer sets 8F-515R (5'-AGAGTTTGATCCTGG-3'/5'-TTACCGCGGCTGCT-3') for bacteria and 340F-1000R (5'-CCCTAYGGGGYGCASCAG-3'/5'-GGCCATGCACYWCYTCTC-3') for archaea (Gantner et al. 2011; Hamady et al. 2008). These primers contained the 454 Life Science primer A sequence and a unique 8-nt multiplex identifier (Hamady et al. 2008). PCR amplifications were performed using iProof High-Fidelity DNA Polymerase

(Bio-Rad, Hercules, CA, USA) with the following cycle conditions: initial denaturation step at 98 °C for 30 s., followed by 30/35 (bacteria/archaea) cycles consisting of 98 °C for 10 s, 58 °C for 30 s and 72 °C for 45 s, completed by a final extension at 72 °C for 7 s. Triplicate amplification of each sample was carried out under identical conditions, but with unique multiplex identifier. DNA quality was checked for DNA degradation and protein impurities by agarose gel electrophoresis. The concentrations of bacterial amplicons were quantified using a Qubit™ fluorometer and the Quant-iT™ dsDNA BR Assay Kit (Invitrogen), while the concentration of archaeal amplicons was quantified by agarose gel electrophoresis and the software *Quantity One band intensity calculation* (Bio-Rad Laboratories). Equimolar concentrations of bacterial and archaeal amplicons were pooled prior to purification with NucleoSpin® Extract II columns (Machery-Nagel, Düren, Germany). Four hundred fifty four pyrosequencing was performed in a GS FLX system (Roche) at the Norwegian High-Throughput Sequencing Centre (NSC, Oslo, Norway).

All reads were processed using the QIIME v.1.6.0 software package (Caporaso et al. 2010), and reads were removed if they contained homopolymer run exceeding 6 nt, were shorter than 350 nt in length and/or had a mean quality score below 25. Chimera reads were removed from the dataset using UCHIME incorporated in USEARCH (Edgar et al. 2011). A threshold of 3 % dissimilarity ('species level') between 16S ribosomal RNA (rRNA) gene sequences was used to cluster reads into operational taxonomic units (OTUs) (Edgar 2010). Ribosomal Database Project (RDP) Classifier with a

confidence threshold of 0.8 was used to assign the OTUs to known taxons (Wang et al. 2007). Singletons were excluded by filtering out OTUs observed fewer than two times across all samples. The samples were further normalized to the smallest library to remove sample heterogeneity, thus generating the final datasets used for diversity analysis. A principal coordinate analysis (PCoA) of unweighted UniFrac distances was used to determine how the diversity among samples changed in response to storage time and temperature. To determine if the differences observed in the PCoA plot were significant, a statistical significant test was applied on the unweighted UniFrac distance matrices. The parametric *p*-values were calculated performing two-sample Student's *t*-tests, while nonparametric *p*-values were calculated using Monte Carlo permutation ($n=1000$). Community profiles were visualized as OTU heatmaps with hierarchical clustering that were generated using Calypso v.3.4 (<http://bioinfo.qimr.edu.au/calypso/>).

Data accessibility

Sequence data are available at NCBI Short Read Archive under accession number SRP049062.

Results

Biogas production from inocula stored under different conditions

The performance of fresh as well as stored inoculum samples was analyzed by determining the BMP of cellulose. Cumulative methane production curves for all samples are shown in Fig. 2. The final methane yield from the fresh inoculum was 372 mL/gVS (Fig. 2a) and reached a plateau after about 20 days of incubation, most likely due to complete degradation of cellulose. Figure 2 shows that storage time up to 1 month did not affect methane yields, regardless of the storage temperature. However, although the final biogas yields for the frozen inoculum were similar to those for inocula stored at RT or 4 °C, the initial rate of the biogas production was lower, indicating slow recovery of the microbial community after preservation by freezing (Fig. 2b and c). Longer term storage (between 2 and 11 months) resulted in both reduced rates and yields of biogas production for all storage conditions (Fig. 2d–f), with storage at RT giving the best results and storage at –20 °C the worst. Moreover, inocula stored for 6 and 11 months performed equally.

Characterization of microbial communities

Microbial community compositions were characterized using 16S rRNA gene sequencing. In total, 336, 107 and 236,824 raw reads were obtained from the amplicon library originating

from this inoculum storage study. Of these, 296,287 bacterial and 226,558 archaeal 16S rRNA sequences had sufficient quality (longer than 350 nt, mean quality score above 25) for downstream analysis. Of the sequences, 19.9 and 9.8 % (bacteria and archaea, respectively) were further discharged as chimeras or singletons. Finally, an average of 2508 and 2684 (bacteria and archaea, respectively) reads per amplicon sample were obtained, and normalized to the smallest library size (1210 bacteria reads/amplicon sample and 1000 archaea reads/amplicon sample) for downstream analysis. Sample coverage (Good's coverage) for each amplicon sample is given in Supplemental Table S1. Figure 3 shows community-level comparisons of the samples based on unweighted UniFrac (qualitative β -diversity) phylogenetic distances. Each point represents the community in a specific sample (three points per sample due to triplicated amplification), and points within dashed circles originate from samples collected prior to AD of cellulose. Statistical analyses performed on unweighted UniFrac distance matrices for significance testing can be found in the Supplementary material, Figure S1 and Table S2.

Comparison of the two principle coordinate (PCoA) plots in Fig. 3 (a and b), color coded for either temperature or time, shows that bacterial communities cluster more distinctly due to time of storage (Fig. 3b) than temperature of storage (Fig. 3a). The bacterial communities present after storage and before AD (inside dashed circles) appear in two clusters; one comprising the samples originating from fresh inoculum and those stored for less than 1 month, whereas the other contains the majority of samples originating from inoculum stored for 1 month or longer (with the exception of samples stored at –20 °C for 1 month; Fig. 3b). Notably, the present analysis does not discriminate between dead and viable cells and both factors need to be taken into account when interpreting Fig. 3. In particular, the clustering of inocula frozen for 1 month with fresh inocula, rather than with inocula stored for 1 month under other conditions, could be due to better preservation of the DNA of dead bacteria.

Comparison of the data for samples taken after 40 days of AD shows clustering of the fresh inocula and inocula stored for 1 week at RT or 4 °C. Similar to the samples taken prior to AD, time of storage (Fig. 3b) had greater influence on the community composition than temperature (Fig. 3a). The data clearly show that freezing (Fig. 3a, Fig. S1a) and long-time storage (11 months; Fig. 3b, Fig. S1b) have a significant effect on the community, as suggested by the effect of both factors on biogas production (Fig. 2). Somewhat surprisingly, inocula stored for 1 month at RT or 4 °C cluster in the proximity of less-well-performing inocula stored for longer periods, while they perform as well as fresh inocula in terms of methane yield (Fig. 2c). With exception of this observation, the bacterial community data displayed in Fig. 3 show clear effects of storage that correlate with observed changes in the performance of the inoculum in AD. In terms of the archaeal communities

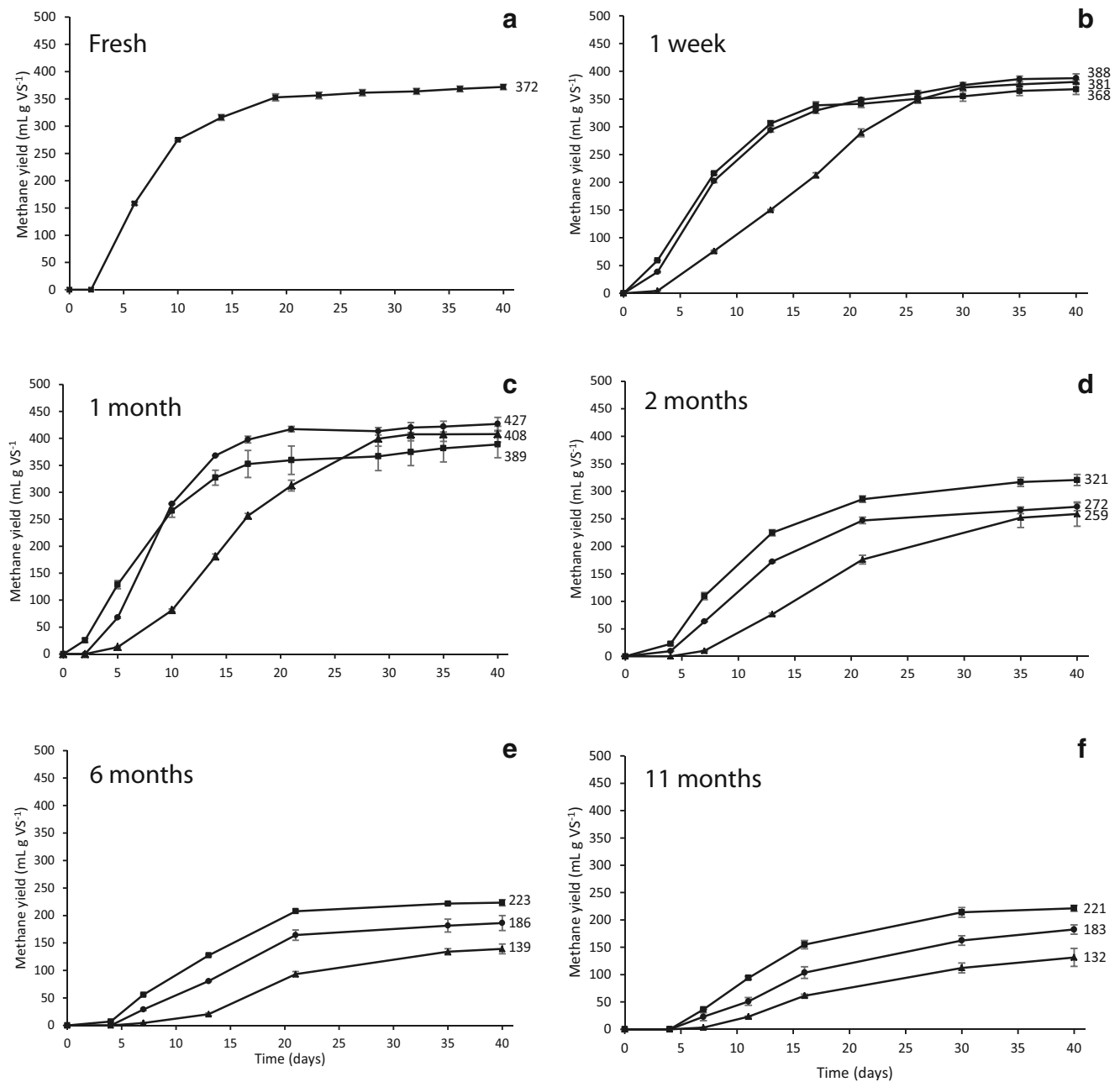


Fig. 2 Methane production from fresh and stored inocula. **a**, fresh; **b**, 1 week; **c**, 1 month; **d**, 2 months; **e**, 6 months; **f**, 11 months. (■), room temperature (RT); (●), 4 °C; (▲), -20 °C. Endogenous methane

production from the inoculum alone, measured in parallel control digestions without added substrate, was subtracted. The error bars indicate the standard deviation for the triplicates

before AD, the samples cluster more or less together (Fig. 3c and d), yet are less defined than the bacterial component of the communities. Samples collected after AD show clustering of the archaeal communities based on temperature (Fig. 3c) rather than time (Fig. 3d). The samples stored at -20 °C segregate from the other samples, which form a dispersed cluster. The structural shift in the archaeal composition of inoculum stored at freezing compared to fresh and/or to those stored at room temperature and 4 °C was statistically significant (Supplemental Figure S1c-e).

Figure 4a shows that overall, *Bacteroidetes*, *Firmicutes* and *Spirochaetes* dominated the bacterial phyla, whereas the less abundant but still consistently observed phyla included *Synergistetes*, *Chloroflexi* and *Proteobacteria*. It also illustrates considerable variation in the microbial communities in relation to both time and storage temperature. Quite consistently, conditions that reduced biogas yields, i.e. storage for longer time and/or lower temperature (Fig. 2) were associated with a decrease in the abundance of *Bacteroidetes* accompanied by an increase in the relative abundance of the

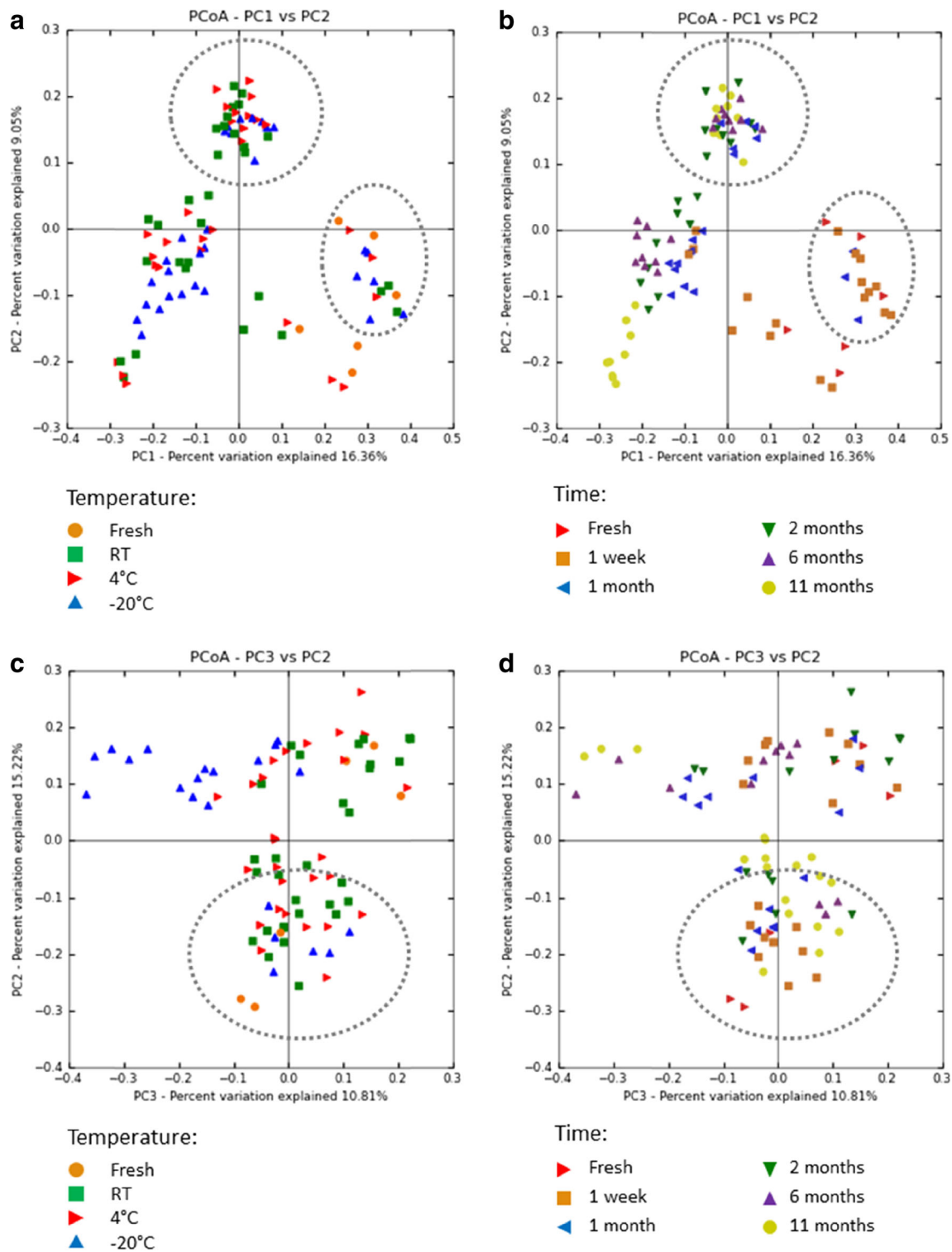


Fig. 3 Principal coordinate analysis (PCoA) of unweighted UniFrac phylogenetic distances between bacterial (**a,b**) and archaeal (**c,d**) communities. The PCoA plots address the effect of storage temperature (*left panels*; **a**, bacteria; **c**, archaea) and the duration of storage (*right panels*; **b**, bacteria; **d**, archaea). The *dots* found within the *dashed circle* (*s*)

originate from samples taken prior to the addition of cellulose, while the other dots represent samples taken after 40 days of digestion. The total number of samples in each plot is 96: 45 samples before adding cellulose (three storage conditions, five storage times, three replicates) + 45 samples after digestion of cellulose + 3 fresh samples before and after digestion of cellulose)

Firmicutes. Although the relative abundance of several bacteria phylotypes fluctuated in relation to storage conditions, overall

community compositions look quite similar as also indicated by the clustering, albeit disperse, shown in Fig. 3a and b. The

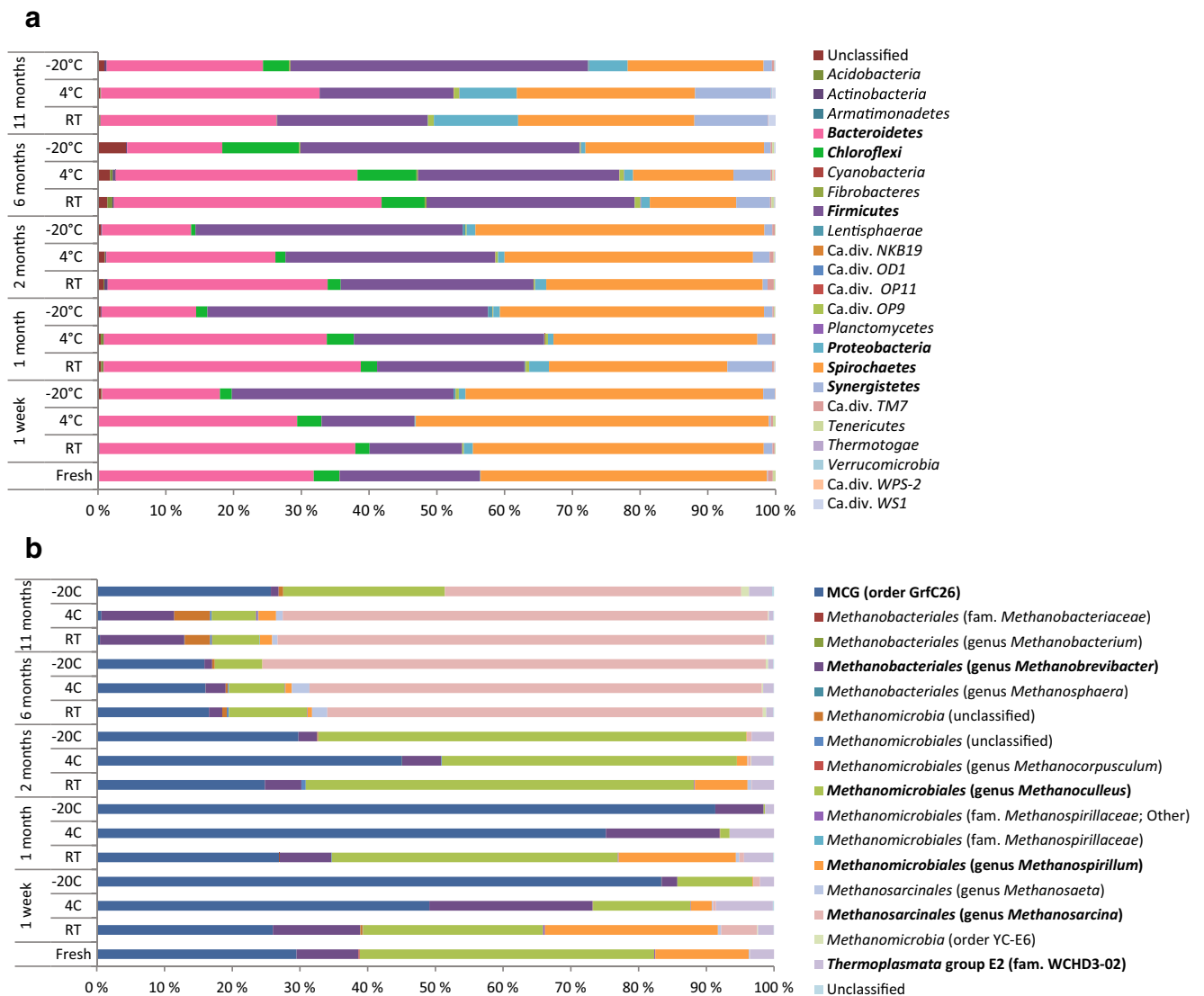


Fig. 4 Abundance of phylotypes in inoculum stored under different conditions. The graphs show the relative abundance (% of total 16S rRNA sequences) of bacteria, at the phylum level (a), and archaea, at the order level (b) identified in batch digesters after anaerobe digestion of cellulose for 40 days at 37 °C, using an inoculum stored at room

temperature, 4 or –20 °C for different periods of time. In this graph, sequences representing triplicated amplicon for the same sample were compiled. The names of the most abundant phylotypes are printed in bold face

three conditions that seem to segregate from the dispersed cluster of Fig. 3a and b (fresh + storage for 1 week at RT or 4 °C) show quite similar bacterial communities (Fig. 4a). Samples stored for 11 months form a subcluster in Fig. 3b. Figure 4a shows that one of the most prominent peculiarities of these samples is a relatively large fraction of *Proteobacteria*.

Figure 4b shows large variation in the archaeal communities. Freezing had a considerable effect, regardless of storage time, initially manifested as an increasing dominance of “Miscellaneous Crenarchaeota Group” (MCG) and reduction in the relevant abundance of the hydrogenotrophic *Methanomicrobiales*. Generally, *Methanomicrobiales* (genus; *Methanoculleus*) and MCG (clone GrfC26) were the prominent

archaea after AD with inoculum stored up to 2 months. After 1 month of storage, major shifts occurred. First, after 2 months of storage, increased relative abundance of hydrogenotrophic *Methanomicrobiales* was observed, also in the frozen samples, but longer storage led to a marked shift from hydrogenotrophic methanogens to methanogens also capable of acetolastic methanogenesis, reflected in a strong dominance of *Methanosarcinales* (genus; *Methanosarcina*) in all samples stored for 6 or 11 months (Fig. 4b). The marked changes in archaeal community composition were also evident in the UniFrac analysis (Fig. 3c and d), indicating that storing the inoculum for more than 2 months at RT, 4 and –20 °C not only affected the relative abundance of specific organisms

but also the overall community composition and the ability of specific subpopulations to recover from storage.

Identification of microorganisms sensitive to storage

Because the storage strategy clearly affected the composition of the microbial community and the relative abundance of several bacterial and archaeal lineages, we attempted to identify the effect of storage on specific species. The abundance of operational taxonomic units (OTUs) was assessed for all samples collected after AD. In total, 1308 bacterial OTUs and 177 archaeal OTUs were obtained and a listing of the most abundant OTUs is shown in Table 1.

Overall, the most abundant bacterial OTUs in the total dataset for samples collected after 40 days of AD revealed a predominance of BAC_OTU2 (*Bacteroidales*), BAC_OTU1 (*Candidatus Cloacimonas*) and BAC_OTU 253 (*Candidatus Cloacimonas*). The most abundant Archaeal OTU by far was ARC_OTU1 (MCG), followed by OTUs like ARC_OTU 4 (*Methanoculleus*), ARC_OTU5 and ARC_OTU9 (both *Methanosarcina*). To assess the sensitivity of individual species, the OTUs were clustered into bacterial (Fig. 5a) and archaeal (Fig. 5b) heatmaps. In the bacterial community, BAC_OTU1 and BAC_OTU253 (Fig. 5a), both classified as *Candidatus Cloacimonas*, diminished upon storage for longer than 1 month. The relative abundance of two major OTUs related to *Bacteroidetes/Bacteroidales* (BAC_OTU2 and BAC_OTU14) also decreased with more extreme storage conditions, as well as a decline of the *Ruminococcaceae*-related OTU, BAC_OTU3. On the other hand, an increase of several OTUs was seen in inoculum stored over longer time, e.g. BAC_OTU38 and BAC_OTU46 (both β -*Proteobacteria* belonging to the family *Alcaligenaceae*).

The heatmap for the archaea (Fig. 5b) indicates that predominant ARC_OTU2, affiliated to hydrogenotrophic *Methanospirillum*, is sensitive to storing, as the scaled and normalized abundance decreased drastically when kept at cold temperature (both 4 and -20 °C) as well as at room temperature for more than 1 month. The same pattern was observed for ARC_OTU4 and ARC_OTU145, both affiliated to the overall dominant lineage of hydrogenotrophic *Methanoculleus*. Another dominant hydrogenotrophic methanogen, *Methanobravibacter* (ARC_OTU3) seemed to thrive at 4 °C, but tolerated storage over longer time poorly. The heatmap further shows that the relative abundance of several *Methanosarcinales*-related OTUs, including ARC_OTU0, ARC_OTU5, ARC_OTU9, OTU20, ARC_OTU24 and ARC_OTU44, increases after storage for 6 or 11 months (Fig. 4b). Additionally, ARC_OTU21, ARC_OTU75 and ARC_OTU179 all belonging to *Methanosarcinales* also show a similar pattern in the heatmap, but are overall less abundant (not shown in Table 1).

Discussion

The present study provides a comparison of a starter culture (inoculum) stored at different temperatures and times to investigate how such storage influences the microbial community and its ability to produce methane. The result reveals that storage of inoculum affects both methane production and microbial community composition.

The methane production data (Fig. 2) show that room temperature is the best storage temperature for the inoculum applied in this study. Storing the inoculum at -20 °C for 6 and 11 months had the most negative impact, reducing the methane yield by more than 60 % compared to the yield obtained with fresh inoculum. As for acceptable storage times, the results presented in Fig. 2 clearly show that storage of inocula used for anaerobic degradation should not exceed 1 month. The observed methane yields from this experiment are in good agreement with methane yields from cellulose reported by other researchers (Díaz et al. 2011; Risberg et al. 2013). Thus, the fresh inoculum was a well-functioning microbial community for biogas production from cellulose. The microbial groups dominating in this inoculum, *Bacteroidales*, *Candidatus Cloacimonas*, MCG, *Methanoculleus* and *Methanosarcina* are in agreement with the microbial community compositions found in CSTR biogas reactors inoculated from the same biogas plant (Hagen et al. 2014).

Previous studies attempting to assess the impact of storage on microbial communities have yielded conflicting results. In a recent study, Rubin et al. concluded that both storage time (up to 14 days) and temperature (RT, 4 and -20 °C) affect the microbial community composition in soil samples, yet only to a minor extent compared to the diversity of communities across individual sample sites (Rubin et al. 2013). Lauber et al. (2010) observed that storage for up to 14 days at different storage temperatures (20, 4, -20 or -80 °C) did not have significant effects on microbial communities in samples from a variety of habitats. In contrast, both Ott et al. (2004) and Tzeneva et al. (2009) observed considerable changes in the microbial diversity after storing of fecal and soil samples, respectively. All these previous studies focused on the bacterial composition immediately after storage, which yield limited information due to the inability to separate dead and live cells.

The unique contribution of this study is the evaluation of longer storage times and the investigation of the functional potential of the community, which relates to viability, after storage. To the best of our knowledge, this is also the first study to investigate storage effects on both archaea and bacteria. Our findings indicate that storage up to 1 month has only moderate effects on community performance in AD.

A large fraction of the microbial community in the fresh inoculum belonged to the *Bacteroidetes* and the *Spirochaetes* phyla. In general, *Bacteroidetes* seemed to handle extreme

Table 1 Lists of archaeal (ARC) and bacterial (BAC) operational taxonomic units (OTU) that were most abundant after anaerobic digestion (40 days, 37 °C) of cellulose in reactors that were inoculated with stored inoculum

ID archaea	Count ^a	% of total count ^b	Consensus lineage	ID bacteria	Count ^a	% of total count ^b	Consensus lineage
ARC_OTU1	6281	13.09	MCG (pGrfC26)	BAC_OTU2	5579	9.61	<i>Bacteroidetes</i> ; o_ <i>Bacteroidales</i>
ARC_OTU5	3803	7.92	<i>Methanosarcinales</i> ; g_ <i>Methanosarcina</i>	BAC_OTU1	5380	9.26	<i>Spirochaetes</i> ; g_ <i>Candidatus</i> <i>Cloacimonas</i>
ARC_OTU4	3348	6.98	<i>Methanomicrobiales</i> ; g_ <i>Methanoculleus</i>	BAC_OTU253	5084	8.75	<i>Spirochaetes</i> ; g_ <i>Candidatus</i> <i>Cloacimonas</i>
ARC_OTU9	3304	6.88	<i>Methanosarcinales</i> ; g_ <i>Methanosarcina</i>	BAC_OTU1221	3394	5.84	<i>Spirochaetes</i> ; g_ <i>Candidatus</i> <i>Cloacimonas</i>
ARC_OTU3	2881	6.00	<i>Methanobacteriales</i> ; g_ <i>Methanobrevibacter</i>	BAC_OTU6	3275	5.64	<i>Spirochaetes</i> ; g_ <i>Treponema</i>
ARC_OTU163	2509	5.23	MCG (pGrfC26)	BAC_OTU3	1799	3.10	<i>Firmicutes</i> ; f_ <i>Ruminococcaceae</i>
ARC_OTU36	2204	4.59	MCG (pGrfC26)	BAC_OTU7	1502	2.59	<i>Firmicutes</i> ; g_ <i>Clostridium</i>
ARC_OTU2	2111	4.40	<i>Methanomicrobiales</i> ; g_ <i>Methanospirillum</i>	BAC_OTU0	1469	2.53	<i>Bacteroidetes</i> ; o_ <i>Bacteroidales</i>
ARC_OTU25	2084	4.34	MCG (pGrfC26)	BAC_OTU4	1457	2.51	<i>Bacteroidetes</i> ; f_ <i>Porphyromonadaceae</i>
ARC_OTU12	1889	3.94	<i>Methanomicrobiales</i> ; g_ <i>Methanoculleus</i>	BAC_OTU12	1077	1.85	<i>Firmicutes</i> ; c_ <i>Clostridia</i> (OPB54)
ARC_OTU7	1326	2.76	MCG (pGrfC26)	BAC_OTU5	940	1.62	<i>Chloroflexi</i> ; f_ <i>Anaerolineaceae</i> (T78)
ARC_OTU32	1324	2.76	<i>Methanomicrobiales</i> ; g_ <i>Methanoculleus</i>	BAC_OTU24	865	1.49	<i>Firmicutes</i> ; g_ <i>Clostridium</i>
ARC_OTU24	1128	2.35	<i>Methanosarcinales</i> ; g_ <i>Methanosarcina</i>	BAC_OTU11	747	1.29	<i>Bacteroidetes</i> ; f_ <i>Porphyromonadaceae</i>
ARC_OTU0	1087	2.26	<i>Methanosarcinales</i> ; g_ <i>Methanosarcina</i>	BAC_OTU14	522	0.90	<i>Bacteroidetes</i> ; o_ <i>Bacteroidales</i>
ARC_OTU63	1003	2.09	<i>Methanomicrobiales</i> ; g_ <i>Methanoculleus</i>	BAC_OTU13	513	0.88	<i>Firmicutes</i> ; g_ <i>Clostridium</i>
ARC_OTU8	918	1.91	<i>Methanomicrobiales</i> ; g_ <i>Methanoculleus</i>	BAC_OTU593	484	0.83	<i>Bacteroidetes</i> ; f_ <i>Porphyromonadaceae</i>
ARC_OTU26	701	1.46	<i>Methanomicrobiales</i> ; g_ <i>Methanoculleus</i>	BAC_OTU28	449	0.77	<i>Firmicutes</i> ; g_ <i>Clostridium</i>
ARC_OTU44	575	1.20	<i>Methanosarcinales</i> ; g_ <i>Methanosarcina</i>	BAC_OTU21	445	0.77	<i>Synergistetes</i> ; f_ <i>Thermovirgaceae</i>
ARC_OTU13	530	1.10	<i>Methanomicrobiales</i> ; s_ <i>Methanoculleus</i> <i>bourgensis</i>	BAC_OTU10	435	0.75	<i>Firmicutes</i> ; g_ <i>Clostridium</i>
ARC_OTU20	487	1.01	<i>Methanosarcinales</i> ; g_ <i>Methanosarcina</i>	BAC_OTU30	419	0.72	<i>Bacteroidetes</i> ; f_ <i>Marinilabiaceae</i>
ARC_OTU10	472	0.98	Thermoplasmata group E2 (WCHD3-02)	BAC_OTU398	399	0.69	<i>Bacteroidetes</i> ; o_ <i>Bacteroidales</i>
ARC_OTU145	417	0.87	<i>Methanomicrobiales</i> ; g_ <i>Methanoculleus</i>	BAC_OTU25	385	0.66	<i>Bacteroidetes</i> ; f_ <i>Porphyromonadaceae</i>
ARC_OTU43	399	0.83	MCG (pGrfC26)	BAC_OTU1225	377	0.66	<i>Spirochaetes</i> ; g_ <i>Candidatus</i> <i>Cloacimonas</i>
ARC_OTU15	388	0.81	<i>Methanomicrobiales</i> ; g_ <i>Methanoculleus</i>	BAC_OTU23	370	0.65	<i>Firmicutes</i> ; c_ RF3 (ML615J-28)
ARC_OTU38	310	0.65	MCG (pGrfC26)	BAC_OTU33	328	0.65	<i>Firmicutes</i> ; g_ <i>Sedimentibacter</i>
ARC_OTU179	308	0.64	<i>Methanosarcinales</i> ; g_ <i>Methanosarcina</i>	BAC_OTU130	319	0.64	<i>Spirochaetes</i> ; g_ <i>Candidatus</i> <i>Cloacimonas</i>
ARC_OTU11	298	0.62	Thermoplasmata group E2 (WCHD3-02)	BAC_OTU38	284	0.56	<i>Proteobacteria</i> ; f_ <i>Alcaligenaceae</i>
ARC_OTU21	289	0.60	c_ <i>Methanomicrobia</i>	BAC_OTU46	280	0.55	<i>Proteobacteria</i> ; f_ <i>Alcaligenaceae</i>
ARC_OTU64	279	0.58	MCG (pGrfC26)	BAC_OTU9	264	0.51	<i>Firmicutes</i> ; f_ <i>Clostridiaceae</i>
ARC_OTU75	274	0.57	<i>Methanosarcinales</i> ; g_ <i>Methanosarcina</i>	BAC_OTU499	243	0.49	<i>Spirochaetes</i> ; g_ <i>Treponema</i>
ARC_OTU31	236	0.49	MCG (pGrfC26)	BAC_OTU57	236	0.49	<i>Synergistetes</i> ; g_ <i>Aminobacterium</i>
ARC_OTU6	219	0.46	<i>Methanobacteriales</i> ; g_ <i>Methanobrevibacter</i>	BAC_OTU60	236	0.48	<i>Chloroflexi</i> ; f_ <i>Anaerolineaceae</i> (T78)

Table 1 (continued)

ID archaea	Count ^a	% of total count ^b	Consensus lineage	ID bacteria	Count ^a	% of total count ^b	Consensus lineage
ARC_OTU19	175	0.36	Thermoplasmata group E2 (WCHD3-02)	BAC_OTU51	189	0.47	<i>Proteobacteria</i> ; f_ <i>Alcaligenaceae</i>
ARC_OTU22	171	0.36	MCG (pGrfC26)	BAC_OTU40	187	0.46	Unclassified bacteria
ARC_OTU76	110	0.23	<i>Methanomicrobiales</i> ; g_ <i>Methanoculleus</i>				

The relative abundances relate to the complete dataset comprising all 40-day samples, and the table only displays OTUs representing $\geq 2\%$ of total reads in at least one sample. The development in the relative abundance of these OTUs in response to temperature and storage time is addressed in the main text and in Fig. 5, showing heatmaps. The OTUs were assigned to consensus lineages using RDP classifier. Taxa are mostly indicated at order level (archaea) or phylum level (bacteria); in addition, the deepest possible lineages are displayed (c; class, f; family, g; genus, s; species)

^a Indicates the total number of reads associated to the respective OTU, only captured for samples collected after 40 days of anaerobic digestion with cellulose as reference substrate

^b Proportion of reads associated to the respective OTU, shown as percentage of all reads for archaea after 40 days of AD, including low abundant not given in the current table

storage conditions (i.e. longer time and/or colder temperature) more poorly than members of the phylum *Firmicutes*. Several members of *Bacteroidetes* have the ability to hydrolyze cellulose (Hatamoto et al. 2014; Naas et al. 2014). Thus, the waning presence of in particular two major OTUs related to *Bacteroidetes/Bacteroidales* (BAC_OTU2 and BAC_OTU14), coinciding with an overall decrease in the relative abundance of the phylum *Bacteroidetes* (Fig. 4a), could lead to reduced biomass depolymerization activity and, thus, a decrease in BMP. Moreover, *Ruminococcaceae* (phylum *Firmicutes*) consist of several well-known cellulolytic bacteria species abundant in the digestive tracts of ruminants, and the decline of *Ruminococcaceae*-related OTUs during storage may also, to some extent, explain the decreased BMP. Another bacterium decreasing with inoculum storage was the uncultured bacterium *Candidatus Cloacimonas*. *Candidatus Cloacimonas* is thought to play a central role in syntrophic degradation of acetic acids in cooperation with hydrogen consumers (Chouari et al. 2005; Solli et al. 2014). As several hydrogenotrophic methanogens did also tolerate storage over time poorly, this indicates a reduced methane production by the syntrophic pathway after long term storage. Methane was still produced, albeit at decreased rates, indicating an increased role of the acetoclastic pathway to convert acetate to methane. Interestingly, several bacterial OTUs were enriched after AD with inoculum stored over longer periods. Two of these OTUs, BAC_OTU38 and BAC_OTU46 belong to the family *Alcaligenaceae*, which are known to thrive in cold environments (Zilouei et al. 2006).

The methanogens in the archaeal community were also influenced by storage condition of the inoculum. The increased relative abundance at long time storage of OTUs affiliated to *Methanosarcinales* strongly indicates that species belonging to this mixotrophic (capable of both acetoclastic and hydrogenotrophic methanogenesis) lineage

generally tolerate storage over longer periods and/or lower temperature better than other methanogens found in the current inoculum. In general, *Methanosarcina* sp. is assumed to be more resistant than most other methanogens towards several forms of stress, including temperature (De Vrieze et al. 2012). Moreover, *Methanosarcina* has previously been shown to be active in natural habitats with moderate to cold temperatures (Schmidt et al. 2014). The fact that this methanogen grows in aggregates might make them less vulnerable to external stresses, and they also have a relatively high growth rate (Ferry 1993). Our microbial community data indicates that cold and/or long term storage of methanogenic microbial cultures might lead to a shift from hydrogenotrophic to acetoclastic methane production. This hypothesis is reinforced by the decrease of SAOB. Interestingly, such shifts from hydrogenotrophic to acetoclastic methanogenesis have recently been shown to occur after thawing permafrost (McCalley et al. 2014). However, it should be emphasized that relative abundance in general does not necessarily reflect microbial activity. The lag phase prolonged and methane production declined when the inoculum used for AD was stored for long time and at cold temperatures, indicating that the observed community composition (i.e. increased abundance of *Methanosarcina*) reflects the presence of this methanogens rather than its methanogenic activity. Analysis of short-chain fatty acid concentrations in the batch bottles at day 40 revealed that there were no accumulations of acetic acid, propionic acid or butyric acid. pH was also stable and similar in all the batch bottles (results not included). This indicates that lower production of methane was a result of less degradation of the cellulose substrate, i.e. that the hydrolysis step was rate-limiting. Previous studies have found that the methanogenesis rather than hydrolysis/acidogenesis is the rate-limiting step at psychrophilic temperatures (Bowen et al. 2014; Kotsyurbenko et al. 2001). In

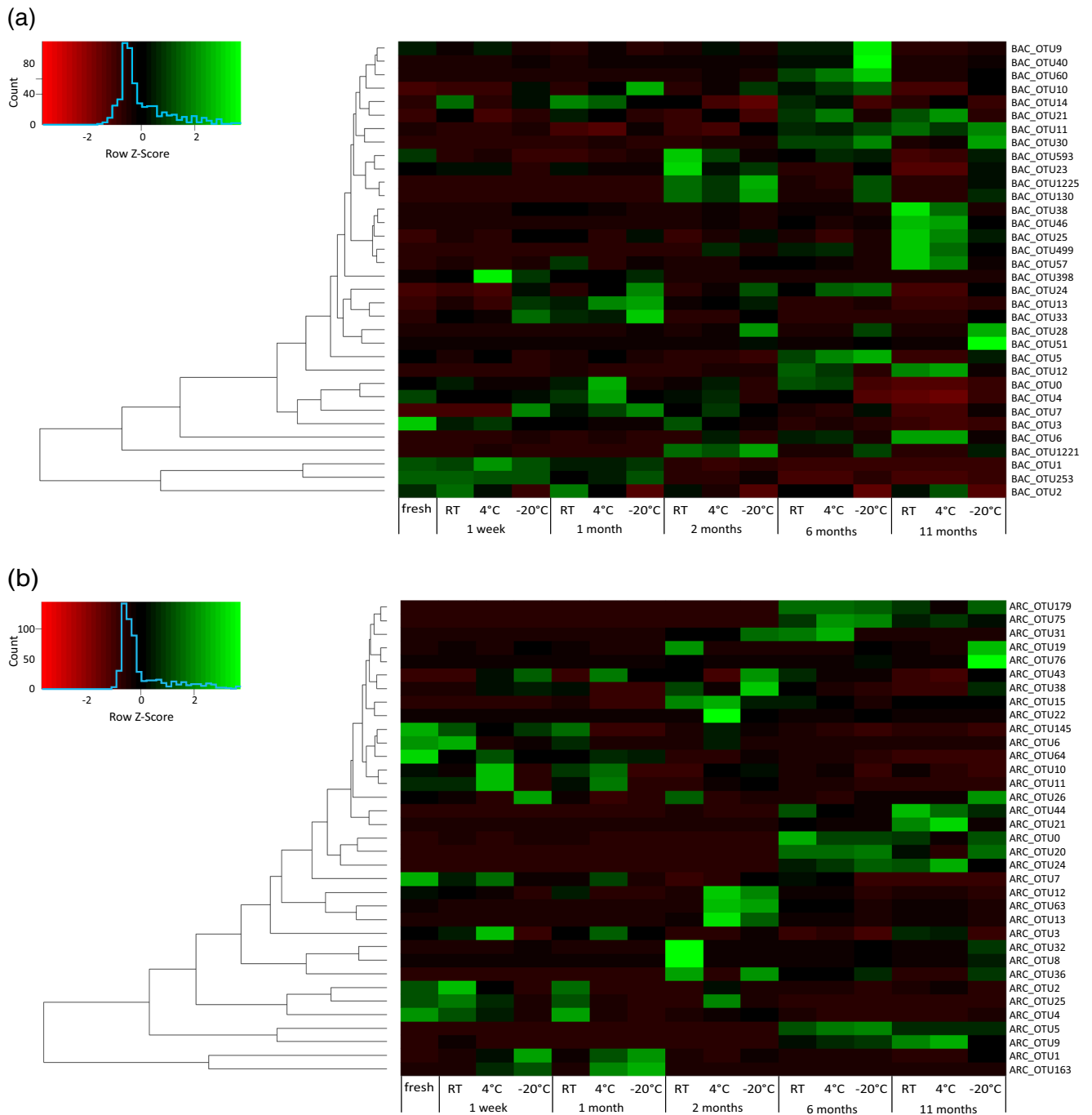


Fig. 5 Heatmaps of the complete sample set collected after AD of cellulose with inoculum stored under different conditions for bacteria (a) and archaea (b). In this graph, sequences representing triplicated amplicon for the same sample were compiled. Storage conditions are ordered vertically and scaled OTUs are ordered horizontally. Low abundant OTUs were removed by only including OTUs representing \geq

2 % of total reads in at least one sample. The scaled and standardized abundance of each OTU, denoted as the row Z-score, is indicated by red-green coloring, with red indicating low abundance and green indicating high abundance; the coloring scale is shown in the insets. Hierarchical clustering-based Euclidean distance between the rows is shown in the dendrogram on the left

addition to the detection of methanogenic archaea, several of the archaeal OTUs were affiliated to an uncultured archaeal lineage assumed to be non-methanogenic, yet often found in biogas reactors. This group, MCG, is a highly versatile

archaeal group with large genetic variation whose physiological functions remain unknown (Meng et al. 2013).

Although microbial analysis immediately after storage (Fig. 3, Supplemental Figure S2) did reveal some changes in

the relative abundance of bacterial and archaeal phylotypes, the distribution of dominant bacteria phyla and, to a lesser extent, archaeal phyla, was preserved during storage. Environmental samples are often stored directly at -20 or -80 °C without addition of glycerol prior to microbial community studies or metagenomic analysis. This sample handling is probably sufficient for revealing the microbial composition, but not for functionality analysis. Our findings suggest that cold storage (4 and -20 °C) over a longer period, as well as long time storage at room temperature does reduce the methanogenic activity of the microbial community. In particular, inocula stored at 11 months at RT or 4 °C showed no large difference in composition before and after AD incubation, reflecting the minor methanogenic activity after long-time storage suggested by a very low BMP.

In Europe, there is a growing interest to use biogas to complement other renewable energy sources, i.e. to produce electricity from biogas when it is dark or the wind is not blowing. This would imply flexible biogas production where the output of a biogas plant is regulated by the feeding regime. In practice, this means that the biogas plant will be “dormant” in periods, before starting up again when the demand of electricity rises. In this way, long term storage of biogas can be reduced and the energy provision can shift between the weather-independent biogas generation and an uncontrolled energy source to maintain a constant energy production. The idea of demand-driven flexible biogas supply is relatively novel, and only a few evaluations of discontinuous gas production have been published recently (Hahn et al. 2014; Mauky et al. 2015). One realistic scenario is to design flexible biogas reactors that operate in combination with solar energy, as the sun provides a highly variable energy source on daily basis as well as seasonal changes. This can be implemented by feeding only during defined periods of the day, both to compensate for limited access to sun light (day vs. night, weather) and to match fluctuation in electricity consumption. Another scenario applicable in the North-European countries, e.g. Norway, is to design flexible biogas reactors operating only during autumn/winter season when the lack of solar energy is high. This would also synchronize well with autumn harvest of possible bioenergy crops. The biogas plant will then be dormant during spring/summer season when other energy sources (i.e. solar) are active, saving biomass and minimizing gas storage needs and operational costs. In order to re-start the biogas process after a dormant period, the microbial starter culture should be of high quality, with functional and adaptive, “ready-to-action” microorganisms. Taking the results from the present study in consideration, we suggest that such “dormant bioreactors” should be fed with fresh substrate at least once every month to maintain the microbial activity in the plant.

In conclusion, to maintain high biogas activity in a microbial starter culture, freezing should be avoided and storage should be limited to a period of maximally 1 month at RT or 4 °C.

Long-time storage in cold environments was shown to be particularly harmful for biogas activity. The most notable change in the microbial community was a shift from dominance of hydrogenotrophic to dominance of acetoclastic methanogens.

Acknowledgments This work was financially supported by the ENERGIX-program of the Norwegian Research Council, grants 203402 and 228747.

Conflict of interest The authors declare that they have no conflict of interest

References

- Ahring BK, Biswas R, Ahamed A, Teller PJ, Uellendahl H (2014) Making lignin accessible for anaerobic digestion by wet-explosion pretreatment. *Bioresour Technol*
- Angelidaki I, Alves M, Bolzonella D, Borzacconi L, Campos J, Guwy A, Kalyuzhnyi S, Jenicek P, Van Lier J (2009) Defining the biomethane potential (BMP) of solid organic wastes and energy crops: a proposed protocol for batch assays
- Aubart C, Bully F (1984) Anaerobic digestion of rabbit wastes and pig manure mixed with rabbit wastes in various experimental conditions. *Agric Wastes* 10(1):1–13
- Bae B-U, Shin H-S, Paik B-C, Chung J-C (1995) Re-activation characteristics of preserved anaerobic granular sludges. *Bioresour Technol* 53(3):231–235
- Bowen EJ, Dolfing J, Davenport RJ, Read FL, Curtis TP (2014) Low-temperature limitation of bioreactor sludge in anaerobic treatment of domestic wastewater. *Water Sci Technol* 69(5):1004–1013
- Caporaso JG, Kuczynski J, Stombaugh J, Bittinger K, Bushman FD, Costello EK, Fierer N, Peña AG, Goodrich JK, Gordon JI (2010) QIIME allows analysis of high-throughput community sequencing data. *Nat Methods* 7(5):335–336
- Castro H, Queirolo M, Quevedo M, Muxi L (2002) Preservation methods for the storage of anaerobic sludges. *Biotechnol Lett* 24(4):329–333
- Chouari R, Le Paslier D, Dauga C, Daegelen P, Weissenbach J, Sghir A (2005) Novel major bacterial candidate division within a municipal anaerobic sludge digester. *Appl Environ Microbiol* 71(4):2145–2153
- De Vrieze J, Hennebel T, Boon N, Verstraete W (2012) *Methanosarcina*: the rediscovered methanogen for heavy duty biomethanation. *Bioresour Technol* 112:1–9
- Díaz I, Donoso-Bravo A, Fdz-Polanco M (2011) Effect of microaerobic conditions on the degradation kinetics of cellulose. *Bioresour Technol* 102(21):10139–10142
- Edgar RC (2010) Search and clustering orders of magnitude faster than BLAST. *Bioinformatics* 26(19):2460–2461
- Edgar RC, Haas BJ, Clemente JC, Quince C, Knight R (2011) UCHIME improves sensitivity and speed of chimera detection. *Bioinformatics* 27(16):2194–2200
- Elbeshbishy E, Nakhla G, Hafez H (2012) Biochemical methane potential (BMP) of food waste and primary sludge: influence of inoculum pre-incubation and inoculum source. *Bioresour Technol* 110:18–25
- Ferry JG (1993) *Methanogenesis: ecology, physiology, biochemistry & genetics*. Chapman & Hall, New York
- Gantner S, Andersson AF, Alonso-Sáez L, Bertilsson S (2011) Novel primers for 16S rRNA-based archaeal community analyses in environmental samples. *J Microbiol Methods* 84(1):12–18
- Hagen LH, Vivekanand V, Linjordet R, Pope PB, Eijsink VG, Horn SJ (2014) Microbial community structure and dynamics during co-

- digestion of whey permeate and cow manure in continuous stirred tank reactor systems. *Bioresour Technol* 171:350–359
- Hahn H, Krautkremer B, Hartmann K, Wachendorf M (2014) Review of concepts for a demand-driven biogas supply for flexible power generation. *Renew Sust Energ Rev* 29:383–393
- Hamady M, Walker JJ, Harris JK, Gold NJ, Knight R (2008) Error-correcting barcoded primers for pyrosequencing hundreds of samples in multiplex. *Nat Methods* 5(3):235–237
- Hatamoto M, Kaneshige M, Nakamura A, Yamaguchi T (2014) *Bacteroides luti* sp. nov., an anaerobic, cellulolytic and xylanolytic bacterium isolated from methanogenic sludge. *Int J Syst Evol Microbiol* 64(Pt 5):1770–1774
- Horn SJ (2013) A tetra-transition away from fossil fuels. In: Sygna L, O'Brien K, Wolf J (eds) *A changing environment for human security: transformative approaches to research, policy and action*. Earthscan, London, p 392
- Jimenez S, Cartagena MC, Arce A (1989) Influence of operating variables on the anaerobic digestion of crude and treated vine shoots. *Biol Wastes* 29(3):211–220
- Kafle GK, Kim SH, Sung KI (2013) Ensiling of fish industry waste for biogas production: a lab scale evaluation of biochemical methane potential (BMP) and kinetics. *Bioresour Technol* 127:326–336
- Kotsyurbenko OR, Glagolev MV, Nozhevnikova AN, Conrad R (2001) Competition between homoacetogenic bacteria and methanogenic archaea for hydrogen at low temperature. *FEMS Microbiol Ecol* 38(2–3):153–159
- Lauber CL, Zhou N, Gordon JI, Knight R, Fierer N (2010) Effect of storage conditions on the assessment of bacterial community structure in soil and human-associated samples. *FEMS Microbiol Lett* 307(1):80–86
- Lopes WS, Leite VD, Prasad S (2004) Influence of inoculum on performance of anaerobic reactors for treating municipal solid waste. *Bioresour Technol* 94(3):261–266
- Lorenz H, Fischer P, Schumacher B, Adler P (2013) Current EU-27 technical potential of organic waste streams for biogas and energy production. *Waste Manag* 33(11):2434–2448
- Mauky E, Jacobi HF, Liebetrau J, Nelles M (2015) Flexible biogas production for demand-driven energy supply—feeding strategies and types of substrates. *Bioresour Technol* 178:262–269
- McCalley CK, Woodcroft BJ, Hodgkins SB, Wehr RA, Kim E-H, Mondav R, Crill PM, Chanton JP, Rich VI, Tyson GW, Saleska SR (2014) Methane dynamics regulated by microbial community response to permafrost thaw. *Nature* 514(7523):478–481
- Meng J, Xu J, Qin D, He Y, Xiao X, Wang F (2013) Genetic and functional properties of uncultivated MCG archaea assessed by metagenome and gene expression analyses. *ISME J*
- Naas A, Mackenzie A, Mravec J, Schückel J, Willats W, Eijsink V, Pope P (2014) Do rumen Bacteroidetes utilize an alternative mechanism for cellulose degradation? *MBio* 5(4):e01401–e01414
- Ott SJ, Musfeldt M, Timmis KN, Hampe J, Wenderoth DF, Schreiber S (2004) *In vitro* alterations of intestinal bacterial microbiota in fecal samples during storage. *Diagn Microbiol Infect Dis* 50(4):237–245
- Raposo F, De la Rubia M, Fernández-Cegri V, Borja R (2012) Anaerobic digestion of solid organic substrates in batch mode: an overview relating to methane yields and experimental procedures. *Renew Sust Energ Rev* 16(1):861–877
- Risberg K, Sun L, Levén L, Horn SJ, Schnürer A (2013) Biogas production from wheat straw and manure—impact of pretreatment and process operating parameters. *Bioresour Technol* 149:232–237
- Rosewarne CP, Pope PB, Denman SE, McSweeney CS, O'Cuiv P, Morrison M (2010) High-yield and phylogenetically robust methods of DNA recovery for analysis of microbial biofilms adherent to plant biomass in the herbivore gut. *Microb Ecol* 61(2):448–454
- Rubin BE, Gibbons SM, Kennedy S, Hampton-Marcell J, Owens S, Gilbert JA (2013) Investigating the impact of storage conditions on microbial community composition in soil samples. *PLoS One* 8(7), e70460
- Schmidt O, Horn MA, Kolb S, Drake HL (2014) Temperature impacts differentially on the methanogenic food web of cellulose-supplemented peatland soil. *Environ Microbiol*. doi:10.1111/1462-2920.12507
- Shehu MS, Abdul Manan Z, Wan Alwi SR (2012) Optimization of thermo-alkaline disintegration of sewage sludge for enhanced biogas yield. *Bioresour Technol* 114:69–74
- Shelton DR, Tiedje JM (1984) General method for determining anaerobic biodegradation potential. *Appl Environ Microbiol* 47(4):850–857
- Shin H-S, Bae B-U, Oh S-E (1993) Preservation characteristics of anaerobic granular sludge. *Biotechnol Lett* 15(5):537–542
- Solli L, Håvelsrud OE, Horn SJ, Rike AG (2014) A metagenomic study of the microbial communities in four parallel biogas reactors. *Biotechnol Biofuels* 7(1)
- Tzeneva VA, Salles JF, Naumova N, de Vos WM, Kuikman PJ, Dolfing J, Smidt H (2009) Effect of soil sample preservation, compared to the effect of other environmental variables, on bacterial and eukaryotic diversity. *Res Microbiol* 160(2):89–98
- Vivekanand V, Olsen EF, Eijsink VG, Horn SJ (2013) Effect of different steam explosion conditions on methane potential and enzymatic saccharification of birch. *Bioresour Technol* 127:343–349
- Wang Q, Garrity GM, Tiedje JM, Cole JR (2007) Naive Bayesian classifier for rapid assignment of rRNA sequences into the new bacterial taxonomy. *Appl Environ Microbiol* 73(16):5261–5267
- Weiland P (2010) Biogas production: current state and perspectives. *Appl Microbiol Biotechnol* 85(4):849–860
- Westerholm M, Levén L, Schnürer A (2012) Bioaugmentation of syntrophic acetate-oxidizing culture in biogas reactors exposed to increasing levels of ammonia. *Appl Environ Microbiol* 78(21):7619–7625
- Wu W-M, Jain MK, Thiele JH, Zeikus JG (1995) Effect of storage on the performance of methanogenic granules. *Water Res* 29(6):1445–1452
- Ziganshin AM, Liebetrau J, Pröter J, Kleinstüber S (2013) Microbial community structure and dynamics during anaerobic digestion of various agricultural waste materials. *Appl Microbiol Biotechnol* 97(11):5161–5174
- Zilouei H, Soares A, Murto M, Guieysse B, Mattiasson B (2006) Influence of temperature on process efficiency and microbial community response during the biological removal of chlorophenols in a packed-bed bioreactor. *Appl Microbiol Biotechnol* 72(3):591–599

Supplementary material

Applied Microbiology and Biotechnology

Investigating the effect of storage conditions on microbial community composition and biomethane potential in a biogas starter culture

Live Heldal Hagen, Vivekanand Vivekanand, Phil Pope, Vincent G.H. Eijsink, Svein J. Horn*

Department of Chemistry, Biotechnology and Food Science, Norwegian University of Life Sciences, P. O. Box 5003, N-1432 Ås, Norway

*Corresponding author. Tel.: +47 67232488; fax: +47 64965901. *E-mail address*:

svein.horn@nmbu.no (S.J. Horn)

Supplemental table

Table S1: Good's coverage values calculated from bacterial and archaeal 16S rRNA amplicon library generated from 454 Roche/pyrosequencing.

	Storage condition	Good's coverage	Storage condition	Good's coverage	Storage condition	Good's coverage
BACTERIA	Start_Fresh_1	0,978	End_1month_RT_1	0,954	Start_6months_-20C_1	0,951
	Start_Fresh_2	0,984	End_1month_RT_2	0,950	Start_6months_-20C_2	0,933
	Start_Fresh_3	0,986	End_1month_RT_3	0,961	Start_6months_-20C_3	0,948
	End_Fresh_1	0,987	End_1month_4C_1	0,955	End_6months_RT_1	0,915
	End_Fresh_2	0,984	End_1month_4C_2	0,953	End_6months_RT_2	0,905
	End_Fresh_3	0,971	End_1month_4C_3	0,954	End_6months_RT_3	0,926
	Start_1week_RT_1	0,983	End_1month_-20C_1	0,957	End_6months_4C_1	0,899
	Start_1week_RT_2	0,988	End_1month_-20C_2	0,962	End_6months_4C_2	0,923
	Start_1week_RT_3	0,983	End_1month_-20C_3	0,961	End_6months_4C_3	0,925
	Start_1week_4C_1	0,974	Start_2months_RT_1	0,937	End_6months_-20C_1	0,929
	Start_1week_4C_2	0,983	Start_2months_RT_2	0,946	End_6months_-20C_2	0,927
	Start_1week_4C_3	0,982	Start_2months_RT_3	0,938	End_6months_-20C_3	0,922
	Start_1week_-20C_1	0,983	Start_2months_4C_1	0,938	Start_11months_RT_1	0,933
	Start_1week_-20C_2	0,990	Start_2months_4C_2	0,932	Start_11months_RT_2	0,941
	Start_1week_-20C_3	0,981	Start_2months_4C_3	0,926	Start_11months_RT_3	0,939
	End_1week_RT_1	0,981	Start_2months_-20C_1	0,951	Start_11months_4C_1	0,940
	End_1week_RT_2	0,970	Start_2months_-20C_2	0,939	Start_11months_4C_2	0,928
	End_1week_RT_3	0,980	Start_2months_-20C_3	0,929	Start_11months_4C_3	0,936
	End_1week_4C_1	0,975	End_2months_RT_1	0,936	Start_11months_-20C_1	0,944
	End_1week_4C_2	0,983	End_2months_RT_2	0,947	Start_11months_-20C_2	0,953
	End_1week_4C_3	0,981	End_2months_RT_3	0,950	Start_11months_-20C_3	0,943
	End_1week_-20C_1	0,966	End_2months_4C_1	0,922	End_11months_RT_1	0,958
	End_1week_-20C_2	0,961	End_2months_4C_2	0,916	End_11months_RT_2	0,958
	End_1week_-20C_3	0,947	End_2months_4C_3	0,919	End_11months_RT_3	0,945
	Start_1month_RT_1	0,961	End_2months_-20C_1	0,941	End_11months_4C_1	0,946
	Start_1month_RT_2	0,957	End_2months_-20C_2	0,942	End_11months_4C_2	0,954
	Start_1month_RT_3	0,965	End_2months_-20C_3	0,939	End_11months_4C_3	0,951
	Start_1month_4C_1	0,961	Start_6months_RT_1	0,950	End_11months_-20C_1	0,935
	Start_1month_4C_2	0,966	Start_6months_RT_2	0,949	End_11months_-20C_2	0,932
	Start_1month_4C_3	0,961	Start_6months_RT_3	0,968	End_11months_-20C_3	0,930
	Start_1month_-20C_1	0,986	Start_6months_4C_1	0,944		
	Start_1month_-20C_2	0,984	Start_6months_4C_2	0,957		
	Start_1month_-20C_3	0,981	Start_6months_4C_3	0,957		
ARCHAEA	Start_Fresh_1	0,999	End_1month_RT_1	0,997	Start_6months_-20C_1	NA
	Start_Fresh_2	NA	End_1month_RT_2	0,994	Start_6months_-20C_2	NA
	Start_Fresh_3	0,999	End_1month_RT_3	0,998	Start_6months_-20C_3	0,800
	End_Fresh_1	0,997	End_1month_4C_1	0,999	End_6months_RT_1	0,992
	End_Fresh_2	0,997	End_1month_4C_2	0,998	End_6months_RT_2	0,986
	End_Fresh_3	0,993	End_1month_4C_3	0,997	End_6months_RT_3	0,983
	Start_1week_RT_1	1,000	End_1month_-20C_1	0,998	End_6months_4C_1	0,989
	Start_1week_4C_2	0,996	End_1month_-20C_2	0,999	End_6months_4C_2	0,976
	Start_1week_RT_3	0,999	End_1month_-20C_3	0,998	End_6months_4C_3	0,984
	Start_1week_4C_1	0,997	Start_2months_RT_1	0,988	End_6months_-20C_1	0,991
	Start_1week_RT_2	0,996	Start_2months_RT_2	0,987	End_6months_-20C_2	0,988
	Start_1week_4C_3	0,998	Start_2months_RT_3	0,989	End_6months_-20C_3	0,985
	Start_1week_-20C_1	0,998	Start_2months_4C_1	0,987	Start_11months_RT_1	0,985

Start_1week_-20C_2	0,995	Start_2months_4C_2	0,989	Start_11months_RT_2	0,990
Start_1week_-20C_3	0,995	Start_2months_4C_3	0,986	Start_11months_RT_3	0,989
End_1week_RT_1	0,996	Start_2months_-20C_1	NA	Start_11months_4C_1	0,991
End_1week_RT_2	0,995	Start_2months_-20C_2	NA	Start_11months_4C_2	0,991
End_1week_RT_3	0,993	Start_2months_-20C_3	NA	Start_11months_4C_3	0,990
End_1week_4C_1	0,994	End_2months_RT_1	0,988	Start_11months_-20C_1	0,993
End_1week_4C_2	0,995	End_2months_RT_2	0,991	Start_11months_-20C_2	0,991
End_1week_4C_3	0,995	End_2months_RT_3	0,990	Start_11months_-20C_3	0,993
End_1week_-20C_1	0,998	End_2months_4C_1	0,981	End_11months_RT_1	0,987
End_1week_-20C_2	0,997	End_2months_4C_2	0,982	End_11months_RT_2	0,990
End_1week_-20C_3	0,997	End_2months_4C_3	0,988	End_11months_RT_3	0,991
Start_1month_RT_1	0,995	End_2months_-20C_1	0,989	End_11months_4C_1	0,987
Start_1month_RT_2	0,995	End_2months_-20C_2	0,991	End_11months_4C_2	0,987
Start_1month_RT_3	0,995	End_2months_-20C_3	0,993	End_11months_4C_3	0,986
Start_1month_4C_1	0,997	Start_6months_RT_1	0,990	End_11months_-20C_1	0,989
Start_1month_4C_2	0,997	Start_6months_RT_2	0,992	End_11months_-20C_2	0,993
Start_1month_4C_3	0,996	Start_6months_RT_3	0,996	End_11months_-20C_3	0,989
Start_1month_-20C_1	NA	Start_6months_4C_1	NA		
Start_1month_-20C_2	1,000	Start_6months_4C_2	0,999		
Start_1month_-20C_3	1,000	Start_6months_4C_3	0,800		

Table S2: The statistical significance of differences in unweighted UniFrac distances between storage conditions of samples after 40 days of anaerobic degradation. The statistical significance is calculated using two-sided student's t-test with 1000 Monte Carlo simulations, and the significance degree is represented as no significance ($p>0.05$) with NS; $p\leq 0.05$ with one asterisk (*); $p\leq 0.01$ with two asterisk (**). The groups complies with the labels in figure S1. The control sample (not stored) is referred to as “Fresh” temperature and “0” time.

	Group 1	Group 2	t statistic	Nonparametric p-value (Bonferroni-corrected)	Significance degree
Bacteria; Compl. Fig S1a	All within Temp	All between Temp	-17.33	0.01	**
	All within Temp	Fresh vs. Fresh	0.77	1	NS
	All within Temp	-20 vs. -20	-0.09	1	NS
	All within Temp	Fresh vs. -20	-17.33	0.01	**
	All between Temp	Fresh vs. Fresh	5.20	0.01	**
	All between Temp	-20 vs. -20	17.20	0.01	**
	All between Temp	Fresh vs. -20	0.00	1	NS
	Fresh vs. Fresh	-20 vs. -20	-0.79	1	NS
	Fresh vs. Fresh	Fresh vs. -20	-5.20	0.01	**
		-20 vs. -20	Fresh vs. -20	-17.20	0.01
Bacteria; Compl. Fig S1b	All within Time	All between Time	-19.35	0.028	*
	All within Time	11M vs. 11M	4.02	0.028	*
	All within Time	0 vs. 0	2.01	0.868	NS
	All within Time	<11M vs. <11M	-0.89	1	NS
	All within Time	11M vs. 0	-15.71	0.028	*
	All within Time	11M vs. <11M	-16.23	0.028	*
	All within Time	0 vs. <11M	-11.63	0.028	*
	All between Time	11M vs. 11M	9.20	0.028	*
	All between Time	0 vs. 0	3.52	0.084	NS
	All between Time	<11M vs. <11M	19.21	0.028	*
	All between Time	11M vs. 0	-7.69	0.028	*
	All between Time	11M vs. <11M	1.73	1	NS
	All between Time	0 vs. <11M	0.12	1	NS
	11M vs. 11M	0 vs. 0	0.39	1	NS
	11M vs. 11M	<11M vs. <11M	-4.62	0.028	*
	11M vs. 11M	11M vs. 0	-9.84	0.028	*
	11M vs. 11M	11M vs. <11M	-8.95	0.028	*
	11M vs. 11M	0 vs. <11M	-7.14	0.028	*
	0 vs. 0	<11M vs. <11M	-2.31	0.588	NS
	0 vs. 0	11M vs. 0	-9.04	0.028	*
0 vs. 0	11M vs. <11M	-3.67	0.028	*	
0 vs. 0	0 vs. <11M	-3.28	0.056	NS	
<11M vs. <11M	11M vs. 0	-17.02	0.028	*	

	<11M vs. <11M	11M vs. <11M	-16.32	0.028	*
	<11M vs. <11M	0 vs. <11M	-12.00	0.028	*
	11M vs. 0	11M vs. <11M	9.14	0.028	*
	11M vs. 0	0 vs. <11M	7.08	0.028	*
	11M vs. <11M	0 vs. <11M	-1.03	1	NS
Archaea; Compl. Fig S1c	All within Temp	All between Temp	-3.27	0.03	*
	All within Temp	Fresh vs. Fresh	3.15	0.01	**
	All within Temp	-20 vs. -20	-0.39	1	NS
	All within Temp	Fresh vs. -20	-3.27	0.05	*
	All between Temp	Fresh vs. Fresh	4.20	0.02	*
	All between Temp	-20 vs. -20	3.04	0.02	*
	All between Temp	Fresh vs. -20	0.00	1	NS
	Fresh vs. Fresh	-20 vs. -20	-3.36	0.01	**
	Fresh vs. Fresh	Fresh vs. -20	-4.20	0.01	**
	-20 vs. -20	Fresh vs. -20	-3.04	0.04	*
Archaea; Compl. Fig S1d	All within Temp	All between Temp	-11.21	0.01	**
	All within Temp	RT vs. RT	1.04	1	NS
	All within Temp	-20 vs. -20	-1.02	1	NS
	All within Temp	RT vs. -20	-11.21	0.01	**
	All between Temp	RT vs. RT	10.69	0.01	**
	All between Temp	-20 vs. -20	8.13	0.01	**
	All between Temp	RT vs. -20	0.00	1	NS
	RT vs. RT	-20 vs. -20	-1.79	0.84	NS
	RT vs. RT	RT vs. -20	-10.69	0.01	**
-20 vs. -20	RT vs. -20	-8.13	0.01	**	
Archaea; Compl. Fig S1e	All within Temp	All between Temp	-5.08	0.01	**
	All within Temp	-20 vs. -20	1.78	0.79	NS
	All within Temp	4 vs. 4	-1.79	0.73	NS
	All within Temp	-20 vs. 4	-5.08	0.01	**
	All between Temp	-20 vs. -20	6.16	0.01	**
	All between Temp	4 vs. 4	2.30	0.22	NS
	All between Temp	-20 vs. 4	0.00	1	NS
	-20 vs. -20	4 vs. 4	-3.14	0.02	*
	-20 vs. -20	-20 vs. 4	-6.16	0.01	**
	4 vs. 4	-20 vs. 4	-2.30	0.2	NS

Supplemental figures

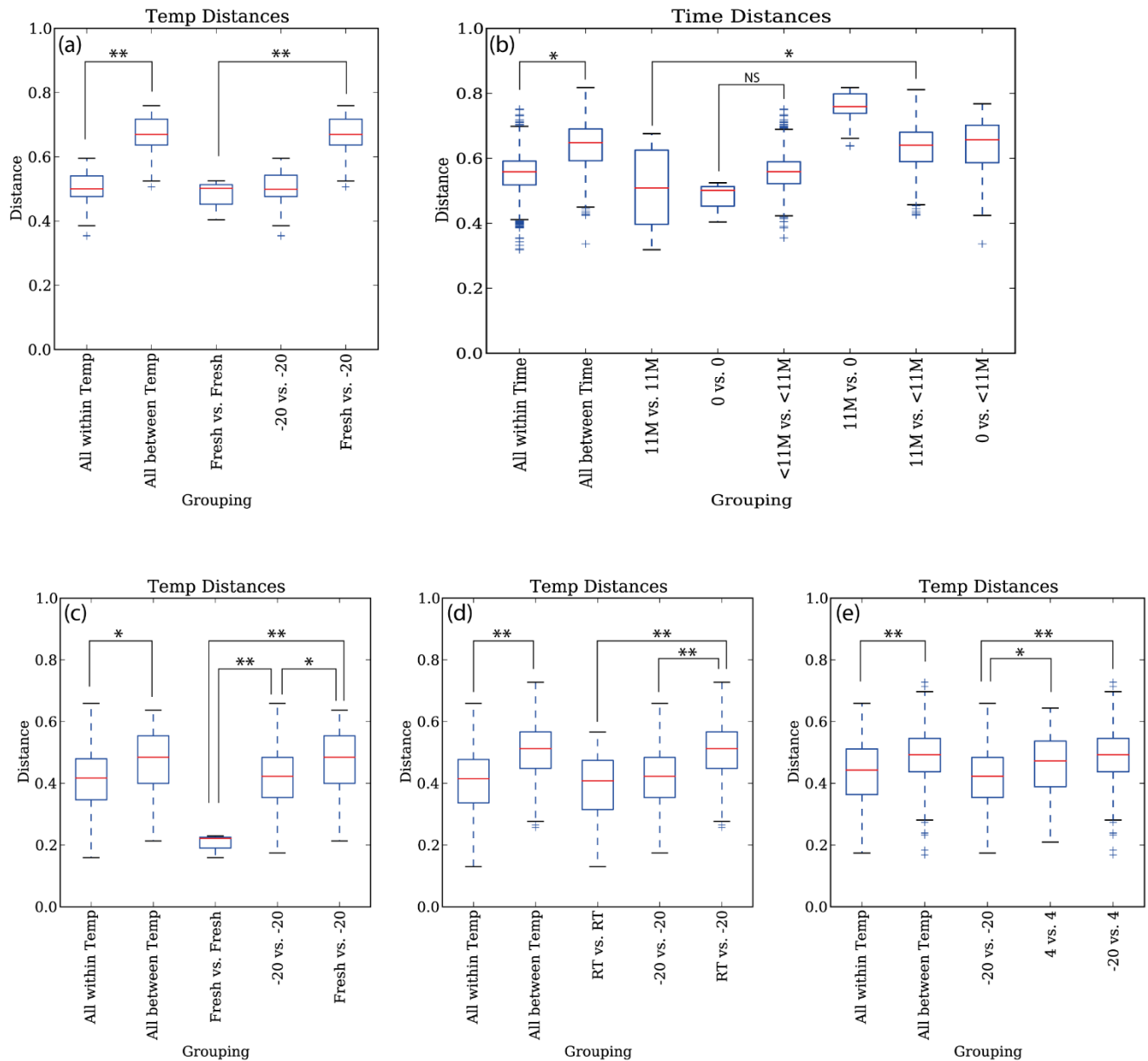


Figure S1: The statistical significance of differences in unweighted UniFrac distances between selected storage conditions. The data represents only samples taken after 40 days of anaerobic degradation. The statistical significance is calculated using student's t-test with 1000 Monte Carlo simulations, and the significance degree is represented as no significance ($p > 0.05$) with NS; $p \leq 0.05$ with one asterisk (*); $p \leq 0.01$ with two asterisk (**). The control sample (not stored) is referred to as “Fresh” temperature and “0” time while 11 months is referred to as 11M. Storage at -20°C (a) and 11 months (b) had a significant effect on the bacterial community structure. Storage at -20°C also had an effect on the archaea community structure, showing significant differences compared to fresh inoculum (c), inoculum stored at 4°C (d), as well as at room temperature – RT (e). See Table S2 for a complete list of p-values for all the compared groups.

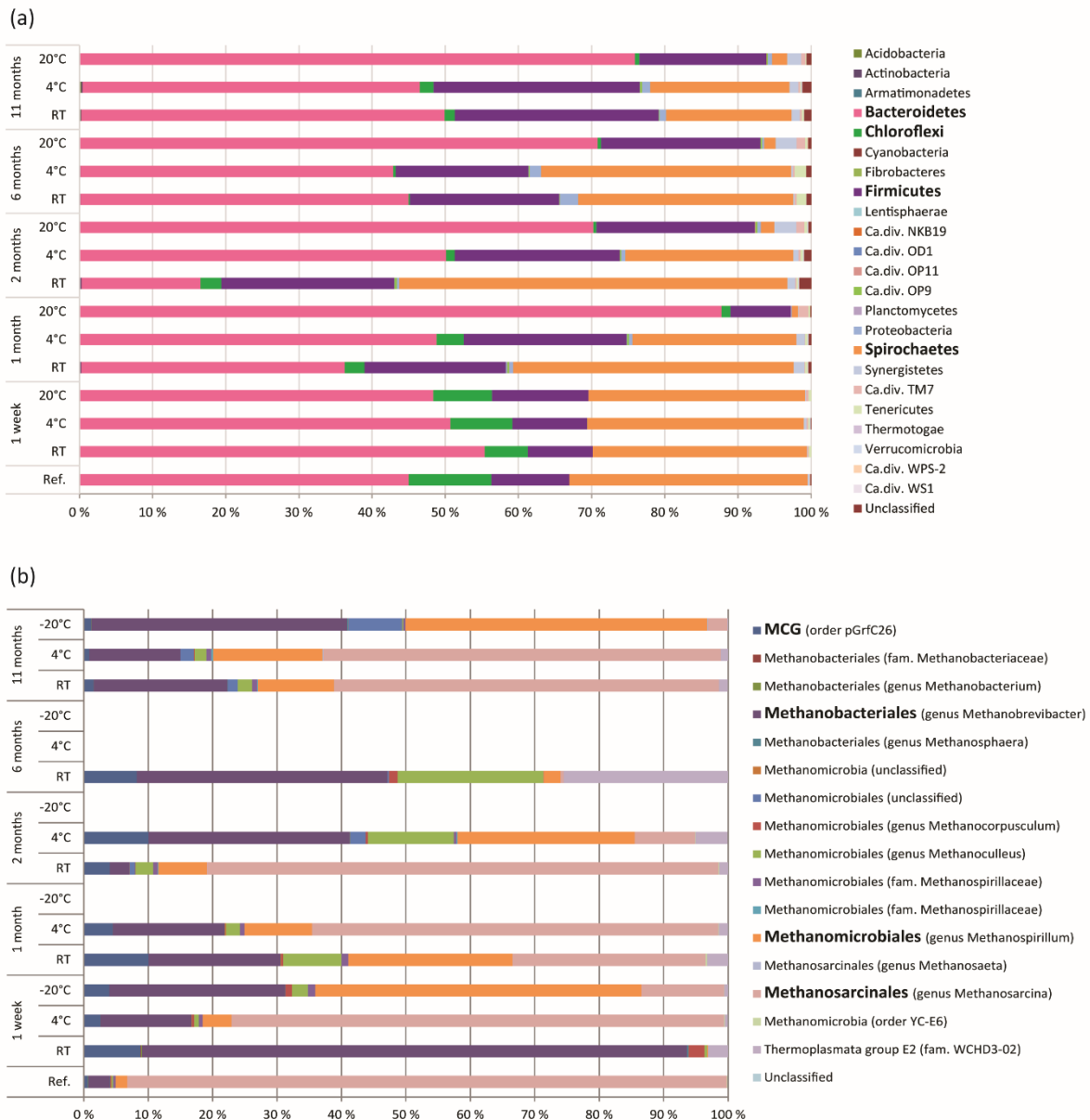


Figure S2: Abundance of phylotypes in inoculum stored at room temperature (RT), 4°C or -20°C for different lengths of time; 1 week, 1 month, 2 months, 6 months and 11 months, as detected in samples taken immediately after ended storage period. Relative abundance is expressed as the percentage of total 16S rRNA sequences of (a), bacterial phyla; (b) archaeal order level, in addition to the deepest lineage assignment given with a 80% bootstrap confidence estimate. No archaeal amplicons were retrieved from several of the samples stored at -20°C (1 month, 2 months, 6 months) and the sample stored at 4°C for 6 months. The names of the most abundant phylotypes are printed in bold face.

Paper III



Anaerobic digestion of food waste – Effect of recirculation and temperature on performance and microbiology

Mirzaman Zamanzadeh ^a, Live H. Hagen ^a, Kine Svensson ^b, Roar Linjordet ^b, Svein J. Horn ^{a,*}

^a Department of Chemistry, Biotechnology and Food Science, Norwegian University of Life Sciences, P. O. Box 5003, N-1432 Ås, Norway

^b NIBIO, Norwegian Institute of Bioeconomy Research, P.O. Box 115, N-1431 Ås, Norway

ARTICLE INFO

Article history:

Received 13 January 2016

Received in revised form

16 March 2016

Accepted 25 March 2016

Available online 28 March 2016

Keywords:

Biomethane

Digestate recirculation

Microbial community

Biogas

Ammonia

Biofuel

ABSTRACT

Recirculation of digestate was investigated as a strategy to dilute the food waste before feeding to anaerobic digesters, and its effects on microbial community structure and performance were studied. Two anaerobic digesters with digestate recirculation were operated at 37 °C (MD + R) and 55 °C (TD + R) and compared to two additional digesters without digestate recirculation operated at the same temperatures (MD and TD). The MD + R digester demonstrated quite stable and similar performance to the MD digester in terms of the methane yield (around 480 mL CH₄ per gVS_{added}). In both MD and MD + R *Methanosaeta* was the dominant archaea. However, the bacterial community structure was significantly different in the two digesters. *Firmicutes* dominated in the MD + R, while *Chloroflexi* was the dominant phylum in the MD. Regarding the thermophilic digesters, the TD + R showed the lowest methane yield (401 mL CH₄ per gVS_{added}) and accumulation of VFAs. In contrast to the mesophilic digesters, the microbial communities in the thermophilic digesters were rather similar, consisting mainly of the phyla *Firmicutes*, *Thermotoga*, *Synergistetes* and the hydrogenotrophic methanogen *Methanothermobacter*. The impact of ammonia inhibition was different depending on the digesters configurations and operating temperatures.

© 2016 Elsevier Ltd. All rights reserved.

1. Introduction

During the last decade, energy recovery from various sources of organic materials has gained increased interest. Bio-methane is a renewable fuel that can be produced from biomass via anaerobic digestion. Internationally, there is a trend to recover the energy

Abbreviations: ADM, anaerobic digestion model; AM, acetoclastic methanogens; bp, base pair; COD, chemical oxygen demand; CODCH₄, COD equivalent of methane; FAN, free ammonia nitrogen; FW, food waste; HM, hydrogenotrophic methanogens; HPLC, high performance liquid chromatography; KI.NH₃, inhibitory ammonia coefficient; MD, mesophilic digester; MD + R, mesophilic digester with recirculation; OUT, operational taxonomic unit; PCOD, particulate chemical oxygen demand; PCR, polymerase chain reaction; rpm, round per minute; SAB, syntrophic acetogenic bacteria; SAOB, syntrophic acetate oxidizing bacteria; SCOD, soluble chemical oxygen demand; SCODE, soluble COD in effluent; SCODin, soluble COD in influent; SNH₃, free ammonia concentration; T, temperature; TAN, total ammonia nitrogen; TCD, thermal conductivity detector; TCOD, total chemical oxygen demand; TD, thermophilic digester; TD + R, thermophilic digester with recirculation; TS, total solids; VFA, volatile fatty acids; VS, volatile solids.

* Corresponding author.

E-mail address: svein.horn@nmbu.no (S.J. Horn).

<http://dx.doi.org/10.1016/j.watres.2016.03.058>

0043-1354/© 2016 Elsevier Ltd. All rights reserved.

content of municipal food wastes through anaerobic digestion instead of landfilling, which has the risk of watershed pollution and greenhouse gas emissions. Food waste (FW), which has a high biogas potential, can make operation of anaerobic digesters and co-digesters more economical through enhanced methane production (Hartmann and Ahring, 2005).

Typically, FW has high solids content and thus it needs to be diluted before feeding to anaerobic digesters. Water can be used to dilute FW before feeding to an anaerobic digester. However, access to water may be limited and costly in some locations. It is also not a sustainable option to use clean water for dilution of food waste. Thus, processed water and/or digestate may be used to dilute the FW, reducing the water consumption in biogas plants.

Even though FW has a high potential for production of renewable energy, it may inhibit certain microbial processes of anaerobic digestion due to its high content of nitrogen-bearing materials or too much acidification (Ganesh et al., 2014; Mata-Alvarez et al., 1992). During the digestion process, nitrogen is released into the bulk liquid and, depending on pH, organic loading and temperature, this may lead to high concentrations of free ammonia in the

digester. Inhibition due to high nitrogen content of the substrate has been reported previously (Sheng et al., 2013; Procházka et al., 2012). Therefore, concern of ammonia inhibition on the methanogenesis process should be taken into account when using FW or recirculating digestate bearing a high content of ammonia back to a digester (Wilson et al., 2012; Gallert et al., 1998).

Anaerobic digestion is a complex bioprocess, in which microorganisms belonging to different functional groups degrade various organic compounds in a concerted effort into methane and carbon dioxide. However, our understanding of the function and metabolic capabilities of microbial communities in anaerobic digestion is limited (Vanwonterghem et al., 2014). Application of culture-independent molecular techniques have provided some information on the complex and diverse microbial communities in anaerobic digesters (Vanwonterghem et al., 2015; De Vrieze et al., 2015). Various parameters may influence microbial community structures, including digester configuration, feedstock, temperature and other operational parameters. Accordingly, several researchers have investigated the microbial ecology in FW-fed anaerobic digesters ran under various operational conditions using molecular techniques (Cardinali-Rezende et al., 2009; Kim et al., 2014, 2015). However, information about the effect of digestate recirculation on microbial community structure of FW-fed anaerobic digesters and its correlation with performance is lacking in the literature.

The primary objective of this study was to characterize and compare the performance of four anaerobic digesters fed with food waste at mesophilic (37 °C) and thermophilic (55 °C) conditions with and without digestate recirculation. The microbial community structures of the four digesters were analyzed to evaluate the influence of temperature and recirculation. In addition, possible correlations between the function of microbial groups and the performance of the mesophilic and thermophilic digesters were investigated.

2. Materials and methods

2.1. Operation of lab-scale digesters

Four 10-L laboratory-scale continuously stirred tank reactors (BelachBioteknik, Sweden) were used in this study and all were fed with food waste (FW). Two digesters were operated as flow-through reactors at mesophilic (MD) and thermophilic (TD) temperatures, and two with digestate recirculation at mesophilic (MD + R) and thermophilic (TD + R) conditions. The mesophilic and thermophilic temperatures were set to 37 °C and 55 °C, respectively. The operational conditions of the digesters are summarized in Table 1. The digesters operated at 37 °C were initially seeded with 3 L of inoculum taken from a full-scale biogas plant digesting food waste at mesophilic conditions (Romerike biogas plant, RBA; Esva, Norway). The digesters were then fed with food waste, gradually increasing the organic loading rate (OLR) from 1 to 3 g VS L⁻¹ d⁻¹ over a period of 3 weeks until a total volume of 6 L was reached. The other two digesters at 55 °C were seeded with 3 L inoculum from a

thermophilic biogas plant digesting food waste (FREVAR; Fredrikstad, Norway), and then fed food waste in the same way as the mesophilic digesters. The working volume of the digesters was 6 L and hydraulic retention time (HRT) was maintained at 20 days through withdrawing 300 mL per day of digested waste and adding the same amount of pretreated food waste after dilution with either tap water or sieved digestate. However, due to the recirculation of the digestate, the actual HRTs in the MD + R and TD + R digesters were longer (approximately 60 days). Prior to the experiments, the food waste was milled to pass a 10-mm sieve and pasteurized at 70 °C for 1 h (in accordance with Norwegian regulations on the use of food waste in biogas plants). The characteristics of the FW used are shown in Table 2. For the digesters with recirculation, the digestate was manually screened using a 2-mm sieve (through which the digestate almost entirely passed) and then used to dilute the feed. The return ratio was approximately 2 (200 mL digestate to 100 mL feed), with some variation over time due to small differences in the volatile solids content of the food waste. The organic loading rate was set at 3 gVS L⁻¹ d⁻¹. Stirrer speed (100 rpm), pH, temperature, gas flow and gas volume was monitored in real time using BIOPHANTOM software (Belach Bioteknik, Sweden). Produced biogas in each anaerobic digester was measured by a water displacement gas-meter and recorded by the software. The digesters were run for 152 days and samples for various analyses were collected throughout the experimental period.

2.2. Analysis of chemical parameters

Samples were taken from the food waste and digesters on a regular basis for analysis of total solids (TS), volatile solids (VS), and total chemical oxygen demand (TCOD). A fraction of the samples was centrifuged for analysis of pH, NH₃ and alkalinity, and filtered (0.45 μm pore size) for analysis of soluble COD and volatile fatty acids (VFAs). The COD, TS and VS analyses were carried out following standard methods (APHA, 1998). Ammonium measurement was done using a probe according to the company's manual (Orion 93; Thermoscientific, USA). In addition to on-line monitoring of the pH, liquid samples were regularly taken to also measure pH by a separate pH instrument (Orion, Thermoscientific, USA). Samples for VFAs were stored at -20 °C. Before VFA analysis, the samples were thawed and the pH of the samples was adjusted to less than 2.5. After centrifugation at 14,000 rpm, the samples were filtered using 0.45-μm syringe filter. VFAs (formate, acetate, propionate, butyrate and valerate) were quantified by a high performance liquid chromatography (HPLC) using a Dionex Ultimate 3000 system (Dionex, Sunnyvale, CA, USA) equipped with a UV detector. The column used was a Zorbax Eclipse Plus C18 (Agilent, USA; 150 × 2.1 mm column; 3.5 μm particles) equipped with a guard column (12.5 × 2.1 mm; 5 μm particles). The column was

Table 1
Operational condition of digesters.

Parameter	Digester			
	MD	TD	MD + R	TD + R
Average OLR, gVS/d	18.5	18.5	18.5	18.5
HRT, d	20	20	60	60
Total Solids, %	16.6 ± 0.8	14.0 ± 1.2	29.5 ± 1.1	26.2 ± 1.7
Temperature, °C	37	55	37	55
Inoculum source	Romerike	Frevar	Romerike	Frevar
Digestate recirculation	NO	NO	YES	YES

Table 2
Food waste characteristics (average ± standard deviation).

Parameters	Unit	Food waste
Total solids	%	17.8 ± 1.2
Volatile Solids	% vs	16.1 ± 1.2
VS/TS		0.90
TCOD	g/L	271 ± 57.5
TCOD/VS		1.7 ± 0.3
SCOD	g/L	95 ± 12
Ammonia	mg/L	504 ± 153
pH		3.9 ± 0.1
Acetate	mg/L	44,642 ± 16,576
Propionate	mg/L	1251 ± 547
i-Butyrate	mg/L	212 ± 14
n-Butyrate	mg/L	244 ± 57

operated at 40 °C at 0.3 mL/min and 1 µL sample was injected. A gradient flow was applied using the eluents methanol and 2.5 mM H₂SO₄. The biogas composition was monitored on-line with an SRI gas chromatograph (Model 8610C) equipped with a thermal conductivity detector (TCD) and a 2 m Haysep-D column. The injector, detector, and column were operated at 41, 153 and 81 °C, respectively. Helium was used as a carrier gas at 20 mL min⁻¹.

2.3. Microbial analysis

At day152 of the experiments, samples were taken from all the digesters for microbial analysis. The samples were frozen immediately and stored at -20 °C. For DNA extraction, the samples were thawed and centrifuged at 14,000 rpm for 7 min to remove the liquid. The pellet was then resuspended in S.T.A.R buffer (Roche Diagnostics Corporation, USA) to stabilize nucleic acid and prevent bacterial growth. Cells were dissociated from large particles by vortex followed by slow spin. Larger particles precipitated to the lower phase, while the upper phase containing cells was transferred to a FastPrep24 tube with acidic washed glass beads. The cells were then mechanically lysed. DNA was extracted using an automated DNA magnetic bead-based method (LGC Genomics, UK) with minor modifications. DNA concentration was measured with Qubit™ fluorometer and the Quant-iT™ dsDNA BR Assay Kit (Invitrogen, USA), and solutions were kept at -20 °C until 16S rRNA sequencing.

For 16S rRNA gene sequencing amplification of V3–V4 hyper variable regions of bacterial and archaeal 16S rRNA genes were carried out using the Pro 341F/Pro805R primer set selected from Takahashi et al. (2014): 5'-CCTACGGGNNBGCASCAG -3'/5'-GAC-TACNVGGGTATCTAATCC -3'. Illumina adaptor overhang was added to the primer pair in addition to the region specific sequences. The amplicon PCR reaction mixture (25 µL) consisted of 12.5 ng microbial gDNA, iProof HF DNA polymerase (BioRad, USA) and 0.2 µM of each primer. The PCR reaction was performed with an initial denaturation step at 98 °C for 30 s, followed by 25 cycles of denaturation at 98 °C in 30 s, annealing at 55 °C in 30 s, extension at 72 °C in 30 s, and completed by a final elongation at 72 °C in 5 min. A PCR clean-up step of the 16S V3–V4 amplicon was conducted with AgencourtAMPure XP beads (Beckman Coulter, USA). An index PCR reaction was carried out to attach unique 6–bp indices (Nextera XT Index Kit) to the Illumina sequencing adaptors to allow multiplexing of samples. The PCR conditions were as followed: 98 °C in 3 min, 8 cycles of 95 °C in 30sec, 55 °C for 30 s, 72 °C for 30 °C, completed by a final elongation step at 72 °C for 5 min. The indexing step was finalized with an additional AMPure XP PCR clean-up. The 16S rRNA amplicons were quantified (Quant-iT™ dsDNA HSAssay Kit and Qubit™ fluorometer, Invitrogen, USA), normalized and pooled in equimolar concentrations. The multiplexed library pool was then spiked with 30% PhiX control to improve base calling during sequencing of low complexity libraries. A final concentration of 8 p.m. denatured DNA was sequenced on an Illumina MiSeq instrument using the MiSeq reagent kit V3.

Sequence analysis was conducted using the Quantitative Insight Into Microbial Ecology (QIIME) version 1.8.0 (Caporaso et al., 2010). Single-end reads were quality filtered (at Phred ≥ Q20) and trimmed to 200 bp before proceeding with downstream analysis. USEARCH61 was used for detection of chimeric sequences, followed by clustering (at 97% sequence identity) of non-chimera sequences and denovo picking of OTUs (Edgar, 2010; Edgar et al., 2011). OTUs were then assigned to taxonomy with QIIME's uclust-based taxonomy assigner. The OTUs observed fewer times than two times and OTUs with a total observation count less than 0.005% were filtered out to remove singletons and reduce the complexity.

2.4. Data accessibility

Sequence data are available at NCBI Short Read Archive under accession number SRP066159.

3. Results and discussion

3.1. Performance of digesters

Table 2 shows the characteristics of the food waste (FW) that was used to feed the digesters. The organic fraction of FW was quite high with a VS/TS ratio of 0.90 ± 0.01. The pH was relatively low, while SCOD, VFAs and NH₃ concentrations were higher than the typical FW values reported previously (Zhang et al., 2011). This was most likely due to the pretreatment and storage of the FW before shipping to the biogas laboratory. Although the FW used had a relatively low pH, the pH within the digesters were quite stable and showed average values of 7.7 ± 0.1, 8.0 ± 0.1, 7.8 ± 0.1 and 8.0 ± 0.1 in the MD, MD + R, TD and TD + R, respectively. The presence of the high alkalinity in the digesters (Table 3) was important in maintaining stable pH.

The average methane yields for the four digesters are shown in Table 3. For the mesophilic digesters the methane yields were quite similar (480 and 475 mL CH₄/gVS_{added}), and higher than the yields in the thermophilic reactors (7% and 18% higher than the TD and TD + R digesters, respectively). A wide range of methane yields of about 350–480 mL CH₄ per gVS_{added} has been reported in the literature for FW digestion (Zhang et al., 2011; El-Mashad and Zhang, 2010; Cho et al., 1995). Thus, the methane yields obtained in this study were in the higher end of values reported earlier. This could be attributed to high degradability of the pretreated FW used in this study.

While recirculation did not affect the methane yield in the mesophilic digesters, recirculation had a clear detrimental effect under thermophilic conditions (Table 3). Therefore, using recirculation for on-site clean water conservation is most applicable under mesophilic condition.

3.2. Solubilization of organic matter

Solubilization of the food waste were compared among the digesters using Equation (1) (Ge et al., 2011). This equation estimates the fraction of particulate COD that is solubilized into soluble material (SCOD). Since part of the SCOD is converted into methane, the COD equivalent of methane needs to be included to estimate the total extent of solubilization.

$$\text{Extent of solubilization (\%)} = \frac{\text{COD}_{\text{CH}_4} + \text{SCOD}_e - \text{SCOD}_{\text{in}}}{\text{PCOD}_{\text{in}}} \quad (1)$$

Where COD_{CH₄} is the COD equivalent of the CH₄ produced; SCOD_e is soluble COD in effluent; SCOD_{in} is soluble COD in influent and PCOD_{in} is the particulate COD in influent.

The extent of solubilization of the substrate in the four digesters are presented in Fig. 1. It clearly shows that the highest solubilization was achieved at the thermophilic conditions without recirculation (TD). The TD digester and its mesophilic counterpart (i.e., MD digester) showed 62.5% and 56.6% solubilization, respectively. For the reactors with recirculation, the solubilization extent in the MD + R and TD + R reactors were 57.2% and 52.2%, respectively. Although the TD reactor showed a higher solubilization extent than the mesophilic digesters, its methane production was lower (Table 3). Partly, this might be explained by the ammonia inhibition and a shift in methane production pathway at the higher temperatures (discussed below). Digester recirculation had a clear

Table 3
Average performance parameters during the stable operation of the digesters.

Parameters	Unit	MD	MD + R	TD	TD + R
Biogas composition	% CH ₄	63	62	62	58
	% CO ₂	37	37	38	42
Methane yield	mL CH ₄ /g VS _{added}	480 ± 33	475 ± 29	448 ± 44	401 ± 45
	mL CH ₄ /g COD _{added}	283 ± 34	280 ± 47	257 ± 61	242 ± 27
Alkalinity	mg/L as CaCO ₃	5329 ± 145	11,267 ± 425	4200 ± 358	8319 ± 335
pH		7.7 ± 0.1	8 ± 0.1	7.8 ± 0.2	8 ± 0.1
Ammonia	mg N–NH ₄ /L	1109 ± 139	2150 ± 204	1258 ± 167	2258 ± 187
Free ammonia ^a	mg N–NH ₃ /L	49	200	198	597
SCOD	mg/L	932 ± 151	3167 ± 540	9413 ± 1915	20,932 ± 1990

^a Calculated from Equation (3).

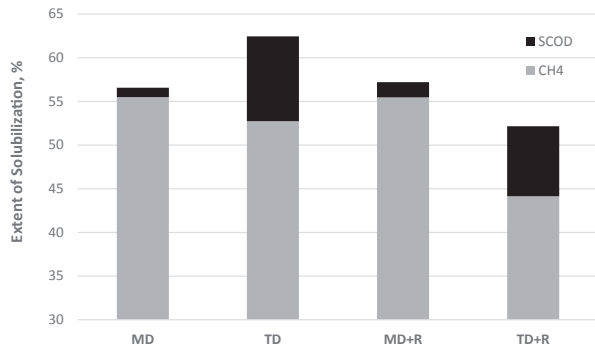


Fig. 1. Average extent of solubilization in the four digesters.

negative effect on solubilization at thermophilic conditions.

A closer analysis of the solubilization data (Fig. 1) revealed an imbalance between hydrolysis and methanogenesis processes in the thermophilic digesters (TD and TD + R), which had higher soluble COD fractions as compared to the mesophilic digesters. Increase in the soluble COD fraction as compared to the methane fraction has been reported previously for anaerobic digestion of waste sludge at elevated temperatures (Ge et al., 2011). The soluble COD fraction accounted for 10% and 8% of the solubilization for the TD and TD + R, respectively, indicating that solubilized products were not removed in these digesters as effectively as in the mesophilic counterparts. This observation agreed with the higher levels of VFAs in the thermophilic digesters as compared to the values obtained for the mesophilic ones (Fig. 2). Acetate and propionate levels were, on average, 175 ± 55 and 10 ± 6 mg/L in the MD and 278 ± 93 and 12 ± 7 mg/L in the MD + R, respectively. The VFA profiles in the thermophilic digesters TD and TD + R were very different. Acetate and propionate concentrations increased over time in the TD and were, on average, 2028 ± 864 and 833 ± 280 mg/L, and the longer VFAs ranged between 230 and 84 mg/L (Fig. 2C). For the TD + R, the main VFA was propionate (2300 ± 1250), followed by iso-valerate, iso-butyrate, *n*-butyrate and *n*-valerate (Fig. 2D). Interestingly, the acetate concentration was very low in the TD + R and averaged 29 ± 7 mg/L.

3.3. Ammonia inhibition

Anaerobic digestion model. No 1 (ADM 1) considers free ammonia inhibition on methanogenesis process in anaerobic digesters (Batstone et al., 2002). Based on the ammonium concentrations and pH values obtained for each digester, the free ammonia fraction was calculated using Equation (2) (Anthonisen et al., 1976; see Table 3).

$$\frac{FAN}{TAN} = \frac{10^{pH}}{10^{pH} + e^{\frac{6344}{(273+T)}}} \quad (2)$$

Where FAN is free ammonia nitrogen in mg/L as N; TAN is total ammonia nitrogen in mg/L as N; T is temperature in °C.

To estimate possible inhibition on the digesters' performance, a non-competitive inhibition (Equation (3)) model was used to evaluate the inhibition effect of free ammonia on methanogenesis (Batstone et al., 2002).

$$\text{Inhibition factor } (I_{nh3}) = \frac{1}{1 + \frac{S_{NH3}}{K_{I,NH3}}} \quad (3)$$

Where, S_{NH3} is the free ammonia concentration (see Table 3) and $K_{I,NH3}$ is the inhibitory ammonia coefficient where 50% reduction happens in methane production. The $K_{I,NH3}$ values for thermophilic and mesophilic temperatures were taken from Gallertand Winter (1998) and were 251 and 92 mg/L NH₃-N, respectively. The inhibition factors (I_{nh3}) computed for the MD, TD, MD + R and TD + R were 0.65, 0.56, 0.32 and 0.30, respectively. High inhibition factor (I_{nh3}) indicates low inhibitory effect on methanogenesis process. Comparison of the digester sets, that is, MD vs. TD and MD + R vs. TD + R, showed 17% and 7.5% greater ammonia inhibition effect on methane production under the thermophilic conditions. In addition, the model estimated a severe inhibition of methanogenesis in the digesters with digestate recirculation, regardless of the operating temperature. The lower performance of the thermophilic digesters (i.e., TD and TD + R) in terms of methane production might partially be explained by ammonia inhibition. However, the methane yields (Table 3) indicated comparable results for the MD and MD + R. It should be noted that the concentration of active microbial biomass might be different at the two temperatures. The microbial decay rates are higher at elevated temperatures, potentially yielding lower active microbial biomass in the thermophilic digesters. Consequently, the overall effect of ammonia inhibition on the acetoclastic methanogenesis pathway was potentially more profound for the thermophilic digesters.

3.4. Microbial analysis

To investigate the effect of digesters configurations (with and without digestate recirculation) operated at mesophilic and thermophilic temperatures on bacterial and archaeal communities, total DNA was isolated from the MD, MD + R, TD and TD + R digesters after 152 days of operation, and analyzed for 16S rRNA sequences. Due to the high microbial diversity that was observed in the digesters, only the phyla with higher than 1% relative abundance were considered for discussion and comparison.

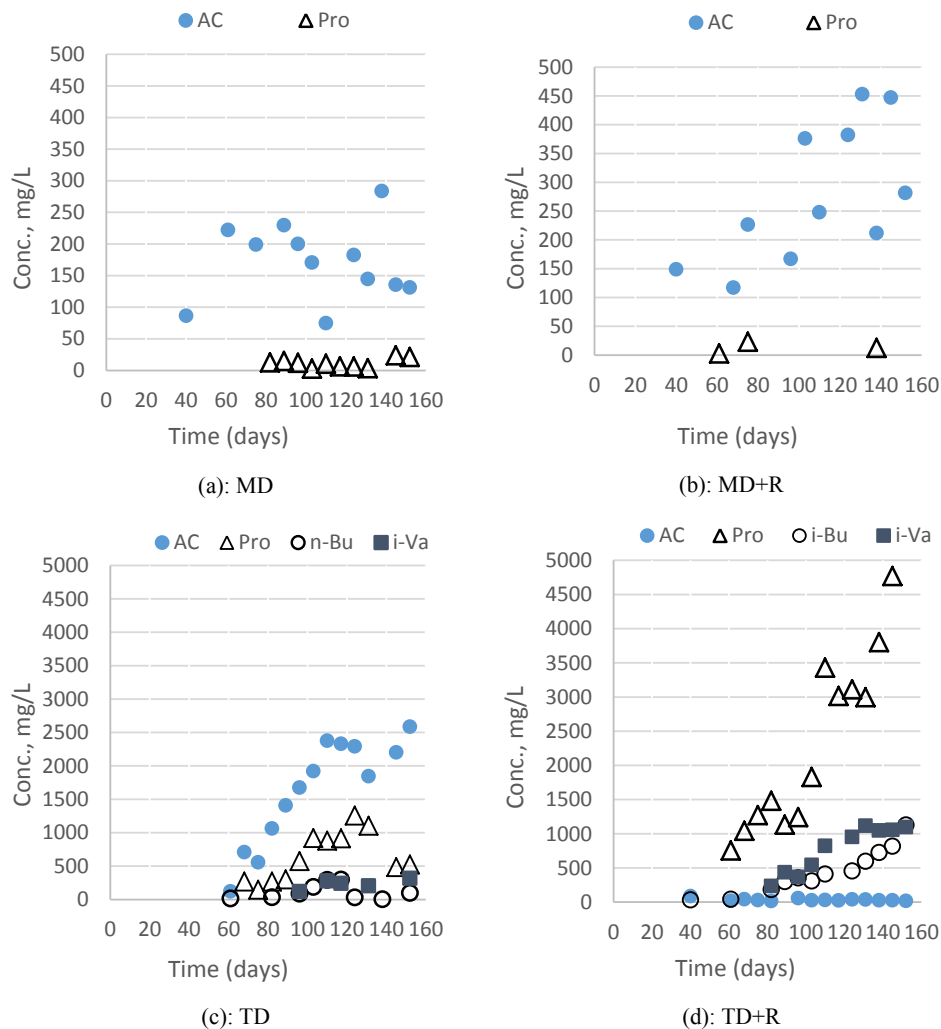


Fig. 2. Concentration of volatile fatty acids in the digesters.

3.4.1. Microbial community structure in mesophilic digesters

The results of the microbial community analysis under stable operation of the MD and MD + R are presented in Fig. 3. The dominant bacterial phyla in both of the mesophilic digesters were *Firmicutes* (25% in the MD and 75% in the MD + R), *Chloroflexi* (54% in the MD and 6% in the MD + R), *Bacteroidetes* (16% in the MD and 7% in the MD + R) and *Actinobacteria* (2% in the MD and 3% in the MD + R). A meta-analysis by Nelson et al. (2011) and an extensive analysis of various full-scale digesters by Sundberg et al. (2013) showed that *Firmicutes*, *Chloroflexi*, *Bacteroidetes* as well as *Proteobacteria* have typically been found as predominant bacterial groups in anaerobic digesters operated under various conditions. *Actinobacteria* was found as the fourth dominant phylum in the MD and MD + R, while the relative abundance of *Proteobacteria* was less than 1% of the total reads in this study. However, this agreed with the previous findings indicating the dominance of either *Actinobacteria* or *Proteobacteria* depending on the digesters operating conditions (Cardinali-Rezende et al., 2012).

Although the bacteria comprising the four most prominent phyla in both mesophilic digesters were the same during the steady-state operation of the mesophilic digesters, the recirculation of the digestate significantly influenced the relative abundance of each of these four bacterial groups. While phyla *Chloroflexi* (mostly represented by the candidate division T78 of the family

Anaerolineaceae) dominated in the MD, *Firmicutes* was by far the most dominant phyla in the MD + R. In total 75% of the reads in the MD + R was affiliated to *Firmicutes*, represented by a major fraction of *Clostridium* (48% of total reads). In strong contrast, only 1% of the total reads of the MD affiliated to this genus. *Firmicutes* in general and the genus *Clostridium* represent members that are versatile in metabolic capabilities and include proteolytic and saccharolytic bacteria, as well as syntrophic species involved in VFA degradation (Riviere et al., 2009; Vanwonterghem et al., 2014; Hippe et al., 1992).

It was also found that 53% of all 16S rRNA gene reads in the MD were affiliated to candidate division T78, while only 5% was observed in the MD + R. Presence of *Anaerolineaceae* in anaerobic digesters fed with various organic wastes has been widely reported in the literature (St-Pierre and Wright, 2014; Kim et al., 2014). Many of the genera that have been identified in this family are strictly anaerobic bacteria and fermentatively use carbohydrates as substrate for growth (Yamada et al., 2006; Sekiguchi et al., 2003). Thus, it would appear that the members of *Anaerolineaceae*, Candidate division T78, contributed to the degradation of carbohydrate fraction of the food waste. Additionally, the remarkable difference observed in the dominance of *Chloroflexi* in the MD and *Firmicutes* in the MD + R might reflect the less tolerance of the *Chloroflexi* members to the high levels of ammonia, which was 2.2 times

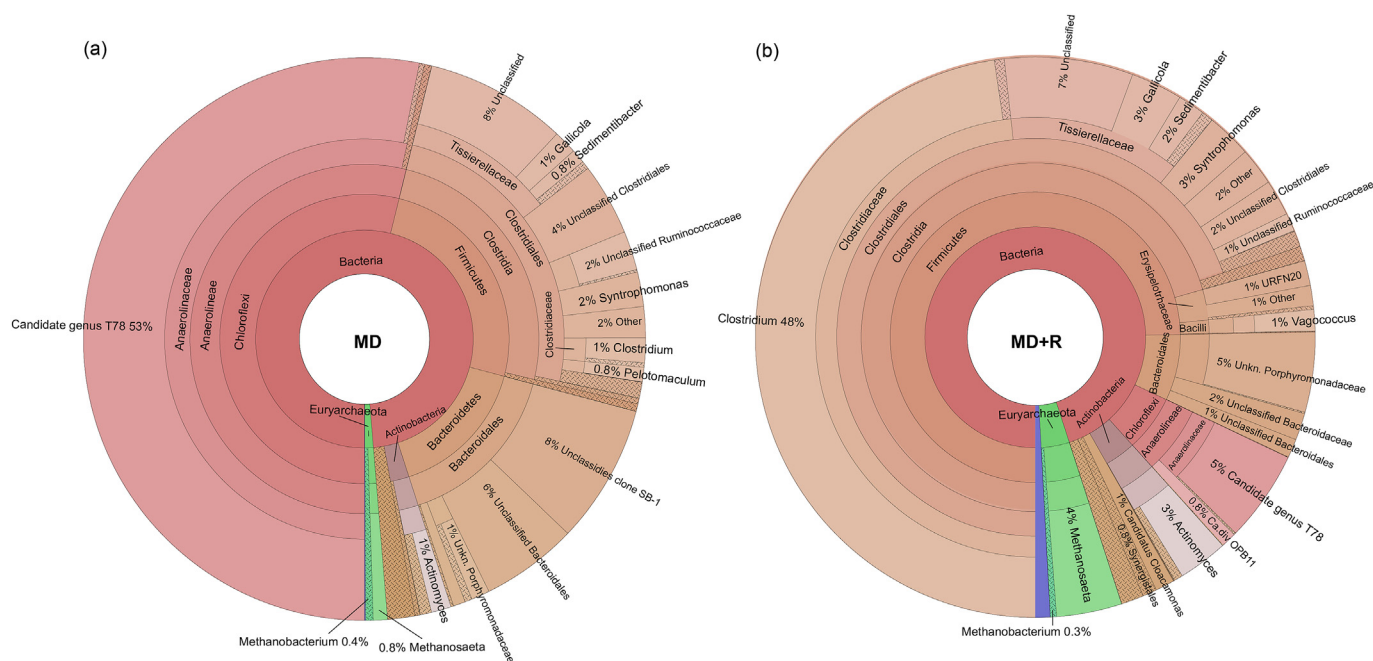


Fig. 3. Microbial structure in MD (a) and MD + R (b) after 153 days of AD, illustrated by simplified Krona plots based on 16S rRNA gene sequencing. The abundance of each taxonomic group corresponds to the percentage of the total number of reads. The shaded areas represent the presence of two or more low abundant taxa.

higher in the MD + R than MD. [Yi et al. \(2014\)](#) reported a reduction of *Anaerolineae* (of *Chloroflexi*) by increasing TS concentration in the anaerobic digesters used for FW treatment. The increase in TS content was accompanied with a severe increase in total ammonia level (from 400 to 1920 mg/L). The results agreed with our observation that the elevated ammonia concentrations led to a decrease in *Chloroflexi* abundance.

Interestingly, analysis of *Firmicutes* revealed a significant difference in distribution of bacterial groups at the family level within the mesophilic digesters. *Tissierellaceae* accounted for 43% of all *Firmicutes*' reads in the MD, while *Clostridiaceae* was the dominant family in the MD + R accounted for 65% of the phylum reads. The family *Clostridiaceae* only constituted 7% of the *Firmicutes* in the MD.

The phyla *Bacteroidetes* and *Actinobacteria* represented respectively 16% and 2% of the readings in the MD, and 7% and 3% in the MD + R. However, the majority (98% in the MD + R and 72% in the MD) of the reads were not affiliated to a known genus of the *Bacteroidetes*. Regarding the *Actinobacteria*, the genus *Actinomyces* was the main member of the phylum found in both mesophilic digesters. The relative abundances were, respectively, 3% and 1% (of the total reads) in the MD + R and MD. The higher relative abundance of the *Actinomyces* in the MD + R was likely due to the effluent recirculation of recalcitrant fiber materials to the digester, since it was previously reported the probable involvement of *Actinomyces* in hydrolysis of cellulose ([Ziganshin et al., 2011, 2013](#)).

Overall, based on the performance results ([Table 3](#)), both MD and MD + R showed stable and comparable performance with high methane production. Thus, the differences in abundance of the predominant phyla did not influence biogas production. This observation support a possible functional redundancy of the *Chloroflexi* and *Firmicutes* members ([Allison and Martiny, 2008](#)).

The phylogenetic analysis of archaea demonstrated that almost all sequences were affiliated with the *Euryarchaeota* phylum ([Fig. 3](#)), comprising 4% and 1% of the microbial community in the mesophilic digesters MD + R and MD, respectively. A notable difference in the relative abundance of methanogens was observed for

the mesophilic digesters. At the genus level, *Methanosaeta* and *Methanobacterium* were dominant genera and accounted for 65% and 32% of all *Euryarchaeota*'s reads in MD, respectively. On the other hand, *Methanosaeta* accounted for 91% of all *Euryarchaeota*'s reads for the MD + R, while *Methanobacterium* constituted 8% of the phylum. Thus, it appeared that the recirculation of the digestate in the MD + R resulted in a high prevalence of *Methanosaeta* species. The prevalence of acetoclastic methanogens (i.e., *Methanosaeta*) over hydrogenotrophic methanogens (*Methanobacterium*) in the MD and MD + R probably demonstrated the acetate cleavage as the main pathway for methane production. Low acetate concentrations in the mesophilic digesters ([Fig. 2](#)), which were, on average, 175 mg/L in the MD and 278 mg/L in the MD + R, supported the efficient conversion of acetate into methane by the acetoclastic methanogenesis pathway.

Additionally, as described earlier, the use of an inhibition model demonstrated a potential severe free ammonia inhibition on the acetoclastic methanogenesis in the MD + R due to high NH_3 levels within the digester, which averaged 198 mg/L. However, the performance and microbial data showed a stable and comparable performance to the MD. Therefore, it interestingly appeared that the recirculation of digestate attenuated the effect of free ammonia on acetoclastic methanogens, since it is well documented that *Methanosaetaceae* are sensitive to high ammonia concentrations ([Ho et al., 2013; Karakashev et al., 2005](#)).

3.4.2. Microbial community structure in thermophilic digesters

The dominant bacterial phyla found in the thermophilic digesters included *Firmicutes*, *Thermotoga*, and *Synergistales* ([Fig. 4](#)). In contrast to the mesophilic digesters where a clear difference in the distribution of prominent groups was observed, the overall community structure was similar in the TD and TD + R. Thus, the effect of recirculation on the microbial community structure was more noticeable under mesophilic conditions. In both thermophilic digesters, *Firmicutes* and *Thermotoga* made up the majority of the reads. *Firmicutes* and *Thermotoga* accounted respectively for 35% and 40% of all reads for the TD and 41% and 37% for the TD + R. As

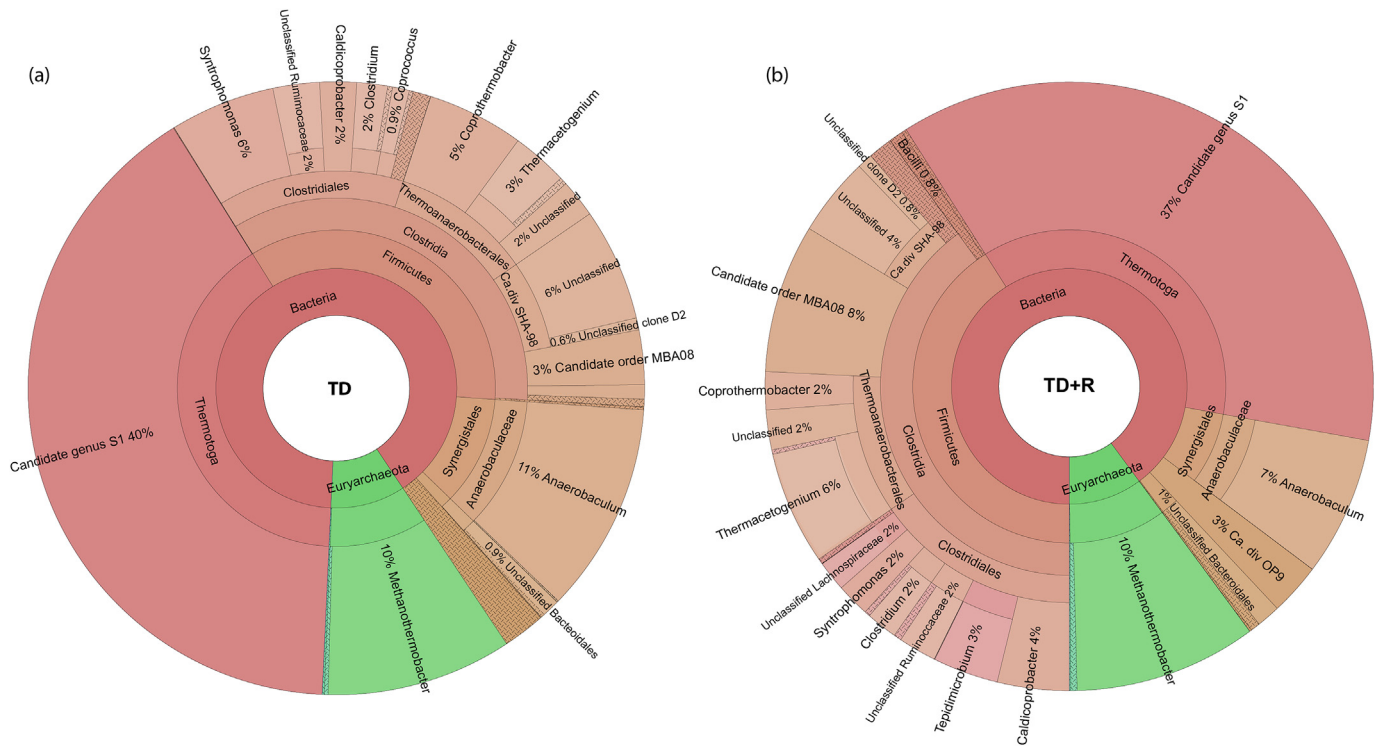


Fig. 4. Microbial community structure in TD (a) and TD + R (b) after 153 days of AD, illustrated by simplified Krona plots based on 16S rRNA gene sequencing. The abundance of each taxonomic group corresponds to the percentage of the total number of reads. The shaded areas represent the presence of two or more low abundant taxa.

with the mesophilic digesters, the diversity within *Firmicutes* was high, comprising several genera mainly within the orders *Clostridiales*, *Thermoanaerobacteriales*, candidate division SHA-98 and the candidate order MBA08. Uncultured representatives from candidate order MBA08 have been observed to dominate in thermophilic (and mesophilic) digesters with high ammonia content (De Vrieze et al., 2015). Additionally, MBA08 has previously been reported to dominate in cellulolytic communities of anaerobic digesters (Sun et al., 2015), thus suggesting that this group was probably responsible for the hydrolysis of cellulosic materials in the food waste.

The genera *Coprothermobacter* and *Thermacetogenium* were dominant members of the order *Thermoanaerobacteriales* in both TD and TD + R. Even though the relative abundance of *Thermoanaerobacteriales* was quite similar in both digesters, the distribution of *Coprothermobacter* and *Thermacetogenium* genera within the order was notably influenced by the digestate recirculation. *Coprothermobacter* was the main genus (49%) of the order *Thermoanaerobacteriales* in the TD, which was followed by *Thermacetogenium* (28%). For TD + R *Thermacetogenium* constituted 60% of the order, followed by *Coprothermobacter* (19%). The genus *Thermacetogenium* grows acetogenically on various hydrolysis products including amino acids, organic acids and H_2/CO_2 . They are also able to oxidize acetate in co-culture with hydrogenotrophic methanogenes (Hattori et al., 2000). This might explain the low concentration of acetate in the TD + R digester (Fig. 2D). Presence of relatively high abundance of *Coprothermobacter* (5% and 2% in TD and TD + R, respectively) was likely due to their contribution to the degradation of proteinaceous fraction of the food waste (Sasaki et al., 2011). The *Coprothermobacter* members are proteolytic bacteria that degrade proteins into acetate, H_2 and CO_2 . In the presence of hydrogenotrophic methanogenes, an increased amount of propionate and butyrate production has been reported (Sasaki et al., 2011). Interestingly, the observation of the relatively high

abundance of *Thermoanaerobacteriales* was concomitant with high concentrations of NH_3 , propionate, butyrate and iso-valerate (Table 3 and Fig. 2). This was likely due to their high ammonium tolerance (up to 6 g/L), which was reported by Ollivier et al., 1985.

A significant difference was observed in the relative abundances of the genera within the *Clostridiales* when the bacterial community structure was compared in the TD and TD + R. *Syntrophomonas* accounted for 40% of the genera found in the order *Clostridiales* in the TD, while this value for the TD + R was only 12%. *Caldicoprobacter* and *Tepidimicrobium* (of the family *Tissierellaceae*) were the predominant genera in the TD + R, accounting for 25% and 23% of the order. *Caldicoprobacter* and *Tepidimicrobium* are both fermentative microorganisms, where the former ferments sugars and the latter grows on a number of proteinaceous substrates (Slobodkin et al., 2006; Yokoyama et al., 2010). As reported previously, the majority of the members of the *Syntrophomonas* are extreme anaerobes, so called syntrophic acetogenic bacteria (SAB), that use β -oxidation process to break down long chain organic acids (C_4 – C_{18}) to acetate, propionate and H_2 in a syntrophic cooperation with hydrogenotrophic methanogenes (Zhao et al., 1993). Consequently, it may be inferred that the relatively greater fraction of *Syntrophomonas* in the TD helped the formation of an enhanced syntrophic degradation of the organic acids and resulted in a better performance. The recirculation of digestate in the TD + R seemed to negatively influence this syntrophic reaction and resulted in the accumulation of the propionate, butyrate and iso-valerate within the digester (Fig. 2). Additionally, the relatively lower abundance of *Anaerobaculum* (phylum *Synergistetes*) in the TD + R (7% of the reads) as compared to the TD (11% of the reads) might account for the accumulation of VFAs in the TD + R. *Anaerobaculum* members are capable of converting organics acids, peptides and a limited number of carbohydrates to acetate, CO_2 and H_2 (Menes and Muxi, 2002).

Thermotoga was solely represented by the candidate division S1

within *Thermotoga* (40% and 37% of the total reads in the TD and TD + R, respectively), a phylum that contains known syntrophic acetate oxidizers (Balk et al., 2002). Additionally, an enhanced growth of *Thermotoga* has been reported in co-culture with a hydrogen consumer (Frock et al., 2012; Conners et al., 2006). Because of its high relative abundance, it is tempting to suggest candidate division S1 as a possible candidate of syntrophic acetate oxidizer.

Analysis of the archaeal composition in the thermophilic digesters revealed that both of the digesters were almost completely dominated by the hydrogenotrophic methanogens (Fig. 4). The genus *Methanothermobacter* (of the order *Methanobacteriales*) accounted for 97% and 96% of the archaea in the TD and TD + R, respectively. Only a small fraction (~1%) of archaeal readings in both digesters was identified as the genus *Methanosarcina*, which is able to use either hydrogenotrophic or acetoclastic methanogenesis pathway. Due to the presence of the various syntrophic members (as discussed above), it was expected to find high abundance of hydrogenotrophic methanogens in the thermophilic digesters. The dominance of H₂ utilizing methanogens has previously been reported in digesters fed with food waste and operated at thermophilic conditions (Guo et al., 2014; Giuliano et al., 2014). The hydrogenotrophic methanogens constituted 10% of the total reads in both TD and TD + R. Based on these observations, it may be inferred that the prevalent pathway for methane production in the thermophilic digesters was hydrogenotrophic methanogenesis.

3.4.3. Dominant microbial pathways for methane production

Based on process data and microbial community data a schematic diagram of probable dominant pathways in the four digesters can be made (Fig. 5). The very low levels of longer VFAs (propionate and butyrate) in both MD and MD + R (Fig. 2a,b) demonstrated an efficient removal of these intermediates into acetate by syntrophic acetogenic bacteria (SAB). These digesters also had relatively low levels of acetate, demonstrating efficient conversion of acetate to methane. Based on microbial data, the main pathway for methane production seemed to be carried out by acetoclastic methanogens (i.e., *Methanosaeta*) in both MD and MD + R (Fig. 5, grey arrows).

Microbial data showed that the dominating pathway for methane production in the thermophilic digesters was hydrogenotrophic methanogenesis, probably due to free ammonia

inhibition of acetoclastic methanogens (Fig. 5, dotted arrows). This means that acetate was metabolized by syntrophic acetate oxidizing bacteria (SAOBs) in the thermophilic digesters. This is supported by the high abundance of *Thermotoga* and *Thermacetogenium* in these digesters, which has been suggested to be syntrophic acetate oxidizers (Hattori et al., 2000). Syntrophic acetate oxidation has been reported to occur under elevated temperatures and high ammonia concentrations (Karakashev et al., 2005). In TD, acetate was accumulating in the digester, while propionate, butyrate and iso-valerate concentrations were relatively low (but higher than in the mesophilic digesters; Fig. 2c). This acetate accumulation demonstrated that the SAOB pathway was more inhibited than the SAB pathway in the TD digester. The accumulation of propionate and longer VFAs in the TD + R digester indicated a much stronger inhibition of the SAB pathway in this digester, probably due to the high concentration of free ammonia (Siegrist et al., 2002). The presence of higher relative abundances of *Syntrophomonas* and *Synergistales* in the TD as compared to the TD + R supported a more effective syntrophic acetogenesis in the TD digester.

4. Conclusion

Regardless of the digestate recirculation, anaerobic digestion of the pretreated FW under mesophilic conditions outperformed the thermophilic digesters in terms of the methane production. Accumulation of VFAs in the thermophilic digesters indicated an imbalance between solubilization of the substrate and the methane production process.

Recirculation of digestate, as a strategy to reduce water consumption, worked very well under mesophilic conditions despite resulting in relatively high levels of ammonia.

In both mesophilic digesters *Methanosaeta* was the dominant archaea, but the bacterial community structure was significantly different. *Firmicutes* dominated in the MD + R, while *Chloroflexi* was the dominant phylum in the MD. In contrast to the mesophilic digesters, the microbial communities in the thermophilic digesters were rather similar, consisting mainly of the phyla *Firmicutes*, *Thermotoga*, *Synergistetes* and the hydrogenotrophic methanogen *Methanothermobacter*. Thus, a combination of digesters configurations, operating temperatures and ammonia concentrations resulted in different dominant pathways for methane production. A conventional acetoclastic methanogenesis appeared to be the main pathway in the mesophilic digesters, while syntrophic acetate oxidation and hydrogenotrophic methanogenesis seemed to be the dominant pathway in the thermophilic digesters. Practically, a mesophilic temperature may be recommended in cases where digestate is to be used for dilution of food waste.

Acknowledgements

This work was financially supported by the ENERGIX-program of the Norwegian Research Council, grant no. 228747. We would like to thank Jane Agger for her help in using liquid chromatography for VFA analysis. A special thank is also extended to Maria Estevez who helped in the preliminary stage of the digesters' set up.

References

- Allison, S.D., Martiny, J.B., 2008. Resistance, resilience, and redundancy in microbial communities. *Proc. Natl. Acad. Sci.* 105 (Suppl. 1), 11512–11519.
- Anthonisen, A., Loehr, R., Prakasam, T., Srinath, E., 1976. Inhibition of nitrification by ammonia and nitrous acid. *J. Water Pollut. Control Fed.* 835–852.
- Balk, M., Weijma, J., Stams, A.J., 2002. *Thermotogalettingae* sp. nov., a novel thermophilic, methanol-degrading bacterium isolated from a thermophilic anaerobic reactor. *Int. J. Syst. Evol. Microbiol.* 52 (4), 1361–1368.
- Batstone, D.J., Keller, J., Angelidaki, I., Kalyuzhny, S., Pavlostathis, S., Rozzi, A., Sanders, W., Siegrist, H., Vavilin, V., 2002. *Anaerobic Digestion Model No. 1*

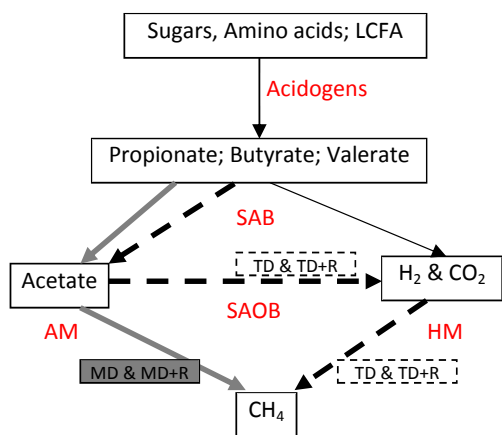


Fig. 5. Dominant methane production pathways in the various digesters. Solid grey arrows indicate a pathway through syntrophic acetogenesis and acetoclastic methanogenesis which dominated in MD and MD + R. Dashed arrows indicate a pathway through syntrophic acetogenesis, acetate oxidation and hydrogenotrophic methanogenesis which dominated in TD and TD + R. SAB: syntrophic acetogenic bacteria; SAOB: syntrophic acetate oxidizing bacteria; AM: acetoclastic methanogens; HM: hydrogenotrophic methanogens.

- (ADM1). IWA publishing.
- Caporaso, J.G., Kuczynski, J., Stombaugh, J., Bittinger, K., Bushman, F.D., Costello, E.K., Fierer, N., Pena, A.G., Goodrich, J.K., Gordon, J.L., 2010. QIIME allows analysis of high-throughput community sequencing data. *Nat. methods* 7 (5), 335–336.
- Cardinali-Rezende, J., Colturato, L.F., Colturato, T.D., Chartone-Souza, E., Nascimento, A.M., Sanz, J.L., 2012. Prokaryotic diversity and dynamics in a full-scale municipal solid waste anaerobic reactor from start-up to steady-state conditions. *Bioresour. Technol.* 119, 373–383.
- Cardinali-Rezende, J., Debarry, R.B., Colturato, L.F., Carneiro, E.V., Chartone-Souza, E., Nascimento, A.M., 2009. Molecular identification and dynamics of microbial communities in reactor treating organic household waste. *Appl. Microbiol. Biotechnol.* 84 (4), 777–789.
- Cho, J.K., Park, S.C., Chang, H.N., 1995. Biochemical methane potential and solid state anaerobic digestion of Korean food wastes. *Bioresour. Technol.* 52 (3), 245–253.
- Connors, S.B., Mongodin, E.F., Johnson, M.R., Montero, C.I., Nelson, K.E., Kelly, R.M., 2006. Microbial biochemistry, physiology, and biotechnology of hyperthermophilic Thermotoga species. *FEMS Microbiol. Rev.* 30 (6), 872–905.
- De Vrieze, J., Saunders, A.M., He, Y., Fang, J., Nielsen, P.H., Verstraete, W., Boon, N., 2015. Ammonia and temperature determine potential clustering in the anaerobic digestion microbiome. *Water Res.* 75, 312–323.
- Edgar, R.C., 2010. Search and clustering orders of magnitude faster than BLAST. *Bioinformatics* 26 (19), 2460–2461.
- Edgar, R.C., Haas, B.J., Clemente, J.C., Quince, C., Knight, R., 2011. UCHIME improves sensitivity and speed of chimera detection. *Bioinformatics* 27 (16), 2194–2200.
- El-Mashad, H.M., Zhang, R., 2010. Biogas production from co-digestion of dairy manure and food waste. *Bioresour. Technol.* 101 (11), 4021–4028.
- Frock, A.D., Gray, S.R., Kelly, R.M., 2012. Hyperthermophilic Thermotoga species differ with respect to specific carbohydrate transporters and glycoside hydrolases. *Appl. Environ. Microbiol.* 78 (6), 1978–1986.
- Gallert, C., Bauer, S., Winter, J., 1998. Effect of ammonia on the anaerobic degradation of protein by a mesophilic and thermophilic biowaste population. *Appl. Microbiol. Biotechnol.* 50 (4), 495–501.
- Ganesh, R., Torrijos, M., Soubie, P., Lugardon, A., Steyer, J.P., Delgenes, J.P., 2014. Single-phase and two-phase anaerobic digestion of fruit and vegetable waste: comparison of start-up, reactor stability and process performance. *Waste Manag.* 34 (5), 875–885.
- Ge, H., Jensen, P.D., Batstone, D.J., 2011. Temperature phased anaerobic digestion increases apparent hydrolysis rate for waste activated sludge. *Water Res.* 45 (4), 1597–1606.
- Giuliano, A., Zanetti, L., Micolucci, F., Cavinato, C., 2014. Thermophilic two-phase anaerobic digestion of source-sorted organic fraction of municipal solid waste for bio-hythane production: effect of recirculation sludge on process stability and microbiology over a long-term pilot-scale experience. *Water Sci. Technol.* 69 (11), 2200–2209.
- Guo, X., Wang, C., Sun, F., Zhu, W., Wu, W., 2014. A comparison of microbial characteristics between the thermophilic and mesophilic anaerobic digesters exposed to elevated food waste loadings. *Bioresour. Technol.* 152, 420–428.
- Hartmann, H., Ahring, B.K., 2005. Anaerobic digestion of the organic fraction of municipal solid waste: influence of co-digestion with manure. *Water Res.* 39 (8), 1543–1552.
- Hattori, S., Kamagata, Y., Hanada, S., Shoun, H., 2000. Thermacetogeniumphaeum gen. nov., sp. nov., a strictly anaerobic, thermophilic, syntrophic acetate-oxidizing bacterium. *Int. J. Syst. Evol. Microbiol.* 50 (4), 1601–1609.
- Hippe, H., Andreesen, J., Gottschalk, G., 1992. The genus Clostridium—nonmedical. *prokaryotes* 2, 1800–1866.
- Ho, D.P., Jensen, P.D., Batstone, D.J., 2013. Methanosarcinaceae and acetate-oxidizing pathways dominate in high-rate thermophilic anaerobic digestion of waste-activated sludge. *Appl. Environ. Microbiol.* 79 (20), 6491–6500.
- Karakashev, D., Batstone, D.J., Angelidaki, I., 2005. Influence of environmental conditions on methanogenic compositions in anaerobic biogas reactors. *Appl. Environ. Microbiol.* 71 (1), 331–338.
- Kim, S., Bae, J., Choi, O., Ju, D., Lee, J., Sung, H., Park, S., Sang, B.-I., Um, Y., 2014. A pilot scale two-stage anaerobic digester treating food waste leachate (FWL): performance and microbial structure analysis using pyrosequencing. *Process Biochem.* 49 (2), 301–308.
- Kim, Y.M., Jang, H.M., Lee, K., Chantrasakdakul, P., Kim, D., Park, K.Y., 2015. Changes in bacterial and archaeal communities in anaerobic digesters treating different organic wastes. *Chemosphere* 141, 134–137.
- Mata-Alvarez, J., Cecchi, F., Llabrés, P., Pavan, P., 1992. Anaerobic digestion of the Barcelona central food market organic wastes. Plant design and feasibility study. *Bioresour. Technol.* 42 (1), 33–42.
- Menes, R.J., Muxí, L., 2002. Anaerobaculum mobile sp. nov., a novel anaerobic, moderately thermophilic, peptide-fermenting bacterium that uses crotonate as an electron acceptor, and emended description of the genus Anaerobaculum. *Int. J. Syst. Evol. Microbiol.* 52 (1), 157–164.
- Nelson, M.C., Morrison, M., Yu, Z., 2011. A meta-analysis of the microbial diversity observed in anaerobic digesters. *Bioresour. Technol.* 102 (4), 3730–3739.
- Ollivier, B.M., Mah, R.A., Ferguson, T.J., Boone, D.R., Garcia, J.-L., Robinson, R., 1985. Emendation of the genus Thermobacteroides: thermobacteroidesproteolyticus sp. nov., a proteolytic acetogen from a methanogenic enrichment. *Int. J. Syst. Bacteriol.* 35 (4), 425–428.
- Procházka, J., Dolejš, P., Máca, J., Dohányos, M., 2012. Stability and inhibition of anaerobic processes caused by insufficiency or excess of ammonia nitrogen. *Appl. Microbiol. Biotechnol.* 93 (1), 439–447.
- Riviere, D., Desvignes, V., Pelletier, E., Chaussonnerie, S., Guermazi, S., Weissenbach, J., Li, T., Camacho, P., Sghir, A., 2009. Towards the definition of a core of microorganisms involved in anaerobic digestion of sludge. *ISME J.* 3 (6), 700–714.
- Sasaki, K., Morita, M., Sasaki, D., Nagaoka, J., Matsumoto, N., Ohmura, N., Shinozaki, H., 2011. Syntrophic degradation of proteinaceous materials by the thermophilic strains Coprothermobacterproteolyticus and Methanothermobacterthermautotrophicus. *J. Biosci. Bioeng.* 112 (5), 469–472.
- Sekiguchi, Y., Yamada, T., Hanada, S., Ohashi, A., Harada, H., Kamagata, Y., 2003. Anaerolineathermophila gen. nov., sp. nov. and Caldilineaerophila gen. nov., sp. nov., novel filamentous thermophiles that represent a previously uncultured lineage of the domain Bacteria at the subphylum level. *Int. J. Syst. Evol. Microbiol.* 53 (6), 1843–1851.
- Sheng, K., Chen, X., Pan, J., Kloss, R., Wei, Y., Ying, Y., 2013. Effect of ammonia and nitrate on biogas production from food waste via anaerobic digestion. *Biosyst. Eng.* 116 (2), 205–212.
- Siegrist, H., Vogt, D., Garcia-Heras, J.L., Gujer, W., 2002. Mathematical model for meso- and thermophilic anaerobic sewage sludge digestion. *Environ. Sci. Technol.* 36 (5), 1113–1123.
- Slobodkin, A., Tourova, T., Kostrikin, N., Lysenko, A., German, K., Bonch-Osmolovskaya, E., Birkeland, N.-K., 2006. Tepidimicrobiumferriphilum gen. nov., sp. nov., a novel moderately thermophilic, Fe (III)-reducing bacterium of the order Clostridiales. *Int. J. Syst. Evol. Microbiol.* 56 (2), 369–372.
- St-Pierre, B., Wright, A.-D.G., 2014. Comparative metagenomic analysis of bacterial populations in three full-scale mesophilic anaerobic manure digesters. *Appl. Microbiol. Biotechnol.* 98 (6), 2709–2717.
- Sun, L., Pope, P.B., Eijsink, V.G., Schnürer, A., 2015. Characterization of microbial community structure during continuous anaerobic digestion of straw and cow manure. *Microb. Biotechnol.* 8 (5), 815–827.
- Sundberg, C., Al-Soud, W.A., Larsson, M., Alm, E., Yekta, S.S., Svensson, B.H., Sørensen, S.J., Karlsson, A., 2013. 454 pyrosequencing analyses of bacterial and archaeal richness in 21 full-scale biogas digesters. *FEMS Microbiol. Ecol.* 85 (3), 612–626.
- Takahashi, S., Tomita, J., Nishioka, K., Hisada, T., Nishijima, M., 2014. Development of a Prokaryotic Universal Primer for Simultaneous Analysis of Bacteria and Archaea Using Next-generation Sequencing.
- Vanwonterghem, I., Jensen, P.D., Ho, D.P., Batstone, D.J., Tyson, G.W., 2014. Linking microbial community structure, interactions and function in anaerobic digesters using new molecular techniques. *Curr. Opin. Biotechnol.* 27, 55–64.
- Vanwonterghem, I., Jensen, P.D., Rabaey, K., Tyson, G.W., 2015. Temperature and Solids Retention Time Control Microbial Population Dynamics and Volatile Fatty Acid Production in Replicated Anaerobic Digesters. *Scientific reports* 5.
- Wilson, C.A., Novak, J., Takacs, I., Wett, B., Murthy, S., 2012. The kinetics of process dependent ammonia inhibition of methanogenesis from acetic acid. *Water Res.* 46 (19), 6247–6256.
- Yamada, T., Sekiguchi, Y., Hanada, S., Imachi, H., Ohashi, A., Harada, H., Kamagata, Y., 2006. Anaerolineathermolimosa sp. nov., Levilineasaccharolytica gen. nov., sp. nov. and Leptolineaardivitalis gen. nov., sp. nov., novel filamentous anaerobes, and description of the new classes Anaerolineae classis nov. and Caldilineae classis nov. in the bacterial phylum Chloroflexi. *Int. J. Syst. Evol. Microbiol.* 56 (6), 1331–1340.
- Yi, J., Dong, B., Jin, J., Dai, X., 2014. Effect of Increasing Total Solids Contents on Anaerobic Digestion of Food Waste under Mesophilic Conditions: Performance and Microbial Characteristics Analysis.
- Yokoyama, H., Wagner, I.D., Wiegell, J., 2010. Caldicoprobacteroshimai gen. nov., sp. nov., an anaerobic, xylanolytic, extremely thermophilic bacterium isolated from sheep faeces, and proposal of Caldicoprobacteraceae fam. nov. *Int. J. Syst. Evol. Microbiol.* 60 (1), 67–71.
- Zhang, L., Lee, Y.-W., and Jahng, D., 2011. Anaerobic co-digestion of food waste and piggery wastewater: focusing on the role of trace elements. *Bioresour. Technol.* 102 (8), 5048–5059.
- Zhao, H., Yang, D., Woese, C.R., Bryant, M.P., 1993. Assignment of fatty acid- β -oxidizing syntrophic bacteria to Syntrophomonadaceae fam. nov. on the basis of 16S rRNA sequence analyses. *Int. J. Syst. Bacteriol.* 43 (2), 278–286.
- Ziganshin, A.M., Liebetrau, J., Pröter, J., Kleinstuber, S., 2013. Microbial community structure and dynamics during anaerobic digestion of various agricultural waste materials. *Appl. Microbiol. Biotechnol.* 97 (11), 5161–5174.
- Ziganshin, A.M., Schmidt, T., Scholwin, F., Il'inskaya, O.N., Harms, H., Kleinstuber, S., 2011. Bacteria and archaea involved in anaerobic digestion of distillers grains with solubles. *Appl. Microbiol. Biotechnol.* 89 (6), 2039–2052.

Paper IV

Quantitative metaproteomics highlight the metabolic contributions of uncultured phylotypes in a thermophilic anaerobic digester

Live H. Hagen, Jeremy A. Frank, Mirzaman Zamanzadeh, Vincent G.H. Eijsink, Phillip B. Pope, Svein J. Horn*, Magnus Ø. Arntzen

Department of Chemistry, Biotechnology and Food Science, Norwegian University of Life Sciences (NMBU), P. O. Box 5003, N-1432 Ås, Norway

*Corresponding author. Department of Chemistry, Biotechnology and Food Science, Norwegian University of Life Sciences, P. O. Box 5003, N-1432 Ås, Norway. Tel.: + 47 67232488; Fax: + 47 64965901. E-mail address: svein.horn@nmbu.no

Abstract

In this study, we used multiple meta-omic approaches to characterize the microbial community and the active metabolic pathways of a stable industrial biogas reactor operating at thermophilic temperatures (60°C) and elevated levels of free ammonia (367 mg NH₃-N/L). The microbial community was strongly dominated (76% of all 16S rRNA amplicon reads) by a population affiliated to the proteolytic bacterium, *Coprothermobacter thermoautotrophicus*. Multiple *C. thermoautotrophicus* strains were detected, introducing an additional level of complexity seldom explored in biogas studies. Genome reconstructions provided metabolic insight into the microbes that performed biomass deconstruction and fermentation, including, besides *C. thermoautotrophicus*, the deeply branching phyla *Dictyoglomi*, *Planctomycetes* and candidate phylum Atribacteria. These biomass degraders were complemented by a synergistic network of microorganisms that convert key fermentation intermediates (fatty acids) via syntrophic interactions with hydrogenotrophic methanogens, to ultimately produce methane. Interpretation of the proteomics data also suggested activity of a *Methanosaeta* phylotype acclimatized to high ammonia level. In particular, we report a novel bacterium proposed as a syntrophic acetate oxidizer that also exerts high expression of enzymes needed for both the Wood Ljungdahl pathway and β -oxidation of fatty acids to acetyl-CoA. Such an arrangement differs from known syntrophic oxidizing bacteria and presents an interesting hypothesis for futures studies. Collectively, this study provides increased insight into active metabolic roles of uncultured phlotypes and presents new synergistic relationships, both of which may contribute to the remarkable stability of the digester under study .

Importance

Biogas production through anaerobic degradation of organic waste provides an attractive source of renewable energy and a sustainable waste management strategy. A comprehensive understanding of the microbial community that drives anaerobic digesters is essential to ensure stable and efficient energy production. Here, we characterize the intricate microbial networks and metabolic pathways in a thermophilic biogas reactor. We discuss the impact of frequently encountered microbial species as well as the metabolism of newly discovered novel phylotypes that seem to play distinct roles within key microbial stages of anaerobic digestion in this remarkably stable high-temperature system. In particular, we draft a metabolic scenario whereby an uncultured SAOB is capable of syntrophically oxidizing acetate as well as longer-chain fatty-acids (via the β -oxidation and Wood-Ljungdahl pathways) to hydrogen and carbon dioxide, which methanogens subsequently convert to methane.

Keywords: Anaerobic digestion, methane, microbial community, metagenomics, metaproteomics

Introduction

Utilization of more sustainable approaches for waste disposal, rather than landfilling or incineration, has gathered global interest in recent years. Microbial anaerobic digestion (AD) of organic matter for the production of methane is a viable alternative and many research initiatives address optimization of the efficiency of the AD process (e.g. 1, 2-4). AD processes operating under thermophilic conditions have advantages over mesophilic processes with respect to digestion efficiency and substrate sanitation (5-7). However, the microbial community inherent to thermophilic AD conditions are typically less diverse and more vulnerable to environmental changes (8-10).

Generally, AD proceeds via four major steps. A large consortium of bacteria performs the first three stages, called hydrolysis, acidogenesis and acetogenesis, whereas a specialized group of archaea (methanogens) is responsible for the final step, methanogenesis (11, 12). In short, organic polymers such as polysaccharides, proteins and lipids are hydrolyzed to oligomers and monomers in the initial step (Hydrolysis). These monomers are in turn fermented to organic acids, such as volatile fatty acids (VFA) and amino acids (Acidogenesis), which may be further degraded to acetate, hydrogen, carbon dioxide (CO_2) and a few other one-carbon compounds (Acetogenesis). Hydrogenotrophic methanogens subsequently convert CO_2 and H_2 into methane (CH_4), whereas acetate can be converted to methane via two different pathways, namely by direct conversion by acetoclastic methanogenesis (13), or by syntrophic acetate oxidation (SAO) (14) yielding CO_2 and H_2 to feed the hydrogenotrophic methanogens. Oxidation of acetate and longer chain fatty acids (FA) is thermodynamically unfavorable ($\Delta G > 0$) under high partial pressure of H_2 (15) and requires a syntrophic interplay with hydrogen consuming microorganisms such as hydrogenotrophic methanogens. Syntrophic networks become particularly significant in

thermophilic anaerobic digestion, where an increase of free ammonia and temperature inhibits acetoclastic methanogens (8, 16, 17).

Despite the importance of these cooperative interactions in biogas processes, few cultivable syntrophic FA and acetate oxidizing bacteria have been recovered and described (e.g. 18, 19, 20). Such bacteria typically grow poorly as a result of marginal energy acquisition shared between the oxidizing bacteria and hydrogen-consumer, and their growth demands are difficult to simulate in laboratory cultures (21). Utilization of combined culture-independent 'omics'-based technologies has recently enabled detailed characterizations of several putative syntrophic acetate oxidizing bacteria (SAOB) (22).

In this study, we characterized the microbial community of a full-scale biogas plant that has been operating efficiently and stably at an unusually high temperature of 60°C for a decade, with food waste as the dominant feed stocks. We specifically sought to determine the metabolic roles of uncultured phylotypes and explored synergistic relationships that possibly play a role in stability. For this cause, we used a combination of high throughput 16S rRNA gene sequencing and total metagenome analyses, which allowed generation of genomic bins of both classified and novel phylotypes. These data were combined with extensive quantitative metaproteomics data, allowing us to assign abundance values to specific proteins for each genomic bin. By combining these analyses we identified favored metabolic pathways and crucial microbes that drive the different steps of the AD in this thermophilic and stable reactor system.

Materials and methods

Source and basic analysis of the sample

The sample was collected in June 2014 from a 2200 m³ thermophilic biogas plant (FrBGR) in Fredrikstad, Norway. This plant has been operating stably for a decade at 60 °C mainly using food waste as substrate. Total solids (TS), volatile solids (VS), total chemical oxygen demand (TCOD) and soluble COD (SCOD) were analyzed according to Standard Methods (APHA, 1998). For measurement of SCOD and volatile fatty acids (VFAs), an aliquot of the sample was first centrifuged at 14000 rpm for 1 min and then filtered using 0.45 µm filters. Ammonium was determined in the centrifuged filtered samples using an ammonium sensitive electrode (Orion 93 Electrode, Thermoscientific, USA). VFAs were analyzed by reversed phase HPLC (Dionex, Sunnyvale CA, USA) using a Zorbax Eclipse Plus C₁₈ column (Agilent, USA; 150 x 2.1 mm column; 3.5 µm particles) equipped with a guard column (12.5 x 2.1 mm; 5 µm particles). The pH was adjusted to 2.5 using 2.5 mM H₂SO₄ prior to VFA analysis of the sample.

DNA extraction

An aliquot of 1 mL slurry from the biogas reactor was frozen immediately after sampling, and kept frozen (at -20°C) until extraction of protein and DNA. DNA was extracted and processed according to (23), with minor modifications. DNA concentrations were quantified using a Qubit™ fluorometer and the Quant-iT™ dsDNA BR Assay Kit (Invitrogen, Carlsbad, CA, USA).

16S rRNA gene sequencing

16S rRNA gene amplicons for the Illumina MiSeq system (Illumina Inc.) were prepared as described in M. Zamanzadeh, et al. (8), and sequencing was conducted using paired-end, 2 x 300 bp cycle runs with the MiSeq Reagent Kit v3 on an Illumina MiSeq sequencing system. All 16S rRNA gene sequences were processed using the QIIME version 1.8.0 software package (24).

Paired-ends were joined (using `join_paired_ends.py`) and quality filtered as follows: only three sequential low-quality (Phred quality score < 20) bases were allowed per sequence before truncating, and reads with < 75% (of total length) consecutive high-quality base calls were discarded. No N characters or barcodes were allowed in the sequence. Chimeric sequences were removed from the dataset using UCHIME incorporated in USEARCH (25) and a threshold of 3% dissimilarity between 16S rRNA gene sequences was used to cluster sequences into *de novo* operational taxonomic units (OTUs) (26). Taxonomy (up to rank 'genus') was assigned to each OTU using the Usearch-based consensus taxonomy assigner implemented in QIIME with default parameters. The Krona visualization tool (27) (available from: <http://krona.sourceforge.net>) was used to visualize the microbial diversity in the biogas reactor sample. Nucleotide variation among 16S rRNA gene sequences assigned to selected taxonomic phylotypes (e.g. *Coprothermobacter*) was detected with oligotyping in order to explore the occurrence of multiple stains not detected by 3% clustering method or taxonomic classification (28).

Total DNA metagenomics

Shotgun metagenomic sequencing of genomic DNA was performed using two different sequencing technology platforms, Illumina MiSeq and the Pacific Biosciences (PacBio) RS II Single Molecule, Real-Time (SMRT®) DNA Sequencing System (29). TruSeq DNA PCR-free sample preparation and paired-ended (2 x 300) MiSeq sequencing were performed at the Norwegian Sequencing Center (NSC, Oslo, Norway). PacBio circular consensus sequencing (CCS) of in total 8 SMRT-cells (minimum accuracy 0.99) using P4-C2 chemistry were performed at the same facility. The PowerClean DNA Clean-Up kit (MoBio Laboratories, Carlsbad, CA, USA) was used to purify extracted microbial DNA prior PacBio sequencing in order to avoid enzymatic inhibition during downstream sample library preparation. MiRA assembler (version 4)

was applied for hybrid assembly of reads from MiSeq and PacBio. Only contigs above 1 kb were considered for the downstream analysis. Open reading frame (ORF)s identified with MetaGeneMark v.1 (30) were screened for protein encoding marker genes, and these were subsequently converted to into a multiple FASTA file (`aa_from_gff.pl`, included in MetaGeneMark v.1). Comparison of the protein sequences against a set of 31 AMPHORA marker genes using HMMSCAN (HMMER 3.0) was then performed.

GC content and sequencing coverage were calculated for each contig and contigs containing 16S rRNA gene fragments were identified. This information was used to generate high quality training data for phylogenetic annotation ('binning') using PhyloPythia S+ (31), resulting in 43 genomic bins at phyla-, species-, and phylotype-levels. 107 Hidden Markov Models of conserved single-copy genes were used to measure the completeness and level of contig duplication in the genomic bins (contigs > 5kb/contigs). All hybrid MiSeq/PacBio contigs (>1 Kb) and genomic bins were uploaded to Integrated Microbial Genomes (IMG) Expert Review for functional annotation. Nucleotide MUMmer (NUCmer) was used for alignment of FrBGR genomic bins and closely related reference genomes.

Metaproteomics

Proteins were extracted from the FrBGR sample by two approaches, one tailored for extracting proteins from within the bacterial cells, and one for proteins residing in the extracellular liquid; both methods are described in detail in Supplementary Text S1. Proteins were denatured, reduced and carbamidomethylated, and further processed into peptides using trypsin. The peptides were analysed by nanoLC-MS/MS as described previously, using a Q-Exactive hybrid quadrupole orbitrap mass spectrometer (Thermo Scientific, Bremen, Germany) (32), and acquired raw data was analysed using MaxQuant (33) version 1.4.1.2. Proteins were quantified using the MaxLFQ

algorithm (34). The data was searched against a sample-specific database, generated from the FrBGR metagenomic contigs that had been organized into phylogenomic bins using PhyloPythiaS+ (see above) and supplemented with reference genomes (www.ncbi.nlm.nih.gov) included from Supplementary Table S1. In addition, common contaminants such as human keratins, trypsin and bovine serum albumin were concatenated to the database as reversed sequences of all protein entries for estimation of false discovery rates. Protein N-terminal acetylation, oxidation of methionine, conversion of glutamine to pyro glutamic acid, and deamination of asparagine and glutamine were used as variable modifications, while carbamidomethylation of cysteine residues was used as a fixed modification. Trypsin was used as digestion enzyme and two missed cleavages was allowed. All identifications were filtered in order to achieve a protein false discovery rate (FDR) of 1%. Results from both protein extraction methods were combined. For protein quantifications, all measurements were performed in biological replicates for both extraction methods and proteins with only a single quantification, i.e. only detected in one of the replicates, were omitted from further analysis.

Results

Characteristics of the biogas reactor

Table 1 shows the characteristics of the FrBGR biogas reactor. The reactor was operating at 60 °C and the average pH of the effluent was 8.0±0.1. The alkalinity was relatively high (5832 mg/L CaCO₃) at the sampling time, indicating enough buffering capacity for neutralization of organic acids and ensuring pH stability. The concentrations of VFAs were generally low and only acetate (91.0±7.0 mg/L) and propionate (32.0±1.5 mg/L) were detected in the effluent. Analysis of the organic content of the digester demonstrated that the major fraction of the chemical oxygen demand (COD) was in particulate form. The soluble COD fraction was only 7.5% of TCOD,

implying an effective conversion of solubilized organics into biogas. The ammonium concentration in the reactor at the time of sampling was 1057 mg NH₄-N/L. Based on the temperature and pH of the digester, the free ammonia concentration was calculated as 367 mg NH₃-N/L (35), which is a level expected to have an inhibitory effect on acetoclastic methanogens (e.g. 36). All in all, these analytical data are typical for a well performing biogas reactor, apart from a relatively high ammonia level.

Data from combined 'meta-omics' technologies

More than 600 000 16S rRNA gene sequences were obtained using MiSeq sequencing of technical triplicates of the DNA sample. Total DNA metagenomic sequencing provided 54 million paired-end reads (MiSeq) and nearly 220 000 long reads (PacBio). (Supplementary Table S2). The hybrid assembly (MiSeq+PacBio) resulted in 235 738 contigs (totaling 473 Mb), where 69 contigs were longer than 100 kb and 4417 longer than 10 kb. The longest contig was 541 616 bp long, with *Dictyoglomus thermophilum* as closest phylogenomic relative. 142 316 contigs were binned into 43 genomic bins. A total of 2416 proteins were identified by combining the two metaproteomics approaches and requiring proteins to be identified and quantified in both replicates. This resulted in highly reproducible, label-free, quantitative data (Pearson correlation R = 0.98, supplementary Figure S1). Taxonomic assignment of each protein was determined by searching against protein sets generated for each FrBGR genomic bin. Detailed descriptions of the proteins, including the numbers of protein hits in the group, are provided in the supplementary material, Table S3. The data assembled for the 24 most abundant genomic bins is summarized in Table 2.

A microbiome strongly dominated by one proteolytic phylotype

The 16S rRNA gene analysis revealed an uneven genus distribution within the FrBGR microbiome, whereby affiliates of the bacterial genus *Coprothermobacter* were predominant,

representing approximately 76% of the total 16S rRNA gene inventory (Figure 1). The second most abundant phylotype (~7%), also affiliated with the bacterial order *Thermoanaerobacterales*, but to the genus *Thermacetogenium*. An *Anaerobaculum* phylotype, affiliated to the bacterial *Synergistales* order was ranked third, representing ~6% of the total inventory. Moreover, the known cellulolytic bacterial genus *Dictyoglomus* represented ~2% of the 16S rRNA gene sequences, whereas another 2% was assigned to *Syntrophomonas*. Phylogenomic binning of assembled contigs from the metagenomic dataset demonstrated a similar population distribution, whereby *Coprothermobacter proteolyticus* accounted for a majority (54 %) of the contigs, followed by *Anaerobaculum mobile* (12 %) and *Thermacetogenium phaeum* (~5 %) (Table 2).

Whilst the representative genome of *Coprothermobacter proteolyticus* DSM5256 is 2.42 Mbp (37), the size of the *C. proteolyticus*-affiliated FrBGR genomic bin was more than tenfold larger (Table 2). The genome bin was examined for assembly and/or binning errors to explain this discrepancy. Closer inspection revealed gene sequences from more than one strain, which seemingly effected the assembly and binning of this phylogenetic group. In addition to *C. proteolyticus*, poor assembly of some of the other dominating bacteria was observed. High-resolution investigation of the 16S rRNA gene inventory detected potential polymorphisms in the 16S rRNA dataset demonstrating that the OTUs assigned as *Coprothermobacter* comprised at least 11 oligotypes (Supplementary Figure S2a). Furthermore, an alignment between the *C. proteolyticus*-affiliated FrBGR genomic bin and the *C. proteolyticus* DSM5256 genome, revealed multiple contigs that mapped against the same *C. proteolyticus* DSM5256 genome coordinates with varying similarity (between 75-100%) (Supplementary Figure S2b).

A total of nine different proteases and peptidases, and two putative intracellular proteases/amidases, were observed in the proteome of *C. proteolyticus* (supplementary table S3).

An oligoendopeptidase was the most abundant of these proteases, with a $\log_{10}(\text{LQF})$ value of 8.4. Import/export of proteins and peptides was indicated by the detection of putative ABC-type transporter systems related to oligopeptides, dipeptides and branched amino acids ($\log_{10}(\text{LQF})$ ranging from 6.6 to 9.2). As expected, the *C. proteolyticus* proteome contained most enzymes of common amino acid metabolizing pathways, dealing with glycine, serine, threonine, valine, leucine and isoleucine. The proteomes of other FrBGR-phylogenotypes also contained enzymes for amino acid metabolism, such as *A. mobile*-affiliated phylogenotypes that expressed proteins inferred in glycine metabolism and arginine degradation via citrulline and ornithine (Supplementary table S3). Several *A. mobile*-affiliated proteins inferred in oligopeptide uptake and degradation were also detected in the proteome, indicating proteolytic activity (Supplementary table S3).

The FrBGR metagenome revealed a diverse group of microorganisms with cellulolytic potential, among them two uncultured phylogenotypes assigned to deeply branching and scarcely described bacterial clades with known cellulolytic potential, namely phylum *Planctomycetes* and candidate phylum Atribacteria (lineage OP9) (Supplementary table S3). The proteome of the uncultured Atribacteria phylogenotype included beta-glucoside-related glycosidase ($\text{Log}_{10}(\text{LFQ})=7.3$) in addition to galactose mutarotase, L-fucose isomerase and xylose isomerase, indicating that this phylogenotype is participating in the hydrolysis of polysaccharides (e.g. xyloglucan oligomers), potentially derived from (hemi)cellulose degradation. Translocation of sugar compounds through the cell membrane was presumably mediated by ABC-type sugar transport systems (non-redundant ABC-type sugar transport system, $\text{Log}_{10}(\text{LFQ})=6.9$), and almost all key enzymes needed for glycolysis (Embden-Meyerhof pathway, EMP) were found in the proteome (Supplementary table S3). Moreover, peptide uptake (non-redundant ABC-dipeptide transport system; $\text{Log}_{10}(\text{LFQ})=8.8$) and degradation (Trypsine-like serine protease; $\text{Log}_{10}(\text{LFQ})=7.2$) systems were detected in the

proteome of the uncultured Atribacteria bacterium, suggest a broader hydrolytic role that also includes protein and amino acids.

A deeply branched phylotype affiliated to the *Planctomycetes* (referred to as unclassified *Planctomycetes* sp.) was also detected, albeit at relatively low abundance (thus not shown in Fig.1). The predicted metabolic role of *Planctomycetes* sp. in FrBGR is linked to carbohydrate degradation, including hemicellulose. Proteome support for this prediction included proteins with carbohydrate binding domains ($\text{Log}_{10}(\text{LFQ})=7.5$), endoglucanases ($\text{Log}_{10}(\text{LFQ})=6.7$ and 6.5), beta-galactosidases ($\text{Log}_{10}(\text{LFQ})=5.7$), alpha-fucosidase ($\text{Log}_{10}(\text{LFQ})=6.5$), alpha-L-arabinofurosidase ($\text{Log}_{10}(\text{LFQ})=6.5$) as well as xylose- and L-arabinose isomerases (ranging from $\text{Log}_{10}(\text{LFQ})$ 6.3 to 8.3). Additionally, the proteome data showed that all genes needed for glycolysis (EMP pathway) were expressed (Supplementary Table S3). Several *Planctomycetes* sp.-affiliated proteins were also assigned as proteases and peptidases with relative high abundance ($\text{Log}_{10}(\text{LFQ})$ ranging from 6.53 to 8.40) (Supplementary table S3).

A phylotype affiliated to *Dictyoglomus thermophilum* was predicted to degrade xylose via the isomerase pathway, whereby xylose is converted to xylulose by the action of xylose isomerase followed by phosphorylation to xylulose-5-phosphate by xylulokinase. The *D. thermophilum*-affiliated proteome comprised both a xylosidase/arabinosidase ($\log_{10}(\text{LFQ})=7.3$) and xylose isomerase ($\log_{10}(\text{LFQ})=6.5$), in addition to a α -amylase/ α mannosidase ($\log_{10}(\text{LFQ})=8.6$) and an endoglucanase ($\log_{10}(\text{LFQ})=6.6$). A D-xylulose 5-phosphate/D-fructose 6-phosphate phosphoketolase (XFP) was also detected, potentially converting D-xylulose-5-phosphate to acetyl-phosphate and glyceraldehyd-3-phosphate, which may enter the pentose phosphate pathway (PPP) and/or glycolysis (EMP) with acetate as an end-product. Several other genomic bins that affiliated with known cellulolytic bacteria, e.g. *Clostridium stercorarium*, and *Clostridium*

thermocellum were extracted from the FrBGR metagenome. However, only a few proteins from these organisms were detected, indicating a reduced role in the biogas reactor.

Methanogenic population and the methanogenesis pathways

Only 0.04 % of the 16S rRNA sequences was affiliated with the Euryarchaeota, which were dominated by representatives of hydrogenotrophic methanogens (*Methanothermobacter*, 99% of Euryarchaeota sequences) and to a much lesser extent acetoclastic methanogens (*Methanosaeta*, 1%) (Figure 1). Accordingly, the genomic bin of *Methanosaeta thermophila* was incomplete, and therefore supplemented by the corresponding reference genome (*Methanosaeta thermophila* PT, Supplementary Table S1) for proteome analysis. Despite the discrepancy in relative abundance of hydrogenotrophic vs acetoclastic methanogens, proteins for both methanogenic pathways were detected (Figure 2). Proteins related to hydrogenotrophic methanogenesis included the formylmethanofuran dehydrogenase cluster ($\log_{10}(\text{LFQ})= 9.7-10.4$), methyl CoM reductase subunits: $\log_{10}(\text{LFQ})= 9.6-9.7$) and several methyltransferase subunits (mtr cluster; $\log_{10}(\text{LFQ})= 7.8-9.3$). Proteins associated with acetoclastic methanogenesis (reference genome *Methanosaeta thermophila* PT) were generally detected at lower levels, ranging from $\log_{10}(\text{LFQ})$ values of 6.7 to 9.0 (acetyl-CoA decarbonylase/synthase and acetyl-coenzyme A synthetase, respectively) (Figure 2, Supplementary Table S3).

Identification of proteins involved in syntrophic degradation of fermentation intermediates

Syntrophic degradation of fermentation intermediates, especially the fatty acids butyrate, propionate and acetate, is essential for the stability of an anaerobic digester. Butyrate and longer chain FA are oxidized through β -oxidation cycle(s), while oxidation of propionate proceeds through the methyl-malonyl-CoA (MMC) pathway. Syntrophic oxidation of acetate, the major precursor in the process, is usually associated with the reverse Wood Ljungdahl pathway.

Phylotypes affiliated to syntrophic bacteria from the genus *Syntrophomonas* were amongst the most prominent in the the FrBGR 16S rRNA dataset, and a near complete genomic bin was reconstructed for phylotypes closely affiliated with *Syntrophomonas wolfei*. For *S. wolfei*-affiliated phylotypes, all four enzyme classes required for β -oxidation of butyrate and perhaps longer FA (acyl-CoA dehydrogenase, enoyl-CoA hydratase and 3-hydroxyacyl-CoA dehydrogenase, 3-ketoacyl-CoA thiolase), were expressed ($\log_{10}(\text{LQF}) = \sim 7$), demonstrating the phylotype's activity within FrBGR. Several CoA transferases, but no acetyl CoA synthetase were observed in the proteome, indicating that activation of the fatty acids occurred by transfer of the CoA group from acetyl-CoA to the fatty acid. A near complete genomic bin was also recovered for a phylotype closely affiliated to *Syntrophothermus lipocalidus*, although *Syntrophothermus* was not present among the abundant genus in the FrBGR 16S rRNA dataset. A long-chain acyl-CoA synthase was identified ($\log_{10}(\text{LQF}) = 6.8$) in the proteome of the *Syntrophothermus lipocalidus*-like phylotype, indicating uptake and degradation of long-chain FA (LCFA), which could emerge from lipid hydrolysis. Distinct from *S. wolfei*, the expression of an acetyl-CoA hydrolase in *S. lipocalidus* indicated that acetate might be formed by hydrolysis rather than substrate level phosphorylation. A phylotype affiliated with the thermophilic, syntrophic propionate-degrading bacterium *Pelotomaculum thermopropionicum*, (38), was detected in FrBGR, but metabolic reconstruction of this phylotype was not possible due to low genome coverage. The incorporation of the reference genome of *P. thermopropionicum* (supplementary Table S1) improved proteome mapping and suggested metabolism of propionate, as both the methyl-malonyl-CoA (MMC) cluster and propionate CoA transferase (PCT) cluster were expressed in relative high abundance (up to $\log_{10}(\text{LQF}) = 8.1$ and 7.5 respectively; Supplementary table S3).

The most numerically abundant phylotype inferred in acetate oxidation was affiliated to *T. phaeum*, and represented approximately 7 % of the 16S rRNA gene inventory. Genome reconstruction and proteome analysis of phylotype *T. phaeum* revealed a relatively high abundance of proteins that constitute the Wood-Ljungdahl (WL) pathway, which is the mainstay in most syntrophic acetate oxidizers (i.e. formyltetrahydrofolate synthase, 5,10 – methylenetetrahydrofolate dehydrogenase, methylenetetrahydrofolate reductase, trimethylamine:corrinoid methyltransferase, carbon monoxide dehydrogenase/acetyl-CoA, phosphotransacetylase and acetate kinase). In addition, proteomic analyses of an uncultured phylotype affiliated with the *Firmicutes* phylum (referred to as unFirm02_FrBGR; abbreviated to “unFi” in Figure 4 and Supplementary Figure S3), also gave strong indications towards its role as a SAOB. This was based on the proteome detection of nearly all enzymes required for the WL pathway (Figure 3, Supplementary Table S3, Supplementary Figure S3). Moreover, the four β -oxidation enzyme classes needed for the degradation of FA to acetyl-CoA were also detected (39), where an Acyl-CoA synthetase protein had the highest expression level ($\log_{10}(\text{LQF}) = 9.0$). Notably, the expression level of β -oxidation related enzymes was generally higher for unFirm02_FrBGR compared to both *S. lipocalidus* and *S. wolfei* (Supplementary Table S3). However, the broad functioning of many enzymes in these classes made further predictions into the specific FA being oxidized overly speculative, and therefore was not attempted. The proteome also revealed that proteins only related to the lower part of the unidirectional EMP were observed (Figure 3, Supplementary Table S3). A protein cluster encoding Fe-S oxidoreductase and electron transfer flavoprotein (ETF) α - and β -subunits was identified in the unFirm02_FrBGR proteome, suggesting a mechanism for reverse electron transfer (39). Thus, we hypothesize that unFirm02_FrBGR imports and oxidizes fatty acids to acetyl-CoA, which is further oxidized to

CO₂ and H₂ through a reverse WL pathway, as illustrated in Figure 3. Searching the 16S rRNA dataset against the metagenome data demonstrated that this phylotype was among the 10 most abundant microbes in FrBGR, comprising 0.5% of the total 16S rRNA gene sequences. Its representative OTU could not be assigned further than to the order *Natranerobiales* ML1228J-1 in our 16S rRNA gene sequencing analysis (using RDP classifier). A phylogenetic comparison of the unFirm02_FrBGR 16S rRNA sequence with known SAOBs and selected syntrophic acetogens suggests a closer relationship to the thermotolerant SAOB *Tepidanaerobacter acetoxydans* than *T. phaeum* (supplementary Figure S4). The closest relative to the representative sequence for unFirm02_FrBGR was *Candidatus* Contubernalis alkalceticum clone Z-7904, with only 91% 16S rRNA gene sequence similarity (using BLAST).

Discussion

Biomass degradation in an ammonia-rich biogas reactor operating at 60°C

Genome reconstruction and functional interpretation of uncultured phylotypes identified participants within key central metabolic pathways in FrBGR, including hydrolysis of macromolecules, downstream fermentation, syntrophic degradation of intermediates and methanogenesis via two pathways (syntrophic acetate oxidation – hydrogenotrophic methanogenesis and acetoclastic methanogenesis) (Summarized in Figure 4). The high content of protein-rich material in the substrate was reflected by a strong dominance of *C. proteolyticus*- and *A. mobile*-like phylotypes, both proven to express high levels of enzymes essential for protein- and amino acid degradation. *C. proteolyticus* is frequently reported at various abundances in thermophilic digesters treating protein-rich biomass, and its proteolytic activity is clearly

supported by the literature (40, 41). Our data introduces additional complexity for *C. proteolyticus*-like populations by indicating the presence of multiple-strains, however the specific diversity and functional interplay that exists remains to be elucidated.

Several novel phylotypes were identified to actively produce enzymes needed for degradation of polysaccharide, another major compartment of food waste (42). A deeply branching bacteria, *D. thermophilum* was observed at relative high abundance (1 % of all 16S rRNA gene sequences, Figure 1) and with high expression levels of proteins related to xylan degradation, in accordance with literature (43). In addition, functional insight was generated for two phylotypes affiliated to deeply branching phyla, *Planctomycetes* and candidate phylum Atribacteria. Representatives from *Planctomycetes* are only sporadically observed typical in anaerobic digesters (44, 45), while candidate phylum Atribacteria (formerly “OP9”) are widespread within these systems (8, 9, 46, 47). Recent studies have demonstrated carbohydrate-degrading characteristics of uncultivated OP9 members (Atribacteria) (48, 49), and the metabolic insight gained in this study suggests proteolytic activity. The results also imply that the unclassified *Planctomycetes* phylotype is metabolically active in the hydrolysis of both proteins and carbohydrates.

A syntrophic network enable complete degradation of fatty acids

Propionate and longer chain fatty acids are important intermediates in anaerobic digestion, and a rapid degradation of these compounds to acetate, formate or hydrogen is essential to enable a complete degradation of organic matter to methane. Degradation of fatty acids in concert with hydrogen production is highly endergonic under standard conditions (propionate $\Delta G^{\circ} = +76.1 \text{ kJ mol}^{-1}$, butyrate; $\Delta G^{\circ} = +48.6 \text{ kJ mol}^{-1}$ (50)), and only possible when hydrogen is kept at low partial pressures by a secondary organism, e.g. a hydrogenotrophic methanogen. Propionate, originating from e.g. amino acid degradation, polysaccharide fermentation, or as a byproduct from β -

oxidation of LCFA, is often one of the major VFAs in anaerobic digestion processes and insufficient removal can lead to instability (51). Most of the characterized syntrophic propionate oxidizing bacteria degrade propionate through the unidirectional methylmalonyl coenzyme A (MMC) pathway. Within FrBGR, *Pelotomacum thermopropionicum* (38) was seemingly the only organism expressing most of the MMC-related enzymes. Involvement of the aforementioned Atribacteria in syntrophic propionate degradation have also been suggested previously (52), however, no evidence for this was found in our data.

Degradation of butyrate and longer chain fatty acids to acetyl-CoA and acetate proceeds through β -oxidation cycles, of which *S. wolfei* -, *S. lipocaldicus*- and unFirm02_FrGBR- phylotypes expressed enzymes from the required classifications (acyl-CoA dehydrogenase, enoyl-CoA hydratase and 3-hydroxyacyl-CoA dehydrogenase, 3-ketoacyl-CoA thiolase). Both *S. wolfei* and *S. lipocalidus* are well-known FA-degraders, whereby the former can utilize fatty acids of four to eight carbons (C₄ to C₈) to (53, 54) and the latter can degrade C₄ to C₁₀ (55). Interestingly, unFirm02_FrBGR exerted the highest acyl-CoA synthetase and acyl-CoA dehydrogenase expression levels compared to both *S. wolfei* and *S. lipocaldicus*, suggesting this novel phylotype is an important FA degrader in FrBGR.

Protein levels indicate activity of a low abundant acetoclastic methanogen insensitive to ammonia

Generally, acetate serves as one of the most important precursors in AD processes (12). Acetate utilizing populations such as acetoclastic methanogens or SAOBs, are therefore essential to ensure stable carbon flow via acetate with methane as a final product. The operating temperature (60 °C) of FrBGR has been previously proposed as a critical balance temperature for an efficient anaerobic digestion (56). Moreover, the concentration of free ammonia (367 mg NH₃-N/L) was in the upper sensitivity level previously established for acetoclastic methogens (8, 10, 16, 57), presumably a

direct consequence of elevated temperatures (lower pK_a of NH_4^+/NH_3) and the proteinaceous feedstock. Similar high ammonia levels and operating temperatures for methanogenic bioreactors are associated with a decline of acetate-consuming methanogens (particularly *Methanosaeta*) and a poorer biogas reactor performance (56, 58-60). Nevertheless, despite the high temperature and free ammonia concentration in FrBGR, chemical analyses suggested a stable (low VFA concentration, sufficient alkalinity) and efficient (low COD) conversion of biomass to biogas. Inhibition of the acetoclastic methanogenesis was therefore expected as well as promoted importance of SAOBs and hydrogenotrophic methanogens (61, 62).

The overall population structure of methanogens in FrBGR was predominated by the obligate hydrogenotrophic methanogen; *M. thermoautotrophicus*. As expected, low population levels were associated with the obligate acetoclastic methanogenic genus *Methanosaeta* in FrBGR, however surprisingly several *Methanosaeta thermofila* enzymes associated with acetoclastic methanogenesis were detected in the FrBGR metaproteome. This illustrated that despite its very low 16S rRNA abundance, *M. thermofila* is metabolically active under the elevated temperature and high ammonia levels. According to the wide range of NH_3 inhibition coefficients (K_{I,NH_3}) reported in the literature (8, 16, 57), the degree of process inhibition is highly dependent on the operational history of a digester, and whether the microbial community within the digester has acclimatized to high ammonia exposure. Previous studies have shown that communities can adapt to stress, and remain tolerant over several generation times (3). Since FrBGR has been running steadily for several years, the populations of acetoclastic methanogens in FrBGR are seemingly acclimatized to the high free ammonia levels calculated for the reactor. In addition to proteomic detection suggesting acetoclastic methanogenesis, the genomic reconstruction of a well-known SOAB *T. phaeum* (63), with a highly expressed WL pathway suggests that acetate-turnover

predominately occurs via syntrophic acetate oxidation in co-existence with hydrogen consuming *Methanothermobacter thermoautotrophicus*-like phylotypes. This scenario suites well with the hypothesis, suggested by D. Ho, et al. (56), that some levels of acetoclastic methanogenesis may be necessary for removal of residual acetate, while SAOBs removes the bulk, in order to enable an efficient degradation.

Evidence for a novel thermophilic acetate oxidizing bacteria, taking longer chain fatty acids all the way to CO₂

Very few SAOBs have been successfully isolated and characterized to date. This limited collection is only represented by two thermophiles (*T. phaeum* and *Thermotoga lettinga* (64)), one that is thermotolerant (*Tepidanaerobacter acetoxydans* (20)) and three mesophiles (*Pseudothermotoga lettinga* (64), *Clostridium ultunense* (18) and *Syntrophaceticus schinkii* (65)). Recent studies have emphasized that the appearance of SAOBs in anaerobic systems is more widespread than those characterized by culture dependent methods and several genomes representing uncultured putative SAOB have been deduced (22, 52, 66). In this study, we identified genomic data affiliated to *T. phaeum* and *T. acetoxydans*, however only few proteins were mapped to the latter indicating low metabolic activity. Phylotypes affiliated to the genus *Thermoacetogenium* were the second most abundant in the 16S rRNA gene inventory. In addition, *T. phaeum*-affiliated proteins related to the WL-pathway were detected at high-levels, demonstrating the prominence of SAO in FrBGR. Aside from relatively well-known SAOB, our analysis suggested a metabolic role for an uncultured and novel thermophilic SAOB (unFirm02_FrBGR). Interestingly, this phylotype encodes the necessary genes and pathways to syntrophically oxidize acetate as well as longer chain fatty acids. This combination of pathways is documented for non-syntrophic sulphate-reducers (67), but not for the characterized SAOBs. Genomic annotation indicates unFirm02_FrBGR is not

a sulphate reducer, as no genes for sulphate reduction was found. Proteomics showed that nearly all unFirm02_FrBGR proteins essential for the WL-pathway were expressed with particularly high levels of formyltetrahydrofolate synthetase (FTHFS) and CO dehydrogenase (acsB). The expression of a protein cluster encoding Fe-S oxidoreductase and electron transfer flavoprotein (ETF) α - and β -subunits, has been previously shown to serve as reverse electron transfer systems in syntrophic fatty acid oxidizing bacteria (39). And finally, phylogenetic analysis confirmed that unFirm02_FrBGR was closest related to *Candidatus Contubernalis alkaleticum*, an uncultivated obligate syntrophic acetate oxidizer (68). Although cultivation based efforts are required to completely validate the metabolic traits and ecological role of the unFirm02_FrBGR phylotype, we believe that the FrBGR observations infer a syntrophic lifestyle. Overall, this study demonstrates a thermophilic bacterium that seemingly utilizes β -oxidation to degrade longer chain fatty acids to acetate, followed by a further oxidation of acetate to CO₂ through the reductive Wood-Ljungdahl pathway.

Conclusion

Collectively we present an increased understanding of uncultured phylotypes that engage in key microbial process within a stable biogas reactor that is operating under problematic conditions. Multiple strains were detected within reconstructed genomes for several key phylotypes, introducing an additional level of complexity seldom explored in biogas studies. Particular focus on uncultivated and scarcely described microbial groups, such as the candidate phylum Atribacteria, *Planctomycetes* and a novel putative SAOB complement ongoing efforts to characterize the microbial processes that control biogas production. Key findings include evidence for a novel SAOB that is seemingly capable of both β -oxidation of longer chain fatty acids as well as acetate oxidation via a reductive WL-pathway. The “connection” of these two pathways

expands our knowledge into the intricate syntrophic networks that are required to convert important fermentation intermediates into methane. Culture-based confirmation is still required and presents an ongoing challenge.

Acknowledgement

This work was financially supported by the Norwegian Research Council (project No. 228747). JAF, MØA and PBP are supported by a grant from the European Research Council (336355-MicroDE). Reactor material from an industrial anaerobic biogas reactor and operating parameter information was provided by the municipal renovation enterprise «Fredrikstad Vann, Avløp og Renovasjonsforetak FREVAR FK», Fredrikstad, Norway. The sequencing service was provided by the Norwegian Sequencing Centre (NSC) (www.sequencing.uio.no). A special thanks to NSC staff-member Ave Tooming-Klunderud for expertise regarding sequencing. We thank Professor Abigail A. Salyers from the University of Illinois for her helpful advice and correspondence.

Data accession:

Datasets are available at the NCBI Sequence Read Archive under accession number SRP076292

Figure captures

Figure 1. Phylogenetic distribution of the most dominant 16S rRNA gene sequences in FrBGR. Details for the Euryarchaeota (not visible in the major plot because of low abundance) are provided in a separate plot to the lower left. Scattered areas contain two or more phylotypes with low abundance. The phylotype assigned to the order *Natranaerobiales* in the 16S rRNA dataset corresponds to the genomic bin named “unFirm02_FrBGR” in the metagenomic dataset, as indicated. The plot was generated using Krona, and then simplified (i.e. removal of low abundant phylotypes) in order to reduce size.

Figure 2. Methanogenesis pathways in FrBGR operating at high temperature and high ammonia concentration. The coloring of genes (shown as boxes) indicates the quantitative MaxQuant LFQ values of the detected proteins. Acetoclastic methanogenesis is shown by light blue lines, with proteins being mapped to the reference genome of *Methanosaeta thermophila* PT. Pathways illustrated by dark blue lines represent hydrogenotrophic methanogenesis and proteins were mapped to *Methanothermobacter thermoautotrophicus* supplemented by the genomic bins of ‘*Methanothermobacter*’, ‘*Methanobacteriales*’ and ‘Archaea’. Abbreviations used in this figure can be found in supplementary Table S3. Subunits of multimeric protein complexes are indicated, if detected (A, B, C etc.).

Figure 3. Selected metabolic pathways of the putative novel SAOB unFirm02_FrBGR. The pathways are proposed based on genome and proteome comparison, and protein abundances are indicated by color. All enzymes needed for β -oxidation of fatty acids, in addition to most enzymes associated with the Wood Ljungdahl pathway were detected. Only proteins affiliated to the lower part of EMP was represented in the proteome. Acetate kinase (ack) was detected in the

genome, but not in the proteome. More details on the proteins detected can be found in supplementary Table S3, including abbreviations.

Figure 4. Hypothetical model of the carbon flux in FrBGR, with functional roles of dominant phylotypes inferred from comparison of metagenome and metaproteome datasets. Metabolic pathways showing the key stages (arrows) of acetogenesis (pink), and methanogenesis (blue), in addition to syntrophic metabolic processes (green). Only the most prominent (with regards on relative abundance and protein abundance) phylotypes in the FrBGR microbial community were evaluated, and it should be noted that the ‘rare’ portion of the population might account for underlying key metabolic pathways not shown here. Organism abbreviations used in this figure: Atri: uncultured Atribacteria bacterium; Dglo: *Dictyoglomus thermophilum*; Athe: *Anaerolinea thermophile*; Cpro: *Coprothermobacter proteolyticus*; Amob: *Anaerobaculum mobile*; Swol: *Syntrophomonas wolfei*; Slip: *Syntrophothermus lipocalidus*; Tpha: *Thermacetogenium phaeum*; unFi: unFirm2_FrBGR; Ppro: *Pelotomaculum thermopropionicum*; Mbt: *Methanothermobacter thermautotrophicus*; Mst: *Methanosaeta thermophile*; Plan: unclassified Planctomycetes sp.

References

1. **Ward AJ, Hobbs PJ, Holliman PJ, Jones DL.** 2008. Optimisation of the anaerobic digestion of agricultural resources. *Bioresource Technology* **99**:7928-7940.
2. **Regueiro L, Carballa M, Lema JM.** 2016. Microbiome response to controlled shifts in ammonium and LCFA levels in co-digestion systems. *Journal of biotechnology*.
3. **Fotidis IA, Karakashev D, Kotsopoulos TA, Martzopoulos GG, Angelidaki I.** 2013. Effect of ammonium and acetate on methanogenic pathway and methanogenic community composition. *FEMS microbiology ecology* **83**:38-48.
4. **Vivekanand V, Olsen EF, Eijsink VG, Horn SJ.** 2013. Effect of different steam explosion conditions on methane potential and enzymatic saccharification of birch. *Bioresource technology* **127**:343-349.
5. **Zabranska J, Stepova J, Wachtl R, Jenicek P, Dohanyos M.** 2000. The activity of anaerobic biomass in thermophilic and mesophilic digesters at different loading rates. *Water Science and Technology*:49-56.
6. **Bolzonella D, Cavinato C, Fatone F, Pavan P, Cecchi F.** 2012. High rate mesophilic, thermophilic, and temperature phased anaerobic digestion of waste activated sludge: A pilot scale study. *Waste management* **32**:1196-1201.
7. **Sanchez E, Borja R, Weiland P, Travieso L, Martin A.** 2000. Effect of temperature and pH on the kinetics of methane production, organic nitrogen and phosphorus removal in the batch anaerobic digestion process of cattle manure. *Bioprocess Engineering* **22**:247-252.
8. **Zamanzadeh M, Hagen LH, Svensson K, Linjordet R, Horn SJ.** 2016. Anaerobic digestion of food waste-effect of recirculation and temperature on performance and microbiology. *Water Research*.
9. **Leven L, Eriksson ARB, Schnurer A.** 2007. Effect of process temperature on bacterial and archaeal communities in two methanogenic bioreactors treating organic household waste. *Fems Microbiology Ecology* **59**:683-693.
10. **Karakashev D, Batstone DJ, Angelidaki I.** 2005. Influence of environmental conditions on methanogenic compositions in anaerobic biogas reactors. *Applied and Environmental Microbiology* **71**:331-338.
11. **Ferry JG.** 1993. *Methanogenesis: ecology, physiology, biochemistry & genetics.* Chapman & Hall, New York.
12. **Gujer W, Zehnder AJB.** 1983. Conversion processes in anaerobic digestion. *Water Science & Technology* **15**:127-167.
13. **Thauer RK.** 1998. Biochemistry of methanogenesis: a tribute to Marjory Stephenson. *Microbiology* **144**:2377-2406.
14. **Schnürer A, Zellner G, Svensson BH.** 1999. Mesophilic syntrophic acetate oxidation during methane formation in biogas reactors. *Fems Microbiology Ecology* **29**:249-261.
15. **McInerney MJ, Struchtemeyer CG, Sieber J, Mouttaki H, Stams AJM, Schink B, Rohlin L, Gunsalus RP.** 2008. Physiology, ecology, phylogeny, and genomics of microorganisms capable of syntrophic metabolism, p 58-72. *In* Wiegand J, Maier RJ, Adams MWW (ed), *Incredible Anaerobes: From Physiology to Genomics to Fuels*, vol 1125. Blackwell Publishing, Oxford.
16. **Angelidaki I, Ahring BK.** 1993. Thermophilic anaerobic digestion of livestock waste: the effect of ammonia. *Applied Microbiology and Biotechnology* **38**:560-564.

17. **Sasaki K, Morita M, Sasaki D, Nagaoka J, Matsumoto N, Ohmura N, Shinozaki H.** 2011. Syntrophic degradation of proteinaceous materials by the thermophilic strains *Coprothermobacter proteolyticus* and *Methanothermobacter thermoautotrophicus*. *Journal of Bioscience and Bioengineering* **112**:469-472.
18. **Schnürer A, Schink B, Svensson BH.** 1996. *Clostridium ultunense* sp. nov., a mesophilic bacterium oxidizing acetate in syntrophic association with a hydrogenotrophic methanogenic bacterium. *International journal of systematic bacteriology* **46**:1145-1152.
19. **Hattori S, Galushko AS, Kamagata Y, Schink B.** 2005. Operation of the CO dehydrogenase/acetyl coenzyme A pathway in both acetate oxidation and acetate formation by the syntrophically acetate-oxidizing bacterium *Thermacetogenium phaeum*. *Journal of bacteriology* **187**:3471-3476.
20. **Westerholm M, Roos S, Schnürer A.** 2011. *Tepidanaerobacter acetatoxydans* sp. nov., an anaerobic, syntrophic acetate-oxidizing bacterium isolated from two ammonium-enriched mesophilic methanogenic processes. *Systematic and applied microbiology* **34**:260-266.
21. **Schink B.** 1997. Energetics of syntrophic cooperation in methanogenic degradation. *Microbiology and Molecular Biology Reviews* **61**:262-&.
22. **Mosbæk F, Kjeldal H, Mulat DG, Albertsen M, Ward AJ, Feilberg A, Nielsen JL.** 2016. Identification of syntrophic acetate-oxidizing bacteria in anaerobic digesters by combined protein-based stable isotope probing and metagenomics. *The ISME Journal* doi:doi:10.1038/ismej.2016.39. doi:10.1038/ismej.2016.39
23. **Rosewarne CP, Pope PB, Denman SE, McSweeney CS, O’Cuiv P, Morrison M.** 2010. High-yield and phylogenetically robust methods of DNA recovery for analysis of microbial biofilms adherent to plant biomass in the herbivore gut. *Microbial ecology* **61**:448-454.
24. **Caporaso JG, Kuczynski J, Stombaugh J, Bittinger K, Bushman FD, Costello EK, Fierer N, Peña AG, Goodrich JK, Gordon JI.** 2010. QIIME allows analysis of high-throughput community sequencing data. *Nature methods* **7**:335-336.
25. **Edgar RC, Haas BJ, Clemente JC, Quince C, Knight R.** 2011. UCHIME improves sensitivity and speed of chimera detection. *Bioinformatics* **27**:2194-2200.
26. **Edgar RC.** 2010. Search and clustering orders of magnitude faster than BLAST. *Bioinformatics* **26**:2460-2461.
27. **Ondov B, Bergman N, Phillippy A.** 2011. Interactive metagenomic visualization in a Web browser. *BMC bioinformatics* **12**:385.
28. **Eren AM, Zozaya M, Taylor CM, Dowd SE, Martin DH, Ferris MJ.** 2011. Exploring the diversity of *Gardnerella vaginalis* in the genitourinary tract microbiota of monogamous couples through subtle nucleotide variation. *PloS one* **6**:e26732.
29. **Frank JA, Pan Y, Tooming-Klunderud A, Eijsink VG, McHardy AC, Nederbragt AJ, Pope PB.** 2016. Improved metagenome assemblies and taxonomic binning using long-read circular consensus sequence data. *Scientific reports* **6**. doi: 10.1038/srep25373
30. **Zhou Y, Pope PB, Li S, Wen B, Tan F, Cheng S, Chen J, Yang J, Liu F, Lei X.** 2014. Omics-based interpretation of synergism in a soil-derived cellulose-degrading microbial community. *Scientific reports* **4**.
31. **Gregor I, Dröge J, Schirmer M, Quince C, McHardy AC.** 2014. PhyloPythiaS+: a self-training method for the rapid reconstruction of low-ranking taxonomic bins from metagenomes. *arXiv preprint arXiv:14067123*.

32. **Arntzen MØ, Karlskås IL, Skaugen M, Eijsink VGH, Mathiesen G.** 2015. Proteomic Investigation of the Response of *Enterococcus faecalis* V583 when Cultivated in Urine. *PloS one* **10**:e0126694.
33. **Cox J, Mann M.** 2008. MaxQuant enables high peptide identification rates, individualized ppb-range mass accuracies and proteome-wide protein quantification. *Nature biotechnology* **26**:1367-1372.
34. **Cox J, Hein MY, Luber CA, Paron I, Nagaraj N, Mann M.** 2014. Accurate proteome-wide label-free quantification by delayed normalization and maximal peptide ratio extraction, termed MaxLFQ. *Molecular & cellular proteomics* **13**:2513-2526.
35. **Anthonisen AC, Loehr RC, Prakasam TBS, Srinath EG.** 1976. Inhibition of nitrification by ammonia and nitrous acid. *Journal (Water Pollution Control Federation)*:835-852.
36. **Ho DP, Jensen PD, Batstone DJ.** 2013. Methanosarcinaceae and acetate-oxidizing pathways dominate in high-rate thermophilic anaerobic digestion of waste-activated sludge. *Applied and environmental microbiology* **79**:6491-6500.
37. **Alexiev A, Coil DA, Badger JH, Enticknap J, Ward N, Robb FT, Eisen JA.** 2014. Complete genome sequence of *Coprothermobacter proteolyticus* DSM 5265. *Genome announcements* **2**.
38. **Kosaka T, Uchiyama T, Ishii S-i, Enoki M, Imachi H, Kamagata Y, Ohashi A, Harada H, Ikenaga H, Watanabe K.** 2006. Reconstruction and regulation of the central catabolic pathway in the thermophilic propionate-oxidizing syntroph *Pelotomaculum thermopropionicum*. *Journal of bacteriology* **188**:202-210.
39. **Sieber JR, Sims DR, Han C, Kim E, Lykidis A, Lapidus AL, McDonald E, Rohlin L, Culley DE, Gunsalus R.** 2010. The genome of *Syntrophomonas wolfei*: new insights into syntrophic metabolism and biohydrogen production. *Environmental microbiology* **12**:2289-2301.
40. **Gagliano MC, Braguglia CM, Petruccioli M, Rossetti S.** 2015. Ecology and biotechnological potential of the thermophilic fermentative *Coprothermobacter* spp. *FEMS microbiology ecology*:fiv018.
41. **Tandishabo K, Nakamura K, Umetsu K, Takamizawa K.** 2012. Distribution and role of *Coprothermobacter* spp. in anaerobic digesters. *Journal of bioscience and bioengineering* **114**:518-520.
42. **Zhang RH, El-Mashad HM, Hartman K, Wang FY, Liu GQ, Choate C, Gamble P.** 2007. Characterization of food waste as feedstock for anaerobic digestion. *Bioresource Technology* **98**:929-935.
43. **Saiki T, Kobayashi Y, Kawagoe K, Beppu T.** 1985. *Dictyoglomus thermophilum* gen. nov., sp. nov., a chemoorganotrophic, anaerobic, thermophilic bacterium. *International Journal of Systematic and Evolutionary Microbiology* **35**:253-259.
44. **Nelson MC, Morrison M, Yu ZT.** 2011. A meta-analysis of the microbial diversity observed in anaerobic digesters. *Bioresource Technology* **102**:3730-3739.
45. **Riviere D, Desvignes V, Pelletier E, Chaussonnerie S, Guermazi S, Weissenbach J, Li T, Camacho P, Sghir A.** 2009. Towards the definition of a core of microorganisms involved in anaerobic digestion of sludge. *The ISME Journal* **3**:700-714.
46. **Hagen LH, Vivekanand V, Pope PB, Eijsink VGH, Horn SJ.** 2015. The effect of storage conditions on microbial community composition and biomethane potential in a biogas starter culture. *Applied microbiology and biotechnology* **99**:5749-5761.

47. **Tang Y-Q, Ji P, Hayashi J, Koike Y, Wu X-L, Kida K.** 2011. Characteristic microbial community of a dry thermophilic methanogenic digester: its long-term stability and change with feeding. *Applied microbiology and biotechnology* **91**:1447-1461.
48. **Dodsworth JA, Blainey PC, Murugapiran SK, Swingley WD, Ross CA, Tringe SG, Chain PSG, Scholz MB, Lo C-C, Raymond J.** 2013. Single-cell and metagenomic analyses indicate a fermentative and saccharolytic lifestyle for members of the OP9 lineage. *Nature communications* **4**:1854.
49. **Nobu MK, Dodsworth JA, Murugapiran SK, Rinke C, Gies EA, Webster G, Schwientek P, Kille P, Parkes RJ, Sass H.** 2016. Phylogeny and physiology of candidate phylum 'Atribacteria'(OP9/JS1) inferred from cultivation-independent genomics. *The ISME journal* **10**:273-286.
50. **Thauer RK, Jungermann K, Decker K.** 1977. Energy-conservation in chemotropic anaerobic bacteria. *Bacteriological Reviews* **41**:100-180.
51. **Hagen LH, Vivekanand V, Linjordet R, Pope PB, Eijsink VG, Horn SJ.** 2014. Microbial community structure and dynamics during co-digestion of whey permeate and cow manure in continuous stirred tank reactor systems. *Bioresource Technology* **171**:350-359.
52. **Nobu MK, Narihiro T, Rinke C, Kamagata Y, Tringe SG, Woyke T, Liu W-T.** 2015. Microbial dark matter ecogenomics reveals complex synergistic networks in a methanogenic bioreactor. *The ISME journal* **9**:1710-1722.
53. **McInerney MJ, Bryant MP, Pfennig N.** 1979. Anaerobic bacterium that degrades fatty acids in syntrophic association with methanogens. *Archives of Microbiology* **122**:129-135.
54. **McInerney MJ, Bryant MP, Hespell RB, Costerton JW.** 1981. *Syntrophomonas wolfei* gen. nov. sp. nov., an anaerobic, syntrophic, fatty acid-oxidizing bacterium. *Applied and Environmental Microbiology* **41**:1029-1039.
55. **Sekiguchi Y, Kamagata Y, Nakamura K, Ohashi A, Harada H.** 2000. *Syntrophothermus lipocalidus* gen. nov., sp. nov., a novel thermophilic, syntrophic, fatty-acid-oxidizing anaerobe which utilizes isobutyrate. *International Journal of Systematic and Evolutionary Microbiology* **50**:771-779.
56. **Ho D, Jensen P, Batstone D.** 2014. Effects of temperature and hydraulic retention time on acetotrophic pathways and performance in high-rate sludge digestion. *Environmental science & technology* **48**:6468-6476.
57. **Yenigün O, Demirel B.** 2013. Ammonia inhibition in anaerobic digestion: a review. *Process Biochemistry* **48**:901-911.
58. **Hartmann H, Ahring BK.** 2005. A novel process configuration for anaerobic digestion of source-sorted household waste using hyper-thermophilic post-treatment. *Biotechnology and bioengineering* **90**:830-837.
59. **Krakat N, Westphal A, Satke K, Schmidt S, Scherer P.** 2010. The microcosm of a biogas fermenter: comparison of moderate hyperthermophilic (60 C) with thermophilic (55 C) conditions. *Engineering in Life Sciences* **10**:520-527.
60. **Rademacher A, Nolte C, Schönberg M, Klocke M.** 2012. Temperature increases from 55 to 75 C in a two-phase biogas reactor result in fundamental alterations within the bacterial and archaeal community structure. *Applied microbiology and biotechnology* **96**:565-576.

61. **Müller B, Sun L, Schnürer A.** 2013. First insights into the syntrophic acetate-oxidizing bacteria—a genetic study. *Microbiologyopen* **2**:35-53.
62. **Hattori S.** 2008. Syntrophic acetate-oxidizing microbes in methanogenic environments. *Microbes and Environments* **23**:118-127.
63. **Hattori S, Kamagata Y, Hanada S, Shoun H.** 2000. *Thermacetogenium phaeum* gen. nov., sp. nov., a strictly anaerobic, thermophilic, syntrophic acetate-oxidizing bacterium. *International Journal of Systematic and Evolutionary Microbiology* **50**:1601-1609.
64. **Balk M, Weijma J, Stams AJ.** 2002. *Thermotoga lettingae* sp. nov., a novel thermophilic, methanol-degrading bacterium isolated from a thermophilic anaerobic reactor. *International Journal of Systematic and Evolutionary Microbiology* **52**:1361-1368.
65. **Westerholm M, Roos S, Schnürer A.** 2010. *Syntrophaceticus schinkii* gen. nov., sp. nov., an anaerobic, syntrophic acetate-oxidizing bacterium isolated from a mesophilic anaerobic filter. *FEMS microbiology letters* **309**:100-104.
66. **Müller B, Sun L, Westerholm M, Schnürer A.** 2016. Bacterial community composition and fhs profiles of low-and high-ammonia biogas digesters reveal novel syntrophic acetate-oxidising bacteria. *Biotechnology for biofuels* **9**:1.
67. **Callaghan A, Morris B, Pereira I, McInerney M, Austin RN, Groves JT, Kukor J, Suflita J, Young L, Zylstra G.** 2012. The genome sequence of *Desulfatibacillum alkenivorans* AK-01: a blueprint for anaerobic alkane oxidation. *Environmental Microbiology* **14**:101-113.
68. **Zhilina TN, Zavarzina DG, Kolganova TV, Tourova TP, Zavarzin GA.** 2005. “*Candidatus Contubernalis alkalaceticum*,” an Obligately Syntrophic Alkaliphilic Bacterium Capable of Anaerobic Acetate Oxidation in a Coculture with *Desulfonatronum cooperativum*. *Microbiology* **74**:695-703.

Table 1. Characteristics of the FrBGR reactor

Parameters	Unit	FrBGR effluent
TS	%	4.4±0.1
VS	%	2.3±0.1
TCOD	mg/L	38615±800
TCOD/VS	-	1.67
SCOD	mg/L	2868±345
pH	-	8.0±0.1
NH ₄	mg N/L	1057±12
Propionate	mg/L	32±1.5
Acetate	mg/L	91±7.0
Alkalinity	mg/L as CaCO ₃	5832±200

Table 2. Characteristics of genomic bins extracted from the FrBGR reactor

ID	Genome bins	Genomic bin size (Mbp)	Contigs (%)	Estimated completeness (%)
Cpro	<i>Coprothermobacter proteolyticus</i>	58.48	54.0	88
Amob	<i>Anaerobaculum mobile</i>	23.65	12.0	93
Tpha	<i>Thermacetogenium phaeum</i>	10.66	5.4	96
Atri	Uncultured Atribacteria bacterium (OP9)	8.46	3.5	93
Slip	<i>Syntrophothermus lipocalidus</i>	7.05	2.8	95
unFi	unFirm2_FrBGR	6.54	2.5	94
Plan	Unclassified Planctomycetes sp.	6.25	3.4	67
Swol	<i>Syntrophomonas wolfei</i>	5.89	1.8	71
Cste	<i>Clostridium stercorarium</i>	5.41	1.7	95
Prot	Unclassified Proteobacteria sp.	4.15	0.7	78
Athe	<i>Anaerolinea thermophila</i>	4.06	1.1	92
Fpen	<i>Fervidobacterium pennivorans</i>	3.68	0.5	93
Dglo	<i>Dictyoglomus thermophilum</i>	3.20	0.9	96
Cthe	<i>Clostridium thermocellum</i>	2.93	1.2	64
Tyel	<i>Thermodesulfovibrio yellowstonii</i>	2.19	0.5	95
Lcri	<i>Lactobacillus crispatus</i>	1.96	0.5	82
Bado	<i>Bifidobacterium adolescentis</i>	1.74	1.0	63
Lraf	<i>Lactococcus raffinolactis</i>	1.63	0.8	65
Ther	Unclassified Thermoanaerobacteraceae sp.	1.36	1.4	>20
Tace	<i>Tepidanaerobacter acetatoxydans</i>	1.01	0.5	40
Pthe	<i>Pelotomaculum thermopropionicum</i>	0.99	0.2	22
Fnod	<i>Fervidobacterium nodosum</i>	0.47	0.3	>20
Mbt	<i>Methanothermobacter thermautotrophicus</i>	0.26	0.2	>20
Mst	<i>Methanosaeta thermophila</i>	0.13	0.2	>20

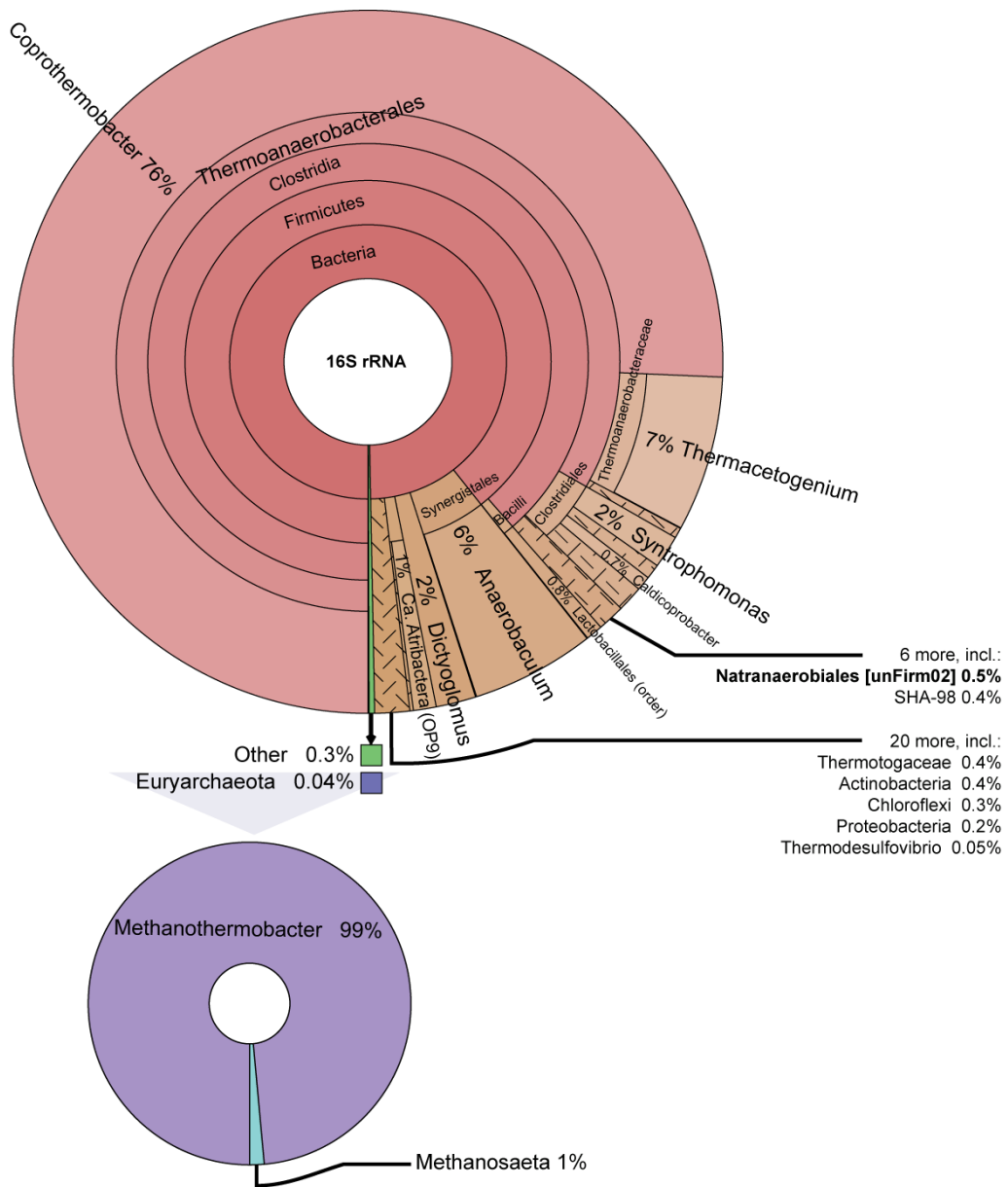


Figure 1

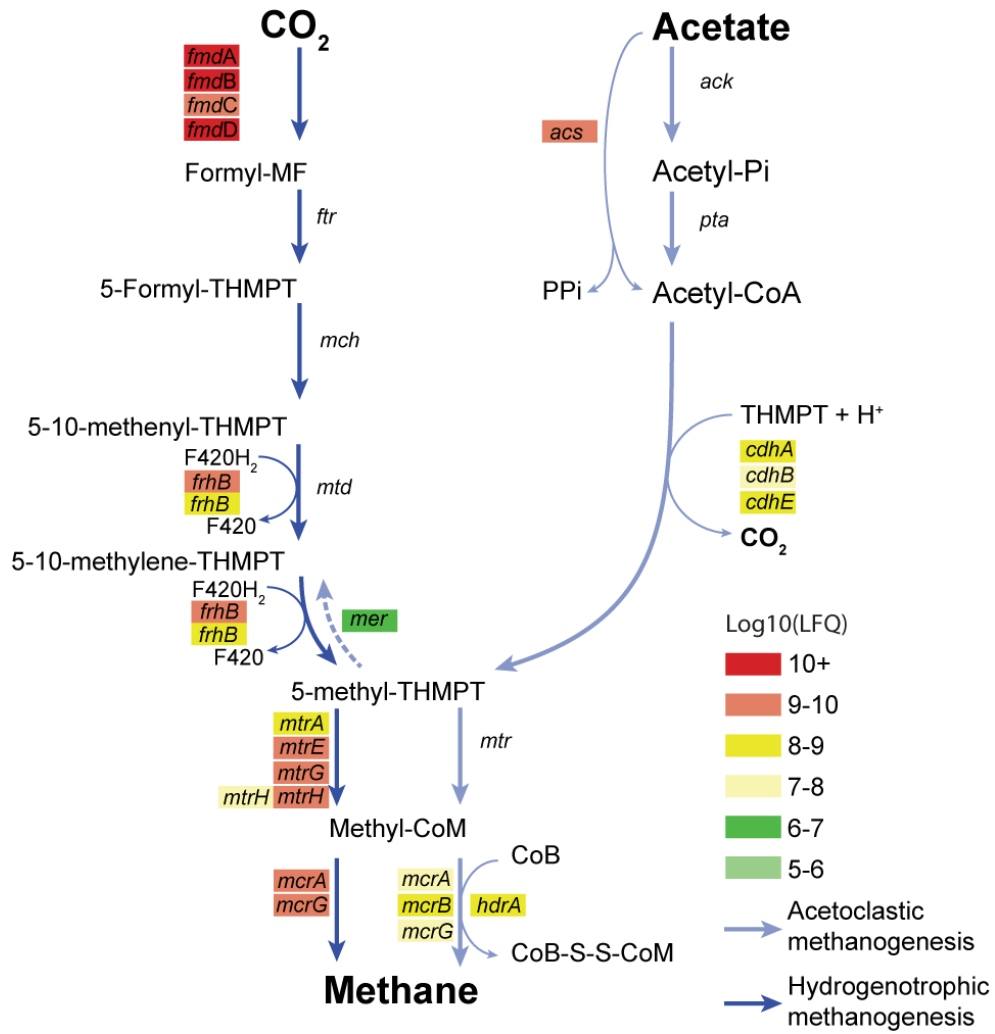


Figure 2

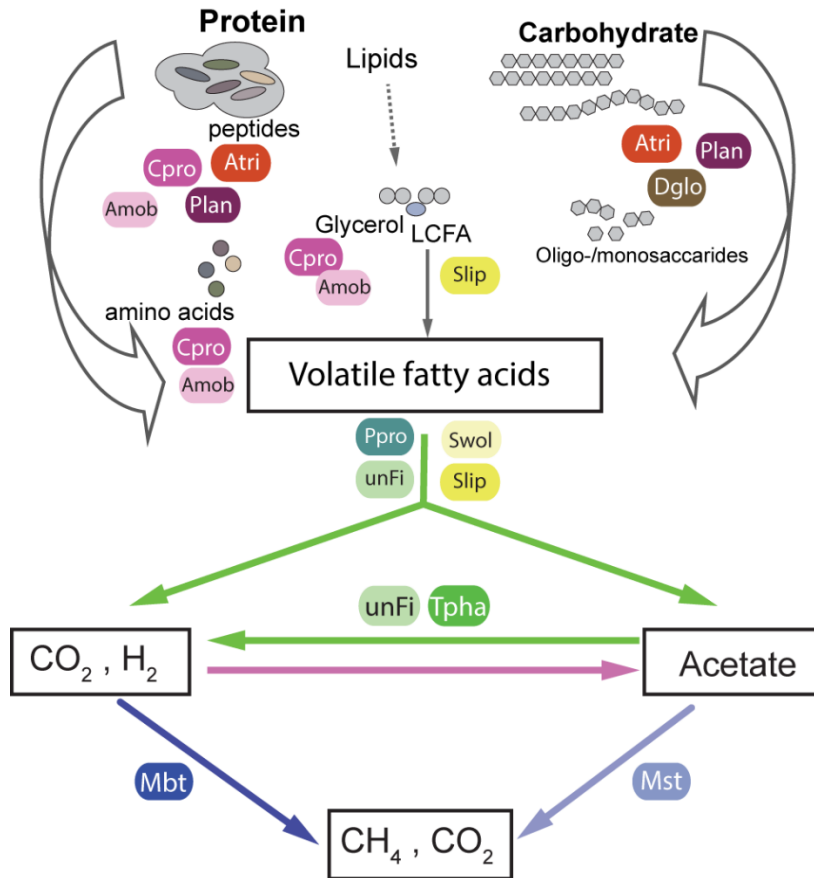


Figure 4

Supplementary material

Quantitative metaproteomics highlight the metabolic contributions of uncultured phylotypes in a thermophilic anaerobic digester

Live H. Hagen, Jeremy A. Frank, Mirzaman Zamanzadeh, Vincent G.H. Eijsink, Phillip B. Pope, Svein J. Horn*, Magnus Ø. Arntzen

Department of Chemistry, Biotechnology and Food Science, Norwegian University of Life Sciences (NMBU), P. O. Box 5003, N-1432 Ås, Norway

*Corresponding author. Department of Chemistry, Biotechnology and Food Science, Norwegian University of Life Sciences, P. O. Box 5003, N-1432 Ås, Norway. Tel.: + 47 67232488; Fax: + 47 64965901. E-mail address: svein.horn@nmbu.no

Supplementary Text S1

Materials and methods

Metaproteomics – protein extraction

Sample was collected in June 2014 from a 2200 m³ thermophilic biogas plant (FrBGR) in Fredrikstad, Norway, and proteins were extracted from the sample in two approaches. In the first method, cells and substrate were pelleted at 16.600 x g for 2 minutes and liquid removed. In order to separate cells from substrate, the pellet was dissolved in 1% (v/v) MeOH, 1% (v/v) tert-Butanol, 0.1% (v/v) Tween-80, pH 2.0 and substrate pelleted by gentle centrifugation at 100 x g for 20 seconds. The cell containing supernatant was transferred to a new tube and the pellet washed again. This was repeated three times to increase the cell count. Cells, now dissociated from the substrate, were finally pelleted and washed in 10 mM Tris-HCl, 1M NaCl, pH 8.0 prior to cell lysis. Lysis was performed using a bead beating approach where glass beads (size $\leq 106 \mu\text{m}$) were added together with lysis buffer (50 mM Tris-HCl, 0.1% (v/v) Triton X-100, 200 mM NaCl, 1 mM DTT) and cells were disrupted in 3 x 60 second cycles using a FastPrep24 (MP Biomedicals, Santa Ana, CA, USA). Debris were removed by centrifugation at 16.600 x g for 20 minutes and proteins were precipitated overnight in 16% ice cold TCA. The next day, proteins were dissolved in SDS sample buffer, separated by SDS-PAGE using an Any-kD Mini-PROTEAN gel (Bio-Rad Laboratories, Hercules, CA, USA) and stained using Coomassie Brilliant Blue R250. The gel was cut in 16 slices and reduced, alkylated and digested as described previously (Arntzen et al. 2015). Prior to mass spectrometry, peptides were desalted using C₁₈ ZipTips (Merck Millipore, Darmstadt, Germany) according to manufacturer's instructions.

A second method was also used, but optimized to extract proteins from the culture liquid. An aliquot of the FrBGR sample (15 mL biomass) was centrifuged at 4500 x g for 10 minutes and the supernatant were transferred to a 10 kDa molecular weight cutoff filter and concentrated to 500 μL . Proteins were then processed for mass spectrometric analysis while residing in the cutoff filter according to the FASP procedure (Wisniewski et al. 2009). In brief, denaturing, alkylation and digestion were accomplished by subsequently passing through 8M urea, 50 mM iodoacetamide and 2 μg trypsin in Tris-HCl, pH 7.8. Trypsination was performed overnight on filter, and peptides were collected the next day by

centrifugation as these would now pass through the cutoff filter. Peptides were desalted by C₁₈ ZipTips as described above.

Supplementary Figures

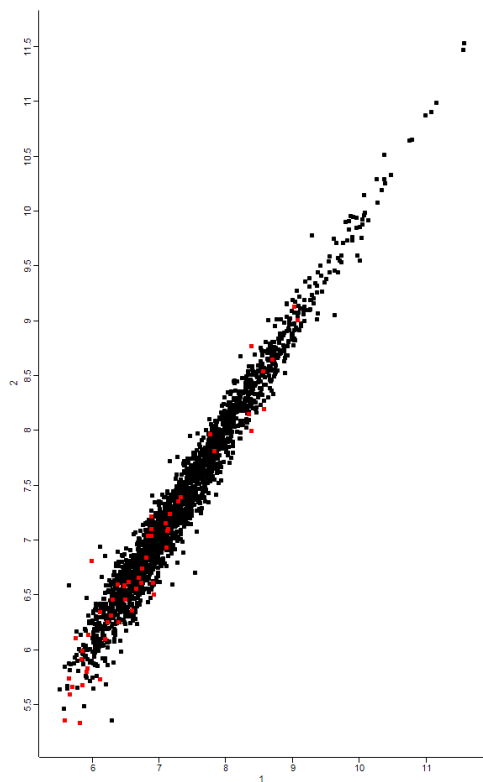


Figure S1: Quality of protein quantification. The figure shows the pairwise reproducibility of label-free quantification (LFQ) between the two biological replicates (Pearson correlation $R=0.98$). Proteins quantified in only one replicate were omitted from further analysis and are not shown in this figure. Proteins identified with a single peptide are indicated in red.

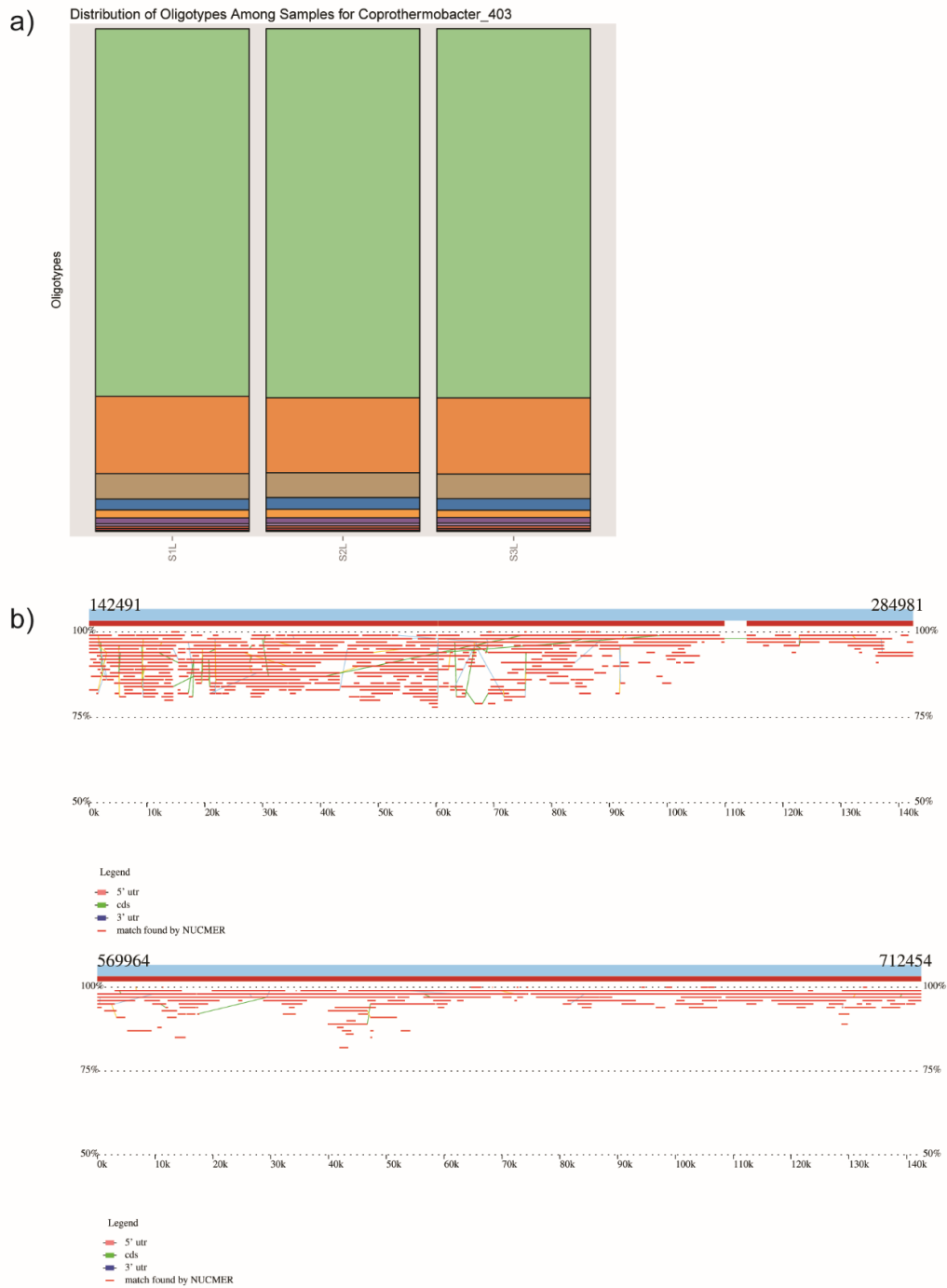
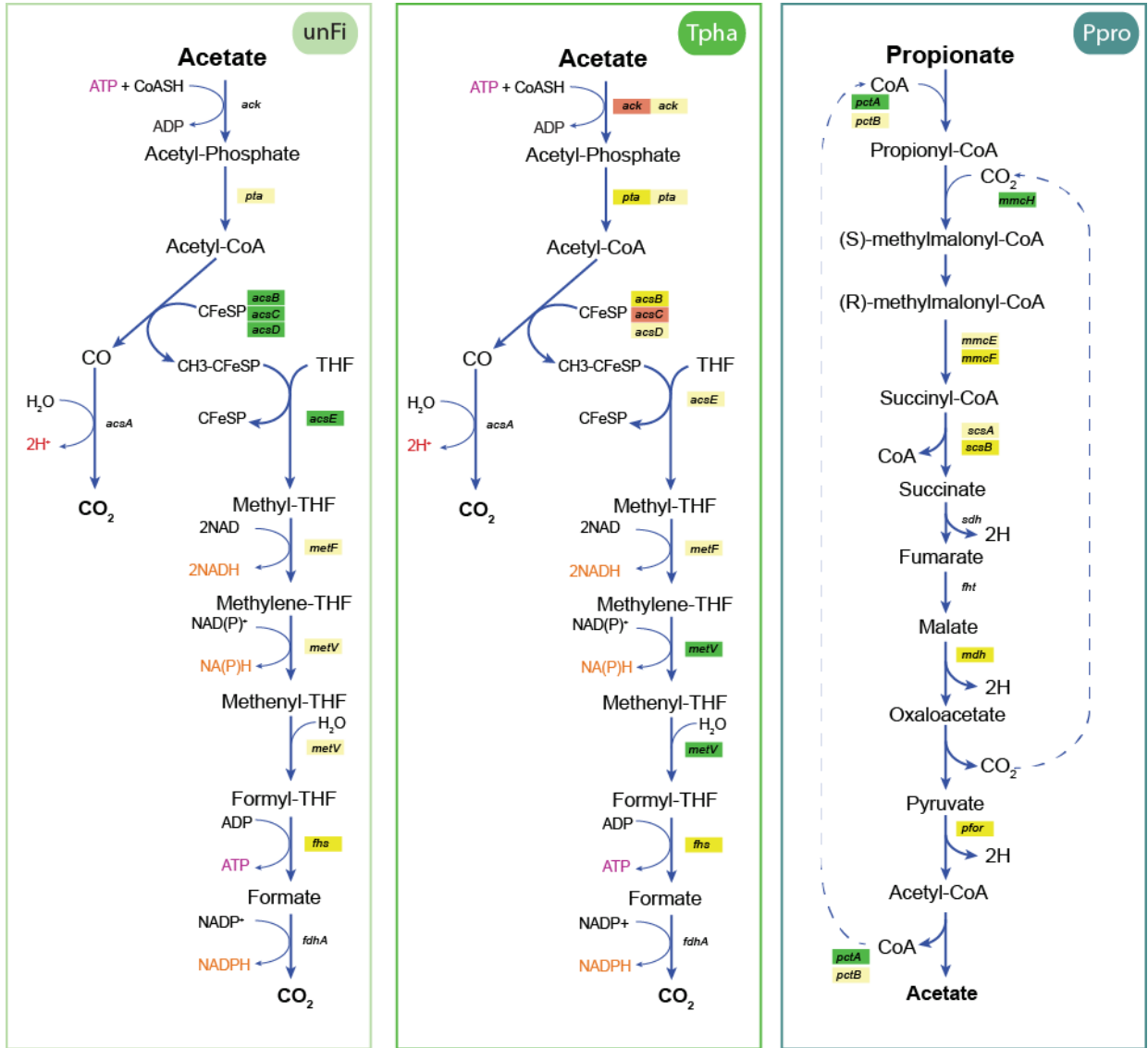


Figure S2 Indication of several strains of *Coprothermobacter proteolyticus* showed by (a) identification of several oligotypes within OTUs assigned to *Coprothermobacter* in the triplicated (S1L, S2L and S3L) 16S rRNA gene sequence data, and (b) alignment (NUCmer) of the draft genome against the representative sequenced genome, *Coprothermobacter proteolyticus* DSM5256.



(Figure continues on text page)



Figure S3 Metabolic pathways for syntrophic oxidation of acetate via Wood-Ljungdahl pathway (Tpha; *Thermacetogenium phaeum* and unFi; unFirm02_FrBGR), propionate via methylmalonyl-CoA pathway (Ppro; *Pelotomaculum thermopropionicum*) and butyrate and longer chain fatty acids via β -oxidation (Slip; *Syntrophothermus lipocalidus*) and (Swol; *Syntrophomonas wolfei*, respectively). The pathways are proposed based on genome and proteome comparison, and protein abundances are indicated by color. Protein abbreviations used in this figure are given in supplementary Sable S3. See Figure 3 for an extended illustration of metabolic pathways of proposed for unFirm02_FrBGR, including β -oxidation.

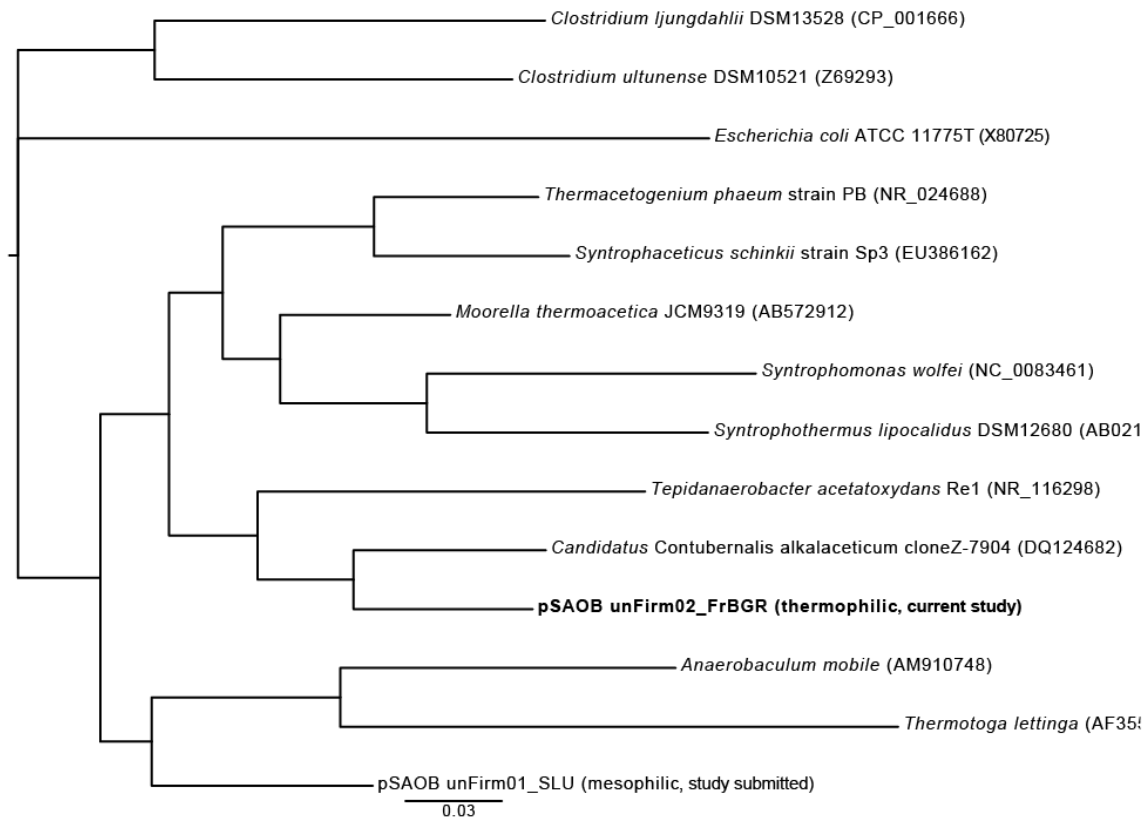


Figure S4 Phylogenetic tree based on 16S rRNA gene sequences highlighting the relationship of the putative novel SAOB unFirm02_FrBGR relative to known SAOBs, selected acetogens and one other potential novel SAOB recently assembled from a similar study of a mesophilic digester (*study submitted*). *Anaerobaculum mobile* and *Escherichia coli* was included as outgroups. The 16S rRNA-based alignment was carried out using MUSCLE, and the phylogenetic tree was generated with FastTree.

Supplementary Tables

Table S1. List of reference genomes included in the protein mapping and the interpretation of the results. The reference genomes is only used if specified in the text, otherwise FrBGR genomic bins were used.

Genomes	Accession number	Identical RefSeq and GeneBank
<i>Methanosaeta thermophila</i> PT	CP000477.1	yes
<i>Methanothermobacter thermautotrophicus</i> strain Delta H	NC_000916.1	yes
<i>Dictyoglomus thermophilum</i> H-6-12	NC_011297	yes
<i>Pelotomaculum thermopropionicum</i> SI	NC_009454	yes
<i>Tepidanaerobacter acetatoxydans</i> Re1	NC_019954	yes
<i>Clostridium stercorarium</i> subsp. stercorarium DSM 8532	NC_020134	yes

Table S2. Sequencing statistics (yields after quality filtration as described in Materials and Methods)

	MiSeq 16S rRNA (n=3, high quality)	MiSeq Metagenomics (Q > 30)	8 SMRT cells Pac Bio RS (min. accuracy 99.0 %)
Reads (bp)	616 687	54 025 934	217 815
Average read length	300 PE	300 PE	1 253
Sequence information (Mb)	180	16 200	274
Contigs after assembly (n)	-	235 738	
Average contig size (nt)	-	2009	

Supplementary Table S3. Proteins related to key metabolic pathways. The number of protein hits for each protein group is given (P(n)). Protein abundance is given as average (AVG) Log10(LFQ) value for the two replicate protein analysis. with standard deviated (STD) specified.

Polysaccharide hydrolysis						
			uncultured Atribacteria bacterium			
Pathway	Enzyme	Contid ID	P(n)	AVG Log10(LFQ)	STD	Max seq. cov. (%)
Transport systems	ABC-type sugar transport system. periplasmic component	Ga0101770_10146014	1	6.874	0.016	21.4
	ABC-type sugar transport system. periplasmic component	Ga0101770_10175443	1	6.881	0.042	25.9
	ABC-type dipeptide transport system. periplasmic component	Ga0101770_101953929	1	8.840	0.024	79.9
	ABC-type sugar transport system. periplasmic component	Ga0101770_102130523	10	8.230	0.003	81.5
	Galactose mutarotase and related enzymes	Ga0101770_102130525	5	8.143	0.075	51.3
	Galactose mutarotase and related enzymes	Ga0101770_101962835	5	8.143	0.075	51.3
	Galactose mutarotase and related enzymes	Ga0101770_10730162	5	8.143	0.075	51.3
	Beta-glucosidase-related glycosidases	Ga0101770_10517754	4	7.297	0.009	14.8
	Xylose isomerase-like TIM barrel	Ga0101770_10783681	10	6.191	0.035	9.3
	Xylose isomerase-like TIM barrel	Ga0101770_11033971	10	6.191	0.035	9.3
	Enolase	Ga0101770_101973712	6	6.815	0.075	24.9
	Dehydrogenases with different specificities (related to short-chain alcohol dehydrogenases)	Ga0101770_101973715	4	6.206	0.014	15.8
	ABC-type sugar transport system. periplasmic component	Ga0101770_101973716	6	8.642	0.022	54.2
	L-fucose isomerase and related proteins	Ga0101770_101973720	8	6.692	0.024	3.8
	ABC-type phosphate transport system. periplasmic component	Ga0101770_101973721	4	6.247	0.051	14.0
	Predicted oxidoreductases (related to aryl-alcohol dehydrogenases) - COG0667	Ga0101770_101973725	8	6.421	0.055	11.7
	ABC-type sugar transport system. periplasmic component	Ga0101770_101973726	8	7.897	0.049	70.2

Glycolysis/Gluconeogenesis							
	Transaldose	Ga0101770_10658732	7	7.016	0.024	55.8	
	6-phosphofructokinase	Ga0101770_10687432	11	6.948	0.131	19.6	
	Fructose/tagatose biphosphate aldolase	Ga0101770_10325923	9	6.756	0.017	27.7	
	Glyceraldehyde-3-phosphate dehydrogenase/erythrose-4-phosphate dehydrogenase	Ga0101770_10343685	8	6.936	0.025	43.5	
	Phosphoenolpyruvate synthase/pyruvate phosphate dikinase	Ga0101770_10195325	22	7.518	0.028	22.0	
	Phosphoenolpyruvate synthase/pyruvate phosphate dikinase	Ga0101770_10781444	6	7.829	0.009	35.9	
	3-phosphoglycerate kinase	Ga0101770_101914671	12	6.610	0.066	12.2	
Uncultured <i>Planctomycetes</i> sp.							
Pathway	Enzyme	Contid ID	P(n)	AVG Log10(LFQ)	STD	Max seq. cov. (%)	
	Phosphotransferase system mannitol/fructose-specific IIA-domain (Ntr-type)	Ga0101770_10002497	1	6.875	0.157	34.6	
	Beta-galactosidase/beta-glucuronidase	Ga0101770_10008434	3	6.725	0.016	2.7	
	Beta-galactosidase/beta-glucuronidase	Ga0101770_10194131	3	6.725	0.016	2.7	
	Beta-galactosidase/beta-glucuronidase	Ga0101770_10012956	6	7.660	0.109	15.4	
	Beta-galactosidase/beta-glucuronidase	Ga0101770_10114081	6	7.660	0.109	15.4	
	Beta-galactosidase/beta-glucuronidase	Ga0101770_10016871	6	7.660	0.109	15.4	
	Endoglucanase	Ga0101770_10014442	1	6.475	0.172	11.9	
	Predicted cobalamin binding protein - COG5012	Ga0101770_10014446	3	6.647	0.129	31.7	
	Sugar phosphate isomerases/epimerases	Ga0101770_10014471	2	7.209	0.113	14.7	
	Domain of Unknown Function (DUF1080)	Ga0101770_10014472	2	6.555	0.182	24.8	
	Uncharacterized conserved protein - COG4274	Ga0101770_10014475	2	7.114	0.118	34.8	
	Endoglucanase	Ga0101770_10022533	2	6.719	0.196	9.0	

	Predicted bile acid beta-glucosidase	Ga0101770_10035255	3	5.680	0.278	4.3
	Predicted bile acid beta-glucosidase	Ga0101770_10822051	3	5.680	0.278	4.3
	Predicted dehydrogenases and related proteins - COG0673	Ga0101770_10082194	3	6.798	0.110	10.0
	Carbohydrate binding domain	Ga0101770_10082195	1	7.551	0.076	16.1
Glycan-structure degradation	Alpha-L-fucosidase	Ga0101770_10208864	3	6.359	0.078	4.1
	Alpha-L-fucosidase	Ga0101770_10208865	3	6.359	0.078	4.1
Arabinose (hemicellulose/pectin)	L-arabinose isomerase	Ga0101770_10004636	1	6.278	0.164	6.2
	Alpha-L-arabinofuranosidase	Ga0101770_10004638	2	6.526	0.264	3.1
Xylose (hemicellulose)	Xylose isomerase-like TIM barrel	Ga0101770_10270493	3	7.185	0.129	39.4
	Xylose isomerase-like TIM barrel	Ga0101770_10011768	3	7.185	0.129	
	Xylose isomerase	Ga0101770_10015354	7	8.149	0.134	53.8
	Xylose isomerase-like TIM barrel	Ga0101770_10620022	5	6.802	0.163	23.3
	Xylose isomerase-like TIM barrel	Ga0101770_10208912	5	6.802	0.163	23.3
	Xylose isomerase-like TIM barrel	Ga0101770_10809971	5	6.802	0.163	23.3
	Predicted dehydrogenases and related proteins - COG0673	Ga0101770_10208913	7	7.826	0.125	45.6
	Xylose isomerase-like TIM barrel	Ga0101770_10246252	3	6.610	0.142	38.6
Glycolysis/Gluconeogenesis						
	Phosphotransferase system mannitol/fructose-specific IIA domain (Ntr-type)	Ga0101770_10002497	1	6.875	0.157	34.6
	Phosphopentomutase	Ga0101770_10027061	55	6.999	0.038	26.2
	Sugar phosphate isomerases/epimerases	Ga0101770_10001539	3	7.381	0.158	32.0
	Sugar phosphate isomerases/epimerases	Ga0101770_10008795	3	6.832	0.202	29.7
	Sugar phosphate isomerases/epimerases	Ga0101770_10014471	2	7.209	0.113	14.7
	Sugar phosphate isomerases/epimerases	Ga0101770_10024763	1	6.620	0.051	19.6
	Sugar phosphate isomerases/epimerases	Ga0101770_10027972	3	6.610	0.142	38.6
	Sugar phosphate isomerases/epimerases	Ga0101770_100277512	2	7.485	0.076	25.6

	Sugar phosphate isomerases/epimerases	Ga0101770_10033342	3	7.185	0.129	39.4
	Sugar phosphate isomerases/epimerases	Ga0101770_10138574	3	8.381	0.101	72.1
	Predicted phosphosugar isomerases - COG2222	Ga0101770_10117116	3	6.481	0.017	23.5
	6-phosphofructokinase	Ga0101770_100034110	3	6.983	0.091	22.9
	6-phosphofructokinase	Ga0101770_10010393	1	6.376	0.208	8.4
	Fructose/tagatose biphosphate aldolase	Ga0101770_10026592	3	6.773	0.112	19.3
	Triosephosphate isomerase	Ga0101770_100205310	1	6.666	0.213	22.1
	Glyceraldehyde-3-phosphate dehydrogenase/erythrose-4-phosphate dehydrogenase	Ga0101770_10006276	6	8.060	0.081	69.4
	3-phosphoglycerate kinase	Ga0101770_10010123	5	7.747	0.070	36.5
	Predicted phosphoglycerate mutase	Ga0101770_10222504	3	6.847	0.218	7.9
	Enolase	Ga0101770_10003117	2	7.554	0.111	49.7
	Phosphoenolpyruvate synthase/pyruvate phosphate dikinase	Ga0101770_100052616	1	8.369	0.050	54.2
	Pyruvate:ferredoxin oxidoreductase and related 2-oxoacid:ferredoxin oxidoreductases. beta subunit	Ga0101770_10010822	2	7.789	0.007	41.5
	Pyruvate:ferredoxin oxidoreductase and related 2-oxoacid:ferredoxin oxidoreductases. alpha subunit	Ga0101770_10059592	1	8.038	0.115	42.4
<i>Dictyoglomus thermophilum</i>						
<i>Pathway</i>	<i>Enzyme</i>	Contid ID	P(n)	AVG Log10(LFQ)	STD	Max seq. cov. (%)
	ABC-type sugar transport system. periplasmic component	Ga0101770_1018957173	2	7.350	0.085	20.4
	ABC-type sugar transport system. periplasmic component	Ga0101770_1018957176	3	7.500	0.032	24.2
	ABC-type oligopeptide transport system. periplasmic component	Ga0101770_101895816	2	7.962	0.073	53.8
	Glycerol-3-phosphate responsive antiterminator (mRNA-binding)	Ga0101770_101895877	5	7.404	0.010	65.6

	Bacterial extracellular solute-binding proteins. family 5 Middle	Ga0101770_10268101	6	8.549	0.013	52.2
	Bacterial extracellular solute-binding proteins. family 5 Middle	Ga0101770_10268102	6	8.549	0.013	52.2
Polysaccharide hydrolysis						
	Alpha-amylase/alpha-mannosidase	Ga0101770_10356912	3	8.622	0.070	50.5
	Alpha-amylase/alpha-mannosidase	Ga0101770_10195581	3	8.622	0.070	50.5
	Alpha-amylase/alpha-mannosidase	Ga0101770_11213565	3	8.622	0.070	50.5
	Endoglucanase	Ga0101770_1018993174	2	6.639	0.160	7.8
	Beta-glucosidase-related glycosidases (In ref.: xylosidase/arabinoxidase)	Ga0101770_10201157	4	7.297	0.009	14.8
	Alpha-galactosidases/6-phospho-beta-glucosidases. family 4 of glycosyl hydrolases	Ga0101770_101895849	4	7.207	0.075	27.9
Xylose						
	Carbohydrate binding domain	Ga0101770_1018957212	2	7.149	0.053	28.1
	Xylose isomerase-like TIM barrel	Ga0101770_1018957218	3	6.536	0.197	9.2
	Maltose-binding periplasmic proteins/domains	Ga0101770_10201153	4	7.740	0.072	55.0
	XFP	Ga0101770_10689251	9	6.670	0.044	8.3
	Phosphoketolase (In ref.: D-xylose 5-phosphate)	Ga0101770_101950352	9	6.670	0.044	8.3
	D-xylose 5- phosphate	DICTH_0096_941*	9	6.670	0.044	8.3
	xylosidase/arabinoxidase	DICTH_0696_680*	4	7.297	0.009	14.8
Glycolysis/Gluconeogenesis						
	3-phosphoglycerate kinase	Ga0101770_1018956127	5	7.488	0.028	14.9
	3-phosphoglycerate kinase	Ga0101770_10961401	5	7.488	0.028	14.9
	Enolase	Ga0101770_1018956349	2	6.916	0.043	22.2
	Glyceraldehyde-3-phosphate dehydrogenase/erythrose-4-phosphate dehydrogenase	Ga0101770_1018956482	5	7.659	0.068	28.8
	6-phosphofructokinase	Ga0101770_10421763	3	7.078	0.014	39.3
	Phosphoenolpyruvate synthase/pyruvate phosphate dikinase	Ga0101770_101943762	11	7.609	0.003	9.0

	Pyruvate:ferredoxin oxidoreductase and related 2-oxoacid:ferredoxin oxidoreductases. gamma subunit	Ga0101770_101901213	6	7.095	0.006	20.0
	Pyruvate:ferredoxin oxidoreductase and related 2-oxoacid:ferredoxin oxidoreductases. alpha subunit	Ga0101770_101901215	4	6.623	0.015	2.8

*Reference genome

Protein hydrolysis and amino acid degradation						
Pathway	Enzyme	Contid ID	P(n)	AVG Log10(LFQ)	STD	Max seq. cov. (%)
Oligo-/dipeptide and amino acid transporters	ABC-type oligopeptide transport system. ATPase component	Ga0101770_100178710	56	6.698	0.065	17.9
	ABC-type oligopeptide transport system. ATPase component	Ga0101770_10252809	53	6.776	0.001	37.6
	ABC-type oligopeptide transport system. periplasmic component	Ga0101770_10387981	11	9.184	0.003	75.8
	ABC-type branched-chain amino acid transport systems. ATPase component	Ga0101770_101914311	44	5.915	0.215	22.7
	ABC-type branched-chain amino acid transport systems. periplasmic component	Ga0101770_10244214	13	6.649	0.034	18.4
	Oligopeptide/dipeptide transporter. C-terminal region	Ga0101770_102934812	56	6.698	0.065	17.9
	Oligopeptide/dipeptide transporter. C-terminal region	Ga0101770_10378281	53	6.776	0.001	37.6
	ABC-type dipeptide transport system. periplasmic component*	Ga0101770_10374102	1	7.454	0.034	60.3
	ABC-type dipeptide transport system. periplasmic component*	Ga0101770_10426592	5	7.034	0.055	64.3
	ABC-type dipeptide transport system. periplasmic component*	Ga0101770_10358803	9	8.051	0.056	75.7
	Subtilisin-like serine proteases	Ga0101770_10296594	15	8.272	0.010	21.6
	Subtilisin-like serine proteases	Ga0101770_10189225	42	7.505	0.075	17.1
	Bacterial surface proteins containing Ig-like domains	Ga0101770_10189227	6	8.097	0.004	28.5
	Predicted Zn-dependent proteases and their inactivated homologs - COG0312	Ga0101770_10189311	38	7.340	0.029	46.4
Proteases and peptidases	Predicted Zn-dependent proteases and their inactivated homologs - COG0312	Ga0101770_10189312	45	7.088	0.020	19.4
	Putative intracellular protease/amidase	Ga0101770_10203764	31	8.208	0.126	92.3
	Putative intracellular protease/amidase	Ga0101770_101989111	6	6.182	0.237	92.3
	Putative translation initiation inhibitor. yjgF family	Ga0101770_101989112	27	7.621	0.059	83.1
	Membrane protease subunits. stomatin/prohibitin homologs	Ga0101770_103243810	79	6.692	0.094	43.8
	Xaa-Pro aminopeptidase	Ga0101770_11199462	52	6.774	0.039	38.9
	D-aminopeptidase	Ga0101770_10195866	46	6.389	0.135	34.2
	Di- and tripeptidases	Ga0101770_10201593	20	7.657	0.048	35.9

	Zn-dependent carboxypeptidase	Ga0101770_10392511	59	8.357	0.057	50.7
	Pyroglutamate carboxylase (N-terminal pyroglutamate)	Ga0101770_10354463	10	6.787	0.087	37.5
	Predicted aminopeptidases - COG2234	Ga0101770_10569803	94	6.974	0.088	20.3
	Aspartyl aminopeptidase	Ga0101770_11279061	64	7.747	0.032	42.5
	Oligonucleotidase F	Ga0101770_10524711	156	8.380	0.016	44.2
	Peptidase dimerisation domain/Acetylornithine deacetylase/Succinyl-diaminopimelate desuccinylase and related deacylases	Ga0101770_10749836	74	8.100	0.069	59.4
Amino acid degradation						
Glycine 1 (Glycine cleavage)	Glycine cleavage system T protein (aminomethyltransferase)	Ga0101770_10209433	37	7.001	0.054	34.5
	Glycine cleavage system protein P (pyridoxal-binding). N-terminal domain	Ga0101770_10209434	75	7.599	0.028	41.8
	Glycine cleavage system protein P (pyridoxal-binding). C-terminal domain	Ga0101770_10209435	82	7.742	0.043	40.7
	Glycine cleavage system H protein (lipoate-binding)	Ga0101770_102006814	24	6.525	0.466	51.2
	Glycine cleavage system H protein (lipoate-binding)	Ga0101770_102107912	15	7.211	0.129	38.6
	Pyruvate/2-oxoglutarate dehydrogenase complex. dihydrolipoamide dehydrogenase (E3) component. and related enzymes	Ga0101770_10027156	78	7.239	0.073	32.2
	Pyruvate/2-oxoglutarate dehydrogenase complex. dihydrolipoamide dehydrogenase (E3) component. and related enzymes	Ga0101770_10244216	13	6.947	0.133	9.0
	Pyruvate/2-oxoglutarate dehydrogenase complex. dihydrolipoamide dehydrogenase (E3) component. and related enzymes	Ga0101770_10372235	33	7.433	0.089	54.0
	Glycine/serine hydroxymethyltransferase	Ga0101770_101938929	89	7.199	0.000	24.3
	Serine-pyruvate aminotransferase/archaeal aspartate aminotransferase	Ga0101770_10204627	55	8.219	0.046	59.3
Glycine 2 (Glycine to Serine)	Serine-pyruvate aminotransferase/archaeal aspartate aminotransferase	Ga0101770_102186811	35	6.895	0.025	59.3
	Phosphoglycerate dehydrogenase and related dehydrogenases	Ga0101770_10202225	12	7.407	0.011	54.8
	Phosphoglycerate dehydrogenase and related dehydrogenases	Ga0101770_10394261	33	6.422	0.069	54.8
	Glycine/D-amino acid oxidases (deaminating)	Ga0101770_101919912	52	6.708	0.042	30.4
Glycine 3 (glycine to glyxylate)						
Glycine 4	Hypothetical protein	Ga0101770_102062031	51	7.844	0.007	51.4

	Glycine/sarcosine/betaine reductase selenoprotein B (GRDB)	Ga0101770_102062032	73	8.226	0.063	64.4
	Glycine reductase complex selenoprotein A	Ga0101770_102062033	41	7.434	0.233	86.4
	Glycine reductase complex selenoprotein A	Ga0101770_102062034	42	7.372	0.109	80.8
	Glycine/sarcosine/betaine reductase component B subunits	Ga0101770_102062035	31	7.034	0.219	54.4
Valine, Leucine and Isoleucine	Branched-chain amino acid aminotransferase/4-amino-4-deoxychorismate lyase	Ga0101770_10487231	16	6.918	0.079	35.9
	Dihydroxyacid dehydratase/phosphogluconate dehydratase	Ga0101770_10487232	8	6.559	0.076	5.6
	Acyl-CoA dehydrogenases	Ga0101770_11084803	2	6.292	0.115	6.5
	Glutamate dehydrogenase/leucine dehydrogenase	Ga0101770_102997410	9	7.004	0.064	56.0
	Glutamate dehydrogenase/leucine dehydrogenase	Ga0101770_10190902	77	8.811	0.031	61.1
	Pyruvate:ferredoxin oxidoreductase and related 2-oxoacid:ferredoxin oxidoreductases. alpha subunit	Ga0101770_10192314	69	7.017	0.044	46.4
	Pyruvate:ferredoxin oxidoreductase and related 2-oxoacid:ferredoxin oxidoreductases. beta subunit	Ga0101770_10192316	58	7.407	0.022	54.9
	Pyruvate:ferredoxin oxidoreductase and related 2-oxoacid:ferredoxin oxidoreductases. gamma subunit	Ga0101770_10192315	62	6.626	0.104	40.3
	Acetyl-CoA acetyltransferase	Ga0101770_10191436	30	7.822	0.033	45.1
	Methylmalonyl-CoA mutase. N-terminal domain/subunit	Ga0101770_10266412	24	6.587	0.051	69.2
	Methylmalonyl-CoA mutase. C-terminal domain/subunit (cobalamin-binding)	Ga0101770_10266413	43	8.296	0.038	91.5
	Glutamate dehydrogenase/leucine dehydrogenase	Ga0101770_102997410	9	7.004	0.064	56.0
	Glutamate	Glutamate dehydrogenase/leucine dehydrogenase	Ga0101770_10190902	77	8.811	0.031
Uncharacterized flavoproteins		Ga0101770_10190908	27	7.024	0.016	28.8
Phosphomannomutase		Ga0101770_10190909	69	6.400	0.069	25.9
Aldo/keto reductases. related to diketogulonate reductase		Ga0101770_102101714	106	6.604	0.115	21.8
Cysteine synthase		Ga0101770_102101716	34	6.250	0.092	22.6
Peroxioredoxin		Ga0101770_102101717	89	6.264	0.185	70.8
Histidine ammonia-lyase		Ga0101770_102664110	42	6.825	0.114	13.5
Imidazolonepropionase and related amidohydrolases		Ga0101770_102071196	122	7.841	0.064	46.9
Urocanate hydratase		Ga0101770_10374011	117	7.955	0.041	36.4
Glutamate formiminotransferase		Ga0101770_10374012	13	6.524	0.086	21.8
Cystein	Formyltetrahydrofolate synthetase	Ga0101770_10374014	102	7.492	0.105	36.0
Histidine						

Aspartate	Aspartate/tyrosine/aromatic aminotransferase	Ga0101770_100271512	72	8.259	0.077	70.1
Threonine	Threonine dehydrogenase and related Zn-dependent dehydrogenases	Ga0101770_10027155	40	6.694	0.031	42.6
THF	Glutamate formiminotransferase	Ga0101770_10374012	13	6.524	0.086	21.8
	Formyltetrahydrofolate synthetase	Ga0101770_10374014	21	7.011	0.038	11.9
	Methenyl tetrahydrofolate cyclohydrolase	Ga0101770_101946813	75	6.523	0.135	26.5
	Predicted methyltransferases - COG1568	Ga0101770_101907918	56	6.976	0.027	57.0
<i>Anaerobaculum mobile</i>						
<i>Pathway</i>	<i>Enzyme</i>	Contid ID	P(n)	AVG Log ₁₀ (LFQ)	STD	Max seq. cov. (%)
Proteases and peptidases	Putative intracellular protease/amidase	Ga0101770_102320030	9	6.579	0.188	33.5
	Peptidase dimerisation domain	Ga0101770_11366713	34	7.759	0.098	34.4
	Peptidase family M28	Ga0101770_11325482	16	6.231	0.021	8.1
	Aspartyl aminopeptidase	Ga0101770_10437904	64	7.747	0.032	42.5
TRAP-type and branched-chain amino acid transporters	TRAP-type uncharacterized transport system. periplasmic component	Ga0101770_10515606	9	6.432	0.160	26.6
	Uncharacterized ABC-type transport system. periplasmic component/surface lipoprotein	Ga0101770_101904361	15	6.147	0.106	15.8
	ABC-type branched-chain amino acid transport systems. periplasmic component	Ga0101770_1019036133	6	7.760	0.001	59.7
	ABC-type branched-chain amino acid transport systems. periplasmic component	Ga0101770_101898737	13	6.649	0.034	18.4
	ABC-type branched-chain amino acid transport systems. periplasmic component	Ga0101770_101904330	28	6.606	0.091	16.2
	ABC-type branched-chain amino acid transport systems. periplasmic component	Ga0101770_101910866	21	5.914	0.069	18.0
	ABC-type branched-chain amino acid transport systems. periplasmic component	Ga0101770_101898737	13	6.649	0.034	18.4
	Uncharacterized NAD(FAD)-dependent dehydrogenases component	Ga0101770_101898739	13	6.947	0.133	9.0
	ABC-type phosphate transport system. periplasmic component	Ga0101770_101898743	11	7.091	0.011	44.3
	Glycosyltransferase	Ga0101770_101898746	21	6.953	0.068	34.2
ABC-type oligopeptide transport system. ATPase component	Ga0101770_102171624	53	6.776	0.001	37.6	

Oligo-/dipeptide transport cluster	ABC-type dipeptide/oligopeptide/nickel transport system. ATPase component	Ga0101770_102171625	56	6.698	0.065	17.9
	ABC-type dipeptide/oligopeptide/nickel transport systems. permease components	Ga0101770_102171626	53	6.781	0.025	23.0
	Chaperonin GroEL (HSP60 family)	Ga0101770_102171628	88	8.385	0.017	57.5
	Co-chaperonin GroES (HSP10)	Ga0101770_102171629	54	7.901	0.033	89.8
	ABC-type phosphate transport system. periplasmic component	Ga0101770_102103119	11	7.091	0.011	44.3
	Uncharacterized NAD(FAD)-dependent dehydrogenases	Ga0101770_102103123	13	6.947	0.133	9.0
Amino acid degradation						
Glycine 1 (Glycine cleavage)	Glycine cleavage system protein P (pyridoxal-binding). C-terminal domain	Ga0101770_10306411	21	7.049	0.153	27.2
	Glycine cleavage system protein P (pyridoxal-binding). C-terminal domain	Ga0101770_10216712	7	7.643	0.100	28.0
Glycine 2 (Glycine to Serine)	Pyruvate/2-oxoglutarate dehydrogenase complex. dihydroipoamide dehydrogenase (E3) component. and related enzymes	Ga0101770_10251721	9	6.857	0.150	23.5
	Serine-pyruvate aminotransferase/archaeal aspartate aminotransferase	Ga0101770_101903682	14	7.439	0.157	37.5
	Glycine/serine hydroxymethyltransferase	Ga0101770_101905895	30	6.766	0.020	11.0
	L-serine deaminase	Ga0101770_10729932	9	5.803	0.100	8.2
Glycine 4	Glycine/sarcosine/betaine reductase component B subunits	Ga0101770_10662854	6	7.548	0.247	65.7
	Glycine/sarcosine/betaine reductase selenoprotein B (GRDB)	Ga0101770_10662851	26	7.837	0.003	44.0
<i>Cystein</i>	Cysteine synthase	Ga0101770_102077722	35	8.049	0.079	36.7
Threonine	Threonine synthase	Ga0101770_102077721	17	6.169	0.024	9.9
	Homoserine dehydrogenas	Ga0101770_1018948103	14	6.652	0.054	19.2
	Aspartate-semialdehyde dehydrogenase	Ga0101770_101892538	19	6.409	0.132	22.7
Isoleucine. leucine. valine	Branched-chain amino acid aminotransferase/4-amino-4-deoxychorismate lyase	Ga0101770_1018948123	24	7.542	0.009	57.4
	Pyruvate/2-oxoglutarate dehydrogenase complex. dihydroipoamide dehydrogenase (E3) component. and related enzymes	Ga0101770_10251721	9	6.857	0.150	23.5
	4-aminobutyrate aminotransferase and related aminotransferases	Ga0101770_1018925137	26	8.635	0.134	66.6
	Methylmalonyl-CoA mutase. N-terminal domain/subunit	Ga0101770_10330761	27	8.035	0.124	44.6

	Methylmalonyl-CoA mutase, C-terminal domain/subunit (cobalamin-binding)	Ga0101770_10330773	10	7.586	0.219	73.4
	Pyruvate:ferredoxin oxidoreductase and related 2-oxoacid:ferredoxin oxidoreductases, alpha subunit	Ga0101770_101902786	14	7.023	0.111	21.8
	Pyruvate:ferredoxin oxidoreductase and related 2-oxoacid:ferredoxin oxidoreductases, beta subunit	Ga0101770_101902787	10	6.385	0.195	39.1
	Pyruvate:ferredoxin oxidoreductase and related 2-oxoacid:ferredoxin oxidoreductases, gamma subunit	Ga0101770_101902788	10	7.017	0.234	39.2
Aspartate	Aspartate/tyrosine/aromatic aminotransferase	Ga0101770_10363062	15	7.207	0.168	28.2
	Aspartate/tyrosine/aromatic aminotransferase	Ga0101770_10411181	72	8.259	0.077	70.1
Glutamate	Glutamate dehydrogenase/leucine dehydrogenase	Ga0101770_1019036148	3	7.913	0.070	72.9
	Glutamate dehydrogenase/leucine dehydrogenase	Ga0101770_10660104	18	8.401	0.125	65.3
	Glutamate dehydrogenase/leucine dehydrogenase	Ga0101770_102189517	2	7.250	0.115	64.1
	Glutamate dehydrogenase/leucine dehydrogenase	Ga0101770_10249779	2	7.250	0.115	64.1
	4-aminobutyrate aminotransferase and related aminotransferases	Ga0101770_1018925137	26	8.635	0.134	66.6
Arginine (<i>specific to A. mobile bin</i>)*	Spermidine synthase	Ga0101770_1018925309	5	5.717	0.183	27.2
	Arginine deiminase	Ga0101770_1018925312	11	6.629	0.123	13.6
	Ornithine carbamoyltransferase	Ga0101770_1018925313	14	6.822	0.015	17.8
Histidine	Urocanate hydratase	Ga0101770_1019101101	44	6.933	0.099	6.6
THF	Formyltetrahydrofolate synthetase	Ga0101770_10515605	21	7.011	0.038	11.9
	5,10-methylene-tetrahydrofolate dehydrogenase/Methenyl tetrahydrofolate cyclohydrolase	Ga0101770_10081561	7	7.237	0.052	50.5
	Methylene-tetrahydromethanopterin dehydrogenase, N-terminal	Ga0101770_101910390	40	6.619	0.155	27.0
Other						
	Aerobic-type carbon monoxide dehydrogenase, large subunit CoxL/CutL homologs	Ga0101770_101894822	16	8.668	0.072	64.8
	Aerobic-type carbon monoxide dehydrogenase, small subunit CoxS/CutS homologs	Ga0101770_101894823	11	7.929	0.244	39.5
	Aerobic-type carbon monoxide dehydrogenase, middle subunit CoxM/CutM homologs	Ga0101770_101894824	9	6.817	0.091	52.9
Oxidative Phosphorylation	Archaeal/vacuolar-type H ⁺ -ATPase subunit B	Ga0101770_10394312	13	9.631	0.112	71.3
	Archaeal/vacuolar-type H ⁺ -ATPase subunit A	Ga0101770_10394314	32	10.036	0.071	80.0
	Archaeal/vacuolar-type H ⁺ -ATPase subunit B	Ga0101770_10394318	13	9.631	0.112	71.3

	acetate kinase	Ga0101770_10493251	13	5.981	0.222	21.4
	Phosphotransacetylase	Ga0101770_1018948120	10	7.357	0.105	64.8
	Phosphotransacetylase	Ga0101770_102648011	10	6.222	0.108	35.7
<i>Uncultured Planctomyces sp.</i>						
<i>Pathway</i>	<i>Enzyme</i>	Contid ID	P(n)	AVG Log10(LFQ)	STD	Max seq. cov. (%)
protein/peptide transport and degradation	Putative intracellular protease/amidase	Ga0101770_100021913	1	6.530	0.071	16.8
	Regulatory P domain of the subtilisin-like proprotein convertases and other protease	Ga0101770_10013091	3	8.401	0.058	31.7
	D-aminopeptidase	Ga0101770_10008424	2	6.986	0.022	14.1
	Bacterial pre-peptidase C-terminal domain	Ga0101770_10017651	1	8.280	0.101	33.0
	Predicted Zn-dependent peptidases - COG0612	Ga0101770_10057821	2	6.709	0.081	21.0
	Predicted Zn-dependent peptidases - COG0612	Ga0101770_10714042	2	6.709	0.081	21.0
Prolyl oligopeptidase family	Predicted Zn-dependent peptidases - COG0612	Ga0101770_10714041	3	6.331	0.011	25.0
		Ga0101770_10015069	2	7.774	0.188	26.7
<i>uncultured Atribacteria bacterium</i>						
<i>Pathway</i>	<i>Enzyme</i>	Contid ID	P(n)	AVG Log10(LFQ)	STD	Max seq. cov. (%)
protein/peptide transport and degradation	ABC-type dipeptide transport system. periplasmic component	Ga0101770_101953929	1	8.840	0.024	79.9
	Trypsin-like serine proteases. typically periplasmic. contain C-terminal PDZ domain	Ga0101770_10267613	6	7.235	0.107	13.6
	Trypsin-like serine proteases. typically periplasmic. contain C-terminal PDZ domain	Ga0101770_101961548	6	7.235	0.107	13.6
	Threonine dehydrogenase and related Zn-dependent dehydrogenases	Ga0101770_101958132	5	6.567	0.006	26.6
	Threonine dehydrogenase and related Zn-dependent dehydrogenases	Ga0101770_101920530	5	6.567	0.006	26.6

Threonine dehydrogenase and related Zn-dependent dehydrogenases	Ga0101770_10296083	5	6.567	0.006	26.6
Threonine dehydrogenase and related Zn-dependent dehydrogenases	Ga0101770_10052912	13	7.393	0.092	26.3
Threonine dehydrogenase and related Zn-dependent dehydrogenases	Ga0101770_11256451	13	7.393	0.092	26.3
Threonine dehydrogenase and related Zn-dependent dehydrogenases	Ga0101770_10240709	13	7.393	0.092	26.3
Threonine dehydrogenase and related Zn-dependent dehydrogenases	Ga0101770_11216291	13	7.393	0.092	26.3
Threonine dehydrogenase and related Zn-dependent dehydrogenases	Ga0101770_10206366	13	7.393	0.092	26.3
Threonine dehydrogenase and related Zn-dependent dehydrogenases	Ga0101770_10240718	13	7.393	0.092	26.3
Threonine dehydrogenase and related Zn-dependent dehydrogenases	Ga0101770_10607252	13	7.393	0.092	26.3
ABC-type Fe3+ transport system. periplasmic component	Ga0101770_10607253	8	7.115	0.053	46.7
ABC-type Fe3+ transport system. periplasmic component	Ga0101770_10206367	8	7.115	0.053	46.7
ABC-type Fe3+ transport system. periplasmic component	Ga0101770_10240717	8	7.115	0.053	46.7

Methylmalonyl-CoA pathway (propionate oxidation)							
<i>Pelotomaculum thermopropionicum*</i>							
<i>Pathway</i>	<i>Enzyme</i>	<i>Abbr.</i>	Contid ID	P(n)	AVG Log10(LFQ)	STD	Max seq. cov. (%)
	acyl CoA:acetate/3-ketoacid CoA transferase, beta subunit		BAF60226.1_2045	2	6.952	0.089	49.4
	glyceraldehyde-3-phosphate dehydrogenase/erythrose-4-phosphate dehydrogenase		BAF59188.1_1007	6	6.270	0.011	21.2
	glyceraldehyde-3-phosphate dehydrogenase/erythrose-4-phosphate dehydrogenase		BAF60904.1_2723	6	6.270	0.011	21.2
MMC	succinyl-CoA synthetase, beta subunit	mmcD2	BAF59539.1_1358	1	8.399	0.083	26.1
	succinyl-CoA synthetase, alpha subunit	mmcD1	BAF59541.1_1360	3	7.196	0.136	54.0
	methylmalonyl-CoA mutase, N-terminal domain/subunit	mmcE	BAF59542.1_1361	1	7.470	0.178	27.6
	methylmalonyl-CoA mutase, C-terminal domain/subunit	mmcF	BAF59543.1_1362	7	8.148	0.153	94.7
	methylmalonyl-CoA decarboxylase, alpha subunit	mmcH	BAF59545.1_1364	1	6.696	0.089	7.8
	malate dehydrogenase	mmcK	BAF59548.1_1367	1	8.030	0.053	38.5
	Transcarboxylase, 5S subunit	mmcL	BAF59549.1_1368	3	7.625	0.053	28.0
	pyruvate:ferredoxin oxidoreductase	mmcM	BAF59550.1_1369	2	8.496	0.047	19.5
PCT	acyl CoA:acetate/3-ketoacid CoA transferase, beta subunit	atoA	BAF60223.1_2042	1	7.504	0.153	21.1
	acyl CoA:acetate/3-ketoacid CoA transferase, alpha subunit	atoD	BAF60224.1_2043	1	6.565	0.003	27.2
	acyl CoA:acetate/3-ketoacid CoA transferase, alpha subunit	atoD	BAF60225.1_2044	1	6.827	0.040	12.5
Potential electron transfer complex							
	hypothetical formate dehydrogenase	pth	BAF60827.1_2646	1	7.040	0.120	16.1
	NADH:ubiquinone oxidoreductase, NADH-binding 51 kD subunit	NuoF	BAF60829.1_2648	1	6.498	0.173	9.1
	NADH:ubiquinone oxidoreductase 24 kD subunit	NuoE	BAF60830.1_2649	1	6.519	0.203	23.5

*Reference genome

β-oxidation pathway (butyrate and longer chain fatty acid oxidation)							
<i>Pathway</i>	<i>Enzyme</i>	<i>Abbr.</i>	<i>Contid ID</i>	<i>P(n)</i>	<i>AVG Log10(LFQ)</i>	<i>STD</i>	<i>Max seq. cov. (%)</i>
	CO dehydrogenase/acetyl-CoA synthase delta subunit (corrinoid Fe-S protein)		Ga0101770_100055312	1	6.709	0.003	40.4
	CO dehydrogenase/acetyl-CoA synthase gamma subunit (corrinoid Fe-S protein)		Ga0101770_100055313	1	7.583	0.022	38.0
	CO dehydrogenase/acetyl-CoA synthase beta subunit		Ga0101770_100055314	4	7.501	0.058	27.1
	6Fe-6S prismatic cluster-containing protein		Ga0101770_100055315	1	7.143	0.020	13.0
Acyl-CoA metabolism	Acetyl-CoA acetyltransferase	fadA	Ga0101770_10711792	3	6.688	0.035	23.5
	Acyl-CoA dehydrogenases	fadE	Ga0101770_10711793	3	7.234	0.074	16.5
	Acetyl-CoA acetyltransferase	fadA	Ga0101770_11066643	3	6.688	0.035	23.5
	Acyl-CoA dehydrogenases	fadE	Ga0101770_11066642	3	7.234	0.074	16.5
	Acetyl-CoA acetyltransferase	fadA	Ga0101770_101910914	3	6.688	0.035	23.5
	Acyl-CoA dehydrogenases	fadE	Ga0101770_101910915	3	7.234	0.074	16.5
	Enoyl-CoA hydratase/carnithine racemase	fadB1	Ga0101770_101913064	1	7.411	0.156	57.0
	Acyl-CoA dehydrogenases	fadE	Ga0101770_101913069	2	7.378	0.106	24.0
	Acyl CoA:acetate/3-ketoacid CoA transferase. beta subunit	catB	Ga0101770_101917085	1	7.033	0.036	28.5
	Acyl CoA:acetate/3-ketoacid CoA transferase. alpha subunit	catA	Ga0101770_101917086	2	6.872	0.003	25.3
	3-hydroxyacyl-CoA dehydrogenase	fadB2	Ga0101770_101918915	5	6.571	0.183	27.9
	Acyl-CoA dehydrogenases	fadE	Ga0101770_101918917	2	6.292	0.115	6.5
	Myo-inositol-1-phosphate synthase		Ga0101770_101918920	9	7.492	0.032	40.5
3-hydroxyacyl-CoA dehydrogenase	fadB2	Ga0101770_1019035106	5	6.980	0.112	23.2	
Enoyl-CoA hydratase/carnithine racemase		Ga0101770_1019035107	3	7.555	0.091	65.6	
Phosphotransacetylase	pta	Ga0101770_101896298	6	6.524	0.027	15.8	
Acetate kinase	ack	Ga0101770_101896299	4	7.375	0.062	46.6	
Electron transfer							
	Electron transfer flavoprotein. beta subunit		Ga0101770_101896276	4	7.731	0.034	65.6
	Electron transfer flavoprotein. alpha subunit		Ga0101770_101896277	3	8.154	0.008	77.3

	NADH:ubiquinone oxidoreductase 24 kD subunit		Ga0101770_101966010	4	8.416	0.068	76.9
	NADH:ubiquinone oxidoreductase. NADH-binding (51 kD) subunit		Ga0101770_101966011	11	8.340	0.035	61.7
	Iron only hydrogenase large subunit. C-terminal domain		Ga0101770_101966012	8	8.683	0.073	58.5
<i>Syntrophothermus lipocaldinus</i>							
<i>Pathway</i>	<i>Enzyme</i>	<i>Abbr.</i>	<i>Contid ID</i>	<i>P(n)</i>	<i>AVG Log10(LFQ)</i>	<i>STD</i>	<i>Max seq. cov. (%)</i>
Acyl-CoA metabolism	Long-chain acyl-CoA synthetases (AMP-forming)	LACS	Ga0101770_10039476	1	6.870	0.078	7.8
	Acyl-CoA synthetases (AMP-forming)/AMP-acid ligases II	ACS	Ga0101770_100021615	1	7.010	0.124	18.9
	Acyl CoA:acetate/3-ketoacid CoA transferase. beta subunit	catB	Ga0101770_100004630	2	7.150	0.190	33.7
	Acyl CoA:acetate/3-ketoacid CoA transferase. alpha subunit	catA	Ga0101770_100004631	2	7.020	0.206	29.5
	Acyl-CoA dehydrogenases	fadE	Ga0101770_100004632	2	6.848	0.163	26.3
	3-hydroxyacyl-CoA dehydrogenase	fadB2	Ga0101770_100004633	5	6.571	0.183	27.9
	Acetyl-CoA acetyltransferase	fadA	Ga0101770_100004634	3	7.502	0.179	46.0
	Enoyl-CoA hydratase/carnithine racemase	fadB1	Ga0101770_100010220	2	7.206	0.125	42.5
	Acyl-CoA dehydrogenases	fadE	Ga0101770_100010221	2	7.715	0.116	39.5
	Acetyl-CoA hydrolase	ach	Ga0101770_100010222	4	7.907	0.161	35.3
SLP	Acetyl-CoA acetyltransferase	fadA	Ga0101770_100010223	3	7.799	0.192	51.2
	Acetate kinase	ack	Ga0101770_100025434	3	6.431	0.117	22.9
	Phosphotransacetylase	pta	Ga0101770_100025435	6	6.524	0.027	15.8
Electron transfer							
	Iron only hydrogenase large subunit. C-terminal domain		Ga0101770_10002305	2	7.672	0.075	22.1
	NADH:ubiquinone oxidoreductase. NADH-binding (51 kD) subunit		Ga0101770_10002306	4	7.235	0.146	21.9
	NADH:ubiquinone oxidoreductase 24 kD subunit		Ga0101770_10002307	3	6.693	0.051	20.9
UnFirm02_FrBGR							
<i>Pathway</i>	<i>Enzyme</i>	<i>Abbr.</i>	<i>Contid ID</i>	<i>P(n)</i>	<i>AVG Log10(LFQ)</i>	<i>STD</i>	<i>Max seq. cov. (%)</i>

Acyl-CoA metabolism	Acyl-CoA synthetases (AMP-forming)/AMP-acid ligases II	ACS	Ga0101770_101933521	4	9.034	0.163	45.1	
	Acyl-CoA dehydrogenases	fadE	Ga0101770_1019074199	3	7.267	0.020	40.9	
	Acyl-CoA dehydrogenases	fadE	Ga0101770_101907812	4	7.495	0.042	37.4	
	Acyl-CoA dehydrogenases	fadE	Ga0101770_101915214	1	7.091	0.048	12.1	
	Acyl-CoA dehydrogenases	fadE	Ga0101770_10193733	1	6.872	0.060	26.6	
	Acyl-CoA dehydrogenases	fadE	Ga0101770_101964615	3	8.086	0.035	45.2	
	Acyl-CoA dehydrogenases	fadE	Ga0101770_10894683	2	8.215	0.194	49.1	
	3-hydroxyacyl-CoA dehydrogenase	fadB2	Ga0101770_101905559	1	6.940	0.076	14.2	
	Acetyl-CoA acetyltransferase	fadA	Ga0101770_101905626	2	7.101	0.023	14.0	
	3-hydroxyacyl-CoA dehydrogenase	fadB2	Ga0101770_11029231	6	8.913	0.008	61.1	
	3-hydroxyacyl-CoA dehydrogenase	fadB2	Ga0101770_101917246	6	8.913	0.008	61.1	
	Acetyl-CoA acetyltransferase	fadA	Ga0101770_101917247	3	8.269	0.059	66.3	
	Enoyl-CoA hydratase/carnithine racemase	fadB1	Ga0101770_10203002	2	6.625	0.067	20.9	
	Acyl dehydratase		Ga0101770_10758842	3	6.796	0.016	34.2	
	Phosphotransacetylase	pta	Ga0101770_10439631	38	7.392	0.028	51.8	
	Other:							
	Glycolysis/ gluconeogenesis	ABC-type oligopeptide transport system, periplasmic component		Ga0101770_101933538	1	7.763	0.015	23.8
		Phosphotransacetylase	pta	Ga0101770_10439631	38	7.392	0.028	51.8
		Phosphoenolpyruvate synthase/pyruvate phosphate dikinase	PEPS	Ga0101770_101965811	3	7.312	0.108	26.6
Glyceraldehyde-3-phosphate dehydrogenase/erythrose-4-phosphate dehydrogenase		G3PD	Ga0101770_1019074121	63	8.840	0.001	86.8	
Glyceraldehyde-3-phosphate dehydrogenase/erythrose-4-phosphate dehydrogenase		G3PD	Ga0101770_101909260	15	7.409	0.052	23.6	
Fructose/tagatose biphosphate aldolase		FBA	Ga0101770_10029874	1	6.664	0.049	28.8	
Fructose/tagatose biphosphate aldolase		FBA	Ga0101770_101973810	1	6.846	0.073	31.3	
Enolase		Eno	Ga0101770_101909222	16	6.809	0.025	14.9	

Wood-Ljungdahl pathway (acetate oxidation)								
<i>Thermacetogenium phaeum</i>								
<i>Pathway</i>	<i>Enzyme</i>	<i>Abbr.</i>	Contid ID	P(n)	AVG Log10(LFQ)	STD	Max seq. cov. (%)	
Tetrahydrofolate pathway	Formyltetrahydrofolate synthetase	fhs/FTHFS	Ga0101770_10222277	1	8.345	0.070	80.9	
	5,10-methylene-tetrahydrofolate dehydrogenase/Methenyl tetrahydrofolate cyclohydrolase	metV	Ga0101770_101900819	2			71.0	
	5,10-methylenetetrahydrofolate reductase	metF	Ga0101770_101900541	3	7.697	0.110	76.5	
	Methylene-tetrahydrofolate reductase C terminal		Ga0101770_101900542	4	7.118	0.103	21.1	
	Coenzyme F420-reducing hydrogenase, delta subunit		Ga0101770_101900543	8	6.866	0.037	13.7	
	Methyltransferase	acsE	Ga0101770_101900544	4	7.508	0.103	39.4	
	CO dehydrogenase/acetyl-CoA synthase delta subunit (corrinoid Fe-S protein)	AcsD	Ga0101770_101900545	1	7.179	0.095	65.4	
	CO dehydrogenase/acetyl-CoA synthase gamma subunit (corrinoid Fe-S protein)	acsC	Ga0101770_101900547	4	9.274	0.114	71.8	
	CO dehydrogenase/acetyl-CoA synthase beta subunit	acsB	Ga0101770_101900548	3	8.726	0.041	71.3	
	Acetate Kinase	ack	Ga0101770_10228884	2	7.114	0.145	54.5	
CODH/ACS cluster	Phosphotransacetylase	pta	Ga0101770_10228885	1	7.053	0.012	64.9	
	Phosphotransacetylase	pta	Ga0101770_101991946	5	8.664	0.057	67.8	
	Acetate Kinase		Ga0101770_101991947	4	9.097	0.132	64.6	
	UnFirm02_FrBGR							
	<i>Pathway</i>	<i>Enzyme</i>	<i>Abbr.</i>	Contid ID	P(n)	AVG Log10(LFQ)	STD	Max seq. cov. (%)
	Tetrahydrofolate pathway	5,10-methylene-tetrahydrofolate dehydrogenase/Methenyl tetrahydrofolate cyclohydrolase	metV	Ga0101770_10189438	7	7.237	0.052	50.5
		5,10-methylene-tetrahydrofolate dehydrogenase/Methenyl tetrahydrofolate cyclohydrolase	metV	Ga0101770_101915166	7	7.237	0.052	50.5
		Formyltetrahydrofolate synthetase	fhs	Ga0101770_101921914	13	8.425	0.021	48.6
5,10-methylenetetrahydrofolate reductase		metF	Ga0101770_10203003	1	7.333	0.012	56.4	
Methylene-tetrahydrofolate reductase C terminal			Ga0101770_10203004	1	6.910	0.107	23.7	
CODH/ACS cluster	Methyltransferase	acsE	Ga0101770_10203005	4	6.942	0.018	17.2	
	Methyltransferase	acsE	Ga0101770_101904522	4	6.942	0.018	17.2	

	CO dehydrogenase/acetyl-CoA synthase delta subunit (corrinoid Fe-S protein)	acsD	Ga0101770_101904523	1	6.330	0.054	17.5
	CO dehydrogenase/acetyl-CoA synthase gamma subunit (corrinoid Fe-S protein)	acsC	Ga0101770_101904524	2	6.933	0.008	31.4
	CO dehydrogenase/acetyl-CoA synthase gamma subunit (corrinoid Fe-S protein)	acsC	Ga0101770_101904525	2	6.933	0.008	31.4
	CO dehydrogenase/acetyl-CoA synthase beta subunit	acsB	Ga0101770_10206496	2	6.805	0.024	18.9
	NAD/NADP transhydrogenase alpha subunit		Ga0101770_101904548	1	6.265	0.103	6.1
	6Fe-6S prismane cluster-containing protein		Ga0101770_101923269	5	7.279	0.084	17.6
	CO dehydrogenase/acetyl-CoA synthase beta subunit	acsB	Ga0101770_101923270	6	8.017	0.023	33.9
	CO dehydrogenase/acetyl-CoA synthase beta subunit	acsB	Ga0101770_10290312	6	8.017	0.023	33.9
	CO dehydrogenase/acetyl-CoA synthase gamma subunit (corrinoid Fe-S protein)	acsC	Ga0101770_10290311	4	8.253	0.067	52.3
	CO dehydrogenase/acetyl-CoA synthase gamma subunit (corrinoid Fe-S protein)	acsC	Ga0101770_101923271	4	8.253	0.067	52.3
	CO dehydrogenase/acetyl-CoA synthase delta subunit (corrinoid Fe-S protein)	acsD	Ga0101770_101923272	4	7.125	0.035	50.2
	Phosphotransacetylase	pta	Ga0101770_11386031	38	7.392	0.028	51.8
Potential electron transfer complex							
	Heterodisulfide reductase. subunit A and related polyferredoxins		Ga0101770_101899450	9	7.584	0.053	19.5
	Heterodisulfide reductase. subunit A and related polyferredoxins		Ga0101770_101906740	9	7.584	0.053	19.5
	Heterodisulfide reductase. subunit A and related polyferredoxins		Ga0101770_101894667	9	7.584	0.053	19.5
	Electron transfer flavoprotein. alpha subunit	ETC	Ga0101770_101894668	2	7.616	0.025	59.0
	Electron transfer flavoprotein. beta subunit	ETC	Ga0101770_101894669	2	7.302	0.039	49.2
	Fe-S oxidoreductase	FeS red	Ga0101770_101894670	2	6.646	0.036	9.1
	Electron transfer flavoprotein. beta subunit	ETC	Ga0101770_101899448	1	6.303	0.020	21.8
	Electron transfer flavoprotein. alpha subunit	ETC	Ga0101770_101899449	1	6.885	0.021	42.9
	Heterodisulfide reductase. subunit A and related polyferredoxins		Ga0101770_101899450	9	7.584	0.053	19.5

Methanogenesis		Hydrogenotrophic methanogenesis						
Pathway	Enzyme	Abbr.	Contig Id Archaea	P(n)	AVG Log10(LFQ)	STD	Max seq. cov. (%)	
mtr cluster	Tetrahydromethanopterin S-methyltransferase. subunit H	mtrH	Ga0101770_10104181 c	1	9.035	0.175	56.2	
mtr cluster	Tetrahydromethanopterin S-methyltransferase. subunit G	mtrG	Ga0101770_10104182 c	3	9.234	0.066	39.5	
mcr cluster	Tetrahydromethanopterin S-methyltransferase. subunit F	mtrF	Ga0101770_10104183 c	3	9.035	0.175	56.2	
	Tetrahydromethanopterin S-methyltransferase. subunit H	mtrH	Ga0101770_10242941 a	1	7.809	0.011	85.8	
	Tetrahydromethanopterin S-methyltransferase. subunit B	mtrB	Ga0101770_10271717 a	2	9.340	0.007	79.4	
	Tetrahydromethanopterin S-methyltransferase. subunit A	mtrA	Ga0101770_10271721 a	5	8.915	0.123	58.6	
	Tetrahydromethanopterin S-methyltransferase. subunit E	mtrE	Ga0101770_10271725 a	2	9.054	0.108	16.7	
mcr cluster	Methyl coenzyme M reductase. alpha subunit	mcr	Ga0101770_10271726 a	1	9.728	0.031	72.8	
fmd cluster	Methyl coenzyme M reductase. gamma subunit	mcr	Ga0101770_10271727 a	1	9.634	0.141	92.5	
	Formylmethanofuran dehydrogenase subunit B	fmdB	Ga0101770_10193823 b	2	10.397	0.099	76.2	
fmd cluster	Formylmethanofuran dehydrogenase subunit C	fmdC	Ga0101770_10193824 b	1	9.961	0.115	93.0	
	Formylmethanofuran dehydrogenase subunit A	fmdA	Ga0101770_10193825 b	2	10.332	0.060	90.5	
	Formylmethanofuran dehydrogenase subunit D	fmdD	Ga0101770_10193826 b	2	10.276	0.024	93.9	
	Hypothetical protein		Ga0101770_10193827 b	2	9.004	0.133	98.8	
	Coenzyme F420-reducing hydrogenase. beta subunit	fthB	Ga0101770_10795316 a	1	8.757	0.176	82.0	

^aContid ID 'M.thermoautotrophicus'

^bContid ID 'Methanothermobacter'

^cContig ID 'Methanobacteriales'

^dContig Id Archaea

Methanogenesis		Acetoclastic methanogenesis (Methanoseta thermophila*)					
<i>Pathway</i>	<i>Enzyme</i>	<i>Abbr.</i>	Contid ID (ref. genome)	P(n)	AVG Log10(LFQ)	STD	Max seq. cov. (%)
cdh cluster	acetyl-CoA decarboxylase/synthase beta subunit	cdhB	Mthe_0290_284	1	7.656	0.127	30.3
cdh cluster	acetyl-CoA decarboxylase/synthase epsilon subunit	cdhE	Mthe_0291_285	1	8.309	0.198	67.6
mrc cluster	acetyl-CoA decarboxylase/synthase alpha subunit	cdhA	Mthe_0292_286	1	8.626	0.113	19.9
mrc cluster	methyl-coenzyme M reductase. alpha subunit	mcrA	Mthe_0569_557	1	7.948	0.138	15.7
mrc cluster	methyl-coenzyme M reductase. gamma subunit	mcrG	Mthe_0570_558	1	7.695	0.180	43.9
acs cluster	methyl-coenzyme M reductase. beta subunit	mcrB	Mthe_0572_560	1	8.437	0.140	32.9
acs cluster	acetyl-coenzyme A synthetase	acs	Mthe_1194_1172	1	8.192	0.223	37.5
acs cluster	acetyl-coenzyme A synthetase	acs	Mthe_1195_1173	4	9.034	0.163	45.1
acs cluster	acetyl-coenzyme A synthetase	acs	Mthe_1196_1174	1	8.367	0.093	32.1
acs cluster	methylenetetrahydromethanopterin reductase	mer	Mthe_0205_200	2	6.342	0.054	19.5
	phosphate ABC transporter substrate-binding protein. PhoT family		Mthe_1480_1450	1	7.537	0.210	23.0
	H ⁺ -transporting two-sector ATPase. E subunit		Mthe_1612_1576	1	6.540	0.150	22.5
	H ⁽⁺⁾ -transporting ATP synthase. subunit H		Mthe_1615_1579	1	6.905	0.255	32.4
	triosephosphate isomerase		Mthe_0041_41	1	6.175	0.154	22.1
	ketol-acid reductoisomerase		Mthe_0112_111	1	7.203	0.096	24.4
	glyceraldehyde-3-phosphate dehydrogenase		Mthe_0701_688	1	6.726	0.110	6.8
	protein=CoB--CoM heterodisulfide reductase subunit A	hdrA	Mthe_1576_1543	1			

*Reference genome